*Supporting Information for*

# Cephalotane-Type $C_{20}$ Diterpenoids from *Cephalotaxus fortune* var. *alpina*

Zhan-Peng Ge,[a,b] Bin Zhou,[a,b,d] Flavia M. Zimbres,[c] Reagan S. Haney,[c] Qun-Fang Liu,[a,b] Yan Wu,[a,b] Maria B. Cassera,[c] Jin-Xin Zhao*[,a,b,d] and Jian-Min Yue*[,a,b,d]

[a]State Key Laboratory of Drug Research, Shanghai Institute of Materia Medica, Chinese Academy of Sciences, 555 Zuchongzhi Road, Shanghai 201203, China

[b]Research Units of Discovery of New Drug Lead Molecules, Chinese Academy of Medical Sciences

[c]Department of Biochemistry and Molecular Biology, Center for Tropical and Emerging Global Diseases (CTEGD), University of Georgia, Athens, Georgia 30602, United States

[d]Shandong Laboratory of Yantai Drug Discovery, Bohai Rim Advanced Research Institute for Drug Discovery, 198 East Binhai Road, Yantai, Shandong 264117, China

*Corresponding authors

Tel.: +86 21 50806718. Email: jmyue@simm.ac.cn; jxzhao@simm.ac.cn.

# List of Supporting Information

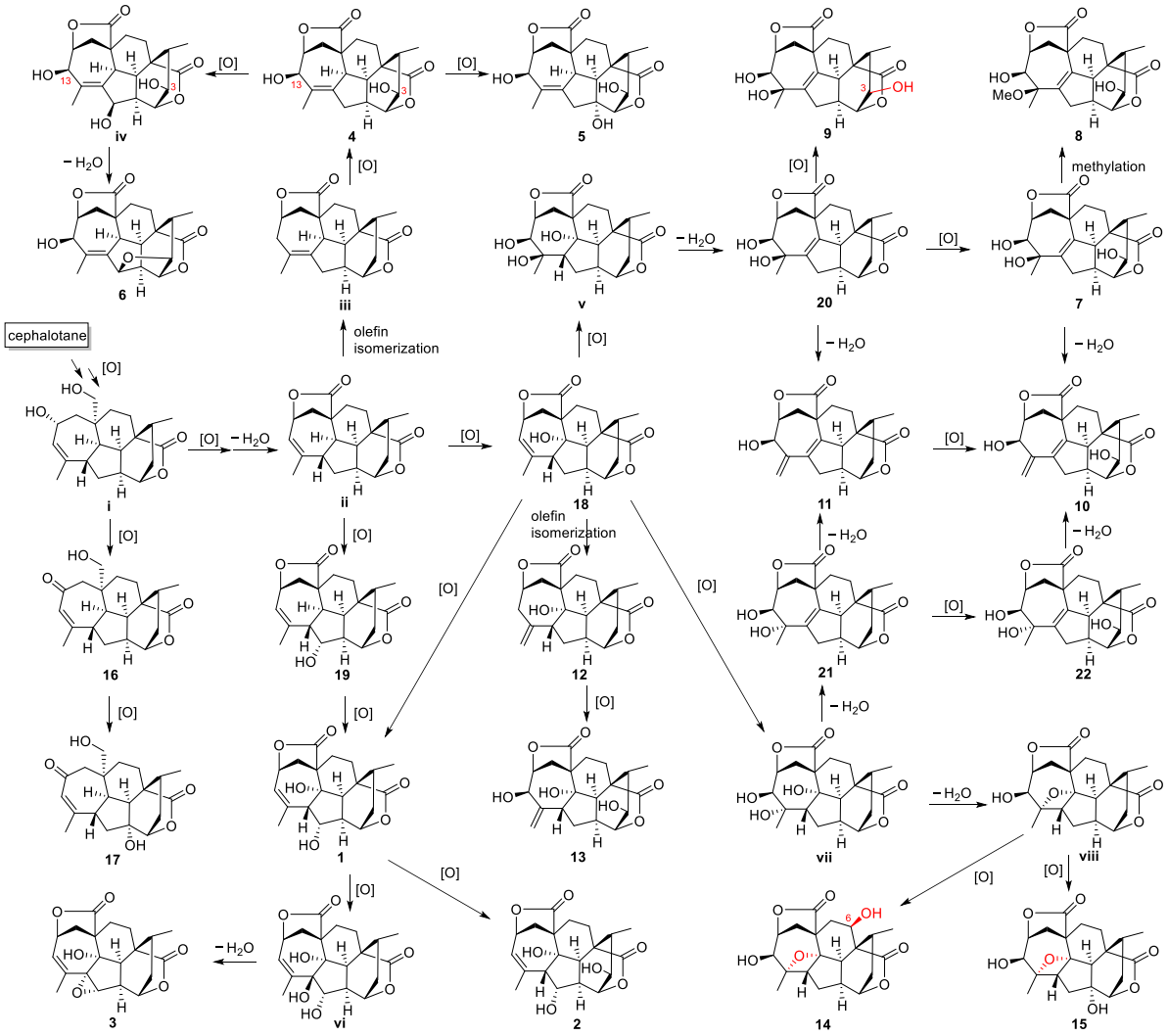


**Scheme S1**. Proposed biosynthetic pathways for compounds **1**−**22**.

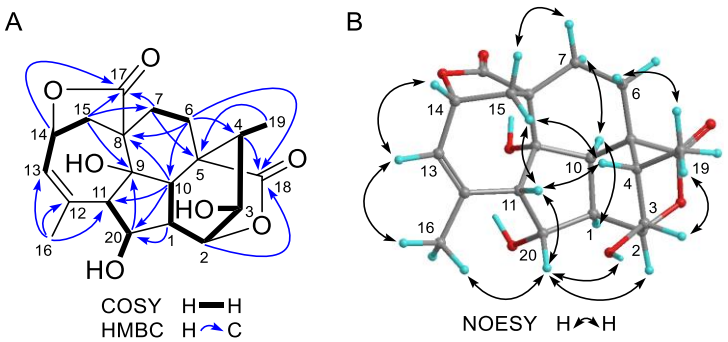


**Figure S1**. Selected 2D NMR correlations of compound **2**.

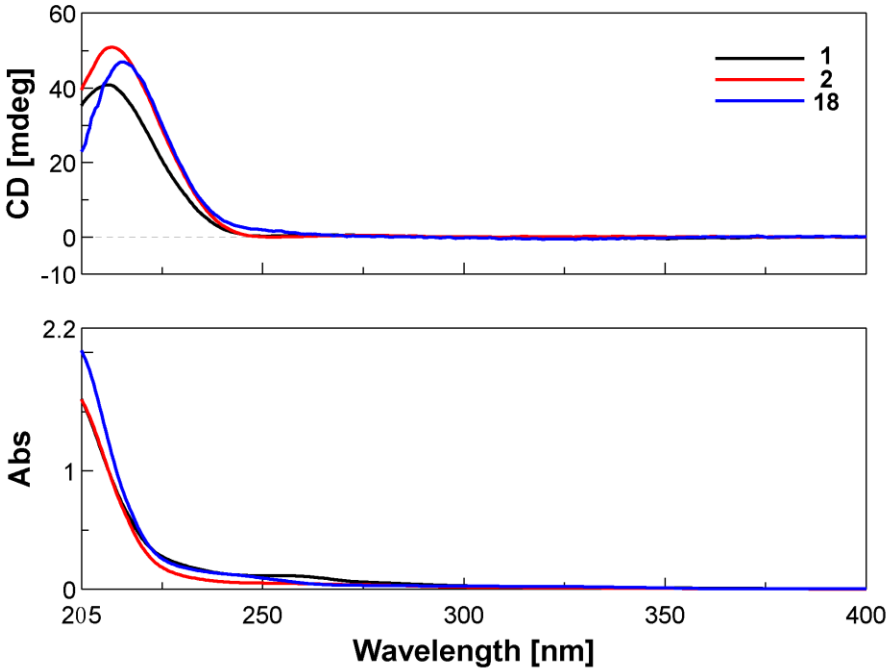


**Figure S2**. ECD spectra of compounds **1**, **2**, and **18**.

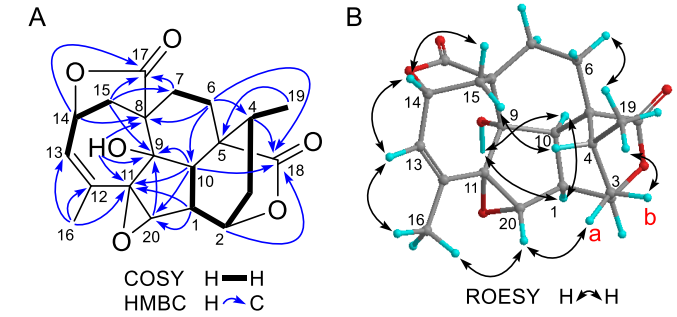


**Figure S3**. Selected 2D NMR correlations of compound **3**.

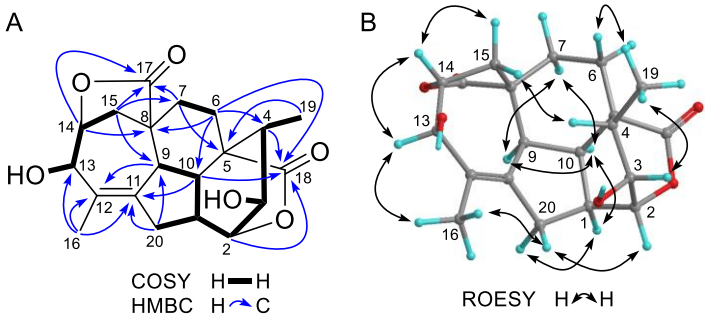


**Figure S4**. Selected 2D NMR correlations of compound **4**.

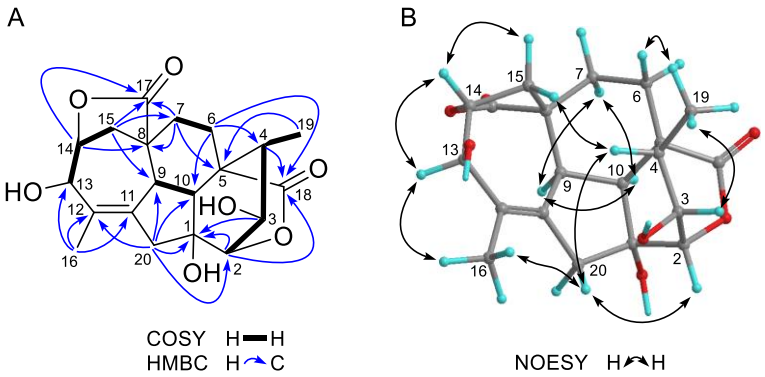


**Figure S5**. Selected 2D NMR correlations of compound **5**.

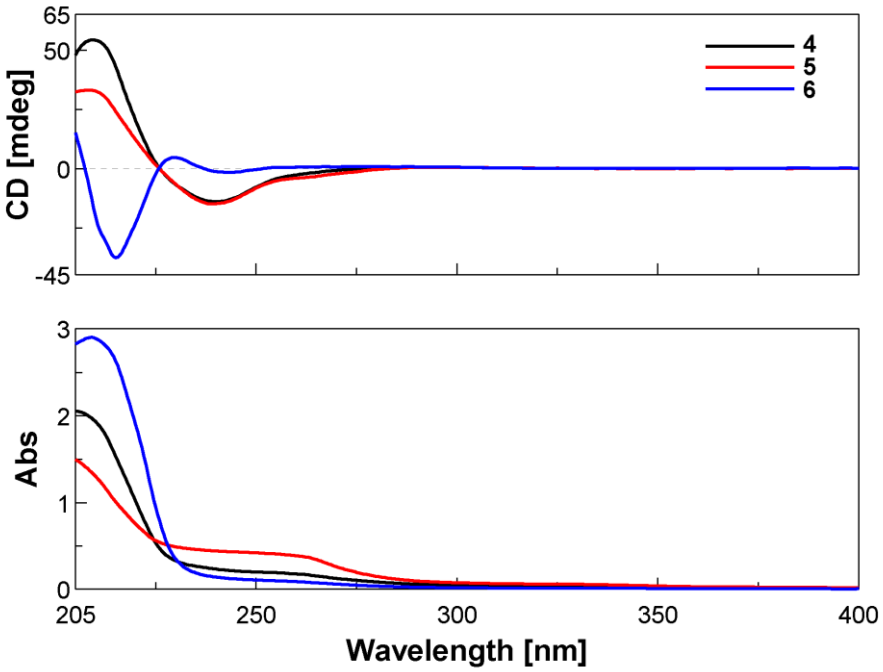


**Figure S6**. ECD spectra of compounds **4**, **5** and **6**.

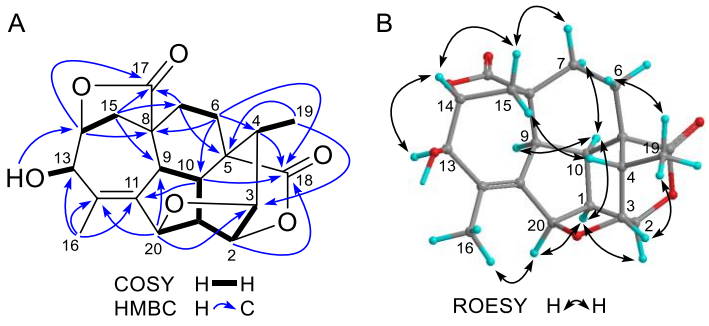


**Figure S7**. Selected 2D NMR correlations of compound **6**.

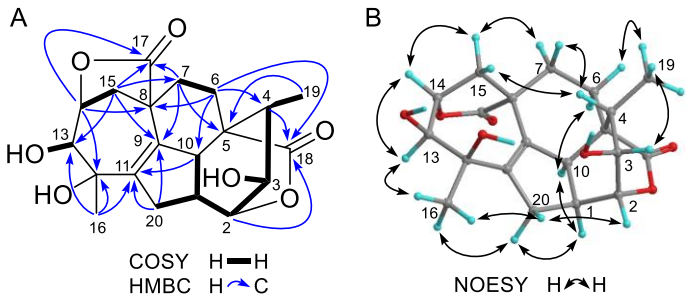


**Figure S8**. Selected 2D NMR correlations of compound **7**.

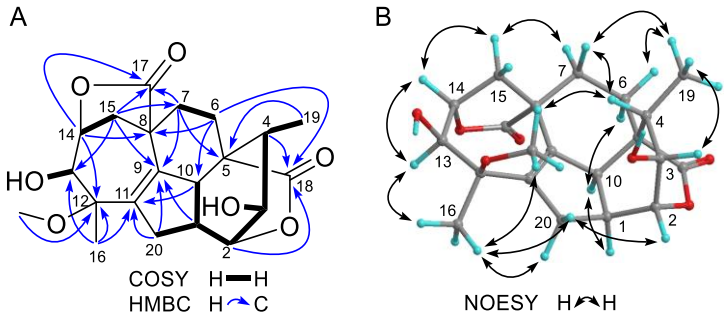


**Figure S9**. Selected 2D NMR correlations of compound **8**.

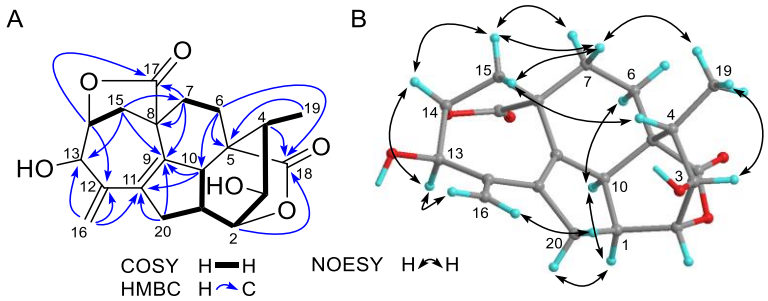


**Figure S10**. Selected 2D NMR correlations of compound **10**.

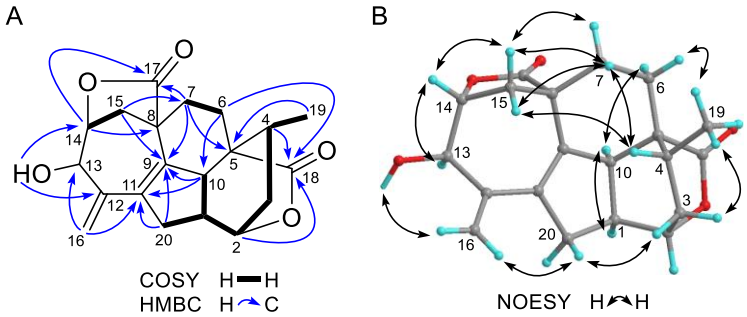


**Figure S11**. Selected 2D NMR correlations of compound **11**.

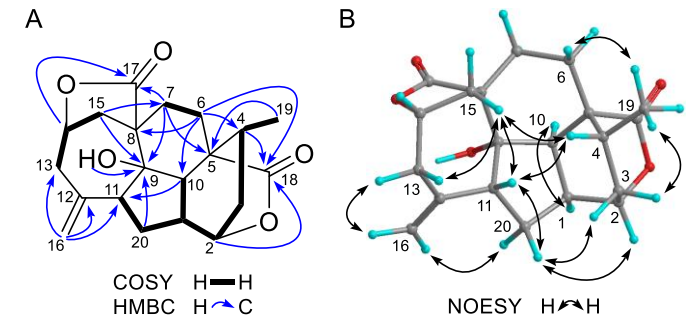


**Figure S12**. Selected 2D NMR correlations of compound **12**.

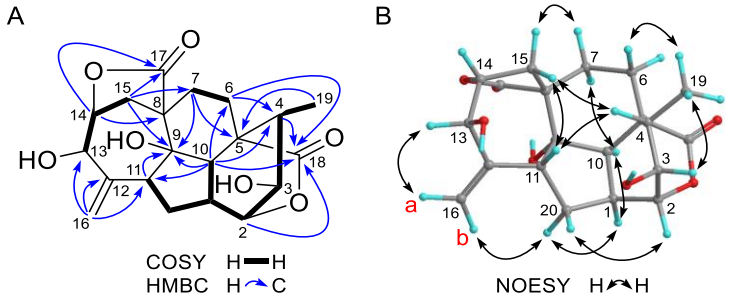


**Figure S13**. Selected 2D NMR correlations of compound **13**.

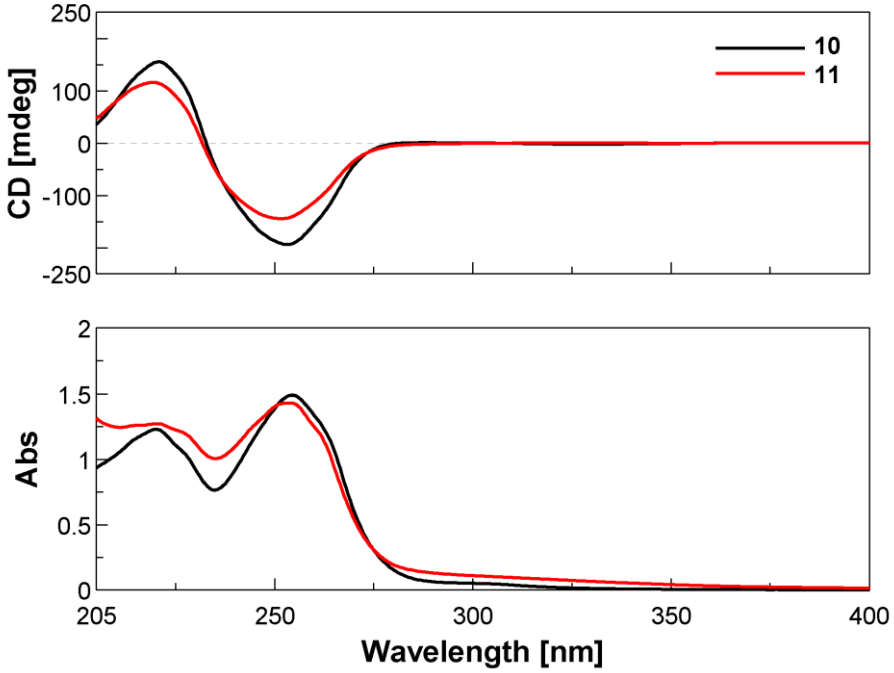


**Figure S14**. ECD spectra of compounds **10** and **11**.

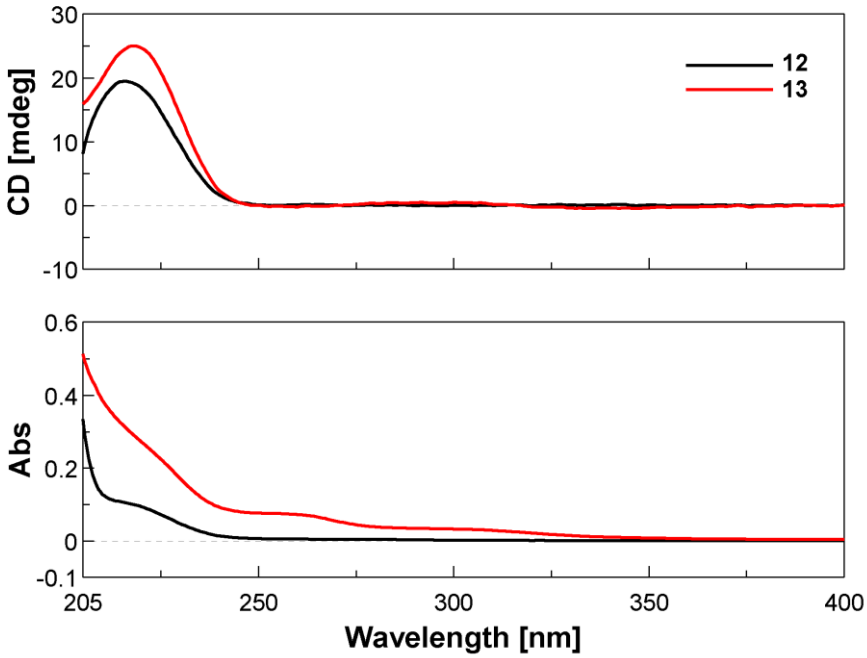


**Figure S15**. ECD spectra of compounds **12** and **13**.

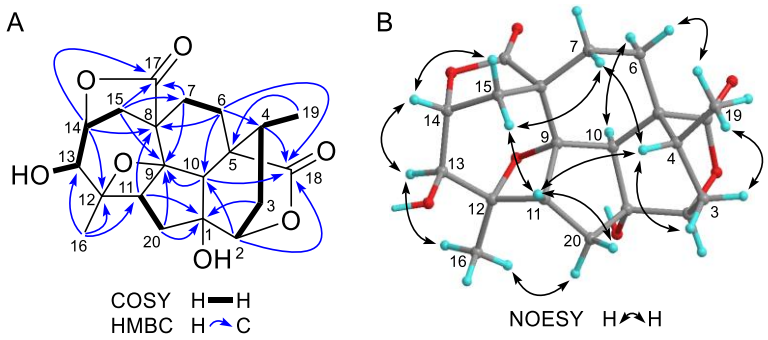


**Figure S16**. Selected 2D NMR correlations of compound **15**.

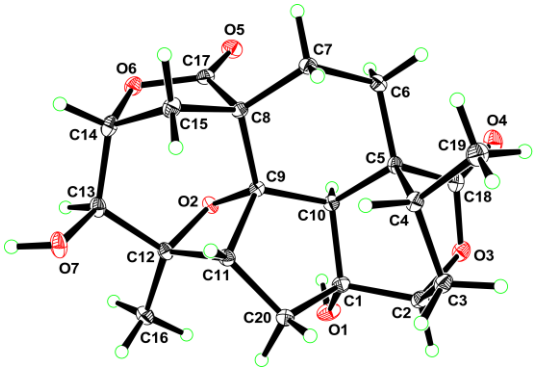


**Figure S17**. ORTEP drawing of compound **15**.

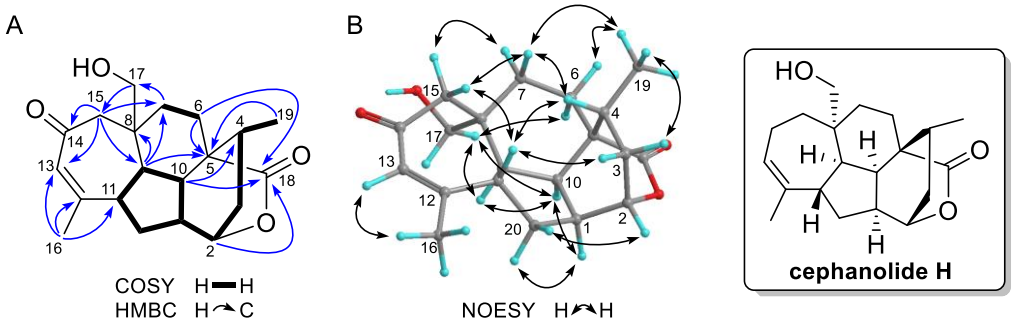


**Figure S18**. Selected 2D NMR correlations of compound **16**.

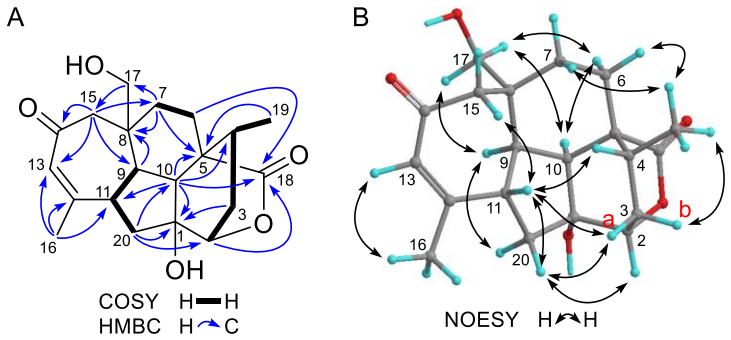


**Figure S19**. Selected 2D NMR correlations of compound **17**.

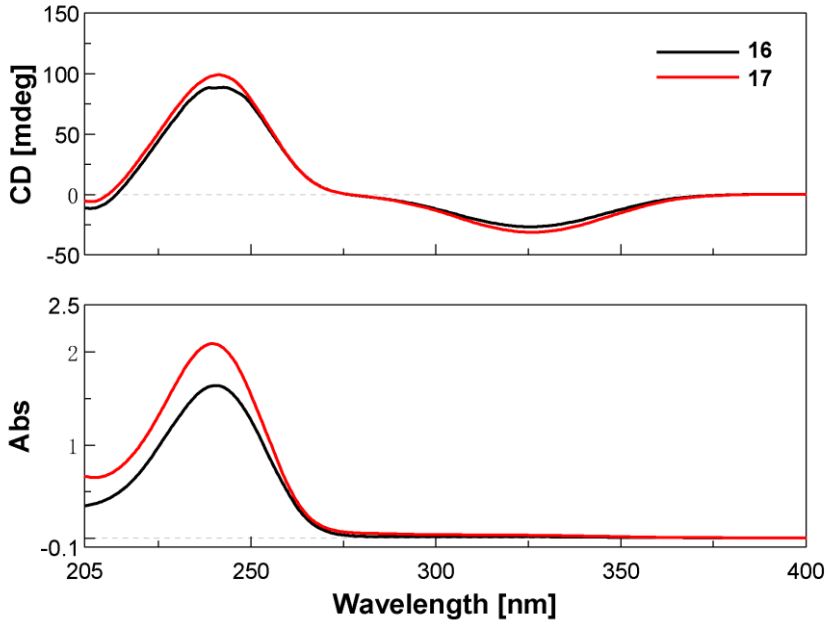


**Figure S20**. ECD spectra of compounds **16** and **17**.

**General experimental procedures**

Melting points were measured on an SGW X-4 melting point apparatus (Shanghai Precision & Scientific Instrument Co. Ltd.) and were uncorrected. Optical rotations (Na lamp, 589 nm) were obtained with an Autopol VI Automatic Polarimeter at room temperature; concentrations were reported in g/100mL. UV and ECD spectra were obtained on a JASCO J-815 spectrometer using a 0.1 cm path length sample cell. IR spectra were recorded on a Thermo Scientific Nicolet iS 5 FT-IR Spectrometer. NMR spectra were acquired on Bruker Avance III 500 and/or 600 spectrometers (Bruker Biospin AG, Switzerland) and referenced to deuterated solvent peaks. HRESIMS were run on a Waters LCT Premier XE mass spectrometer or an Agilent G6520 Q-TOF mass spectrometer. The X-ray crystallographic data were obtained on a Bruker APEX-II CCD diffractometer for compounds **4**, **10**, **14** and **15**, and on a Bruker D8 Venture diffractometer for compound **3**. Silica gel (200–300 and 300–400 mesh, Qingdao Haiyang Chemical Co. Ltd., China), MCI gel (CHP20P, 75–150 $\mu$m, Mitsubishi Chemical Corporation), $C_{18}$ reversed-phase silica gel (20–45 $\mu$m, Fuji Silysia Chemical Ltd., Japan), and Sephadex LH-20 (GE Healthcare, Uppsala, Sweden) were used for column chromatography. Semi-preparative HPLC was performed on a Waters 1525 binary pump with a Waters 2489 detector (254 nm and 210 nm) using a YMC-Pack ODS-A column (250 × 10 mm, S-5 $\mu$m, 12 nm) or a Waters XBridge Prep $C_{18}$ column (250 × 10 mm, S-5 $\mu$m, 130 Å). Precoated silica gel 60 $F_{254}$ plates (Merck Chemicals (Shanghai) Co., Ltd., China) were used for TLC monitors. All solvents were of analytical grade (SCR, Sinopharm Chemical Reagent Co., Ltd., China) except that solvents used for HPLC were of HPLC grade (J&K Scientific Ltd., China).

**Plant material**

The seeds of *Cephalotaxus fortunei* var. *alpina* (H. L. Li) were collected from Shangri-La, Yunnan province, People's Republic of China, and authenticated by Prof. You-Kai Xu of Xishuangbanna Tropical Botanical Garden, Chinese Academy of Sciences. A voucher specimen has been deposited in Shanghai Institute of Materia

Medica, Chinese Academy of Sciences (accession number: Cfsd-2011-1Y-XY).

**Extraction and Isolation**

The air-dried and finely ground seeds of *C. fortunei* var. *alpina* (10 kg) were extracted by maceration in EtOH/$H_2O$ (95:5, 3×20 L) at room temperature to obtain a crude extract (1.2 kg). The crude extract was suspended in water and extracted with petroleum ether and EtOAc, sequentially, and afforded an EtOAc-soluble extract (34 g). The EtOAc-soluble fraction was subjected to an MCI gel column eluted with MeOH/$H_2O$ mixtures (30% to 100% MeOH in $H_2O$) to give seven fractions (A–G). Fraction B (5.7 g) was chromatographed over a silica gel column using $CHCl_3$/MeOH gradient solvent system (100:1 to 5:1) to yield fractions B1–B5 after removal of pigments by Sephadex LH-20 gel chromatography. Fraction C (5.4 g) was subjected to separation with silica gel (petroleum ether/acetone, 10:1 to 1:2) to yield fractions C1–C6. The subfraction B3 (1.2 g) was separated by Sephadex LH-20 with $CHCl_3$/MeOH (1:1) to give five fractions, and the second fraction was purified by HPLC (20% $CH_3CN$ in $H_2O$) to give **14** (2.1 mg, $t_R$ = 14.6 min). The subfraction B4 (1.1 g) was fractioned on a $C_{18}$-reversed phase silica gel column (MeOH/$H_2O$, 20% to 80%) to yield fractions B4a−B4g after using Sephadex LH-20 gel to remove impurities. Fraction B4b was purified by HPLC (15% to 27% $CH_3CN$ in $H_2O$) to give **13** (2.4 mg, $t_R$ = 15.4 min), **22** (12.0 mg, $t_R$ = 19.2 min), **9** (1.3 mg, $t_R$ = 20.3 min), **5** (2.0 mg, $t_R$ = 21.5 min), and **15** (1.5 mg, $t_R$ = 22.5 min). Fraction B4e was separated by HPLC (20% $CH_3CN$ in $H_2O$) to give **17** (1.7 mg, $t_R$ = 13.0 min). Fraction C3 (950 mg) was fractioned over a silica gel column ($CHCl_3$/MeOH, 100:1 to 5:1) to provide fractions C3a–C3g. Fraction C3b was loaded into HPLC system (33.3% $CH_3CN$ in $H_2O$) to give **3** (1.5 mg, $t_R$ = 13.3 min) and **12** (3.8 mg). Similarly, fraction C3d was purified by Sephadex LH-20 gel chromatography and HPLC successively (30% $CH_3CN$ in $H_2O$) to yield **16** (3.4 mg, $t_R$ = 17.1 min), **18** (4.0 mg, $t_R$ = 18.5 min), **8** (6.8 mg, $t_R$ = 10.6 min), **1** (5.9 mg, $t_R$ = 13.0 min), **19** (2.2 mg, $t_R$ = 18.6 min), **11** (0.8 mg, $t_R$ = 21.0 min), and **6** (1.3 mg, $t_R$ = 11.9 min). Fractions C3e and C3f were purified by HPLC to give **20** (8.0 mg, 25% $CH_3CN$ in $H_2O$, $t_R$ = 14.5 min) and **10** (10.9 mg, 20% $CH_3CN$ in $H_2O$, $t_R$ = 23.7 min), respectively. Similar to the fraction C3, fraction C4

(1.5 g) was also subjected to silica and Sephadex LH-20 gel columns and HPLC sequentially to give **21** (8.8 mg), **2** (7.4 mg), **4** (12.4 mg), and **7** (6.4 mg).

*Fortalide A (**1**)*: white solid; $[\alpha]^{20}_{D}$ +21 (*c* 0.1, MeOH); ECD (MeOH) $\lambda$ ($\Delta\varepsilon$) 212 (4.68) nm; IR (KBr) $\nu_{max}$ 3423, 3241, 2981, 2960, 2951, 2873, 1765, 1752, 1464, 1456 $cm^{-1}$; $^{1}H$ and $^{13}C$ NMR (pyridine-$d_5$), see Table 1; (+)-ESIMS *m/z* 383.3 $[M + Na]^+$, 743.3 $[2\ M + Na]^+$; (−)-ESIMS *m/z* 405.2 $[M + HCO_2]^-$; (+)-HRESIMS *m/z* 361.1648 [M + H]+ (calcd for $C_{20}H_{25}O_6$, 361.1646).

*Fortalide B (**2**)*: white solid; $[\alpha]^{20}_{D}$ +30 (*c* 0.1, MeOH); ECD (MeOH) $\lambda$ ($\Delta\varepsilon$) 212 (6.44) nm; IR (KBr) $\nu_{max}$ 3433, 2965, 2887, 1758, 1733, 1461, 1447 $cm^{-1}$; $^{1}H$ and $^{13}C$ NMR (pyridine-$d_5$), see Table 1; (+)-ESIMS *m/z* 440.2 $[M + CH_3CN + Na]^+$, 753.3 $[2\ M + H]^+$, 775.3 $[2\ M + Na]^+$; (−)-ESIMS *m/z* 375.1 $[M - H]^-$, 421.2 $[M + HCO_2]^-$, 751.3 $[2\ M - H]^-$, 797.3 $[2\ M + HCO_2]^-$; (−)-HRESIMS *m/z* 421.1491 $[M + HCO_2]^-$ (calcd for $C_{21}H_{25}O_9$, 421.1499).

*Fortalide C (**3**)*: colorless crystals; 333–336 °C; $[\alpha]^{19}_{D}$ +23 (*c* 0.1, MeOH); UV (MeOH) $\lambda_{max}$ (log $\varepsilon$) 209 (3.80) nm; ECD (MeOH) $\lambda$ ($\Delta\varepsilon$) 219.5 (5.84) nm; IR (KBr) $\nu_{max}$ 3500, 3411, 2962, 2929, 2875, 2855, 1774, 1741, 1449, 1384, 1261, 1182, 1087, 1045, 929, 802, 736 $cm^{-1}$; $^{1}H$ and $^{13}C$ NMR ($CDCl_3$), see Table 1; (+)-ESIMS *m/z* 422.1 $[M + CH_3CN + Na]^+$, 717.3 $[2\ M + H]^+$, 739.2 $[2\ M + Na]^+$, 1097.4 $[3\ M + Na]^+$; (−)-ESIMS *m/z* 403.1 $[M + HCO_2]^-$, 761.3 $[2\ M + HCO_2]^-$; (−)-HRESIMS *m/z* 403.1393 $[M + HCO_2]^-$ (calcd for $C_{21}H_{23}O_8$, 403.1393).

*Fortalide D (**4**)*: colorless crystals; mp 270–272 °C; $[\alpha]^{20}_{D}$ −14 (*c* 0.4, MeOH); UV (MeOH) $\lambda_{max}$ 205 nm; ECD (MeOH) $\lambda$ ($\Delta\varepsilon$) 210 (5.74), 240 (−1.49) nm; IR (KBr) $\nu_{max}$ 3419, 2959, 2928, 2872, 1750, 1447, 1384, 736 $cm^{-1}$; $^{1}H$ and $^{13}C$ NMR ($CDCl_3$), see Table 2; (−)-ESIMS *m/z* 405.2 $[M + HCO_2]^-$, 473.1 $[M + HCO_2 + HCO_2Na]^-$, 765.3 $[2\ M + HCO_2]^-$; (−)-HRESIMS *m/z* 405.1549 $[M + HCO_2]^-$ (calcd for $C_{21}H_{25}O_8$, 405.1549).

*Fortalide E (**5**)*: white solid; $[\alpha]^{19}_{D}$ −20 (*c* 0.1, MeOH); ECD (MeOH) $\lambda$ ($\Delta\varepsilon$) 208 (3.76), 239 (−1.72) nm; IR (KBr) $\nu_{max}$ 3434, 2960, 2925, 2878, 2861, 1753, 1631 $cm^{-1}$; $^{1}H$ NMR and $^{13}C$ NMR (pyridine-$d_5$), see Table 2; (+)-ESIMS *m/z* 775.0 $[2\ M + Na]^+$, 1150.8 $[3\ M + Na]^+$; (−)-ESIMS *m/z* 313.1 $[M - H_2O - CO_2 - H]^-$, 421.2 [M +

$HCO_2]^-$, 751.3 [2 M − H]$^-$, 797.3 [2 M + $HCO_2]^-$; (−)-HRESIMS *m/z* 421.1498 [M + $HCO_2]^-$ (calcd for $C_{21}H_{25}O_9$, 421.1504).

*Fortalide F* ***(6)***: white solid; $[\alpha]^{20}_D$ −29 (*c* 0.1, MeOH); UV (MeOH) $\lambda_{max}$ (log $\varepsilon$) 209 (3.92) nm; ECD (MeOH) $\lambda$ ($\Delta\varepsilon$) 215 (−3.29), 230 (0.39) nm; IR (KBr) $\nu_{max}$ 3460, 2959, 2976, 1761, 1447, 1373, 1051, 736 cm$^{-1}$; $^1$H and $^{13}$C NMR ($CDCl_3$), see Table 2; (+)-ESIMS *m/z* 400.1 [M + $CH_3CN$ + H]$^+$, 717.2 [2 M + H]$^+$; (−)-ESIMS *m/z* 357.1 [M − H]$^-$, 403.1 [M + $HCO_2]^-$, 715.3 [2 M − H]$^-$, 761.3 [2 M + $HCO_2]^-$; (−)-HRESIMS *m/z* 357.1339 [M − H]$^-$ (calcd for $C_{20}H_{21}O_6$, 357.1338).

*Fortalide G* ***(7)***: white solid; $[\alpha]^{20}_D$ −127 (*c* 0.5 MeOH); UV (MeOH) $\lambda_{max}$ (log $\varepsilon$) 203 (3.72), 233 (3.40) nm; ECD (MeOH) $\lambda$ ($\Delta\varepsilon$) 208 (13.11), 237 (−16.26) nm; IR (KBr) $\nu_{max}$ 3589, 3375, 2958, 2929, 2884, 1767, 1731, 1627, 1458, 793 cm$^{-1}$; $^1$H and $^{13}$C NMR (methanol-$d_4$), see Table 3; (+)-ESIMS *m/z* 440.2 [M + $CH_3CN$ + Na]$^+$, 775.3 [2 M + Na]$^+$; (−)-ESIMS *m/z* 375.1 [M − H]$^-$, 421.2 [M + $HCO_2]^-$, 751.3 [2 M − H]$^-$; (−)-HRESIMS *m/z* 751.2969 [2 M − H]$^-$ (calcd for $C_{40}H_{47}O_{14}$, 751.2966).

*Fortalide H* ***(8)***: white solid; $[\alpha]^{19}_D$ −157 (*c* 0.2, MeOH); UV (MeOH) $\lambda_{max}$ (log $\varepsilon$) 204 (3.71), 235 (3.50) nm; ECD (MeOH) $\lambda$ ($\Delta\varepsilon$) 205 (19.01), 238 (−24.80) nm; IR (KBr) $\nu_{max}$ 3440, 2953, 2931, 2875, 1765, 1733 cm$^{-1}$; $^1$H and $^{13}$C NMR (methanol-$d_4$), see Table 3; (+)-ESIMS *m/z* 454.2 [M + $CH_3CN$ + Na]$^+$, 803.3 [2 M + Na]$^+$; (−)-ESIMS *m/z* 435.2 [M + $HCO_2]^-$, 825.3 [2 M + $HCO_2]^-$; (−)-HRESIMS *m/z* 435.1660 [M + $HCO_2]^-$ (calcd for $C_{22}H_{27}O_9$, 435.1655).

*Fortalide I* ***(9)***: white solid; $[\alpha]^{20}_D$ −93 (*c* 0.1, MeOH); UV (MeOH) $\lambda_{max}$ (log $\varepsilon$) 231 (3.40) nm; ECD (MeOH) $\lambda$ ($\Delta\varepsilon$) 206 (13.61), 236 (−13.57) nm; IR (KBr) $\nu_{max}$ 3433, 2927, 2855, 1750, 1626, 1453, 1370, 735 cm$^{-1}$; $^1$H and $^{13}$C NMR (methanol-$d_4$), see Table 3; (+)-ESIMS *m/z* 769.9 [2 M + $NH_4]^+$; (−)-ESIMS *m/z* 375.0 [M − H]$^-$, 751.1 [2 M − H]$^-$; (−)-HRESIMS *m/z* 375.1447 [M − H]$^-$ (calcd for $C_{20}H_{23}O_7$, 375.1449).

*Fortalide J* ***(10)***: colorless crystals; mp 244–246 °C; $[\alpha]^{20}_D$ −290 (*c* 0.2, MeOH); UV (MeOH) $\lambda_{max}$ (log $\varepsilon$) 220 (3.90), 254 (3.99) nm; ECD (MeOH) $\lambda$ ($\Delta\varepsilon$) 221 (30.62), 254 (−38.32) nm; IR (KBr) $\nu_{max}$ 3422, 2928, 2878, 2852, 1750, 1682, 1452 cm$^{-1}$; $^1$H and $^{13}$C NMR (methanol-$d_4$)see Table 4; (+)-ESIMS *m/z* 422.2 [M + $CH_3CN$ + Na]$^+$,

717.3 [2 M + H]$^+$, 739.3 [2 M + Na]$^+$, 1097.4 [3 M + Na]$^+$; (−)-ESIMS *m/z* 357.1 [M − H]$^-$, 403.1 [M + $HCO_2$]$^-$, 715.3 [2 M − H]$^-$, 761.3 [2 M + $HCO_2$]$^-$; (−)-HRESIMS *m/z* 403.1397 [M + $HCO_2$]$^-$ (calcd for $C_{21}H_{23}O_8$, 403.1393).

*Fortalide K* ***(11)***: white solid; [$\alpha$]$^{19}_D$ −182 (*c* 0.1, MeOH); UV (MeOH) $\lambda_{max}$ (log $\varepsilon$) 220 (3.77), 253 (3.82) nm; ECD (MeOH) $\lambda$ ($\Delta\varepsilon$) 220 (16.21), 252 (−20.30) nm; IR (KBr) $\nu_{max}$ 3445, 2926, 2875, 2855, 1761, 1747, 1452, 737 cm$^{-1}$; $^1$H and $^{13}$C NMR ($CDCl_3$) see Table 4; (+)-ESIMS *m/z* 406.2 [M + $CH_3CN$ + Na]$^+$, 707.3 [2 M + Na]$^+$, 1097.4 [3 M + Na]$^+$; (−)-ESIMS *m/z* 387.1 [M + $HCO_2$]$^-$, 729.3 [2 M + $HCO_2$]$^-$; (+)-HRESIMS *m/z* 707.2835 [2 M + Na]$^+$ (calcd for $C_{40}H_{44}O_{10}Na$, 707.2832).

*Fortalide L* ***(12)***: white solid; [$\alpha$]$^{20}_D$ −90 (*c* 0.2, MeOH); ECD (MeOH) $\lambda$ ($\Delta\varepsilon$) 216, (2.18) nm; IR (KBr) $\nu_{max}$ 3505, 2982, 2946, 2852, 1738, 1454, 1188 cm$^{-1}$; $^1$H and $^{13}$C NMR ($CDCl_3$), see Table 5; (+)-ESIMS *m/z* 408.2 [M + $CH_3CN$ + Na]$^+$, 689.3 [2 M + H]$^+$, 711.3 [2 M + Na]$^+$, 1055.5 [3 M + Na]$^+$; (+)-HRESIMS *m/z* 711.3155 [2 M + Na]$^+$ (calcd for $C_{40}H_{48}O_{10}Na$, 711.3145).

*Fortalide M* ***(13)***: white solid; [$\alpha$]$^{20}_D$ −49 (*c* 0.1, MeOH); ECD (MeOH) $\lambda$ ($\Delta\varepsilon$) 218 (2.48) nm; IR (KBr) $\nu_{max}$ 3431, 3390, 3334, 2935, 1758, 1739, 1456, 1042, 1019, 1002 cm$^{-1}$; $^1$H and $^{13}$C NMR (pyridine-$d_5$), see Table 5; (+)-ESIMS *m/z* 439.9 [M + $CH_3CN$ + Na]$^+$, 775.1 [2 M + Na]$^+$; (−)-ESIMS *m/z* 375.0 [M − H]$^-$, 751.2 [2 M − H]$^-$; (−)-HRESIMS *m/z* 421.1499 [M + $HCO_2$]$^-$ (calcd for $C_{21}H_{25}O_9$, 421.1504).

*Fortalide N* ***(14)***: colorless crystals; mp 260–262 °C; [$\alpha$]$^{19}_D$ −61 (*c* 0.2, pyridine); IR (KBr) $\nu_{max}$ 3553, 3431, 2962, 2940, 2884, 1773, 1729, 1465, 1123, 1098, 1071, 1010, 986 cm$^{-1}$; $^1$H NMR and $^{13}$C NMR (pyridine-$d_5$), see Table 6; (+)-ESIMS *m/z* 440.2 [M + $CH_3CN$ + Na]$^+$, 775.3 [2 M + Na]$^+$; (−)-ESIMS *m/z* 421.2 [M + $HCO_2$]$^-$; (−)-HRESIMS *m/z* 421.1505 [M + $HCO_2$]$^-$ (calcd for $C_{21}H_{25}O_9$, 421.1499).

*Fortalide O* ***(15)***: colorless crystals; mp 267–269 °C; [$\alpha$]$^{19}_D$ −16 (*c* 0.1, pyridine); IR (KBr) $\nu_{max}$ 3495, 2968, 2938, 2920, 1780, 1742, 1456, 1349, 1242, 1185, 1068, 1048, 1004, 965 cm$^{-1}$; $^1$H and $^{13}$C NMR (pyridine-$d_5$), see Table 6; (−)-ESIMS *m/z* 375.1 [M − H]$^-$, 751.2 [2 M − H]$^-$; (−)-HRESIMS *m/z* 421.1505 [M + $HCO_2$]$^-$ (calcd for $C_{21}H_{25}O_9$, 421.1499).

*Fortalide P* ***(16)***: white solid; [$\alpha$]$^{19}_D$ −9 (*c* 0.1, MeOH); UV (MeOH) $\lambda_{max}$ (log $\varepsilon$)

241 (3.68) nm; ECD (MeOH) $\lambda$ ($\Delta\varepsilon$) 241 (7.83), 326 (−2.36) nm; IR (KBr) $\nu_{max}$ 3514, 2963, 2920, 2874, 1737, 1652, 1617, 1447, 1371, 1062, 987 $cm^{-1}$; $^{1}H$ and $^{13}C$ NMR ($CDCl_3$), see Table 7; (+)-ESIMS *m/z* 394.2 $[M + CH_3CN + Na]^+$, 683.4 $[2\ M + Na]^+$, 1013.5 $[3\ M + Na]^+$; (+)-HRESIMS *m/z* 683.3564 $[2\ M + Na]^+$ (calcd for $C_{40}H_{52}O_8Na$, 683.3560).

*Fortalide Q* ***(17)***: white solid; $[\alpha]^{20}_D$ −14 (*c* 0.1, MeOH); UV (MeOH) $\lambda_{max}$ (log $\varepsilon$) 240 (3.86) nm; ECD (MeOH) $\lambda$ ($\Delta\varepsilon$) 241 (10.38), 326 (−3.29) nm; IR (KBr) $\nu_{max}$ 3429, 2926, 2875, 1742, 1652, 1450, 1378, 1063, 1029, 738, 701 $cm^{-1}$; $^{1}H$ and $^{13}C$ NMR (methanol-$d_4$), see Table 7; (+)-ESIMS *m/z* 410.2 $[M + CH_3CN + Na]^+$, 715.3 $[2\ M + Na]^+$; (−)-ESIMS *m/z* 345.2 $[M - H]^-$, 391.2 $[M + HCO_2]^-$, 737.4 $[2\ M + HCO_2]^-$; (−)-HRESIMS *m/z* 391.1762 $[M + HCO_2]^-$ (calcd for $C_{21}H_{27}O_7$, 391.1757).

**Supplementary Physical and Spectroscopic Data for Compounds 18, 19, 21 and 22**

*Mannolide A* ***(18)****:* white solid; $[\alpha]^{19.1}_D$ −11 (*c* 0.4, MeOH); ECD (MeOH) $\lambda$ ($\Delta\varepsilon$) 215 (4.50) nm.

*Mannolide B* ***(19)****:* white solid; $[\alpha]^{19.1}_D$ +39 (*c* 0.4, MeOH); ECD (MeOH) $\lambda$ ($\Delta\varepsilon$) 205 (5.60) nm.

*Cephinoid B* ***(21)***: white solid; $^{1}H$ NMR (methanol-$d_4$, 500 MHz) $\delta$ 4.65 (1H, dd, *J* = 8.0, 0.7 Hz), 4.60 (1H, td, *J* = 4.6, 1.2 Hz), 3.98 (1H, s), 3.03 (1H, ddd, *J* = 11.0, 3.8, 1.6 Hz), 2.98 (1H, ddd, *J* = 18.2, 10.5, 1.6 Hz), 2.81 (1H, d, *J* = 13.2 Hz), 2.75 (1H, ttd, *J* = 11.0, 10.5, 4.6, 3.8, 1.8 Hz), 2.44 (1H, dt, *J* = 18.1, 3.8 Hz), 2.31 (1H, ddd, *J* = 13.2, 8.0, 0.7 Hz), 2.25 (1H, ddd, *J* = 14.0, 10.4, 1.2 Hz), 2.18 (1H, dqd, *J* = 10.4, 6.8, 4.3 Hz), 2.02–1.94 (2H, m), 1.89 (1H, ddd, *J* = 14.7, 4.8, 2.8 Hz), 1.61 (1H, ddd, *J* = 14.7, 11.4, 7.8 Hz), 1.54 (3H, s), 1.42 (1H, dtd, *J* = 14.0, 4.4, 1.8 Hz), 0.88 (3H, d, *J* = 6.8 Hz); $^{13}C$ NMR (methanol-$d_4$, 126 MHz) $\delta$ 18.9, 24.4, 24.8, 27.1, 27.4, 30.5, 35.7, 36.5, 36.6, 46.1, 46.2, 53.6, 77.0, 80.2, 81.7, 83.6, 130.7, 146.0, 178.4, 178.9. The reported NMR data for Cephinoid B[1] were actually recorded in methanol-$d_4$, despite that it was incorrectly written as DMSO-$d_6$ in the experimental section.

*Cephinoid A* ***(22)***: colorless crystals; its $^{1}H$ and $^{13}C$ NMR data (DMSO-$d_6$) were consistent with the reported values.[1] Here are supplementary 1D NMR data recorded

in pyridine-$d_5$: $^1$H NMR (500 MHz) $\delta$ 7.44 (1H, s), 6.40 (1H, s), 5.14 (1H, d, $J$ = 8.0 Hz), 4.75 (1H, s), 4.69 (1H, t, $J$ = 4.1 Hz), 4.05 (1H, t, $J$ = 5.0, 4.0 Hz), 3.87 (1H, dt, $J$ = 17.6, 4.1 Hz), 3.47 (1H, dd, $J$ = 11.3, 3.4 Hz), 3.30 (1H, dd, $J$ = 17.5, 11.1 Hz), 3.08 (1H, d, $J$ = 12.8 Hz), 2.82 (1H, ttd, $J$ = 11.0, 4.4, 1.7 Hz), 2.51 (1H, td, $J$ = 13.9, 5.2 Hz), 2.40 (1H, p, $J$ = 7.1, 5.5 Hz), 2.34 (1H, dd, $J$ = 12.9, 8.1 Hz), 2.19 (1H, ddd, $J$ = 14.0, 5.4, 2.0 Hz), 2.07 (2H, s), 2.03 (1H, ddd, $J$ = 14.6, 5.2, 2.1 Hz), 1.69 (1H, td, $J$ = 14.2, 5.4 Hz), 1.11 (2H, d, $J$ = 7.1 Hz); $^{13}$C NMR (126 MHz) $\delta$ 17.0, 25.1, 25.6, 27.7, 35.1, 35.7, 36.0, 36.7, 45.6, 45.7, 53.5, 76.7, 77.0, 79.8, 82.2, 83.8, 128.2, 148.2, 176.6, 177.3; $^1$H NMR (methanol-$d_4$, 400 MHz) $\delta$ 4.65 (1H, d, $J$ = 8.0 Hz), 4.46 (1H, t, $J$ = 4.0 Hz), 3.98 (1H, s), 3.61 (1H, ddd, $J$ = 5.4, 3.8, 1.5 Hz), 3.25 (1H, dt, $J$ = 17.0, 3.3 Hz), 3.05 (1H, ddd, $J$ = 11.1, 3.6, 2.1 Hz), 2.88 (1H, ddd, $J$ = 17.0, 11.0, 2.0 Hz), 2.86–2.72 (1H, m), 2.80 (1H, d, $J$ = 13.1 Hz), 2.33 (1H, dd, $J$ = 13.1, 8.1 Hz), 2.04–1.77 (4H, m), 1.58 (1H, ddd, $J$ = 14.4, 13.1, 6.0 Hz), 1.51 (3H, s), 0.98 (3H, d, $J$ = 7.1 Hz).

**X-ray Crystallographic Analysis for Compounds 3, 4, 10, 14, and 15**

The crystal data were collected on a Bruker APEX-II CCD detector, employing a Ga-K$\alpha$ radiation ($\lambda$ = 1.34139 Å) for compounds **5**, **14** and **15** or a Cu-K$\alpha$ radiation ($\lambda$ = 1.54178 Å) for compound **10**, except that the data of compound **3** were obtained on a Bruker D8 Venture diffractometer with a Ga-K$\alpha$ radiation ($\lambda$ = 1.34139 Å). Using Olex2[2], the structures were solved with the ShelXT[3] structure solution program using Intrinsic Phasing and refined with the ShelXL[4] refinement package using Least Squares minimization.

The corresponding crystal data are included in Tables S1–S5†. The crystallographic data have been deposited at the Cambridge Crystallographic Data Center with deposition numbers CCDC 2205171 (**3**), 2205172 (**4**), 2205173 (**10**), 2205175 (**14**), and 2205176 (**15**).

**Table S1**. X-ray Crystallographic Data for Fortalide C (**3**)[a]

| | |
|---|---|
| Empirical formula | $C_{20}$ $H_{22}$ $O_6$ |
| Formula weight | 358.37 |
| Temperature | 303.3 K |
| Wavelength | 1.34139 Å |
| Crystal system | Orthorhombic |
| Space group | $P2_12_12_1$ |
| Unit cell dimensions | a = 7.8681(4) Å, $\alpha$ = 90°. |
| | b = 11.4609(5) Å, $\beta$ = 90°. |
| | c = 18.4466(9) Å, $\gamma$ = 90°. |
| Volume | 1663.43(14) $Å^3$ |
| Z | 4 |
| Density (calculated) | 1.431 $Mg/m^3$ |
| Absorption coefficient | 0.561 $mm^{-1}$ |
| F(000) | 760 |
| Crystal size | 0.15 x 0.12 x 0.08 $mm^3$ |
| Theta range for data collection | 6.433 to 57.057°. |
| Index ranges | -9<=h<=9, -14<=k<=14, -20<=l<=23 |
| Reflections collected | 17749 |
| Independent reflections | 3328 [R(int) = 0.0378] |
| Completeness to theta = 53.594° | 97.1 % |
| Absorption correction | Semi-empirical from equivalents |
| Max. and min. transmission | 0.7512 and 0.5370 |
| Refinement method | Full-matrix least-squares on $F^2$ |
| Data / restraints / parameters | 3328 / 0 / 238 |
| Goodness-of-fit on $F^2$ | 1.033 |
| Final R indices [I>2sigma(I)] | R1 = 0.0342, wR2 = 0.0915 |
| R indices (all data) | R1 = 0.0351, wR2 = 0.0924 |
| Absolute structure parameter | 0.00(6) |
| Extinction coefficient | n/a |
| Largest diff. peak and hole | 0.314 and -0.287 $e.Å^{-3}$ |

[a]Crystals of **1** were obtained from methanol.

**Table S2**. X-ray Crystallographic Data for Fortalide D (**4**)[a]

| | |
|---|---|
| Empirical formula | $C_{20}H_{30}O_9$ |
| Formula weight | 414.44 |
| Temperature | 169.97 K |
| Wavelength | 1.34139 Å |
| Crystal system | Orthorhombic |
| Space group | $P2_12_12_1$ |
| Unit cell dimensions | a = 8.4147(2) Å a= 90° |
| | b = 10.9726(2) Å b= 90° |
| | c = 21.0590(4) Å g = 90° |
| Volume | 1944.40(7) $Å^3$ |
| Z | 4 |
| Density (calculated) | 1.416 $Mg/m^3$ |
| Absorption coefficient | 0.601 $mm^{-1}$ |
| F(000) | 888 |
| Crystal size | 0.12 x 0.1 x 0.05 $mm^3$ |
| Theta range for data collection | 6.831 to 54.872° |
| Index ranges | -10<=h<=10, -13<=k<=13, -24<=l<=25 |
| Reflections collected | 12965 |
| Independent reflections | 3653 [R(int) = 0.0373] |
| Completeness to theta = 53.594° | 98.8 % |
| Absorption correction | Semi-empirical from equivalents |
| Max. and min. transmission | 0.7508 and 0.5732 |
| Refinement method | Full-matrix least-squares on $F^2$ |
| Data / restraints / parameters | 3653 / 0 / 293 |
| Goodness-of-fit on $F^2$ | 1.064 |
| Final R indices [I>2sigma(I)] | R1 = 0.0308, wR2 = 0.0781 |
| R indices (all data) | R1 = 0.0322, wR2 = 0.0796 |
| Absolute structure parameter | 0.04(9) |
| Extinction coefficient | n/a |
| Largest diff. peak and hole | 0.207 and -0.239 e.$Å^{-3}$ |

[a]Crystals of **4** were crystallized from methanol.

**Table S3**. X-ray Crystallographic Data for Fortalide J (**10**)[a]

| | |
|---|---|
| Empirical formula | $C_{20}H_4O_7$ |
| Formula weight | 376.39 |
| Temperature | 173(2) K |
| Wavelength | 1.54178 Å |
| Crystal system | Monoclinic |
| Space group | P21 |
| Unit cell dimensions | a = 8.9073(2) Å a= 90° |
| | b = 10.3176(2) Å b= 98.1510(10)° |
| | c = 19.2439(4) Å g = 90° |
| Volume | 1750.69(6) $Å^3$ |
| Z | 4 |
| Density (calculated) | 1.428 $Mg/m^3$ |
| Absorption coefficient | 0.901 $mm^{-1}$ |
| F(000) | 800 |
| Crystal size | 0.180 x 0.150 x 0.120 $mm^3$ |
| Theta range for data collection | 4.642 to 67.000°. |
| Index ranges | -10<=h<=10, -12<=k<=12, -22<=l<=22 |
| Reflections collected | 29243 |
| Independent reflections | 6175 [R(int) = 0.0364] |
| Completeness to theta = 67.679° | 97.7 % |
| Absorption correction | Semi-empirical from equivalents |
| Max. and min. transmission | 0.7456 and 0.5492 |
| Refinement method | Full-matrix least-squares on $F^2$ |
| Data / restraints / parameters | 6175 / 5 / 494 |
| Goodness-of-fit on $F^2$ | 1.084 |
| Final R indices [I>2sigma(I)] | R1 = 0.0370, wR2 = 0.1007 |
| R indices (all data) | R1 = 0.0376, wR2 = 0.1015 |
| Absolute structure parameter | 0.04(4) |
| Extinction coefficient | 0.0089(13) |
| Largest diff. peak and hole | 0.661 and -0.346 $e.Å^{-3}$ |

[a]Crystals of **10** were crystallized from methanol.

**Table S4**. X-ray Crystallographic Data for Fortalide N (**14**)[a]

| | |
|---|---|
| Empirical formula | $C_{20}H_{24}O_7$ |
| Formula weight | 376.39 |
| Temperature | 169.97 K |
| Wavelength | 1.34139 Å |
| Crystal system | Monoclinic |
| Space group | P 1 21 1 |
| Unit cell dimensions | a = 6.5730(2) Å a= 90° |
| | b = 14.9361(4) Å b= 91.5960(10)° |
| | c = 8.6462(2) Å g = 90°. |
| Volume | 848.51(4) $Å^3$ |
| Z | 2 |
| Density (calculated) | 1.473 $Mg/m^3$ |
| Absorption coefficient | 0.596 $mm^{-1}$ |
| F(000) | 400 |
| Crystal size | 0.15 x 0.12 x 0.1 $mm^3$ |
| Theta range for data collection | 4.451 to 54.899°. |
| Index ranges | -8<=h<=8, -18<=k<=18, -10<=l<=10 |
| Reflections collected | 10525 |
| Independent reflections | 3199 [R(int) = 0.0413] |
| Completeness to theta = 53.594° | 99.7 % |
| Absorption correction | Semi-empirical from equivalents |
| Max. and min. transmission | 0.7508 and 0.5846 |
| Refinement method | Full-matrix least-squares on $F^2$ |
| Data / restraints / parameters | 3199 / 1 / 251 |
| Goodness-of-fit on $F^2$ | 1.052 |
| Final R indices [I>2sigma(I)] | R1 = 0.0295, wR2 = 0.0724 |
| R indices (all data) | R1 = 0.0320, wR2 = 0.0744 |
| Absolute structure parameter | -0.07(9) |
| Extinction coefficient | n/a |
| Largest diff. peak and hole | 0.199 and -0.176 $e.Å^{-3}$ |

[a]Crystals of **14** were crystallized from methanol/chloroform.

**Table S5**. X-ray Crystallographic Data for Fortalide O (**15**)[a]

| | |
|---|---|
| Empirical formula | $C_{20}H_{24}O_7$ |
| Formula weight | 376.39 |
| Temperature | 170.02 K |
| Wavelength | 1.34139 Å |
| Crystal system | Orthorhombic |
| Space group | $P2_12_12_1$ |
| Unit cell dimensions | a = 6.7694(2) Å a= 90° |
| | b = 14.5049(4) Å b= 90°. |
| | c = 16.9906(5) Å g = 90°. |
| Volume | 1668.30(8) $Å^3$ |
| Z | 4 |
| Density (calculated) | 1.499 $Mg/m^3$ |
| Absorption coefficient | 0.606 $mm^{-1}$ |
| F(000) | 800 |
| Crystal size | 0.08 x 0.06 x 0.03 $mm^3$ |
| Theta range for data collection | 3.486 to 54.859°. |
| Index ranges | -7<=h<=8, -17<=k<=17, -20<=l<=20 |
| Reflections collected | 18448 |
| Independent reflections | 3173 [R(int) = 0.0476] |
| Completeness to theta = 53.594° | 99.9 % |
| Absorption correction | Semi-empirical from equivalents |
| Max. and min. transmission | 0.7508 and 0.5808 |
| Refinement method | Full-matrix least-squares on $F^2$ |
| Data / restraints / parameters | 3173 / 0 / 248 |
| Goodness-of-fit on $F^2$ | 1.044 |
| Final R indices [I>2sigma(I)] | R1 = 0.0258, wR2 = 0.0661 |
| R indices (all data) | R1 = 0.0266, wR2 = 0.0665 |
| Absolute structure parameter | 0.01(7) |
| Extinction coefficient | n/a |
| Largest diff. peak and hole | 0.238 and -0.161 $e.Å^{-3}$ |

[a]Crystals of **15** were crystallized from methanol/pyridine.

## Antiplasmodial bioassay

The antiplasmodial activity was measured using an SYBR-Green I assay against *Plasmodium falciparum* strain Dd2 with artemisinin as the positive control according to the previously reported method.[5]

## References

(1) Ni, L.; Zhong, X. H.; Chen, X. J.; Zhang, B. J.; Bao, M. F.; Cai, X. H. *Phytochemistry.* **2018**, *151*, 50-60.

(2) Dolomanov, O.V., Bourhis, L.J., Gildea, R.J, Howard, J.A.K. & Puschmann, H. (2009), J. Appl. Cryst. 42, 339-341.

(3) Sheldrick, G.M. (2015). Acta Cryst. A71, 3-8.

(4) Sheldrick, G.M. (2015). Acta Cryst. C71, 3-8.

(5) (a) Zhou, B.; Wu, Y.; Gan, L.; Dalal, S.; Cassera, M. B.; Yue, J. *Chin J Chem* **2020**, *38*, 812–816. (b) Smilkstein, M.; Sriwilaijaroen, N.; Kelly, J. X.; Wilairat, P.; Riscoe, M. *Antimicrob Agents Chemother* **2004**, *48*, 1803–1806.

**Figure S21–S30.** 1D and 2D NMR, MS, and IR spectra of fortalide A (**1**)

**Figure S21**. $^{1}$H NMR spectrum of fortalide A (**1**) in pyridine-$d_5$

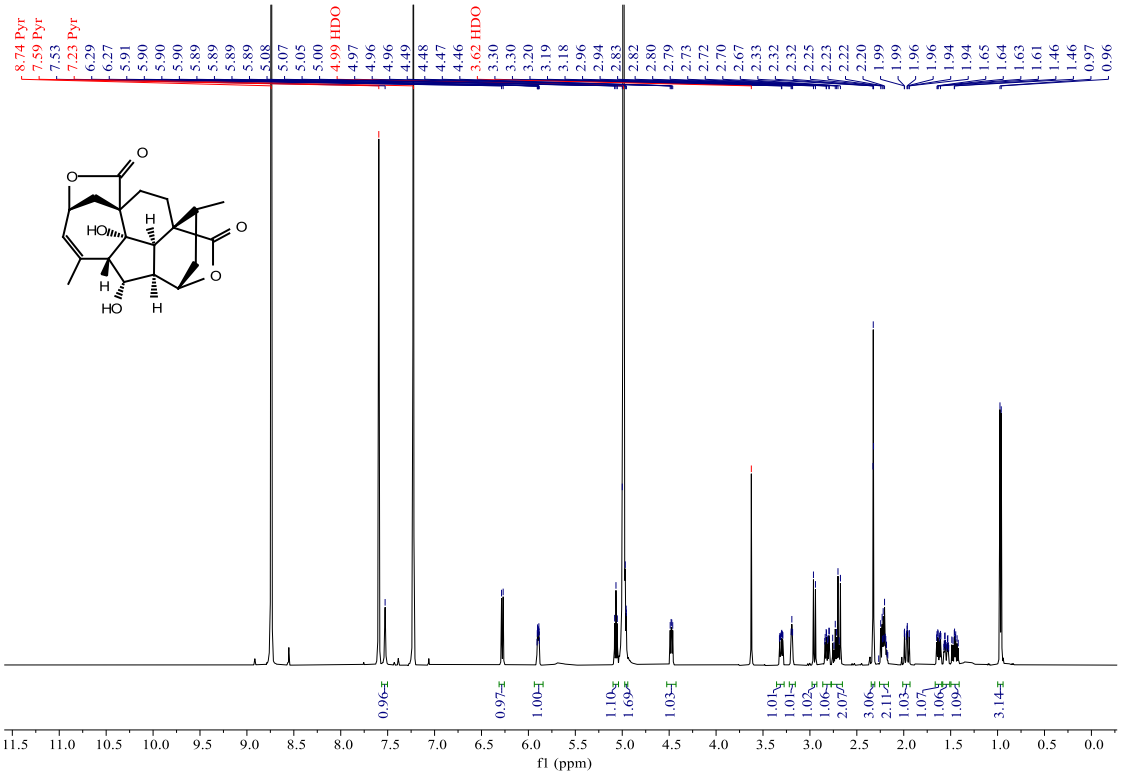


**Figure S22**. $^{13}$C NMR (BB and DEPT-135) spectra of fortalide A (**1**) in pyridine-$d_5$

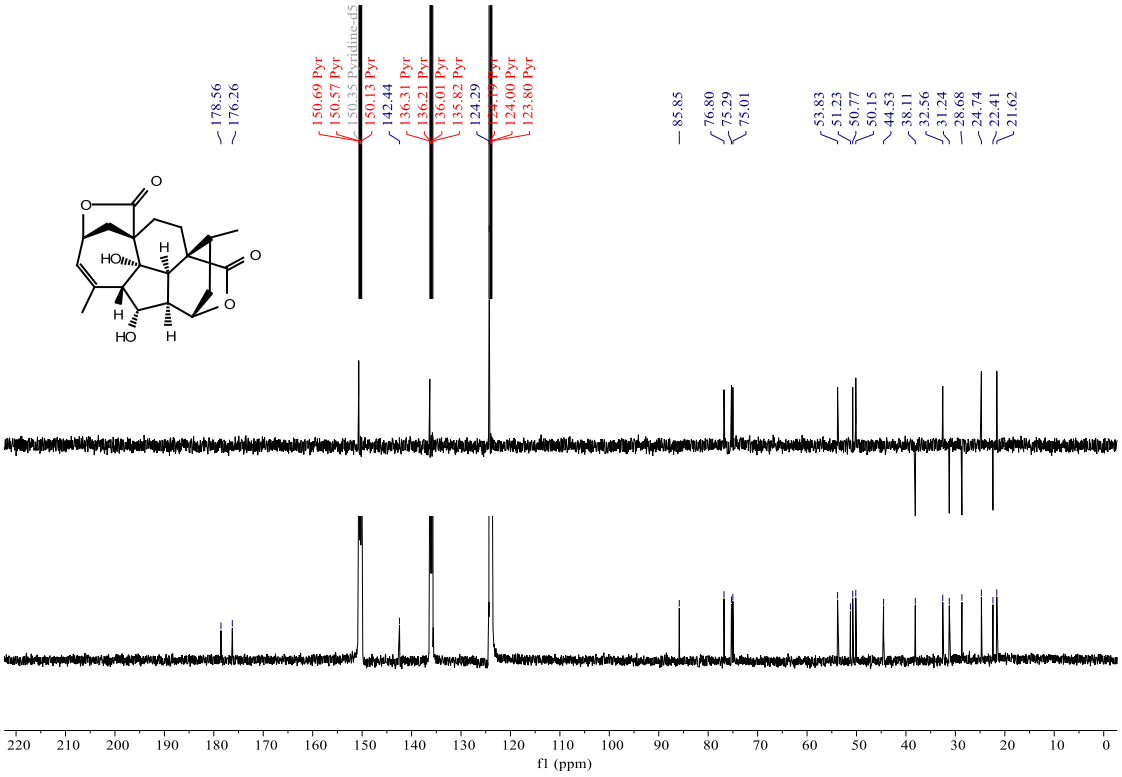

**Figure S23.** HSQC spectrum of fortalide A (**1**) in pyridine-$d_5$

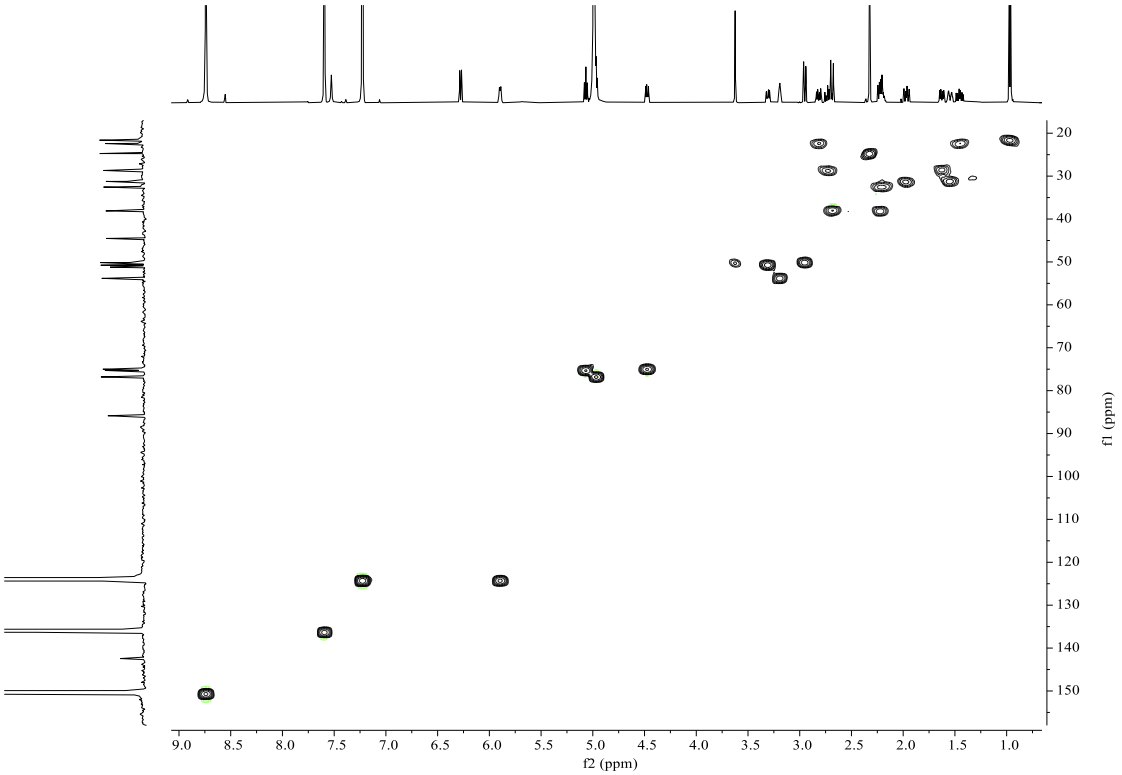


**Figure S24**. HMBC spectrum of fortalide A (**1**) in pyridine-$d_5$

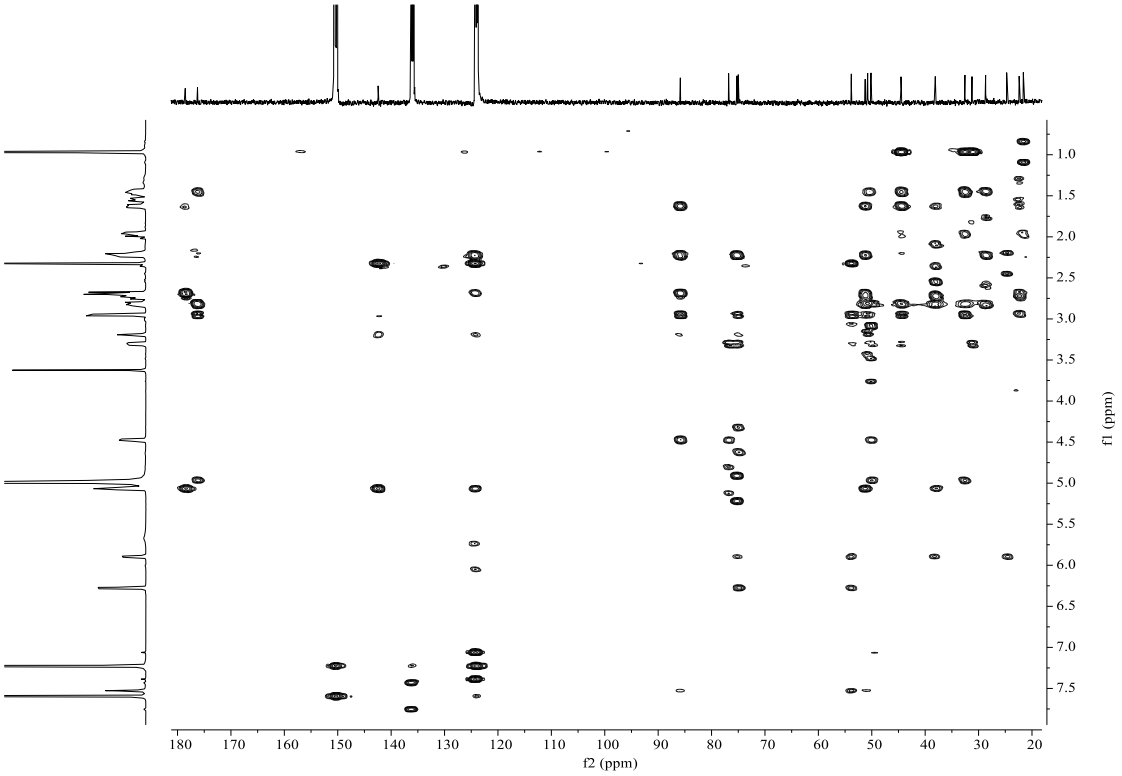

**Figure S25**. $^{1}$H-$^{1}$H COSY spectrum of fortalide A (**1**) in pyridine-$d_5$

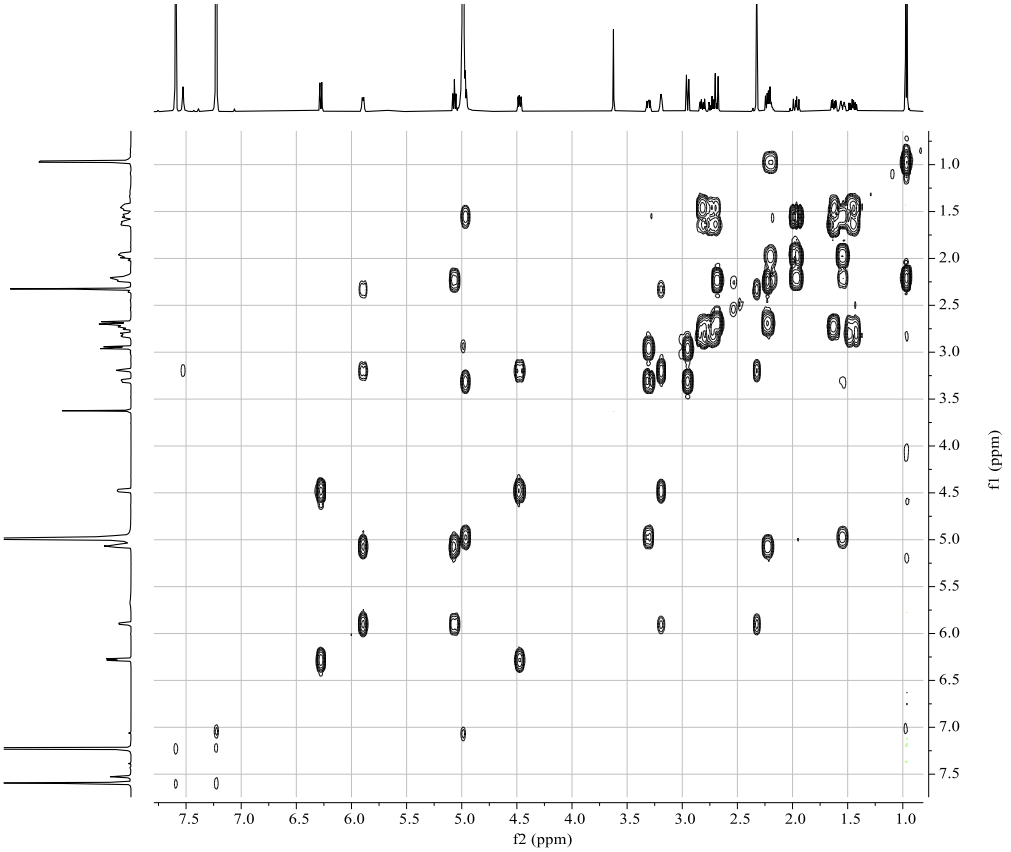


**Figure S26**. NOESY spectrum of fortalide A (**1**) in pyridine-$d_5$

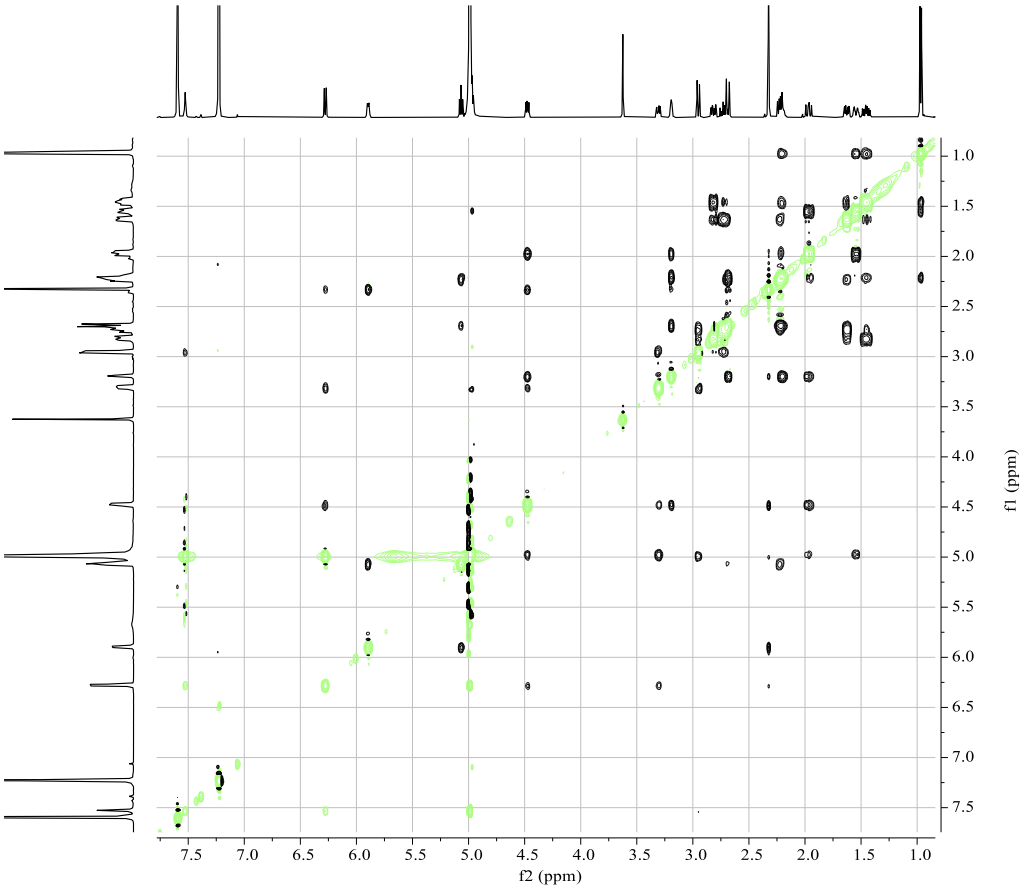

**Figure S27**. (+)-ESIMS spectrum of fortalide A (**1**)

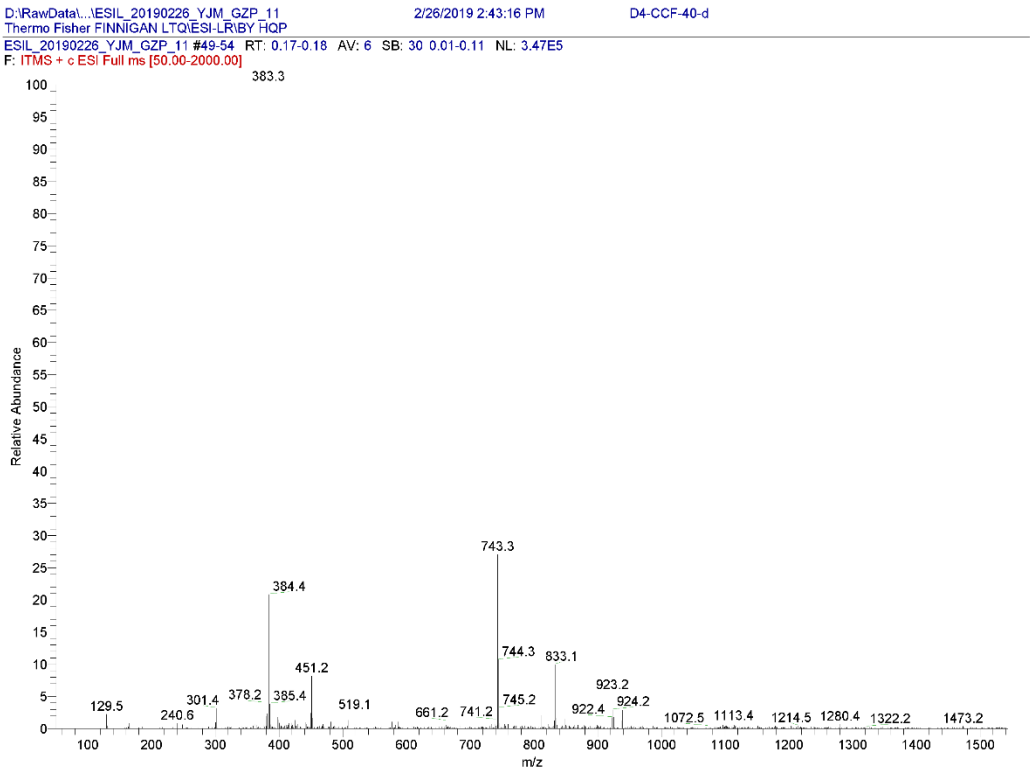


**Figure S28**. (−)-ESIMS spectrum of fortalide A (**1**)

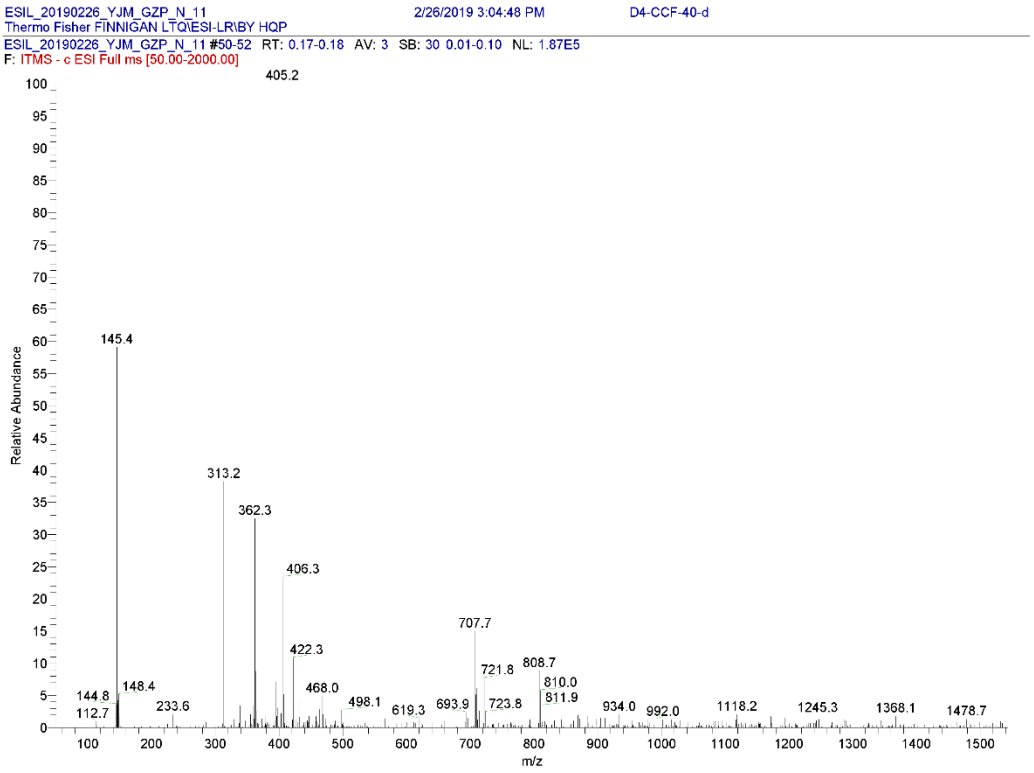

**Figure S29**. (+)-HRESIMS spectrum of fortalide A (**1**)

**Qualitative Analysis Report**

| | | | |
|---|---|---|---|
| **Data Filename** | ESIH_20190227_YJM_GZP_02.d | **Sample Name** | D4-CCF-40-d |
| **Sample Type** | Sample | **Position** | P1-B2 |
| **Instrument Name** | Agilent G6520 Q-TOF | **Acq Method** | 20160322_MS_ESIH_POS_1min.m |
| **Acquired Time** | 2/27/2019 9:30:07 | **IRM Calibration Status** | Success |
| **DA Method** | small molecular data analysis method.m | **Comment** | ESIH by ZZY |

**User Spectra**

| Fragmentor Voltage | Collision Energy | Ionization Mode |
|---|---|---|
| 30 | 0 | ESI |

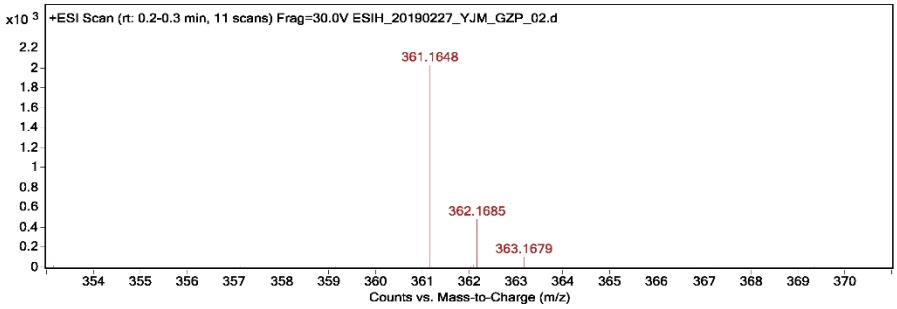


**Formula Calculator Results**

| m/z | Calc m/z | Diff (mDa) | Diff (ppm) | Ion Formula | Ion |
|---|---|---|---|---|---|
| 361.1648 | 361.1646 | -0.23 | -0.63 | C20 H25 O6 | (M+H)+ |

--- End Of Report ---

Agilent Technologies Page 1 of 1 Printed at: 9:43 on: 2/27/2019

**Figure S30**. IR spectrum of fortalide A (**1**)

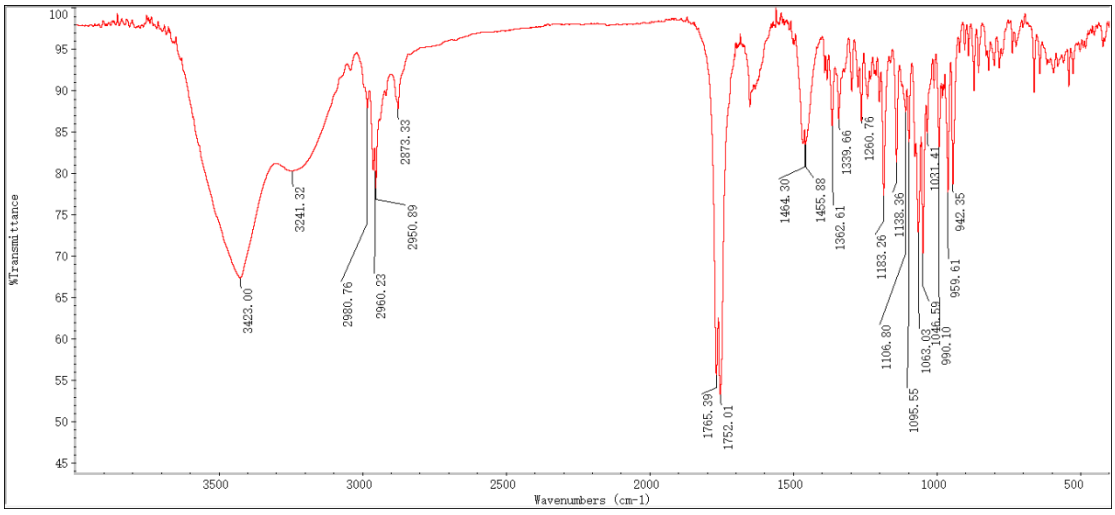

**Figure S31–S40.** 1D and 2D NMR, MS, and IR spectra of fortalide B (**2**)

**Figure S31**. $^{1}$H NMR spectrum of fortalide B (**2**) in pyridine-$d_5$

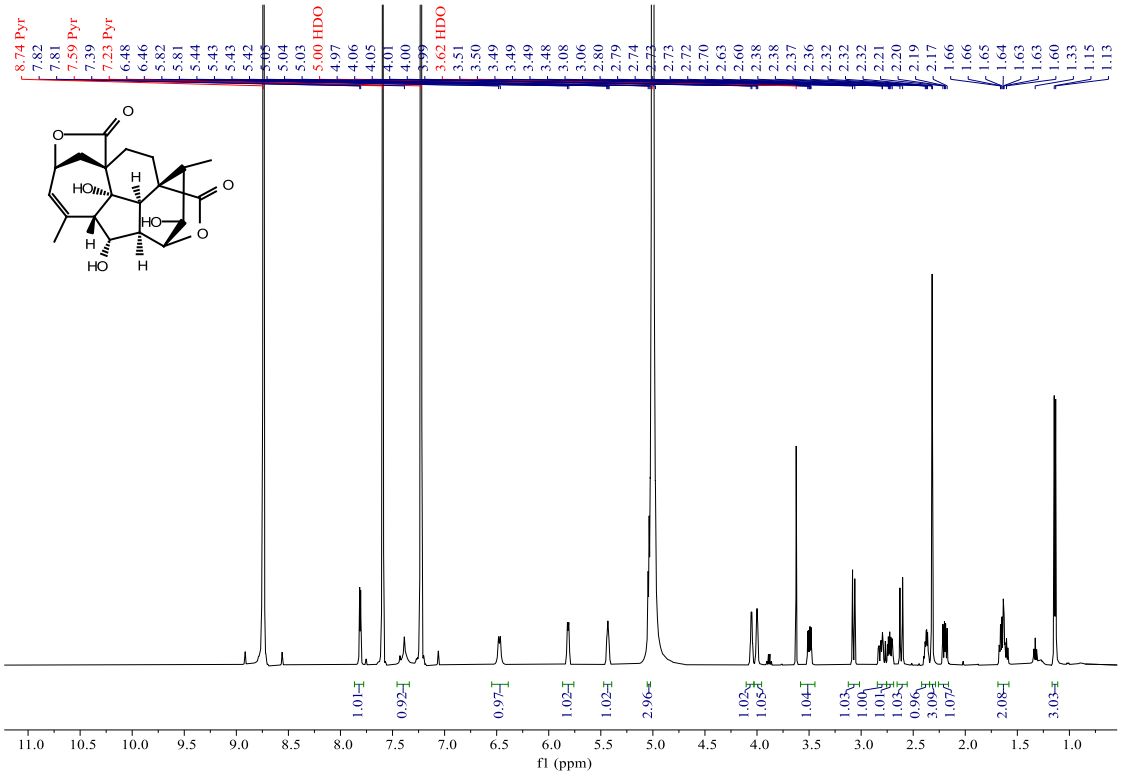


**Figure S32**. $^{13}$C NMR (BB and DEPT-135) spectra of fortalide B (**2**) in pyridine-$d_5$

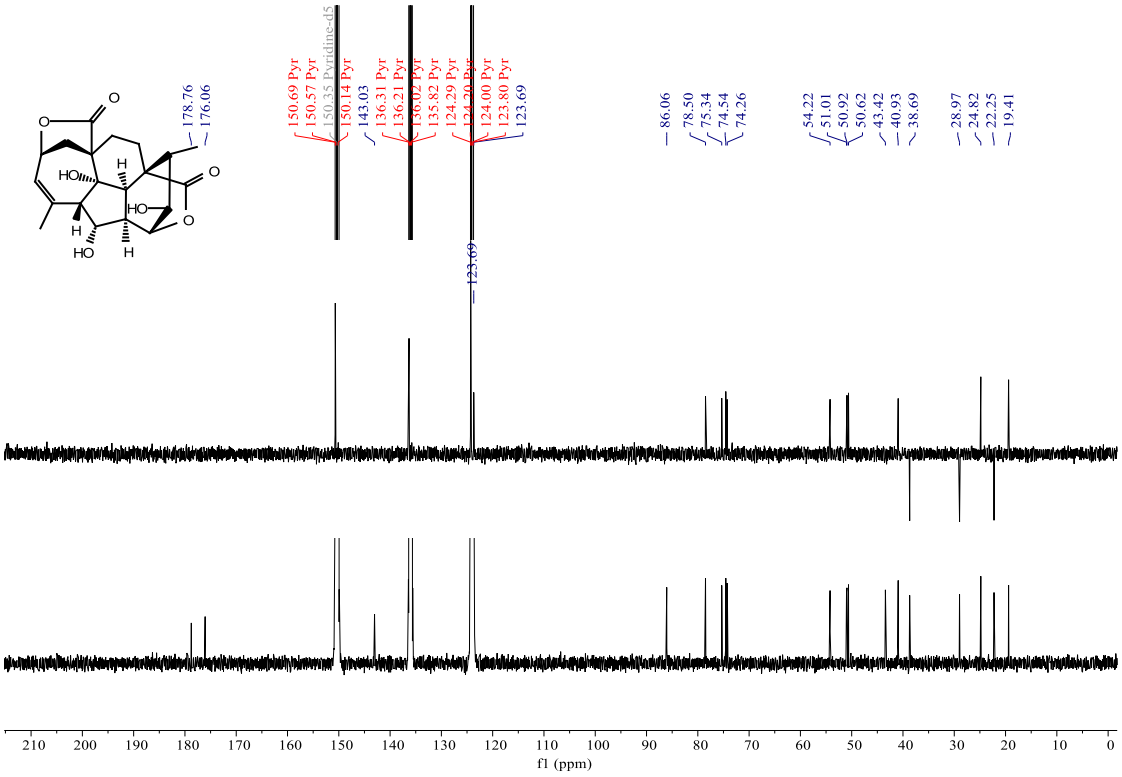

**Figure S33**. HSQC spectrum of fortalide B (**2**) in pyridine-$d_5$

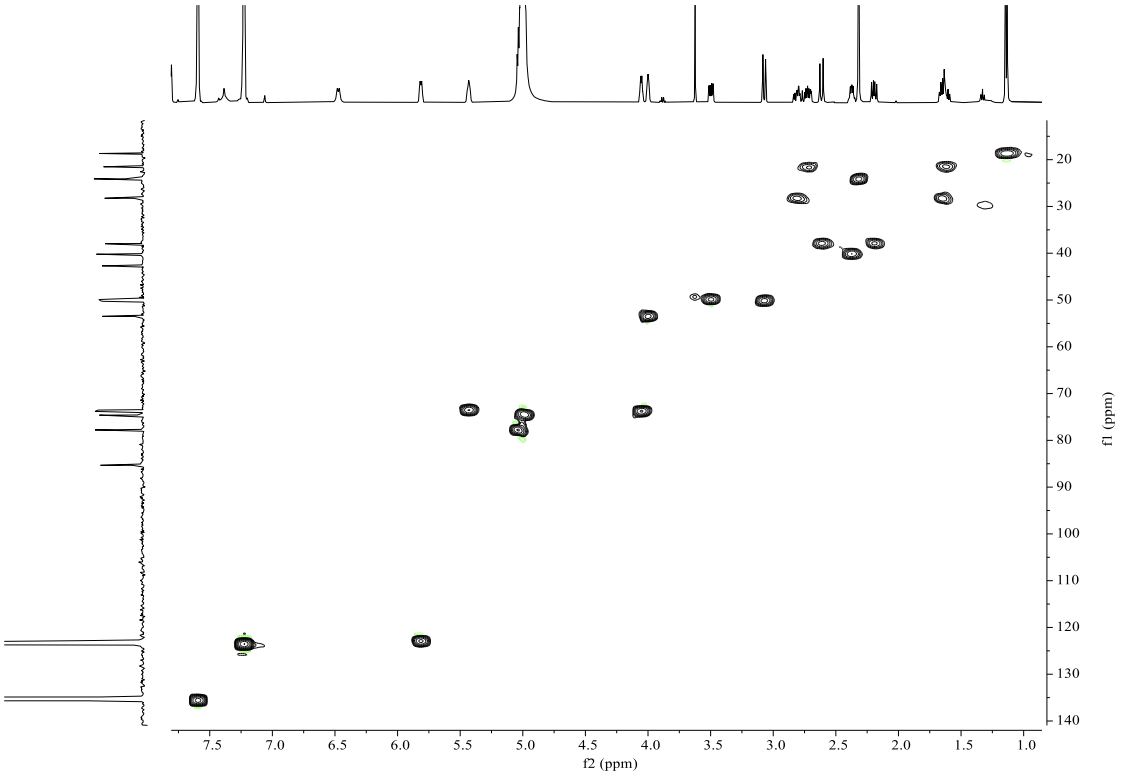


**Figure S34**. HMBC spectrum of fortalide B (**2**) in pyridine-$d_5$

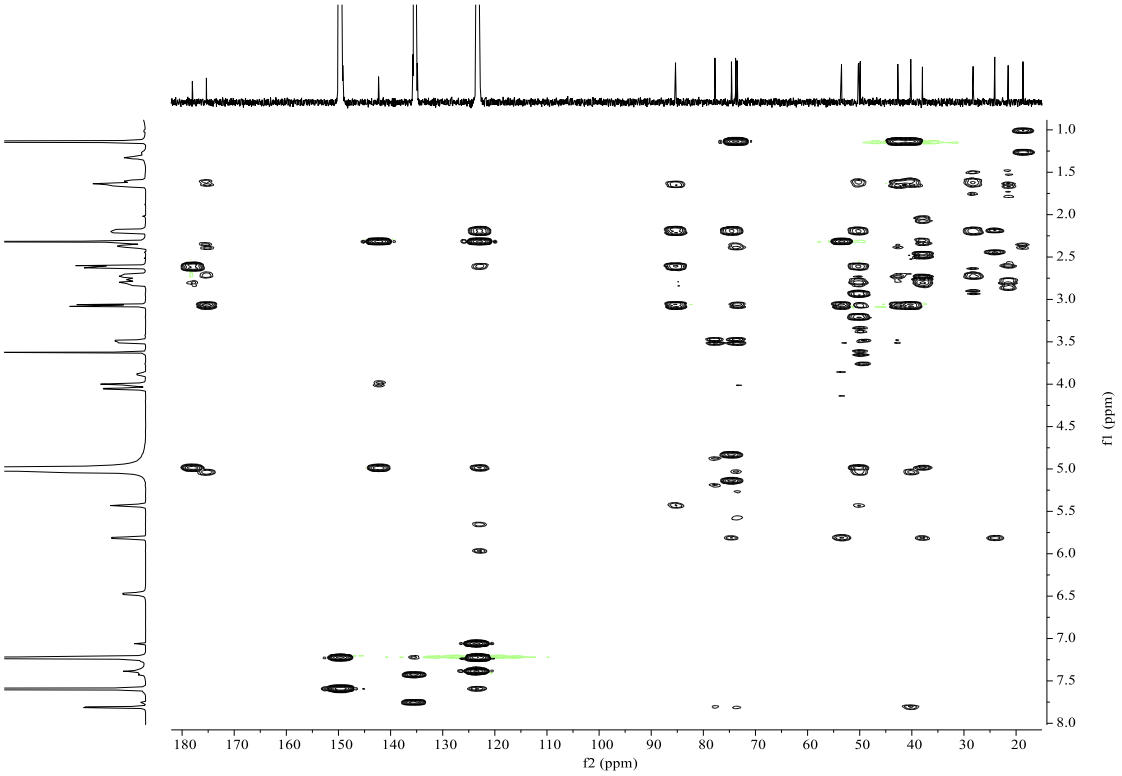

**Figure S35**. $^{1}$H-$^{1}$H COSY spectrum of fortalide B (**2**) in pyridine-$d_5$

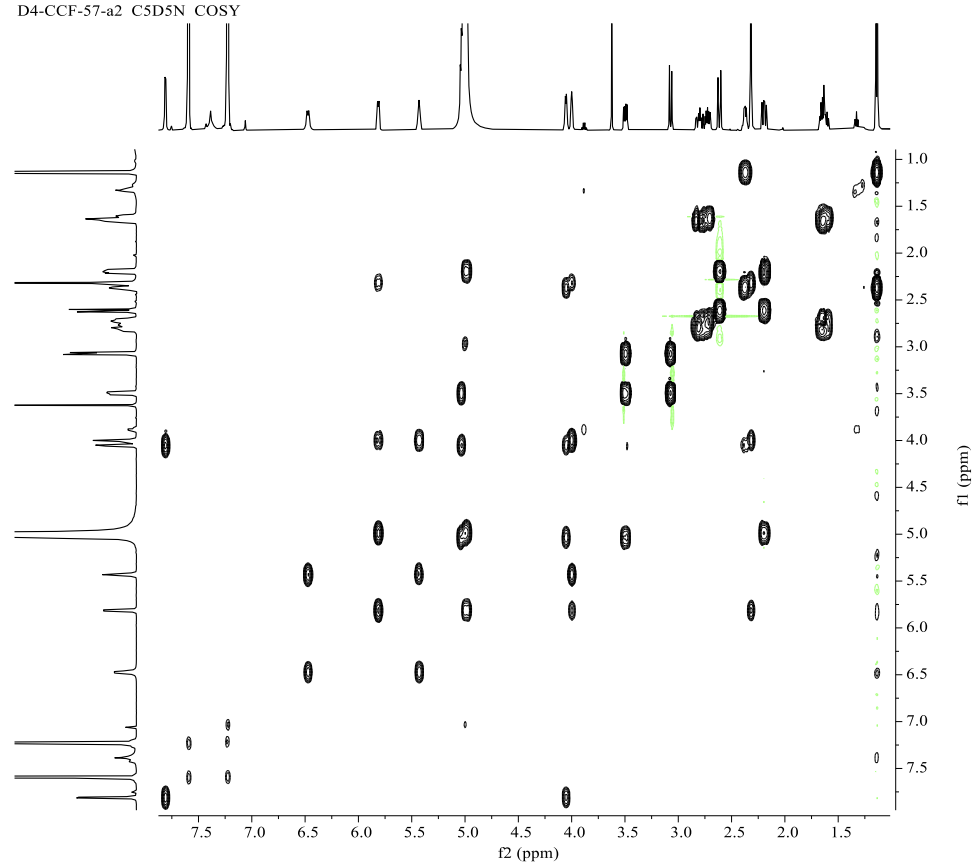


**Figure S36**. NOESY spectrum of fortalide B (**2**) in pyridine-$d_5$

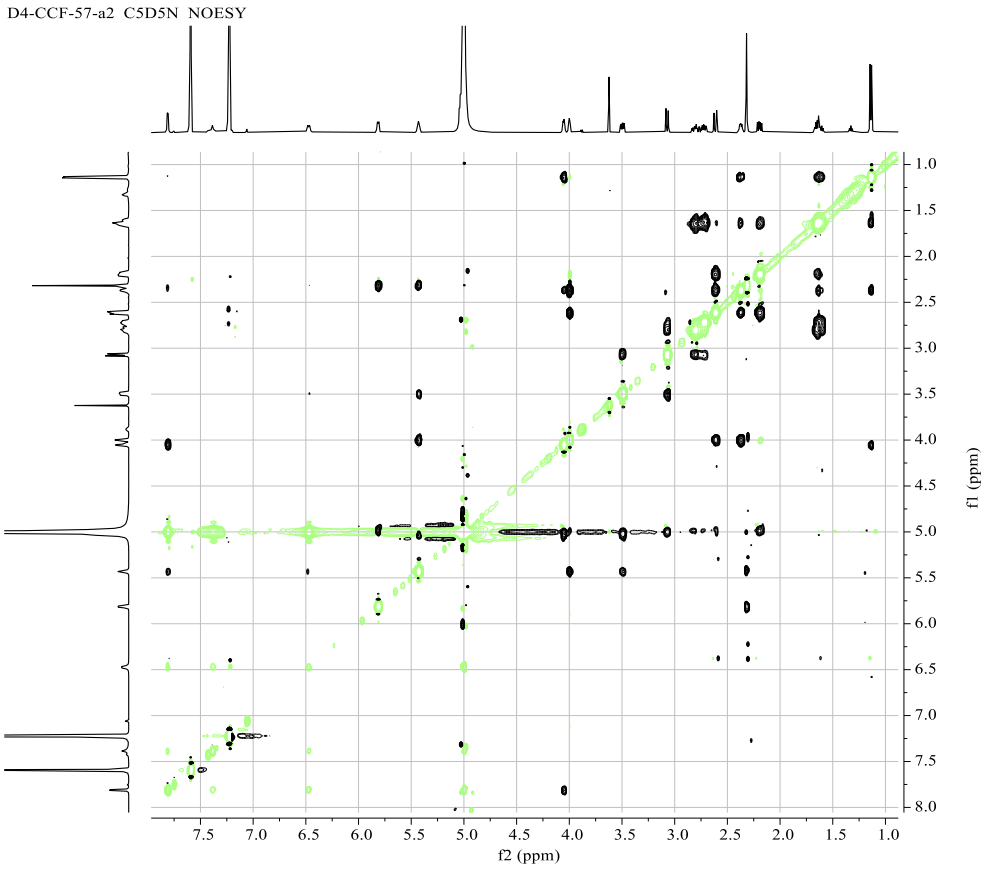

**Figure S37**. (+)-ESIMS spectrum of fortalide B (**2**)

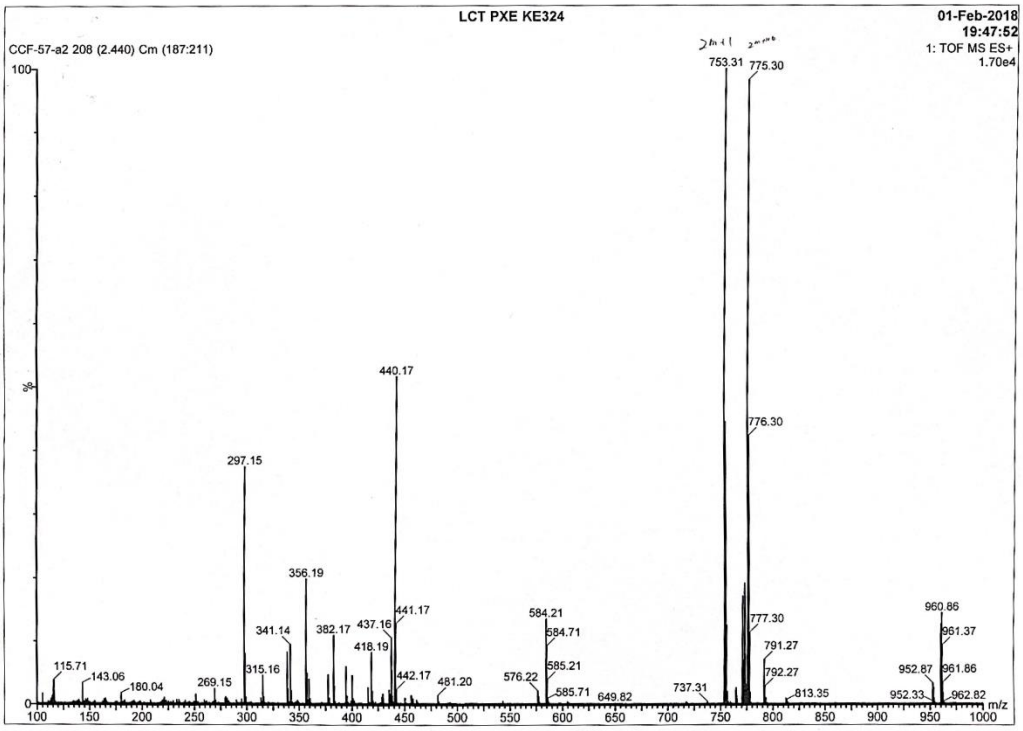


**Figure S38**. (−)-ESIMS spectrum of fortalide B (**2**)

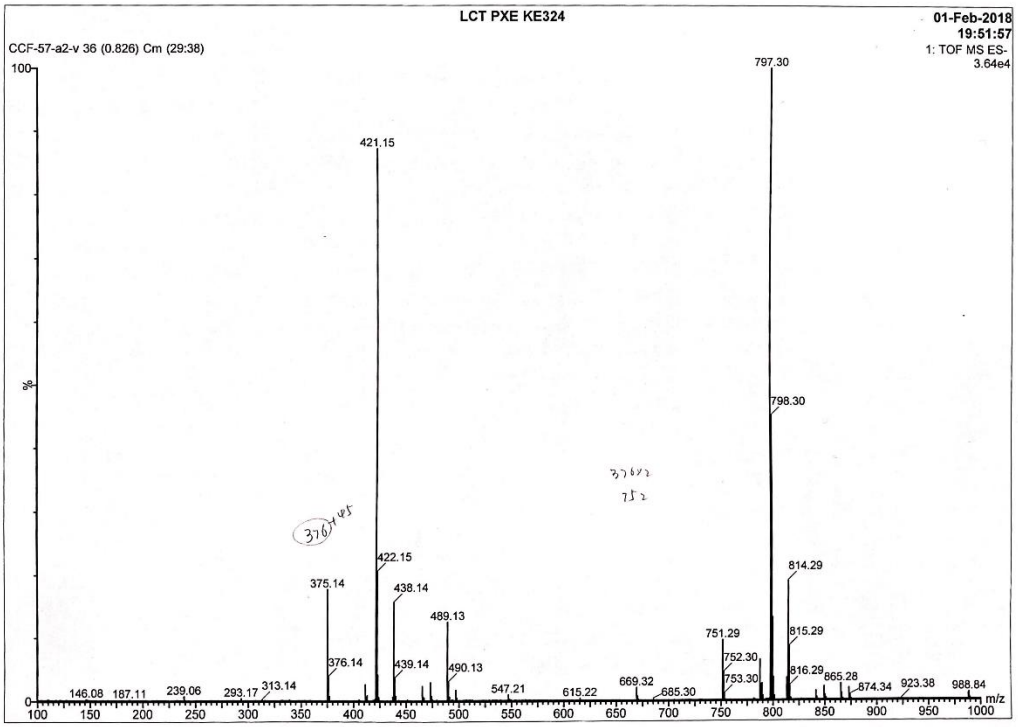

**Figure S39**. (−)-HRESIMS spectrum of fortalide B (**2**)

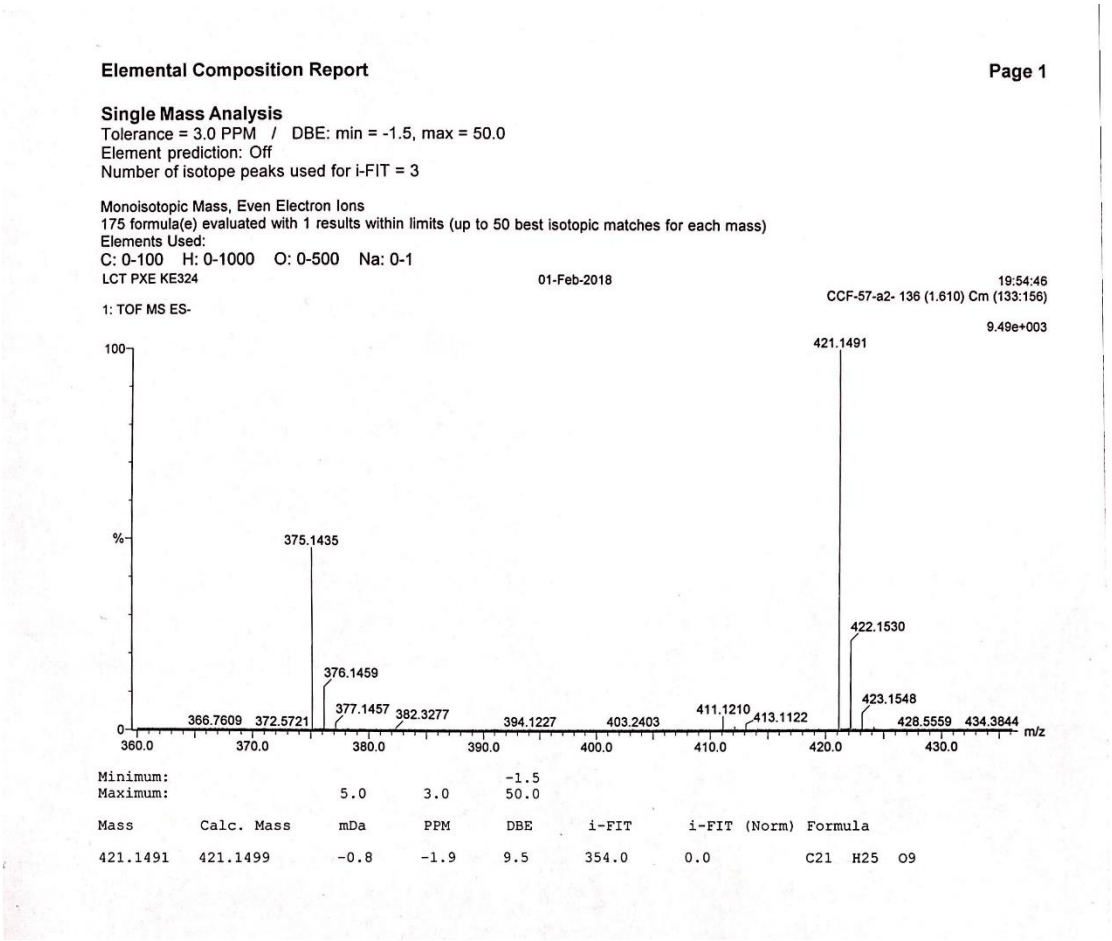


**Figure S40**. IR spectrum of fortalide B (**2**)

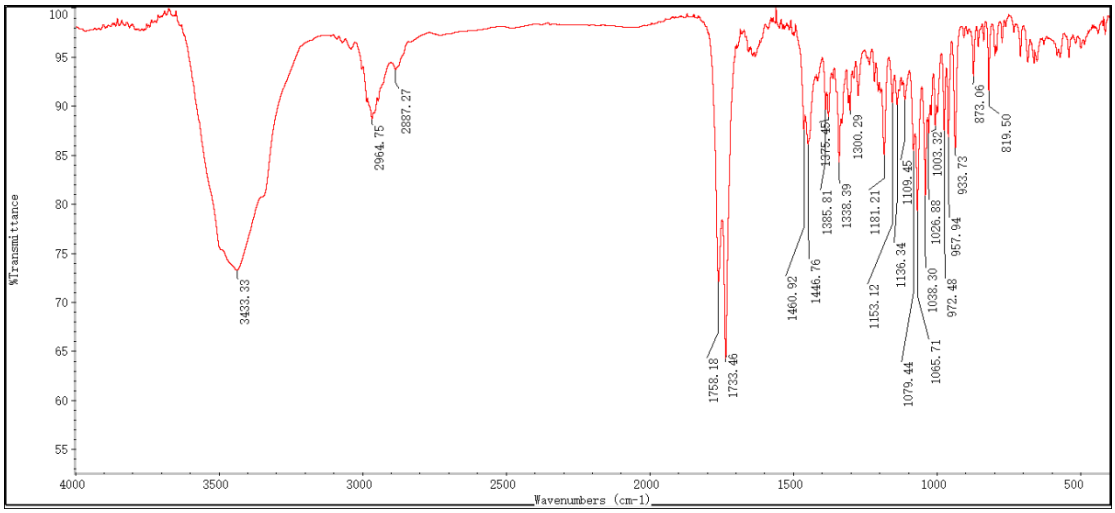

**Figure S41–S51.** 1D and 2D NMR, MS, IR and ECD spectra of fortalide C (**3**)

**Figure S41**. $^{1}H$ NMR spectrum of fortalide C (**3**) in $CDCl_3$

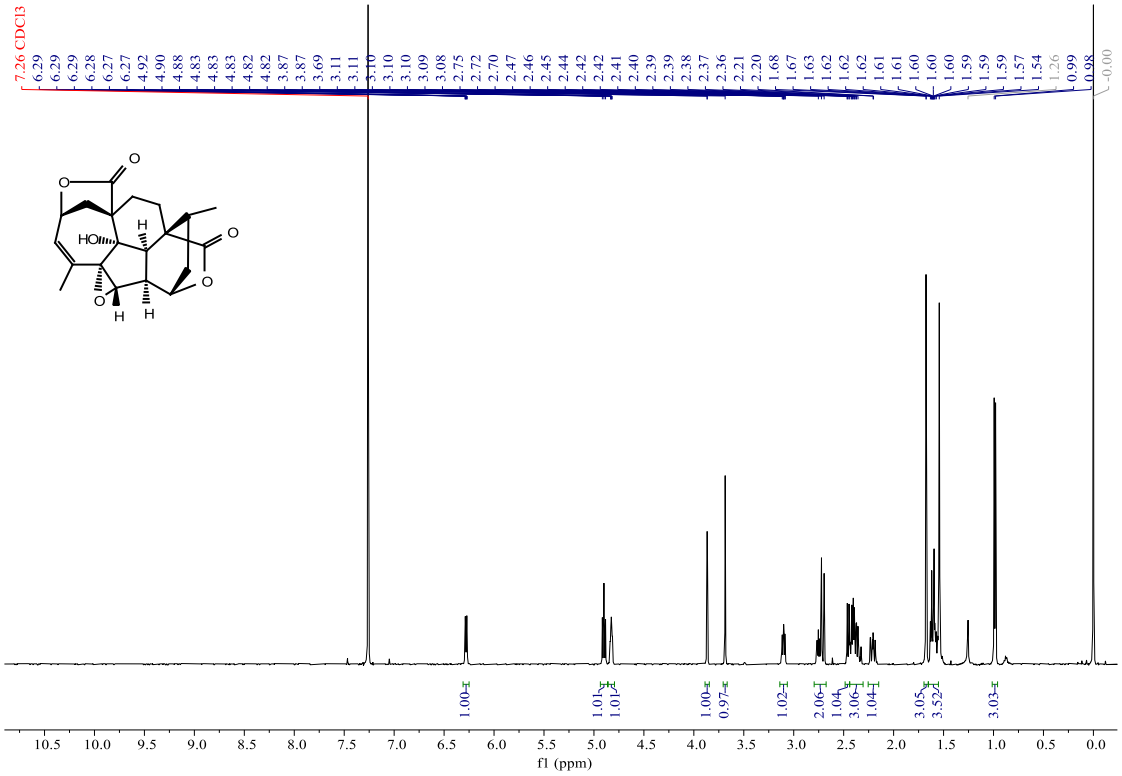


**Figure S42**. $^{13}C$ NMR (BB and DEPT-135) spectra of fortalide C (**3**) in $CDCl_3$

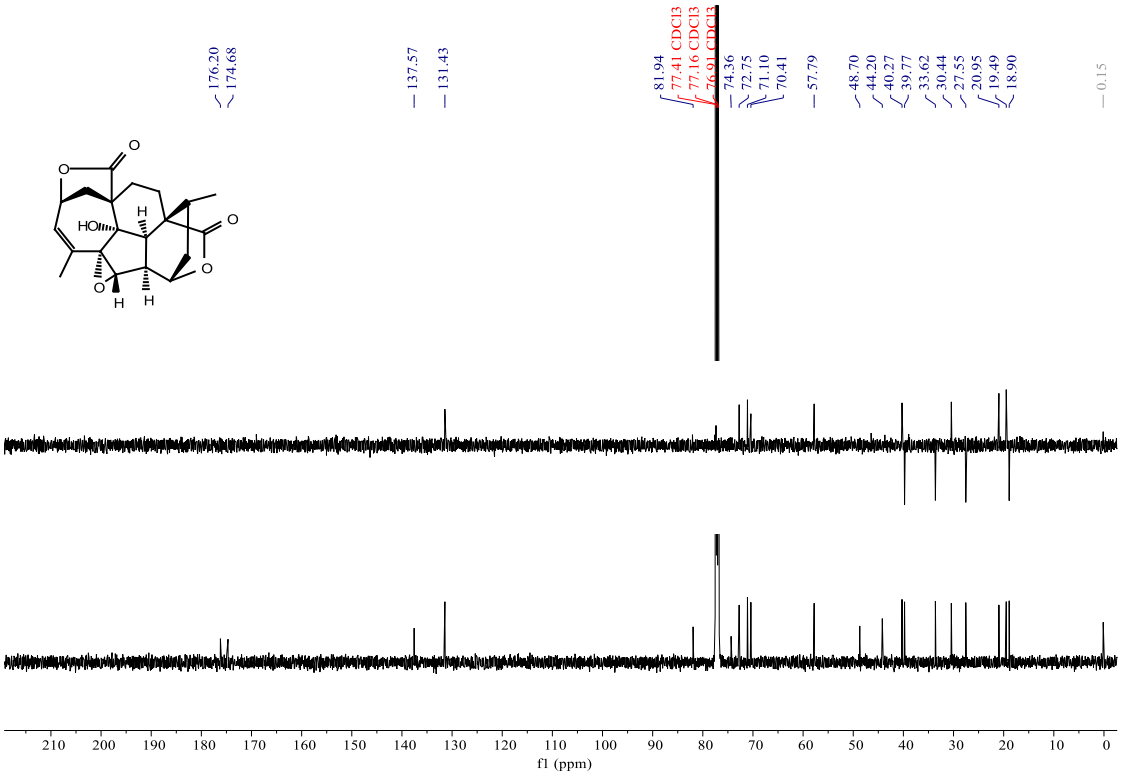

**Figure S43**. HSQC spectrum of fortalide C (**3**) in $CDCl_3$

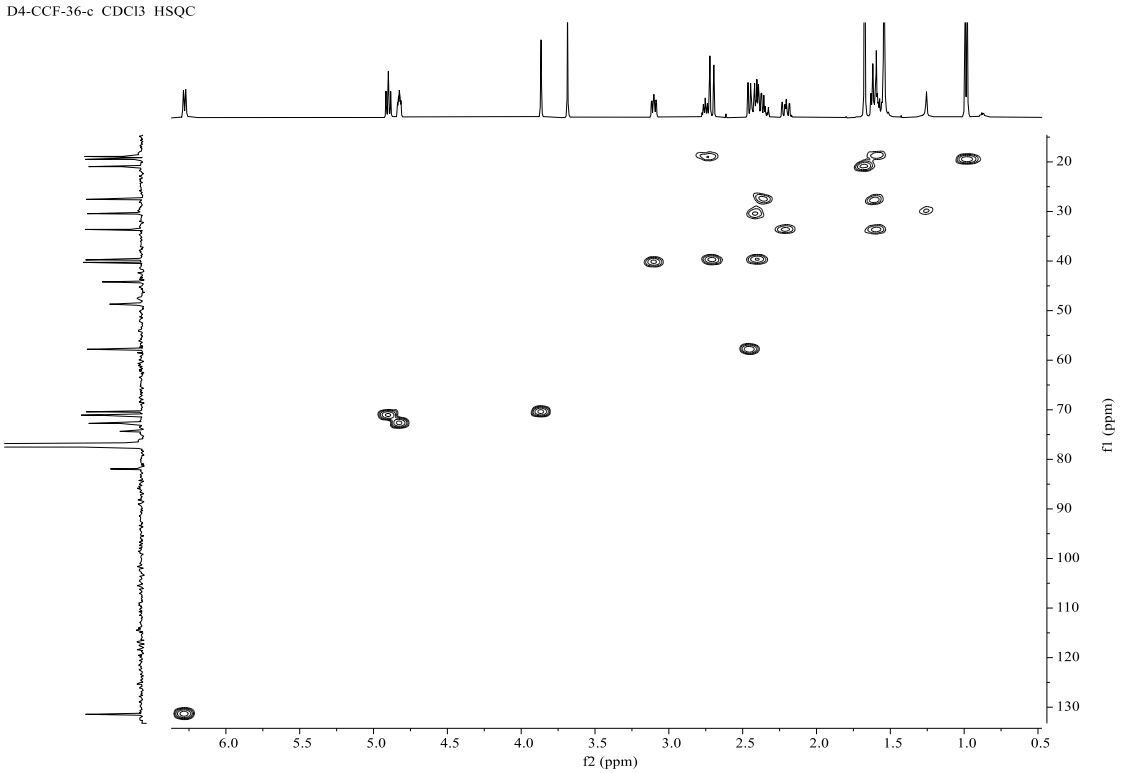


**Figure S44**. HMBC spectrum of fortalide C (**3**) in $CDCl_3$

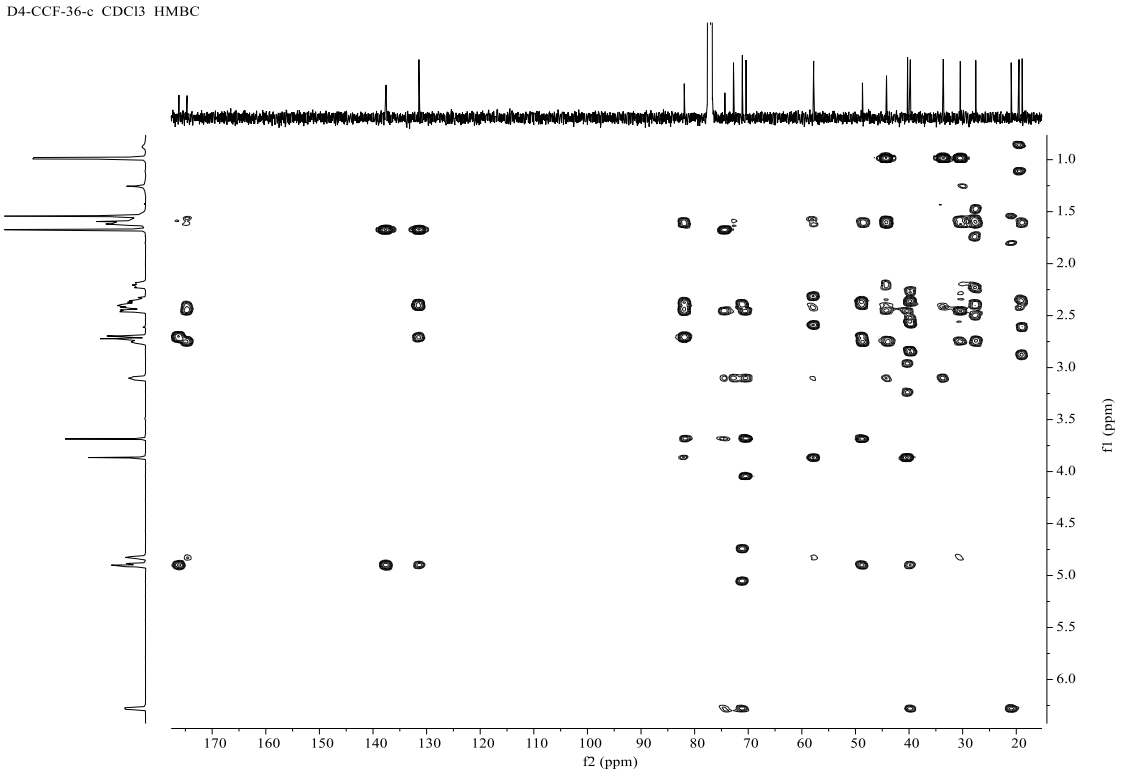

**Figure S45**. $^{1}H$-$^{1}H$ COSY spectrum of fortalide C (**3**) in $CDCl_3$

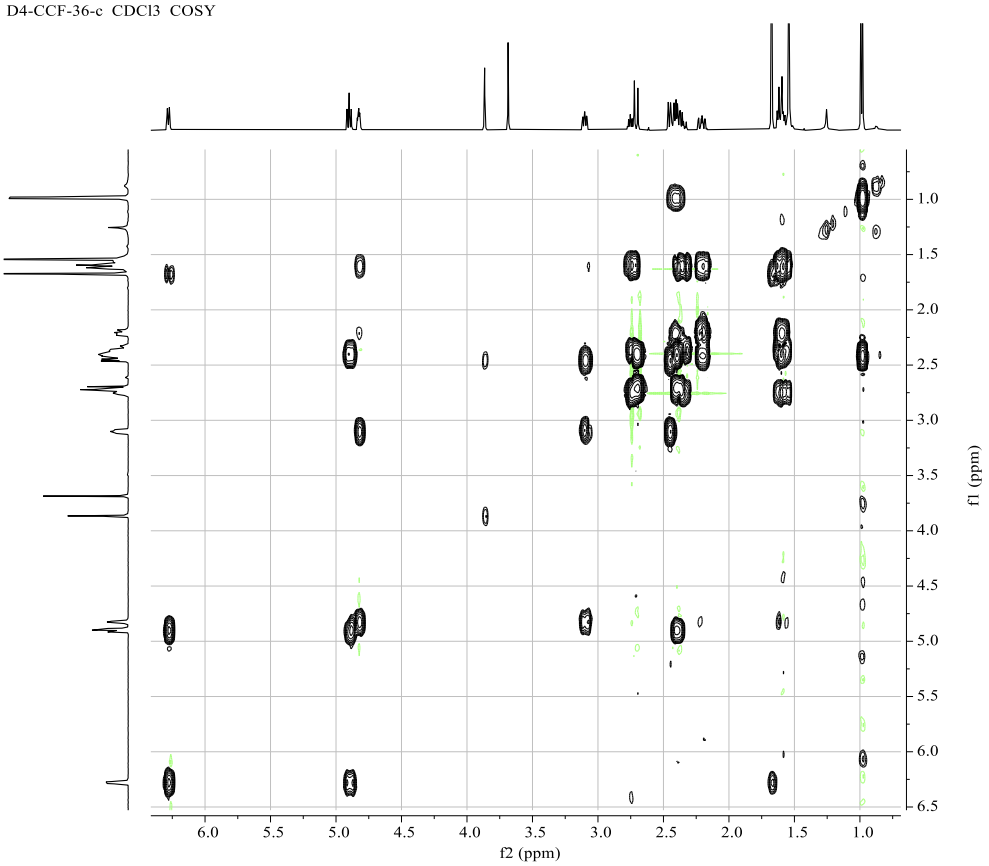


**Figure S46**. ROESY spectrum of fortalide C (**3**) in $CDCl_3$

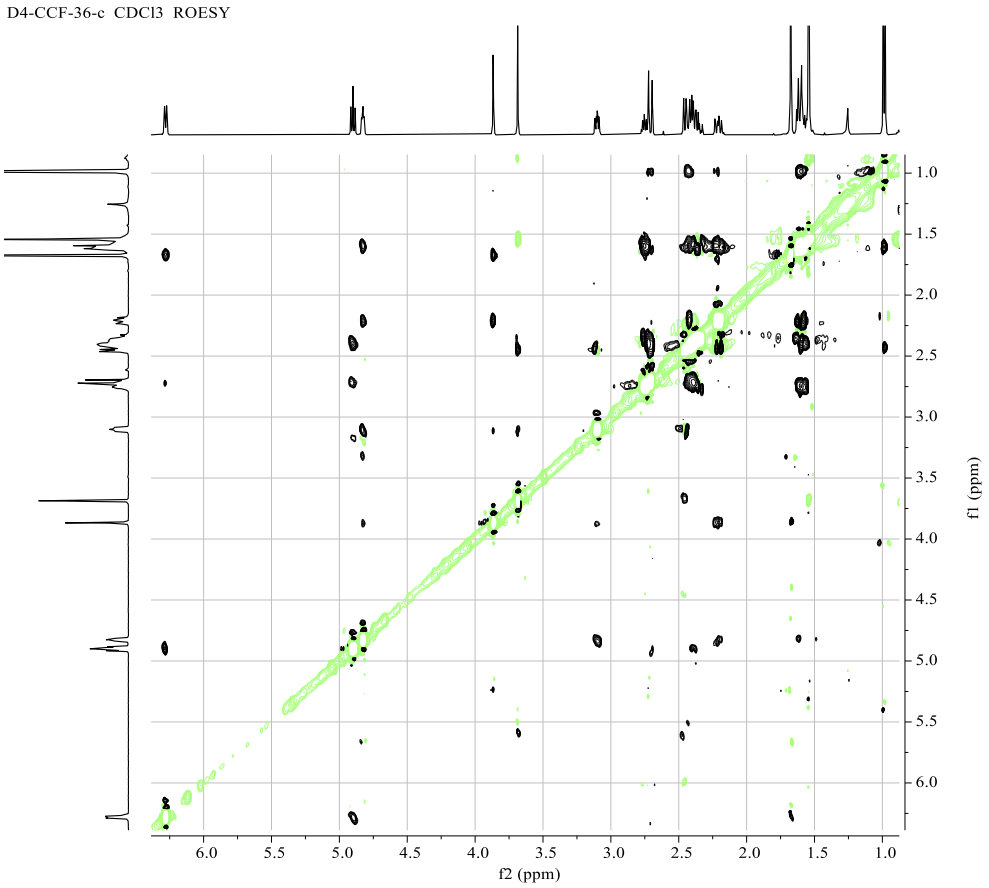

**Figure S47**. (+)-ESIMS spectrum of fortalide C (**3**)

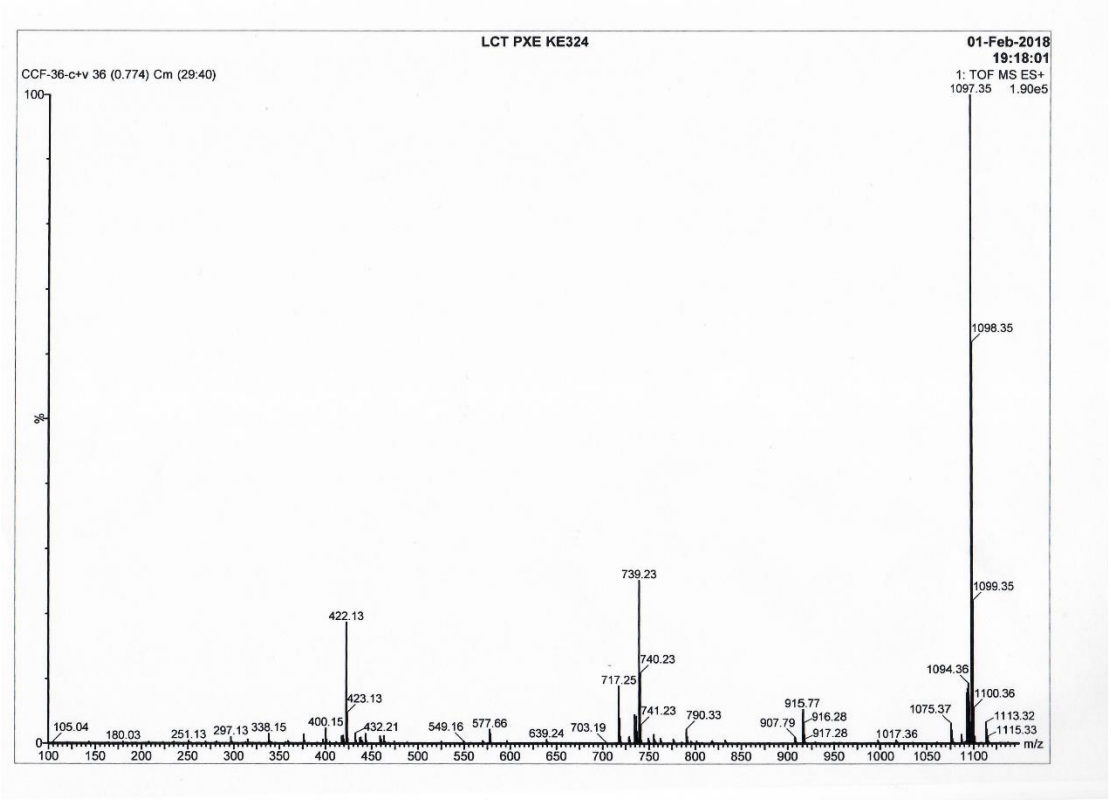


**Figure S48**. (−)-ESIMS spectrum of fortalide C (**3**)

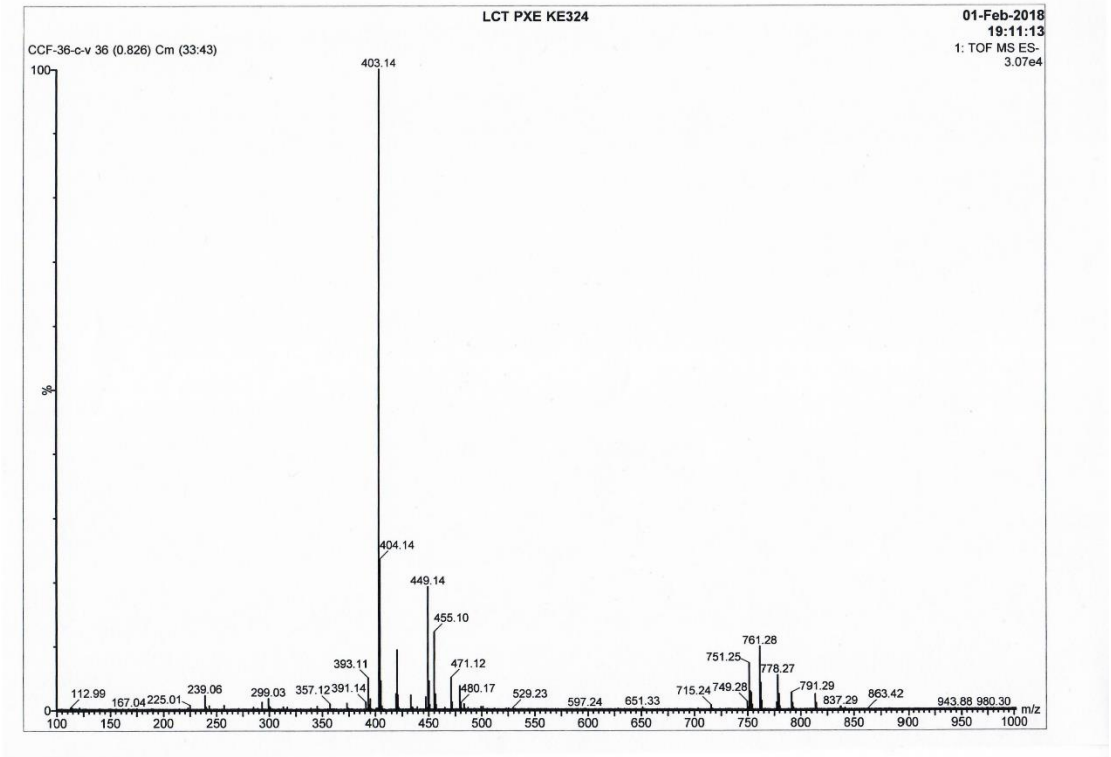

**Figure S49**. (−)-HRESIMS spectrum of fortalide C (**3**)

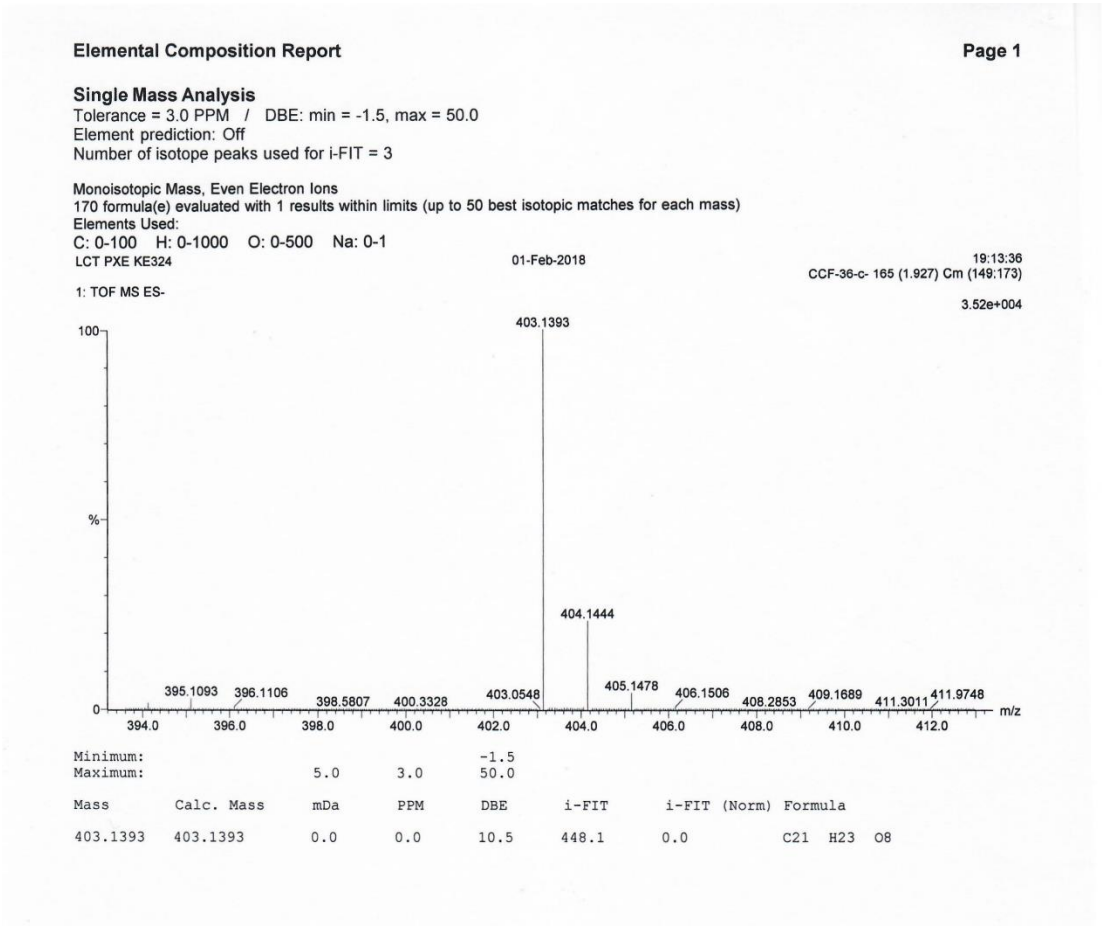


**Figure S50**. IR spectrum of fortalide C (**3**)

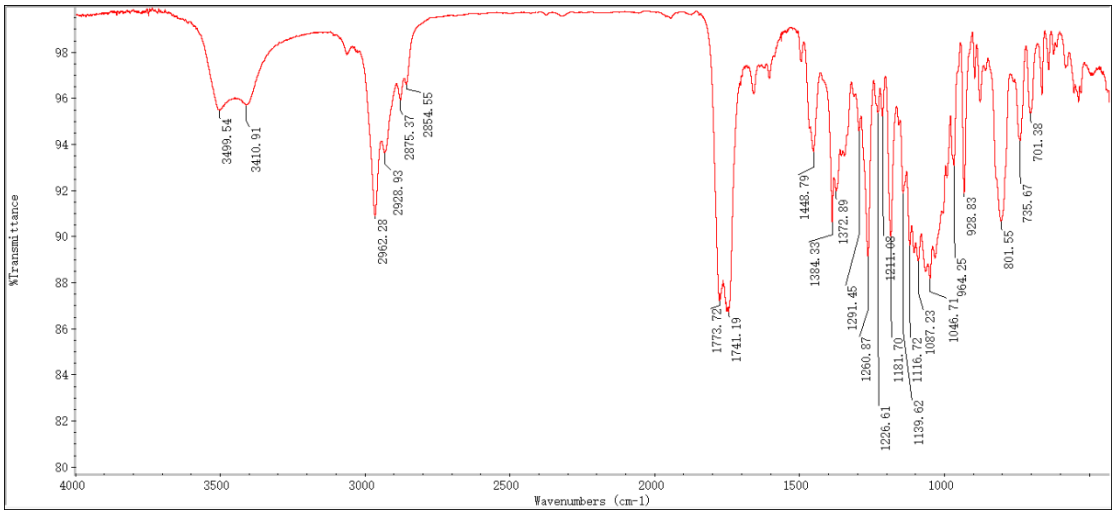

**Figure S51**. UV and ECD spectra of fortalide C (**3**)

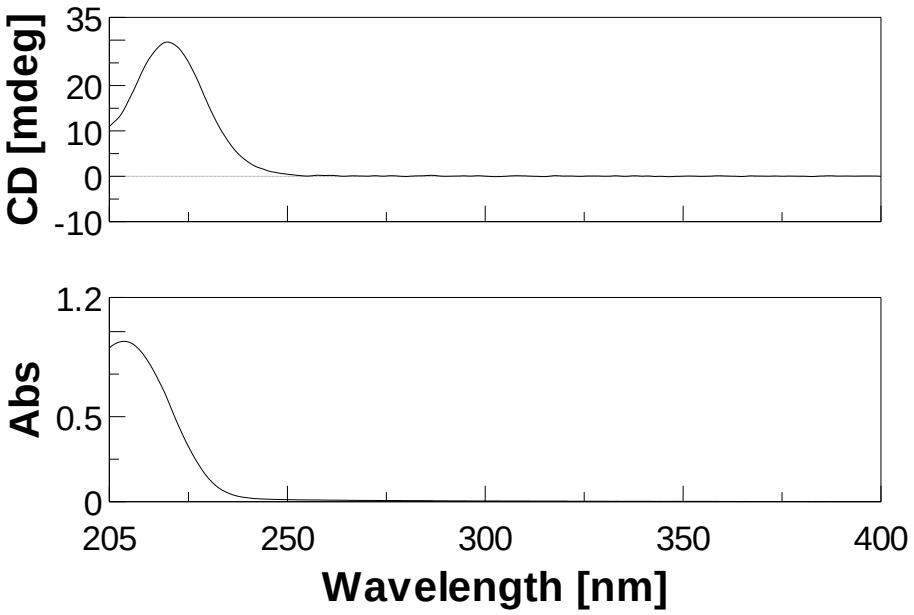


**Figure S52–S60.** 1D and 2D NMR, MS, and IR spectra of fortalide D (**4**)

**Figure S52**. $^{1}H$ NMR spectrum of fortalide D (**4**) in $CDCl_3$

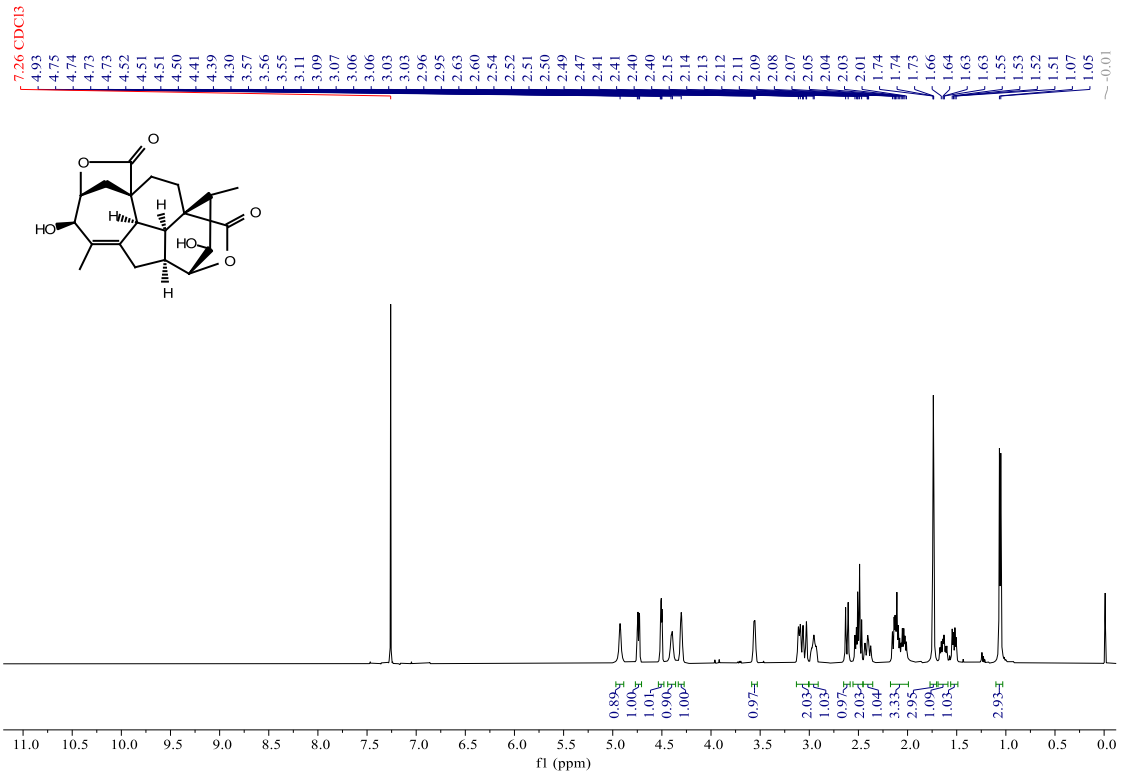

**Figure S53** $^{13}$C NMR (BB and DEPT-135) spectra of fortalide D (**4**) in $CDCl_3$

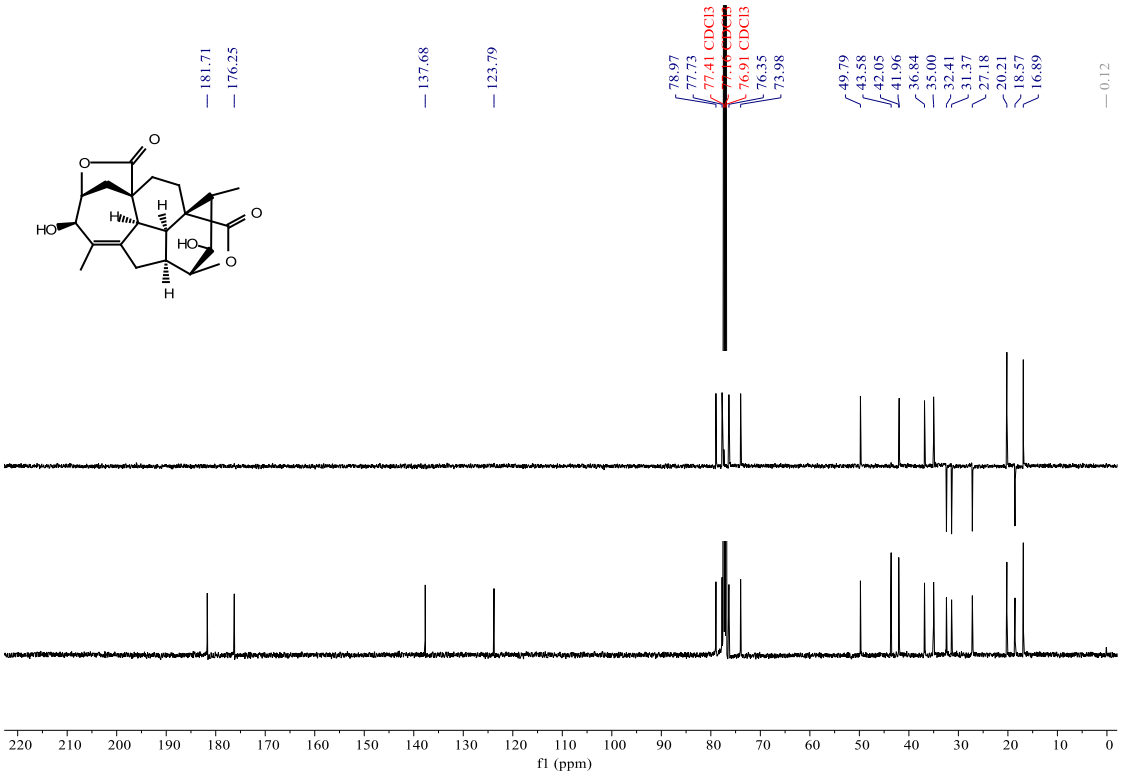


**Figure S54**. HSQC spectrum of fortalide D (**4**) in $CDCl_3$

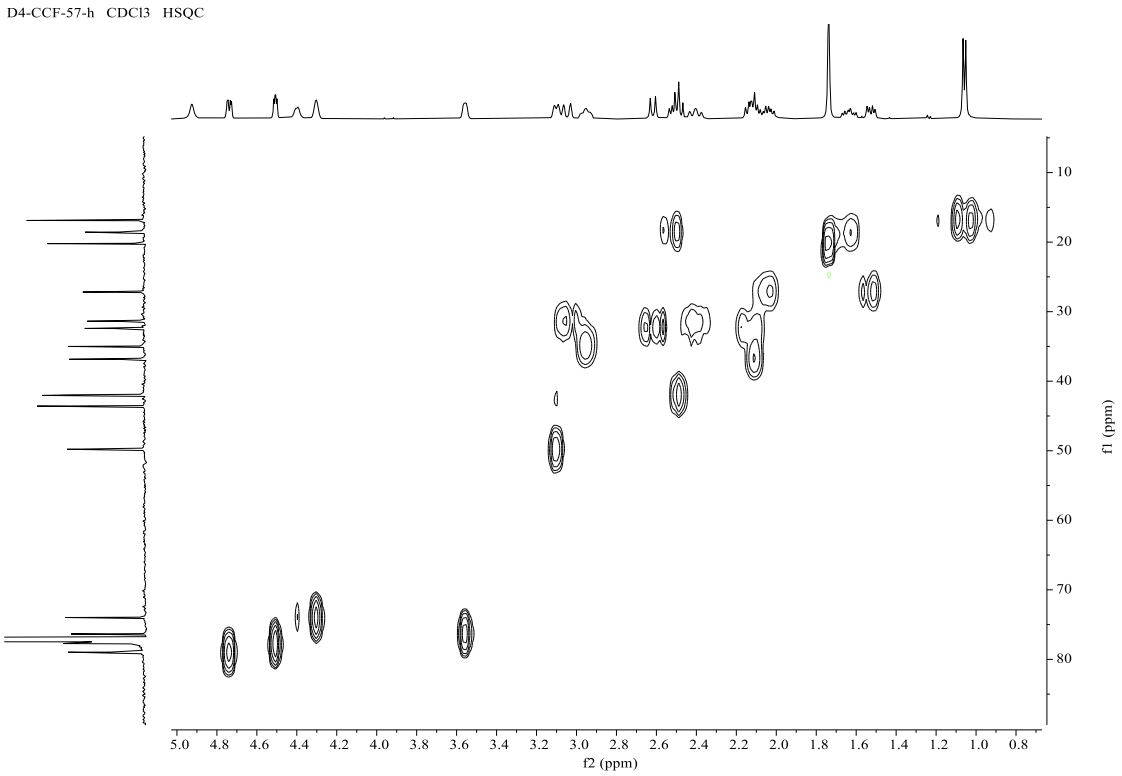

**Figure S55**. HMBC spectrum of fortalide D (**4**) in $CDCl_3$

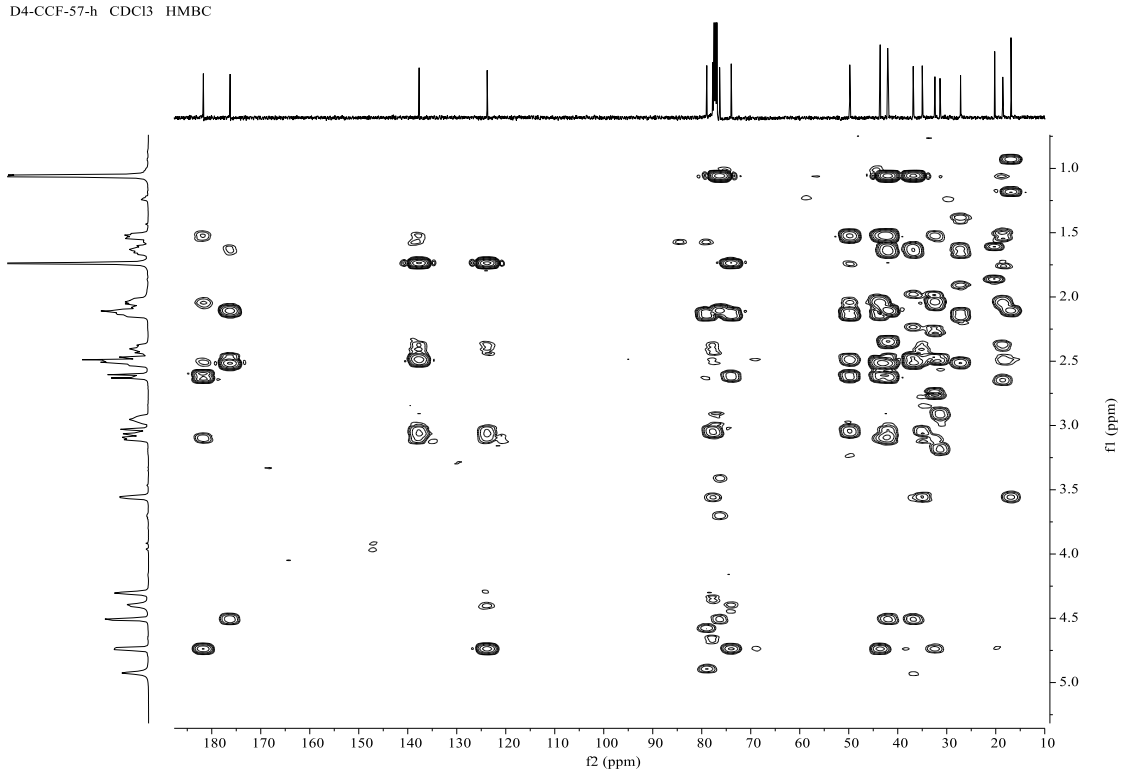


**Figure S56**. $^{1}H$-$^{1}H$ COSY spectrum of fortalide D (**4**) in $CDCl_3$

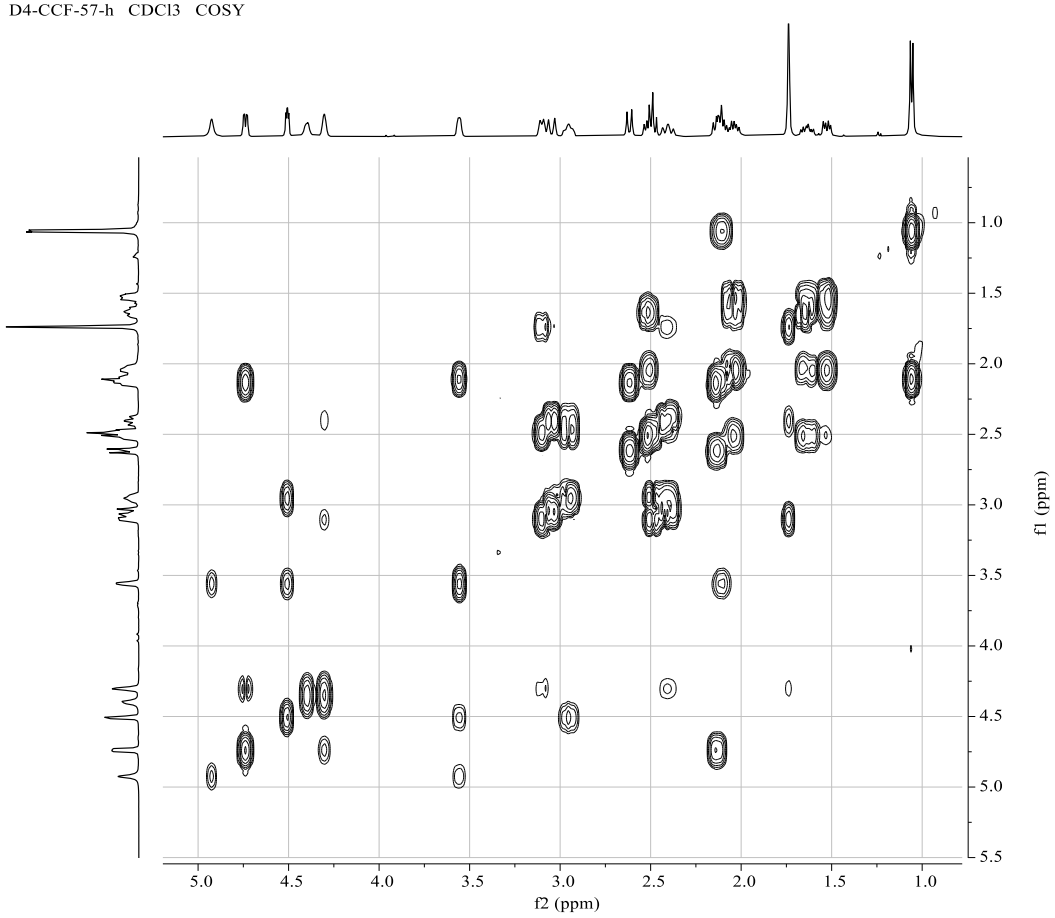

**Figure S57**. ROESY spectrum of fortalide D (**4**) in $CDCl_3$

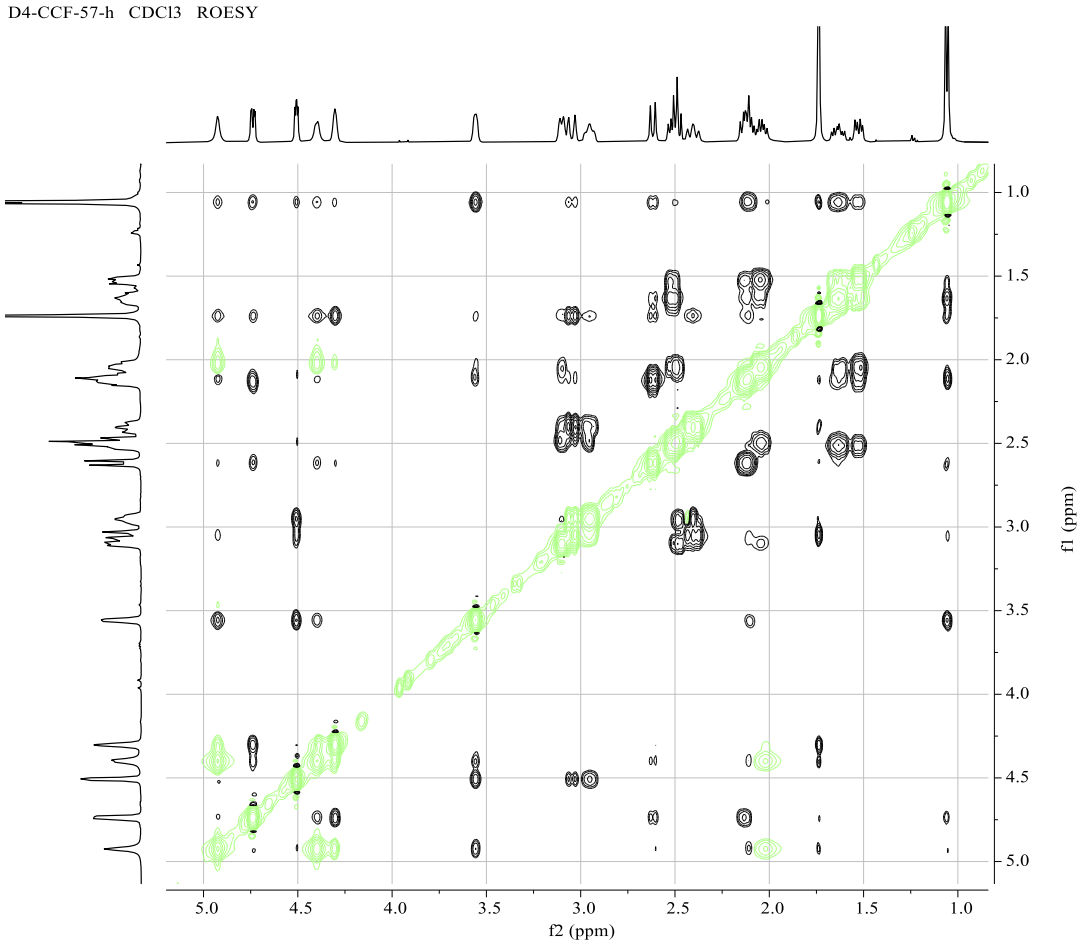


**Figure S58**. (−)-ESIMS spectrum of fortalide D (**4**)

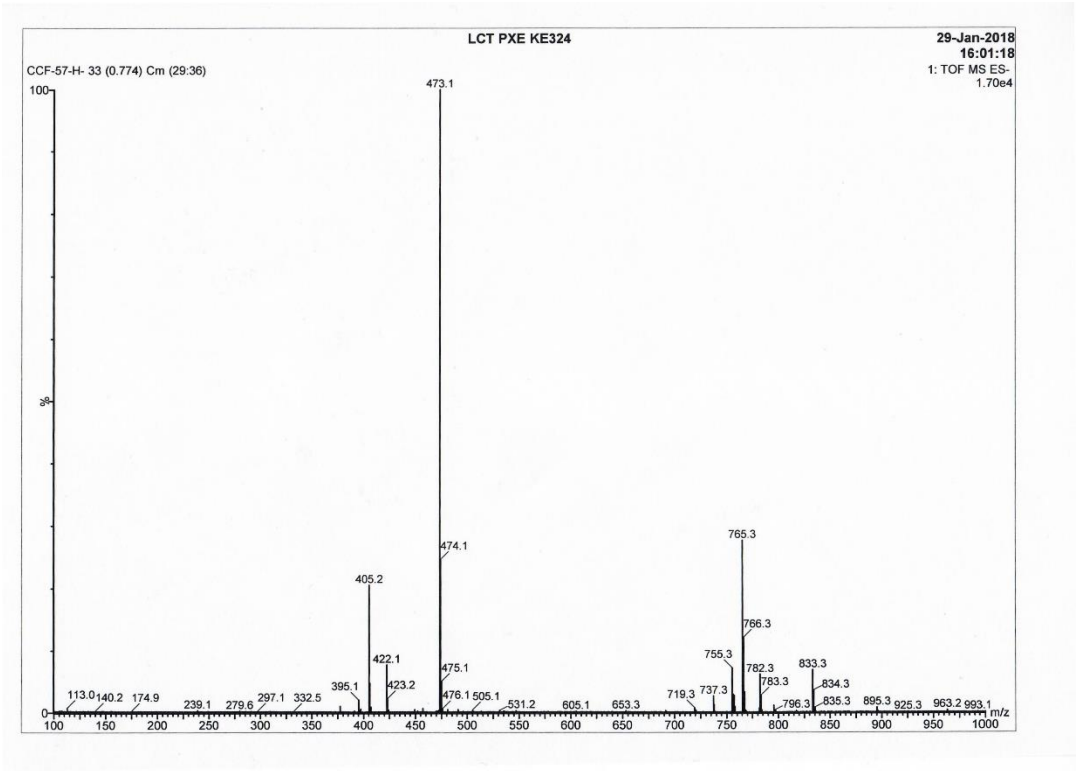

**Figure S59**. (−)-HRESIMS spectrum of fortalide D (**4**)

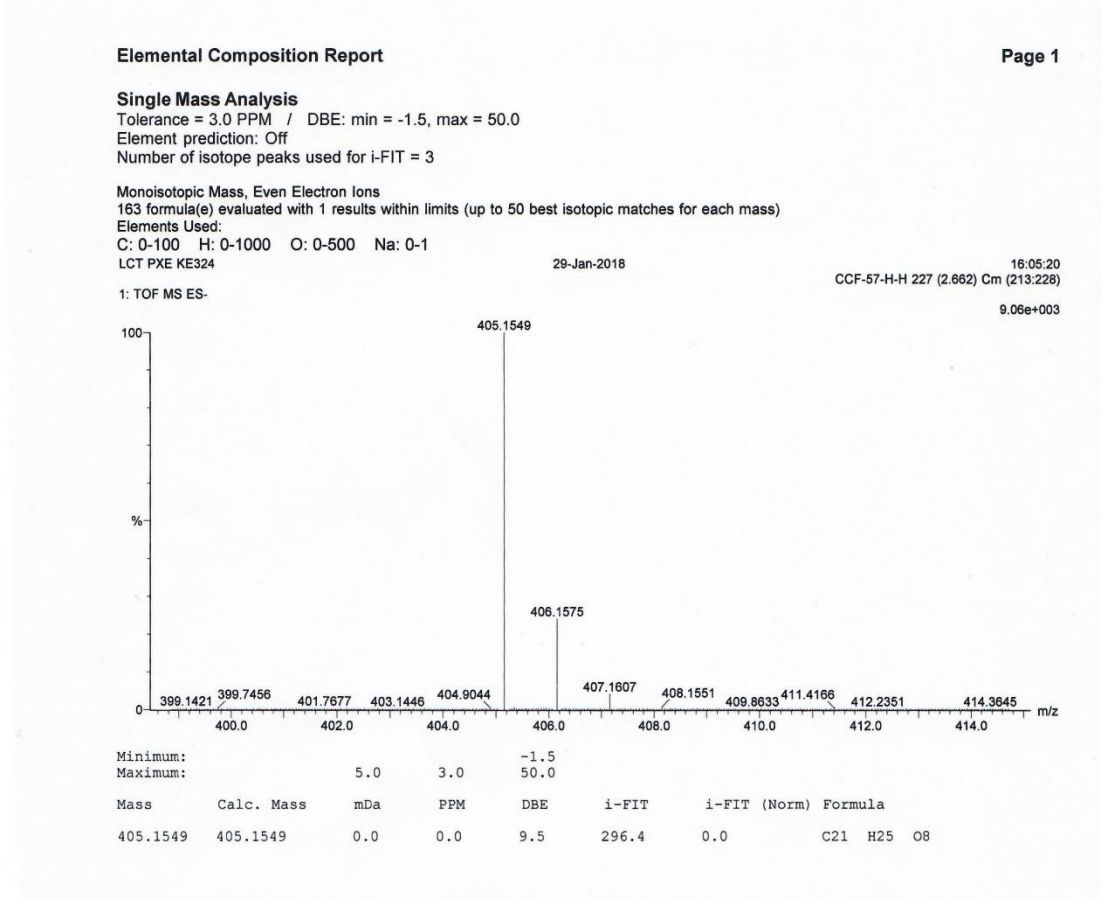

**Elemental Composition Report** Page 1

**Single Mass Analysis**
Tolerance = 3.0 PPM / DBE: min = -1.5, max = 50.0
Element prediction: Off
Number of isotope peaks used for i-FIT = 3

Monoisotopic Mass, Even Electron Ions
163 formula(e) evaluated with 1 results within limits (up to 50 best isotopic matches for each mass)
Elements Used:
C: 0-100 H: 0-1000 O: 0-500 Na: 0-1

LCT PXE KE324 29-Jan-2018 16:05:20
CCF-57-H-H 227 (2.662) Cm (213:228)
1: TOF MS ES- 9.06e+003



| | | | | | | | |
|---|---|---|---|---|---|---|---|
| Minimum: | | | | -1.5 | | | |
| Maximum: | | 5.0 | 3.0 | 50.0 | | | |
| Mass | Calc. Mass | mDa | PPM | DBE | i-FIT | i-FIT (Norm) | Formula |
| 405.1549 | 405.1549 | 0.0 | 0.0 | 9.5 | 296.4 | 0.0 | C21 H25 O8 |

**Figure S60**. IR spectrum of fortalide.D (**4**)

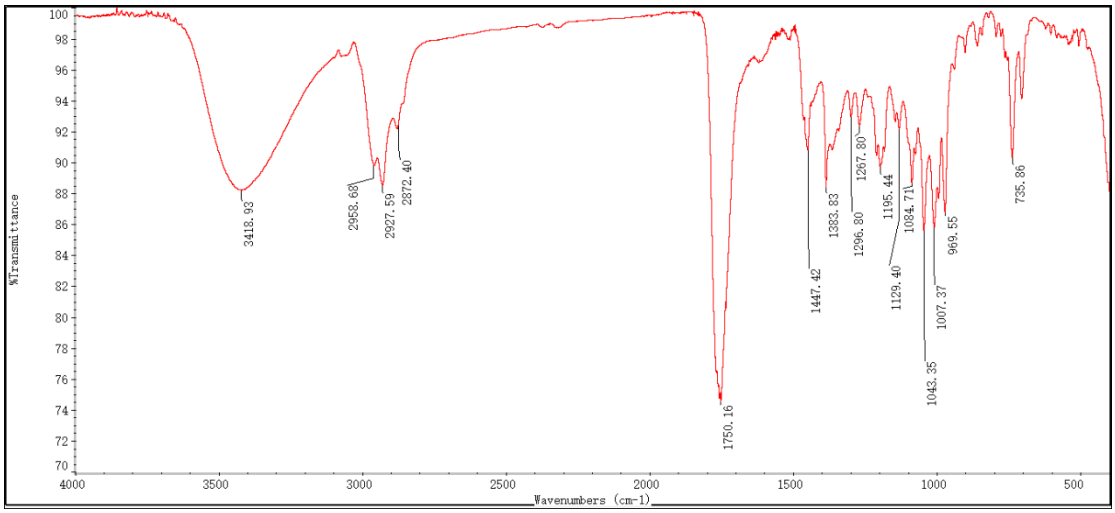

**Figure S61–S70.** 1D and 2D NMR, MS, and IR spectra of fortalide E (**5**)

**Figure S61**. $^{1}$H NMR spectrum of fortalide E (**5**) in pyridine-$d_5$

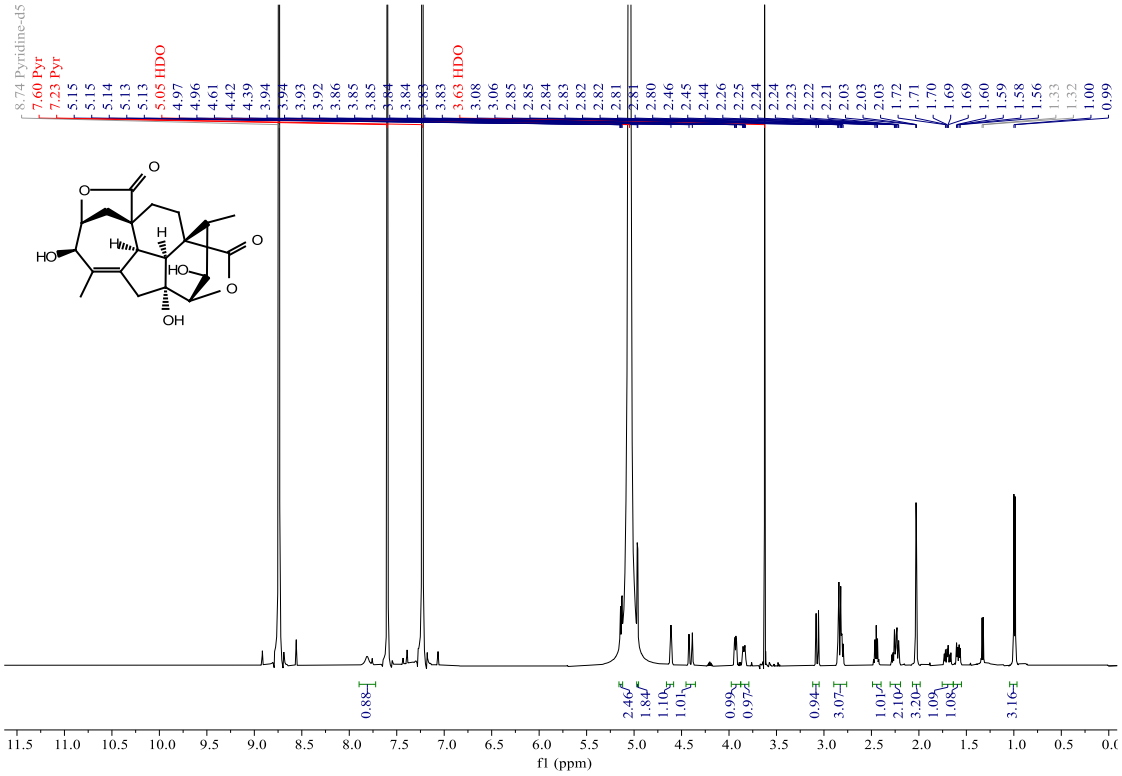


**Figure S62**. $^{13}$C NMR (BB and DEPT-135) spectra of fortalide E (**5**) in pyridine-$d_5$

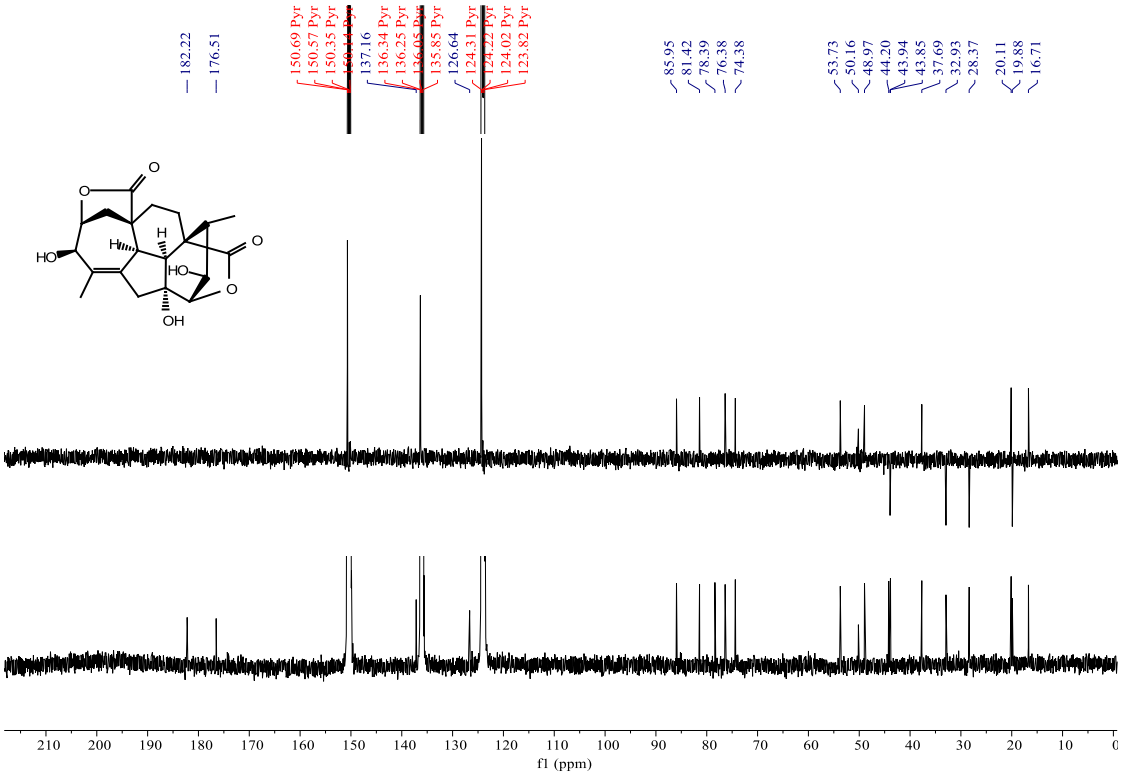

**Figure S63**. HSQC spectrum of fortalide E (**5**) in pyridine-$d_5$

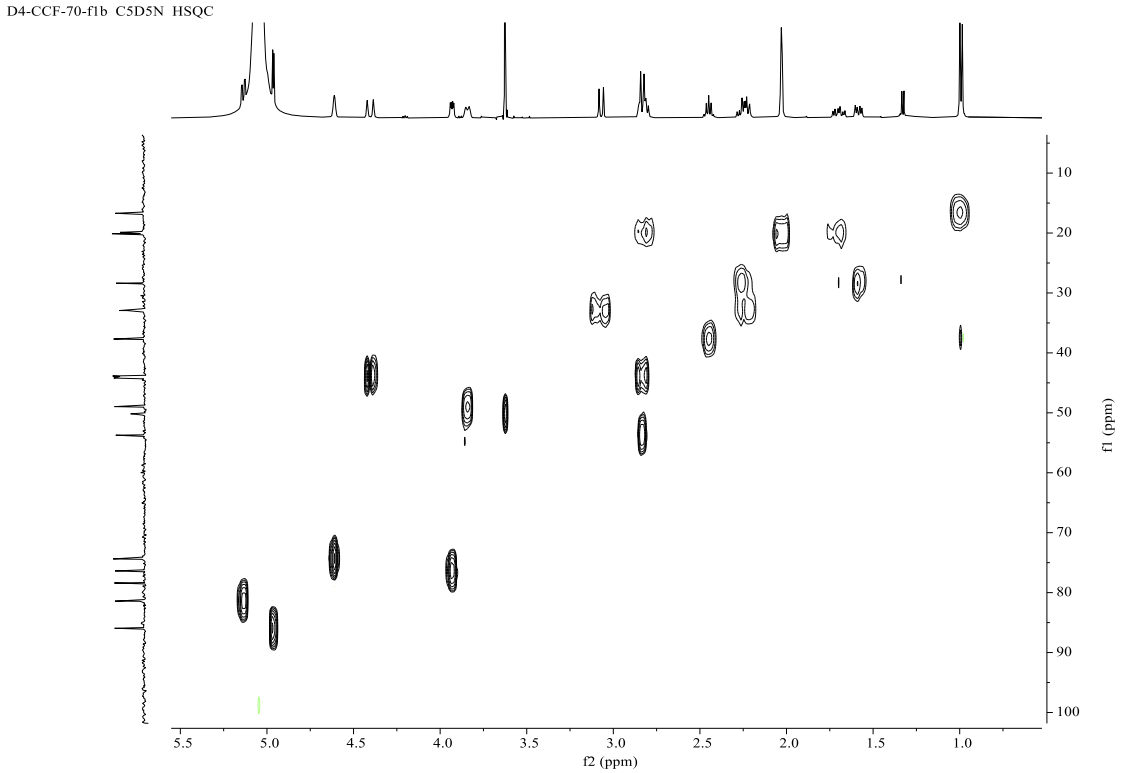


**Figure S64**. HMBC spectrum of fortalide E (**5**) in pyridine-$d_5$

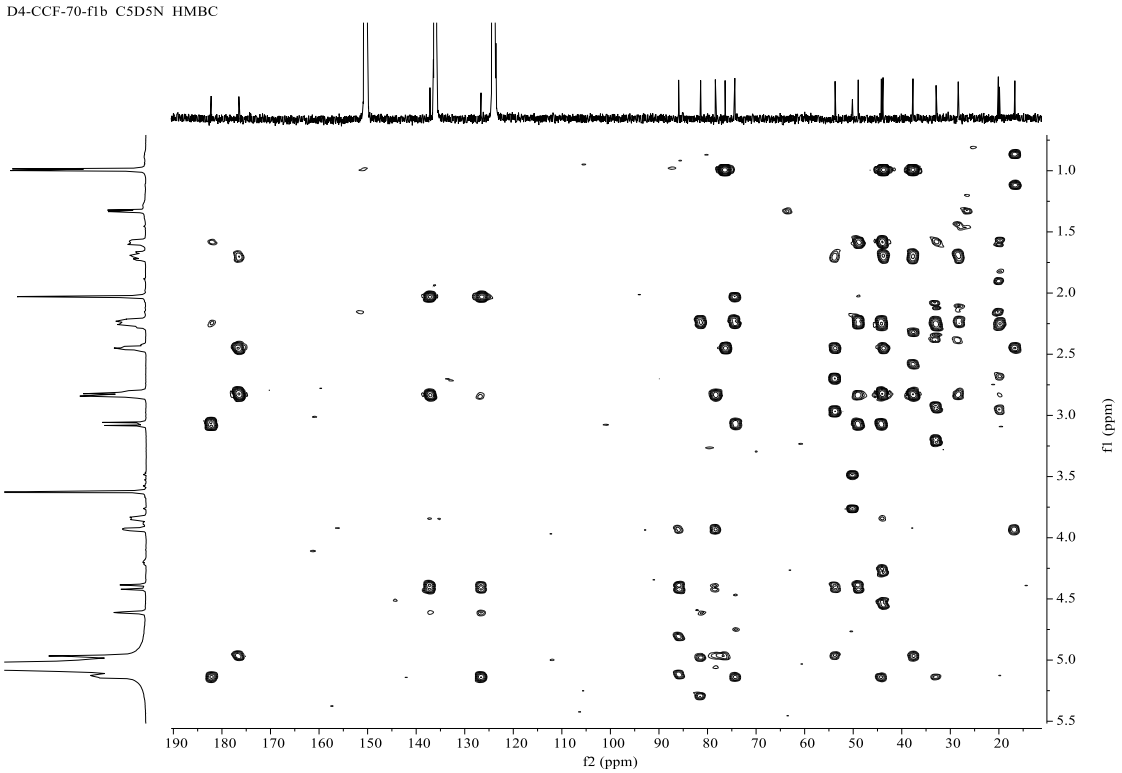

**Figure S65**. $^{1}$H-$^{1}$H COSY spectrum of fortalide E (**5**) in pyridine-$d_5$

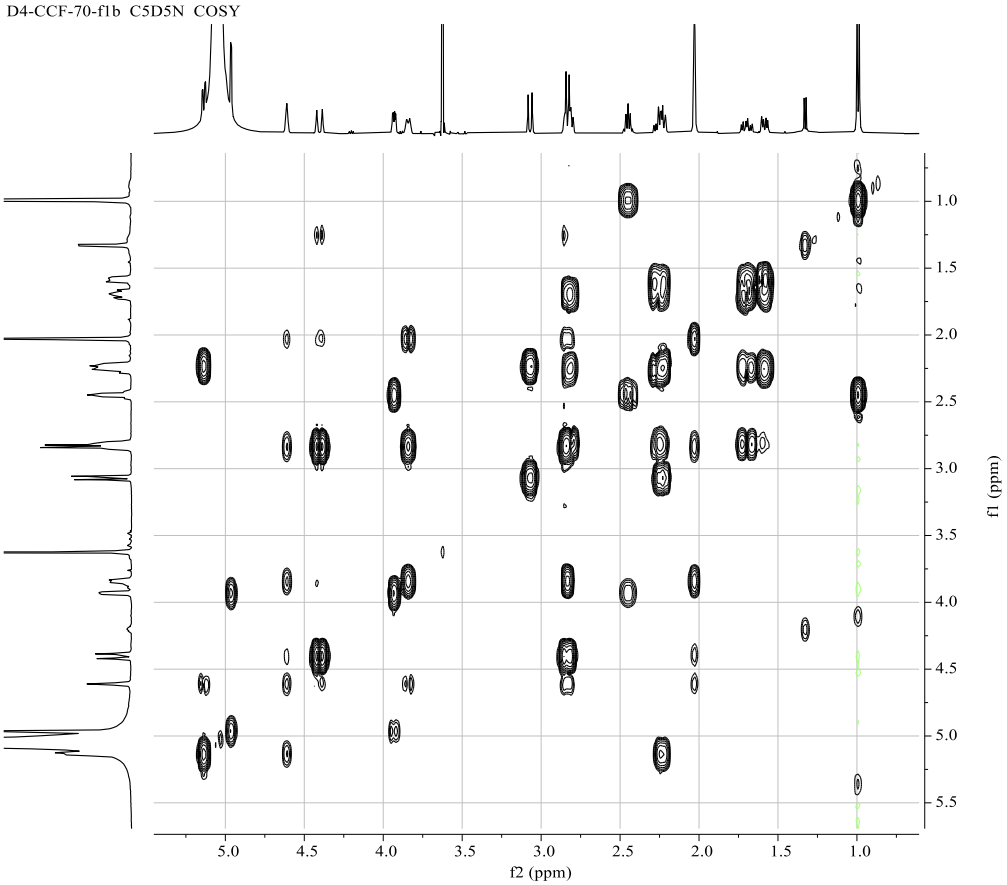


**Figure S66**. NOESY spectrum of fortalide E (**5**) in pyridine-$d_5$

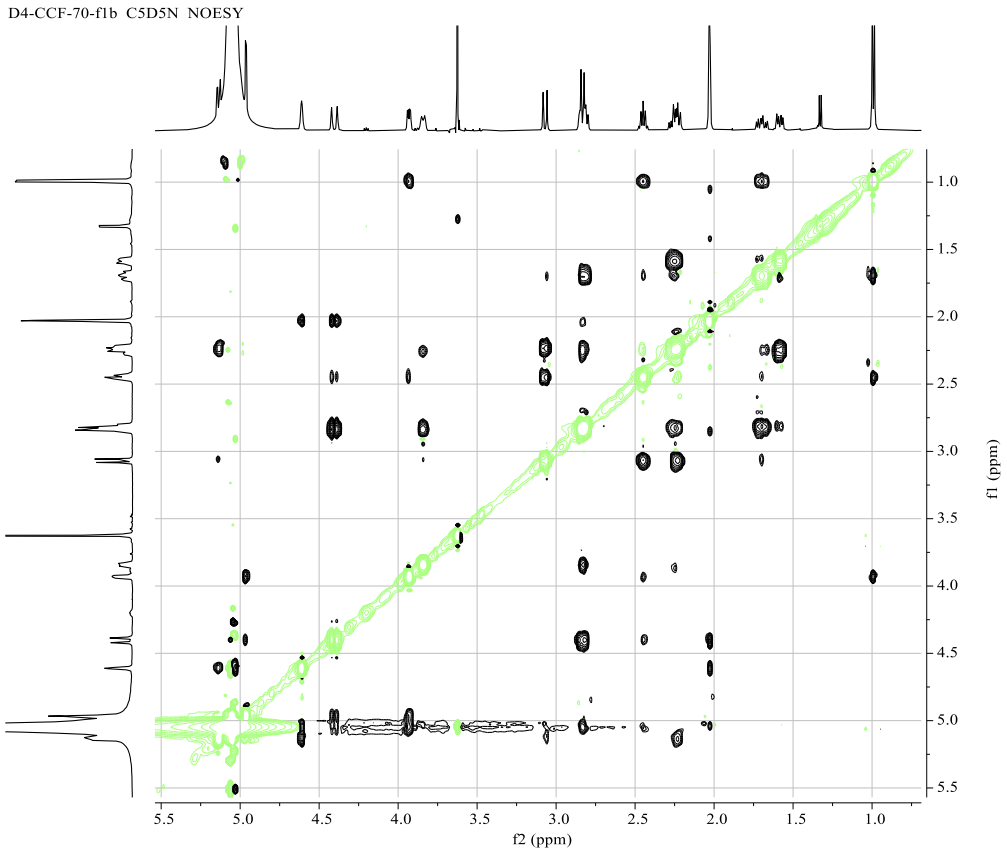

**Figure S67**. (+)-ESIMS spectrum of fortalide E (**5**)

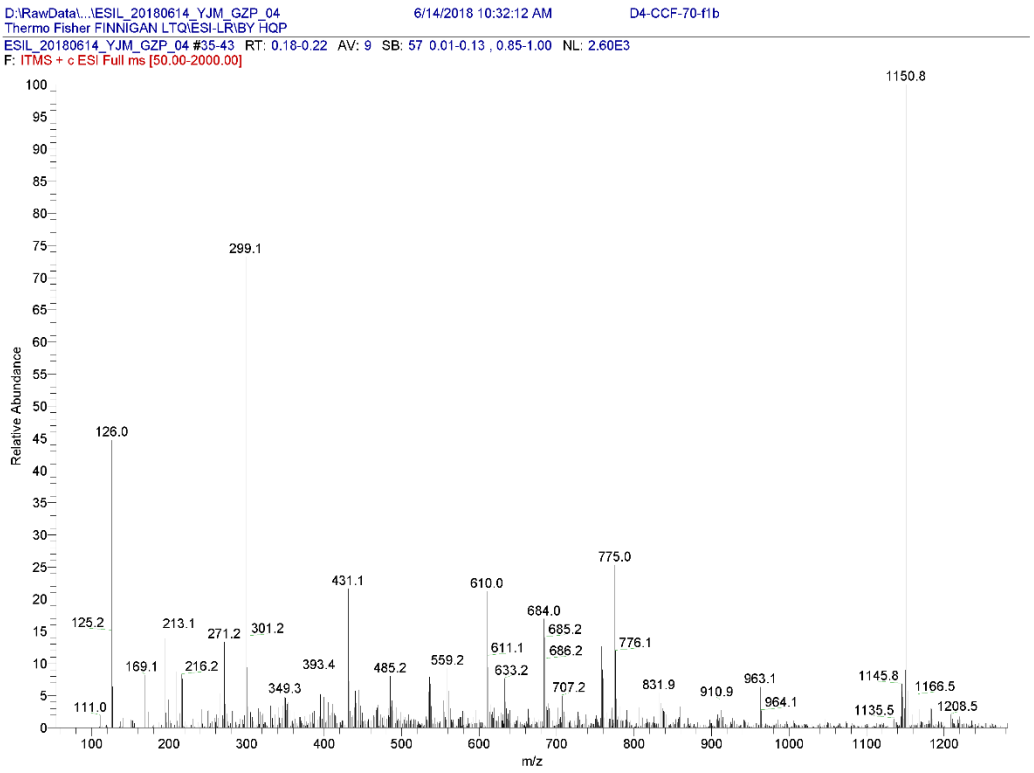


**Figure S68**. (−)-ESIMS spectrum of fortalide E (**5**)

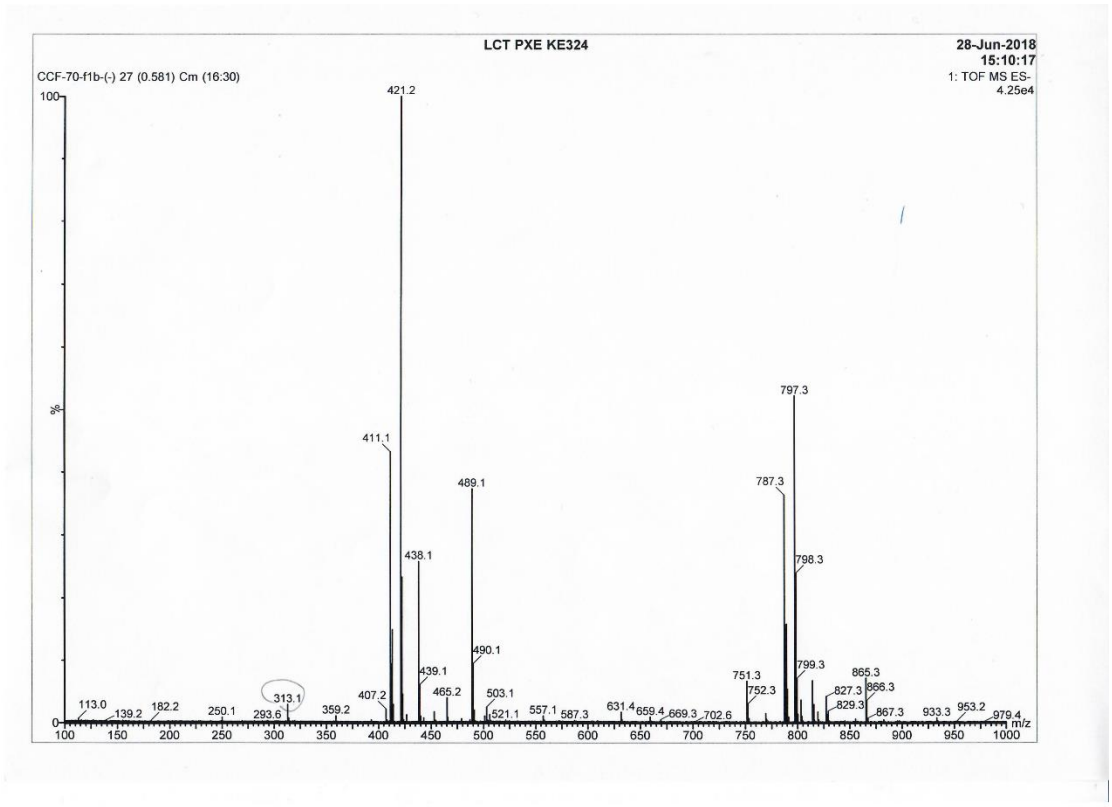

**Figure S69**. (−)-HRESIMS spectrum of fortalide E (**5**)

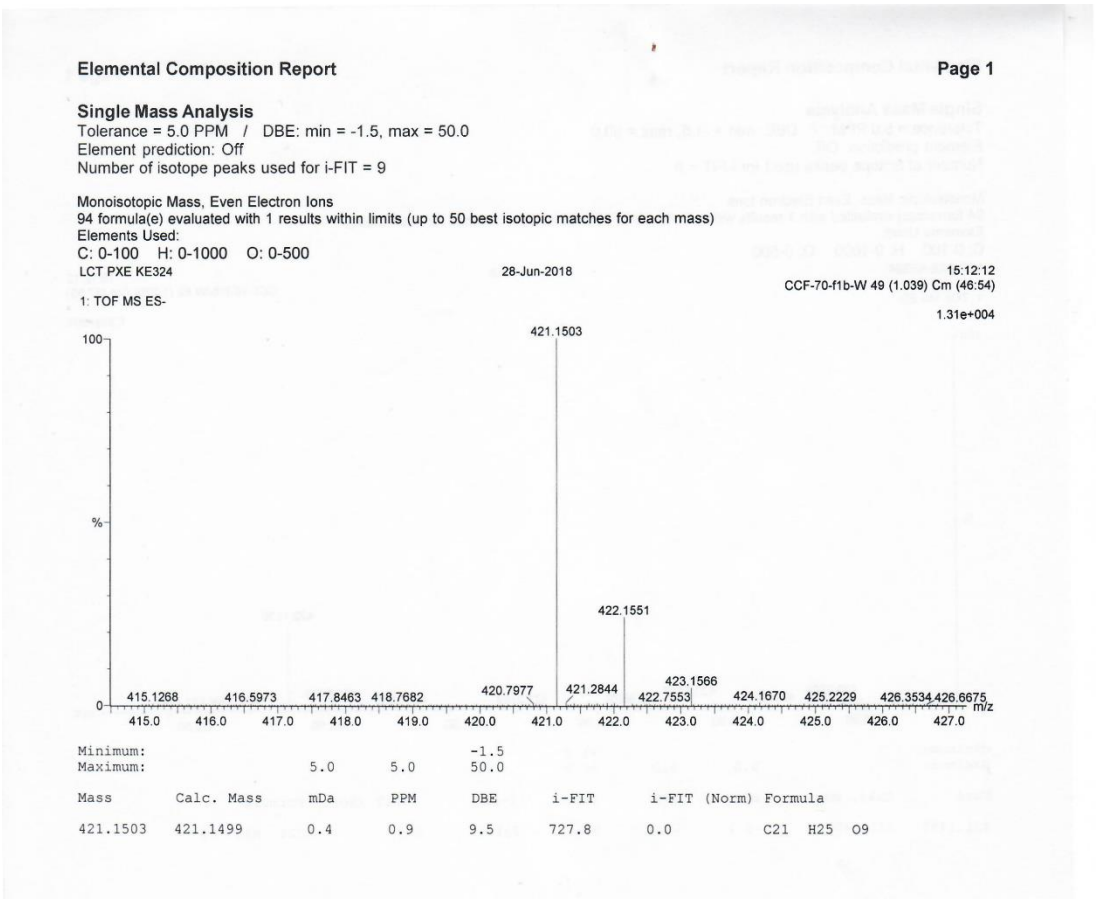


**Figure S70**. IR spectrum of fortalide E (**5**)

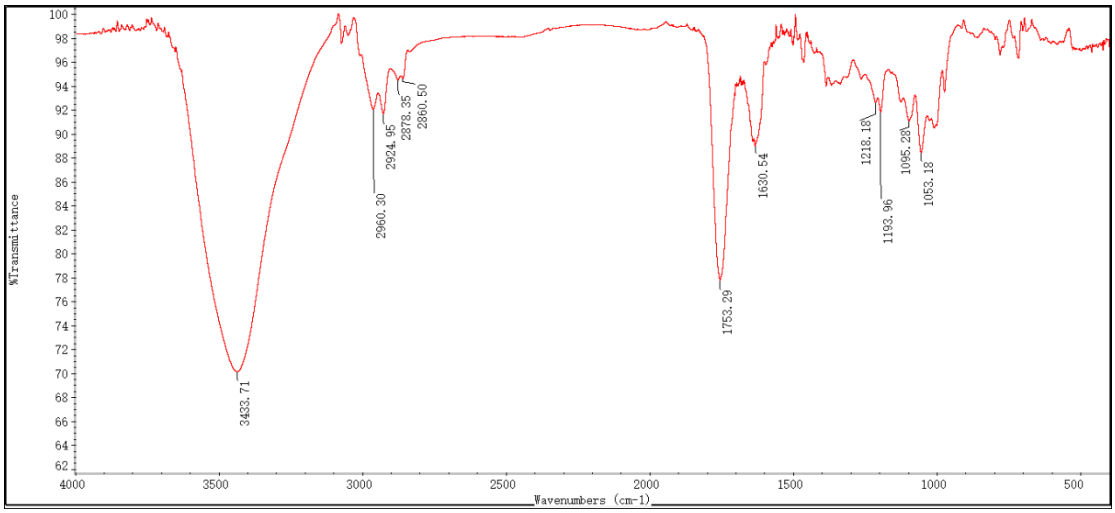

**Figure S71–S80.** 1D and 2D NMR, MS, and IR spectra of fortalide F (**6**)

**Figure S71**. $^{1}$H NMR spectrum of fortalide F (**6**) in $CDCl_3$

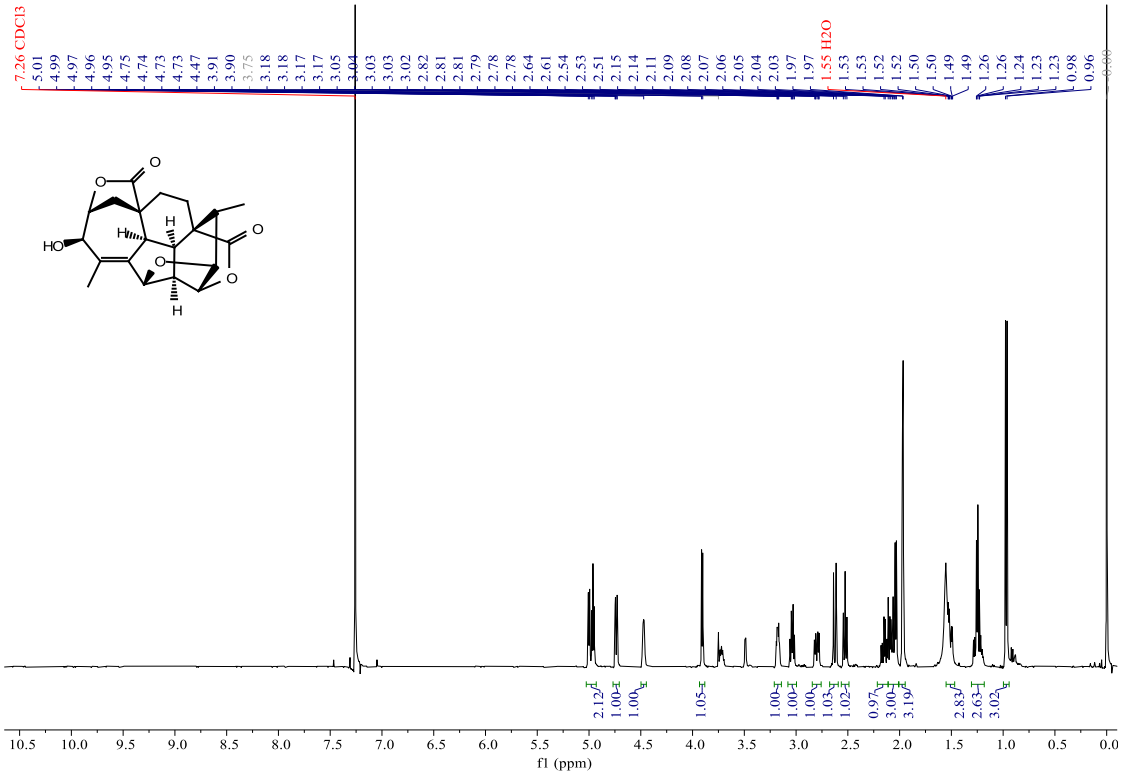


**Figure S72**. $^{13}$C NMR (BB and DEPT-135) spectra of fortalide F (**6**) in $CDCl_3$

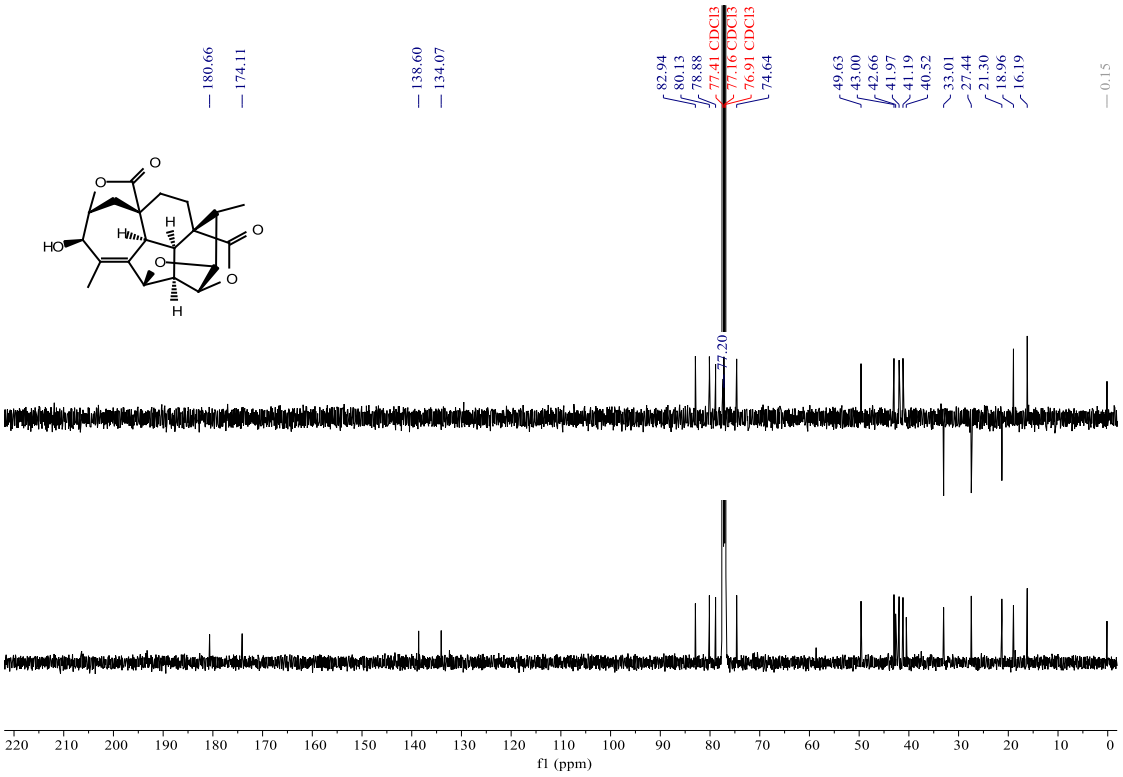

**Figure S73**. HSQC spectrum of fortalide F (**6**) in $CDCl_3$

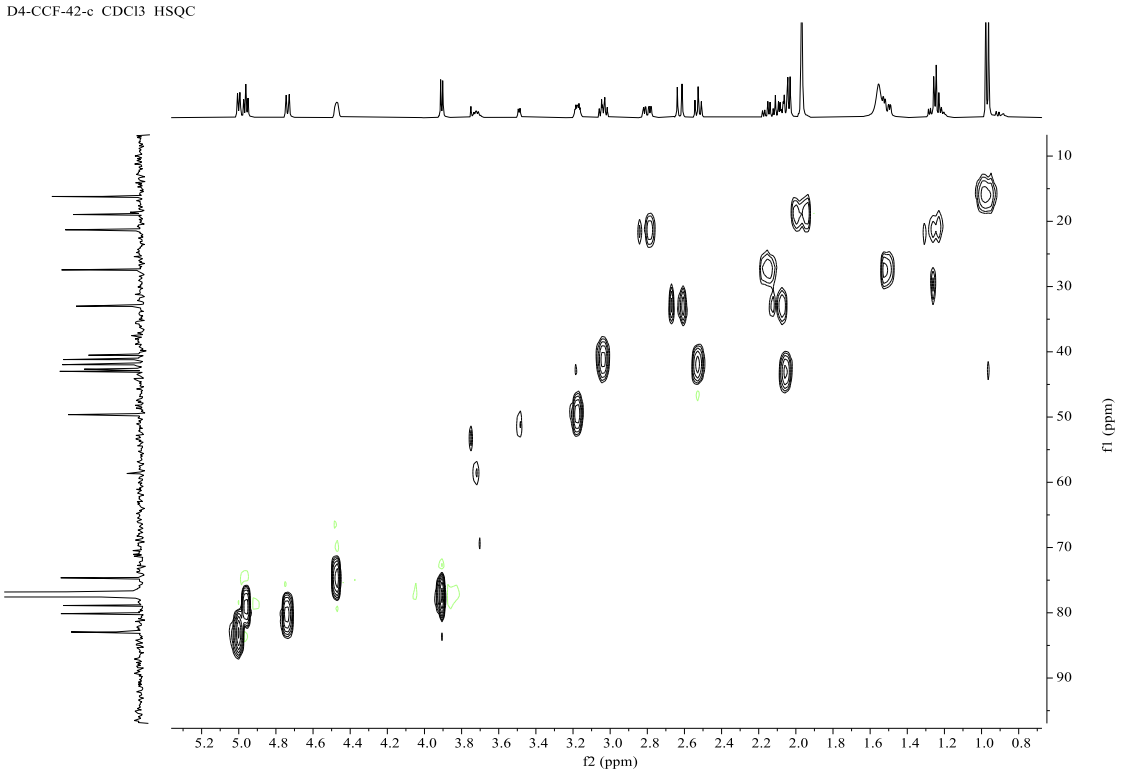


**Figure S74**. HMBC spectrum of fortalide F (**6**) in $CDCl_3$

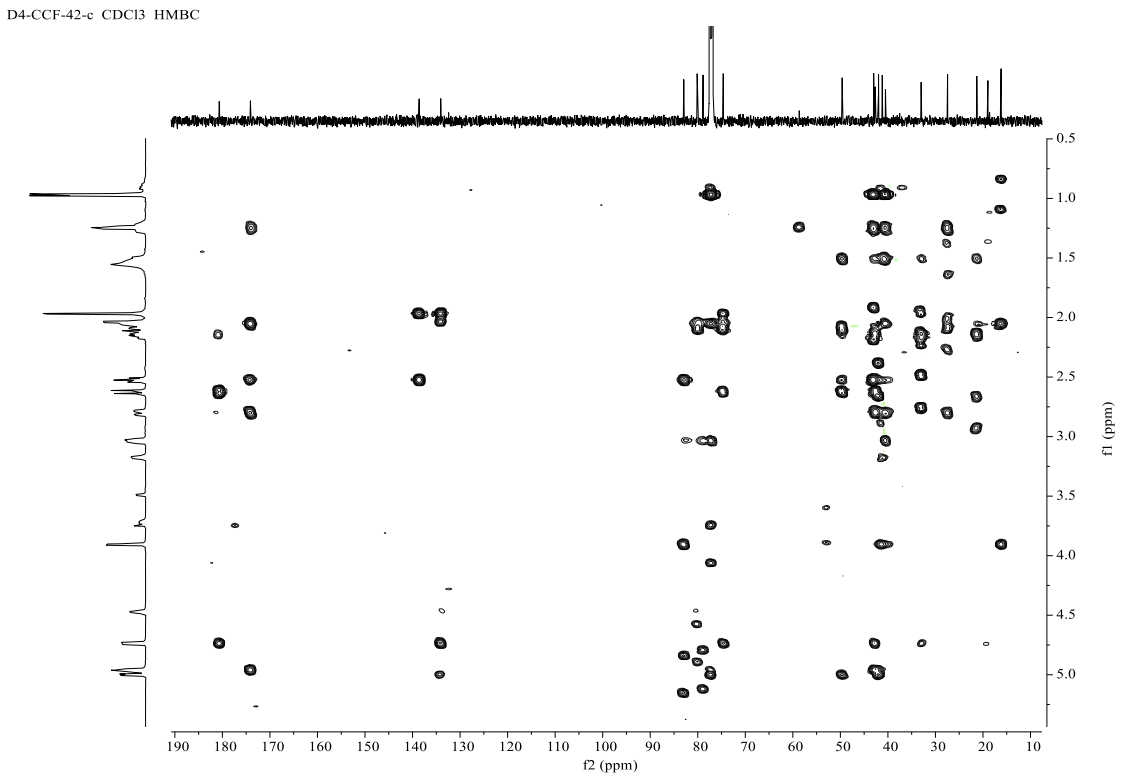

**Figure S75**. $^{1}H$-$^{1}H$ COSY spectrum of fortalide F (**6**) in $CDCl_3$

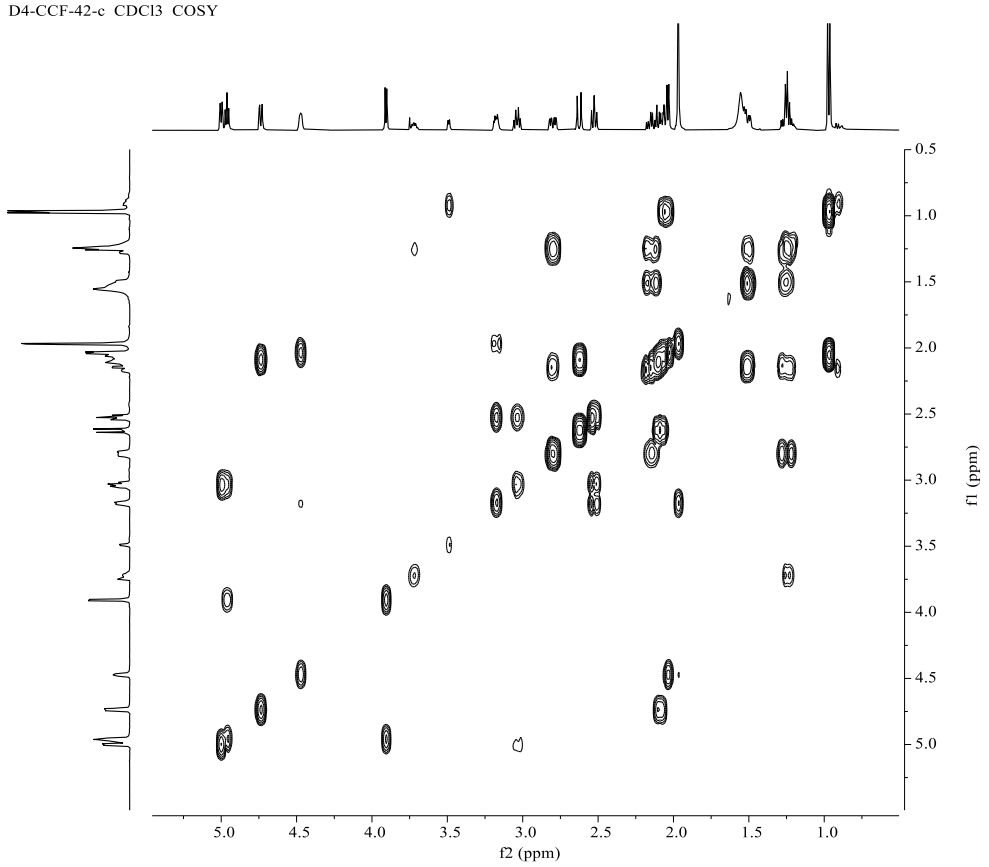


**Figure S76**. ROESY spectrum of fortalide F (**6**) in $CDCl_3$

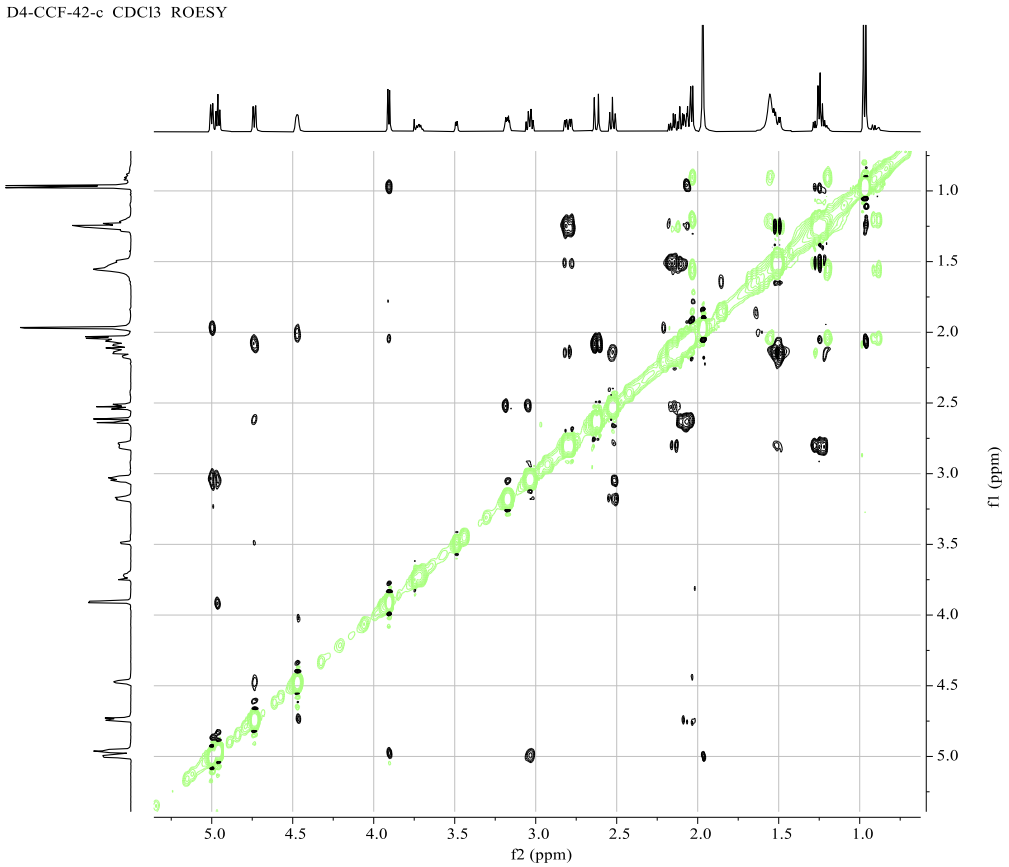

**Figure S77**. (+)-ESIMS spectrum of fortalide F (**6**)

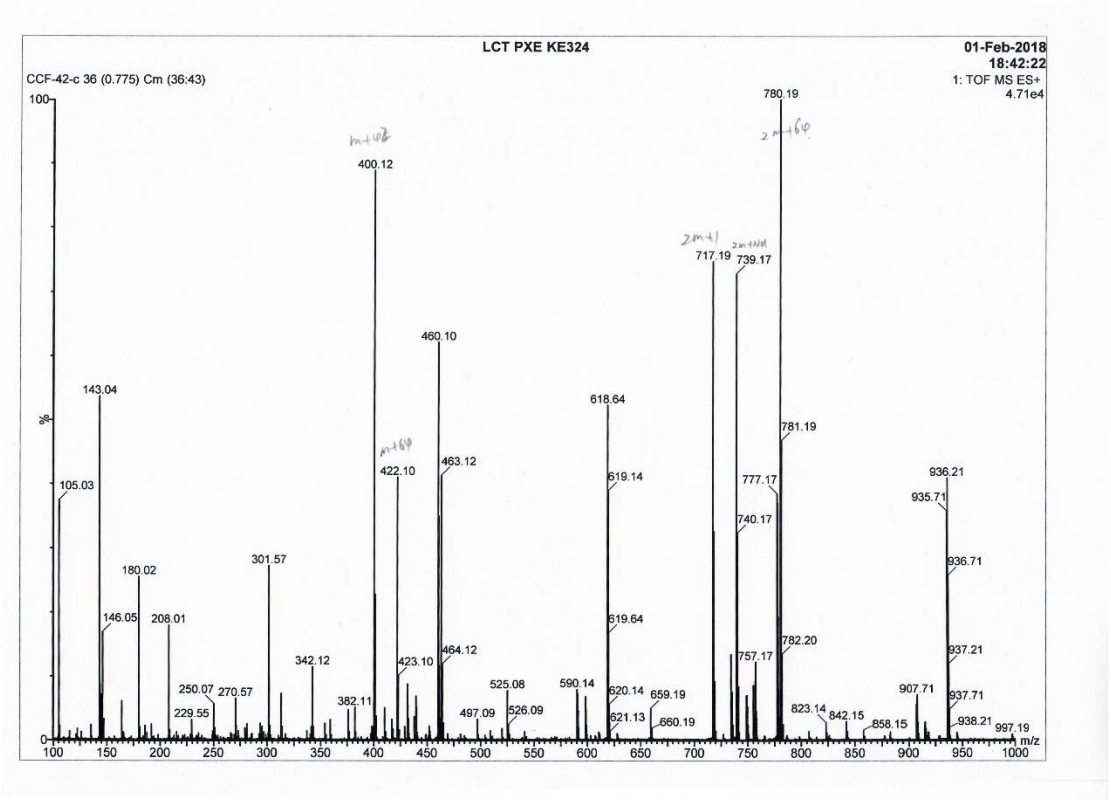


**Figure S78**. (−)-ESIMS spectrum of fortalide F (**6**)

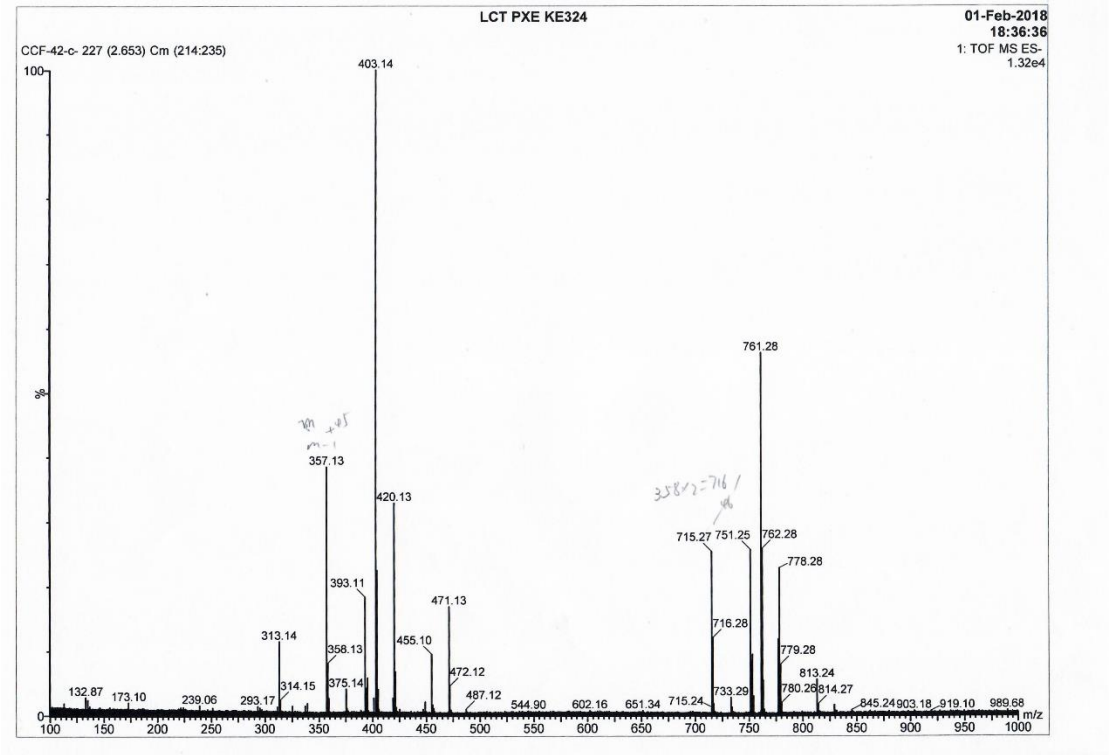

**Figure S79**. (−)-HRESIMS spectrum of fortalide F (**6**)

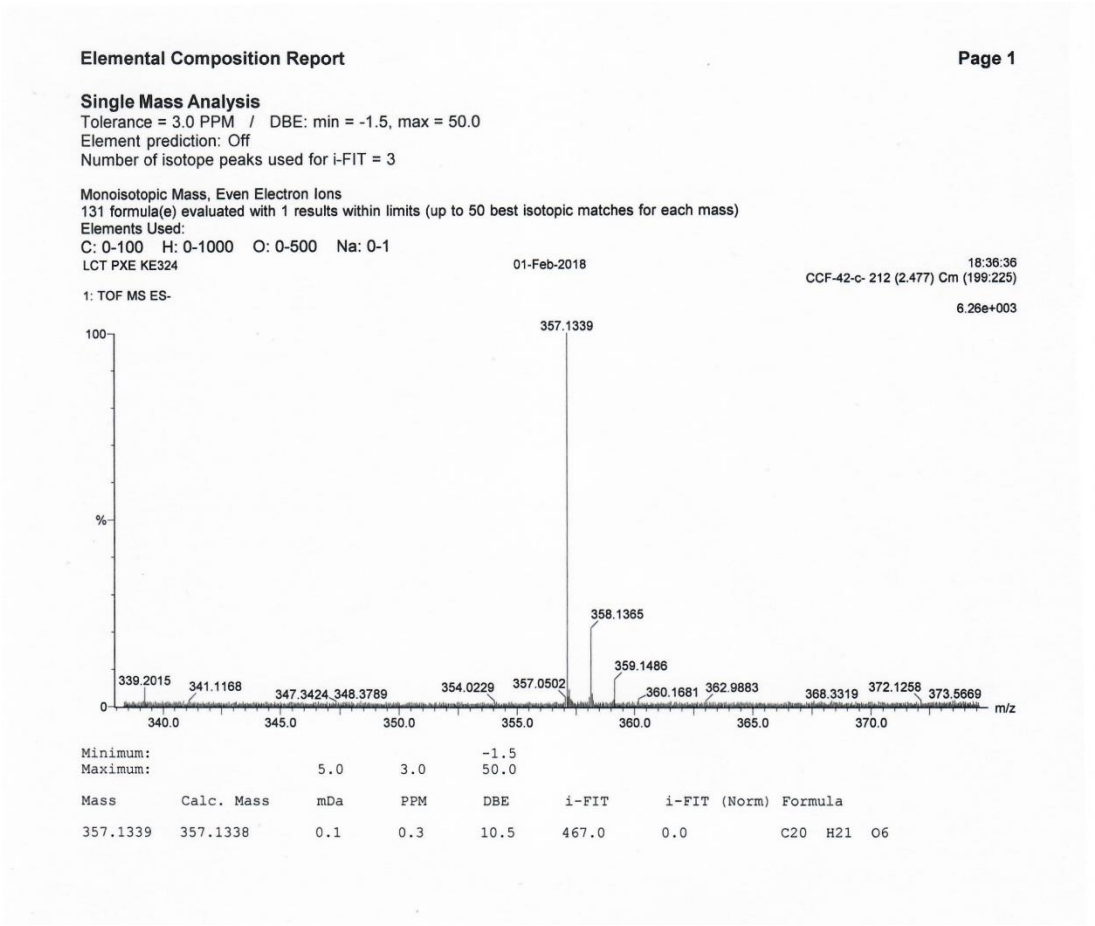


**Figure S80**. IR spectrum of fortalide F (**6**)

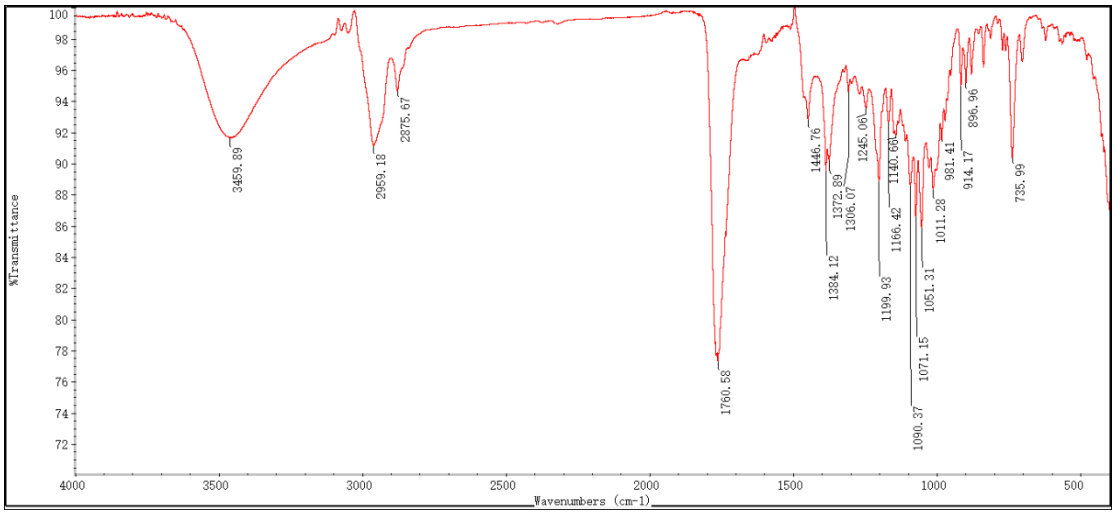

**Figure S81–S92.** 1D and 2D NMR, MS, and IR spectra of fortalide G (**7**)

**Figure S81**. $^{1}$H NMR spectrum of fortalide G (**7**) in methanol-$d_4$.

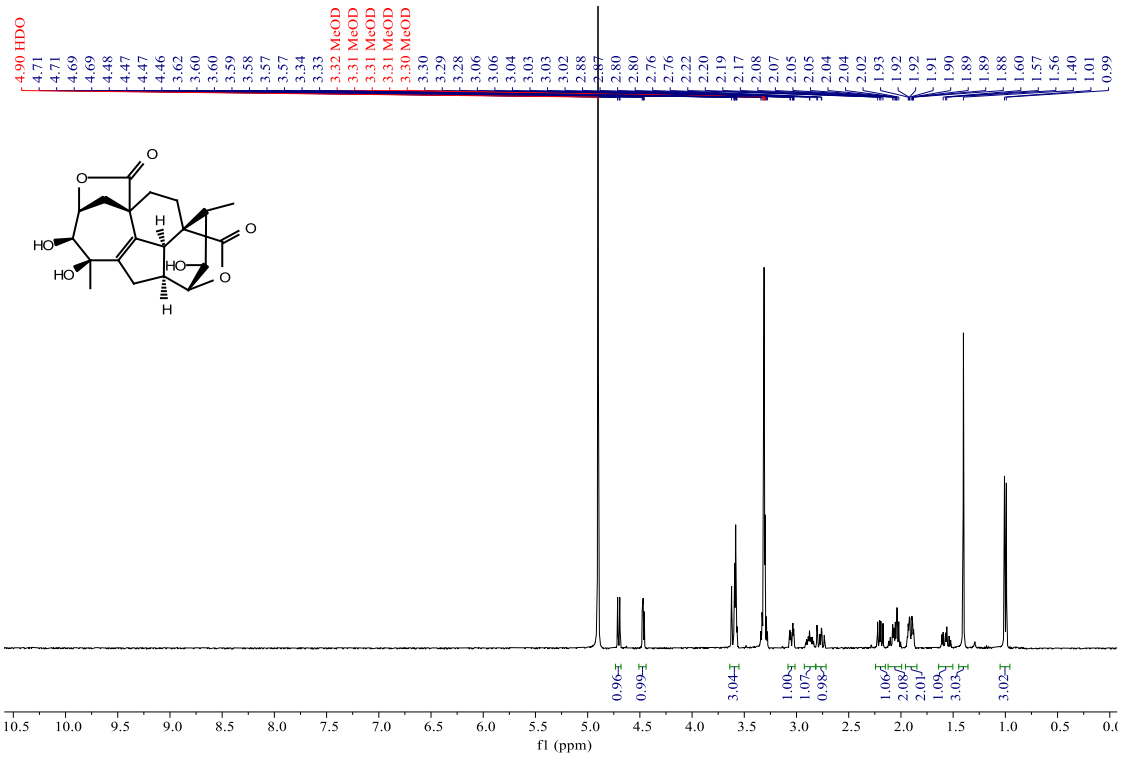


**Figure S82**. $^{1}$H NMR spectrum of fortalide G (**7**) in pyridine-$d_5$.

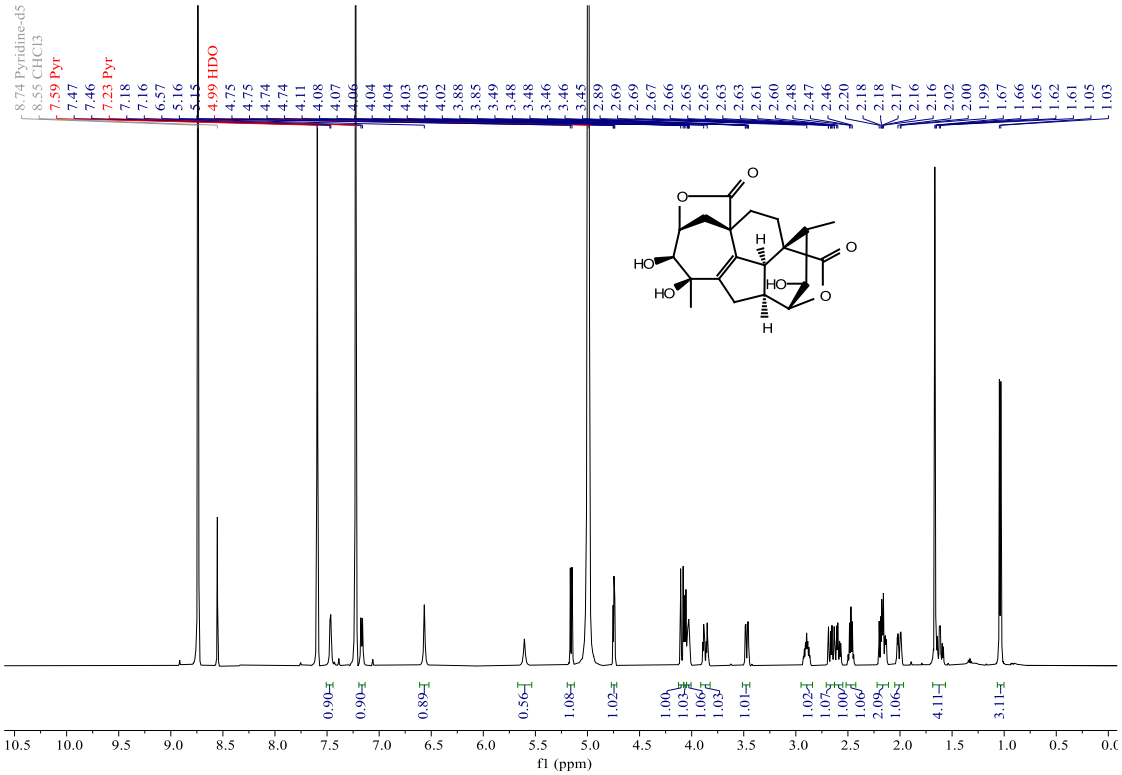

**Figure S83**. $^{13}$C NMR (BB and DEPT-135) spectra of fortalide G (**7**) in methanol-$d_4$.

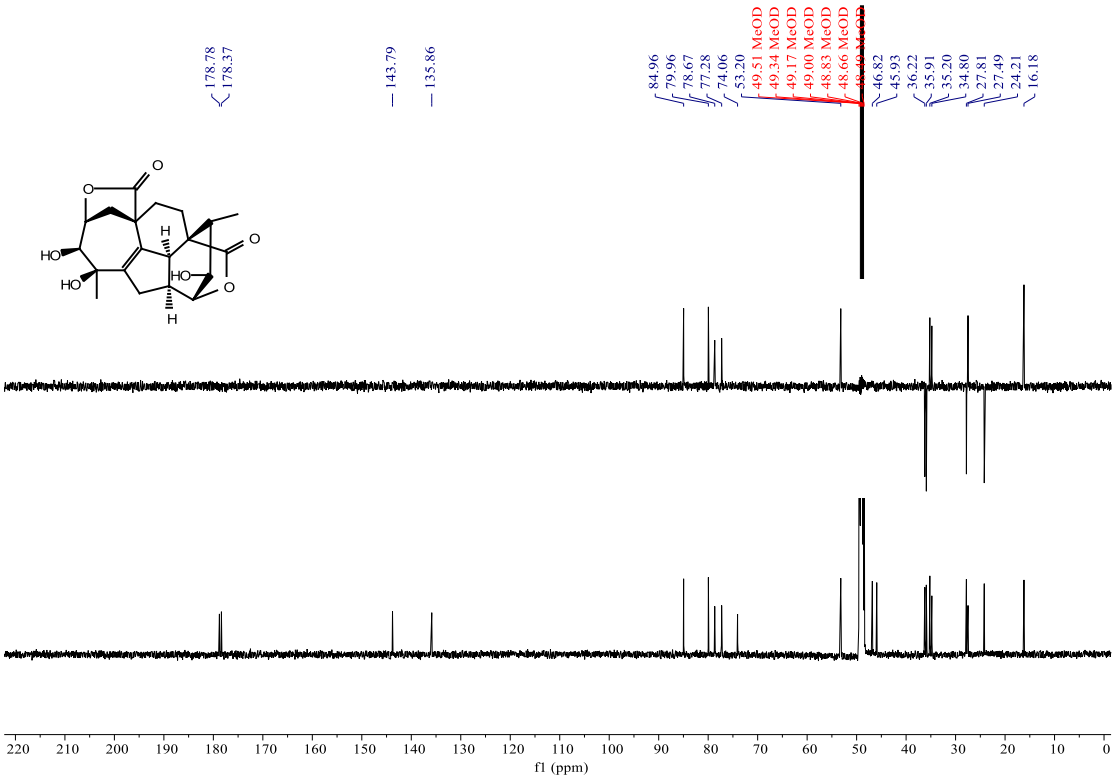


**Figure S84**. $^{13}$C NMR (BB and DEPT-135) spectra of fortalide G (**7**) in pyridine-$d_5$.

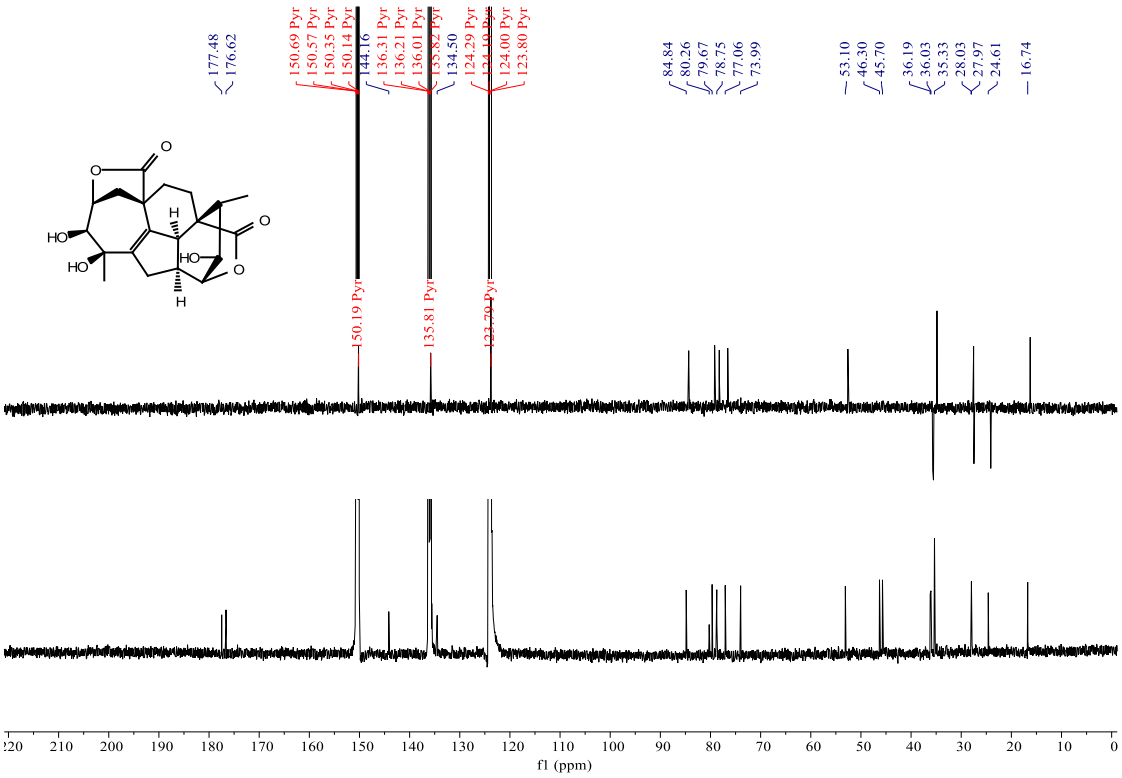

**Figure S85**. HSQC spectrum of fortalide G (**7**) in pyridine-$d_5$.

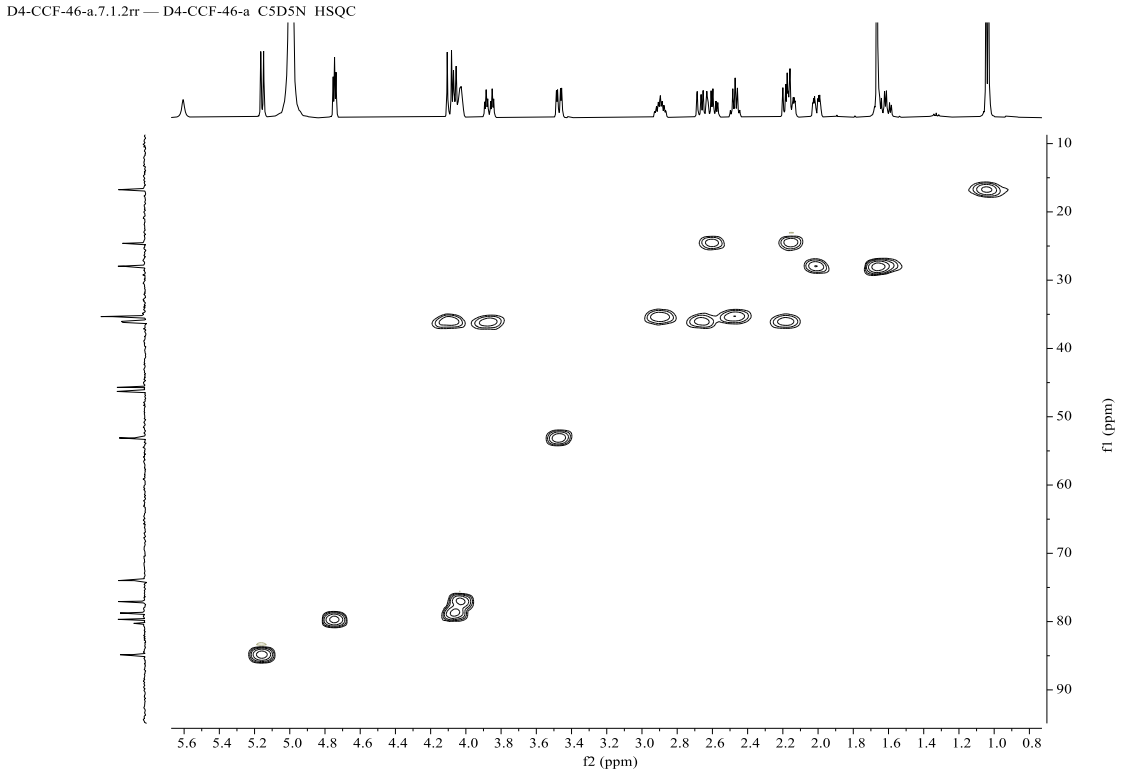


**Figure S86**. HMBC spectrum of fortalide G (**7**) in pyridine-$d_5$.

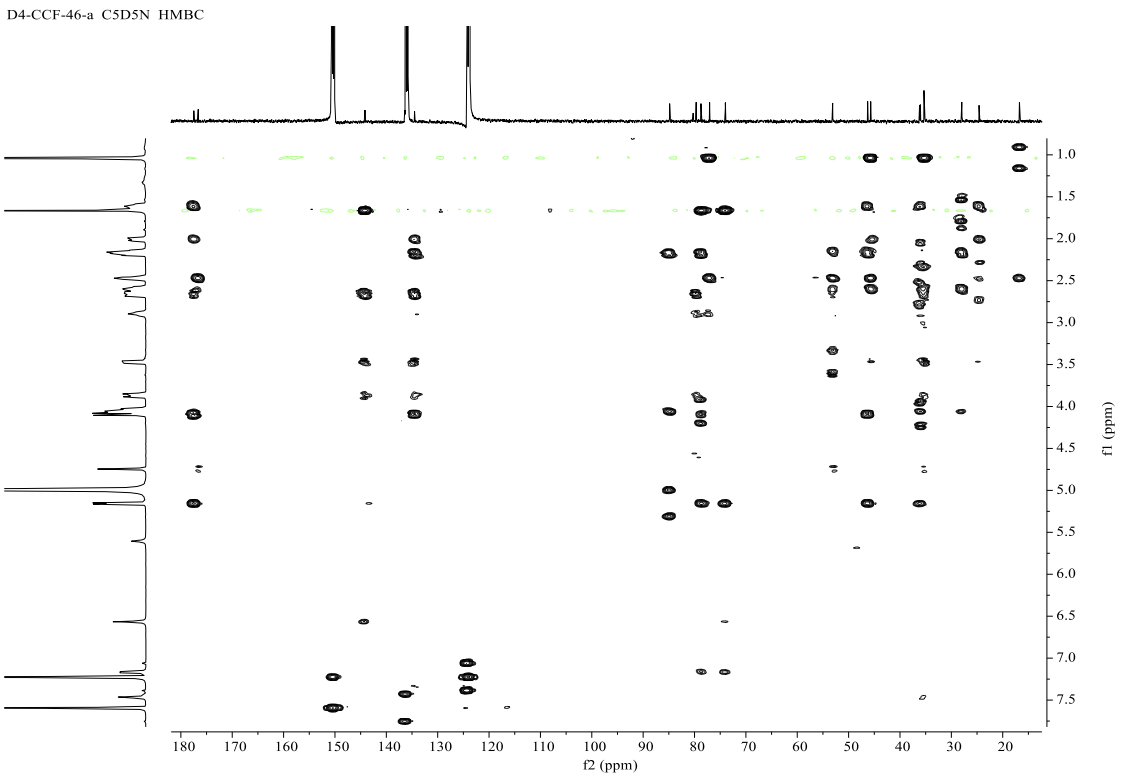

**Figure S87**. $^{1}$H-$^{1}$H COSY spectrum of fortalide G (**7**) in pyridine-$d_5$.

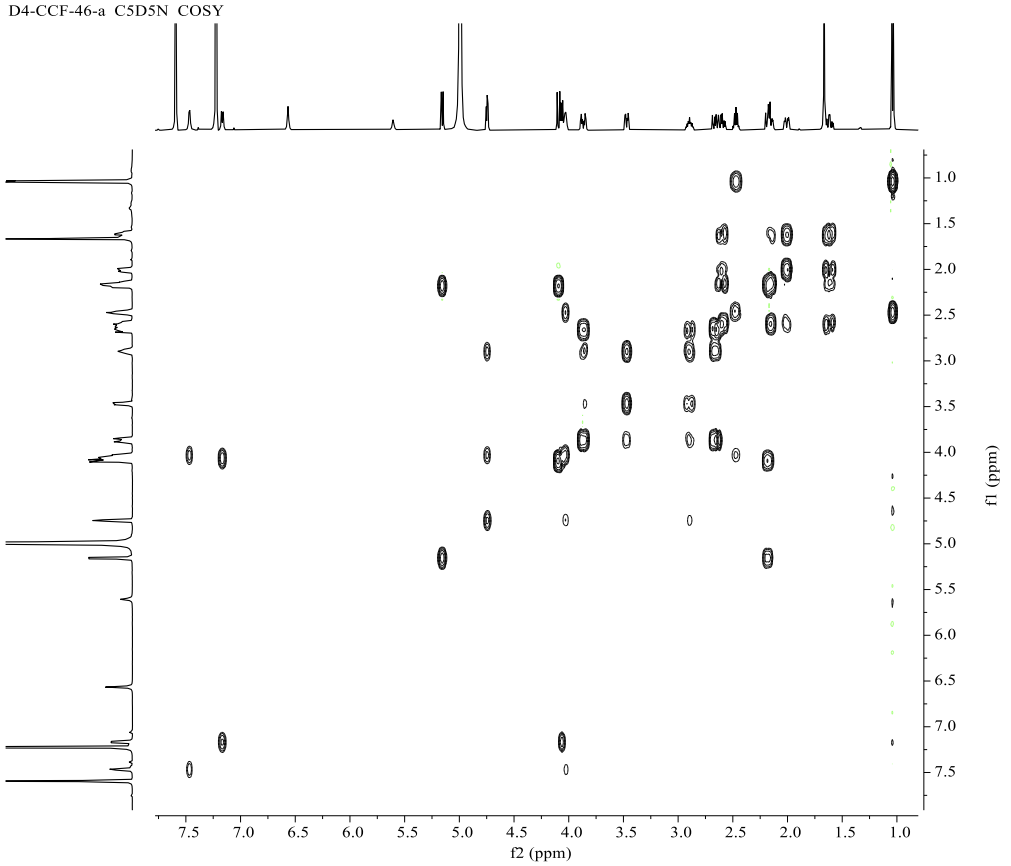


**Figure S88**. NOESY spectrum of fortalide G (**7**) in pyridine-$d_5$.

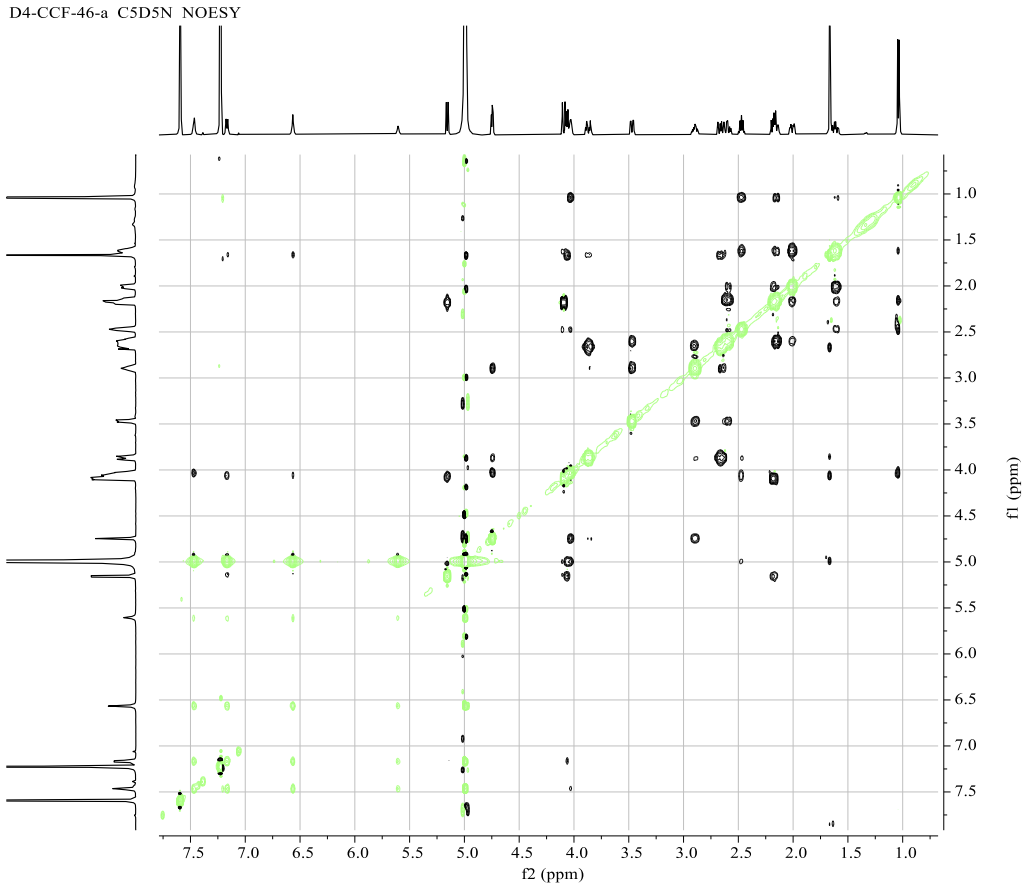

**Figure S89**. (+)-ESIMS spectrum of fortalide G (**7**).

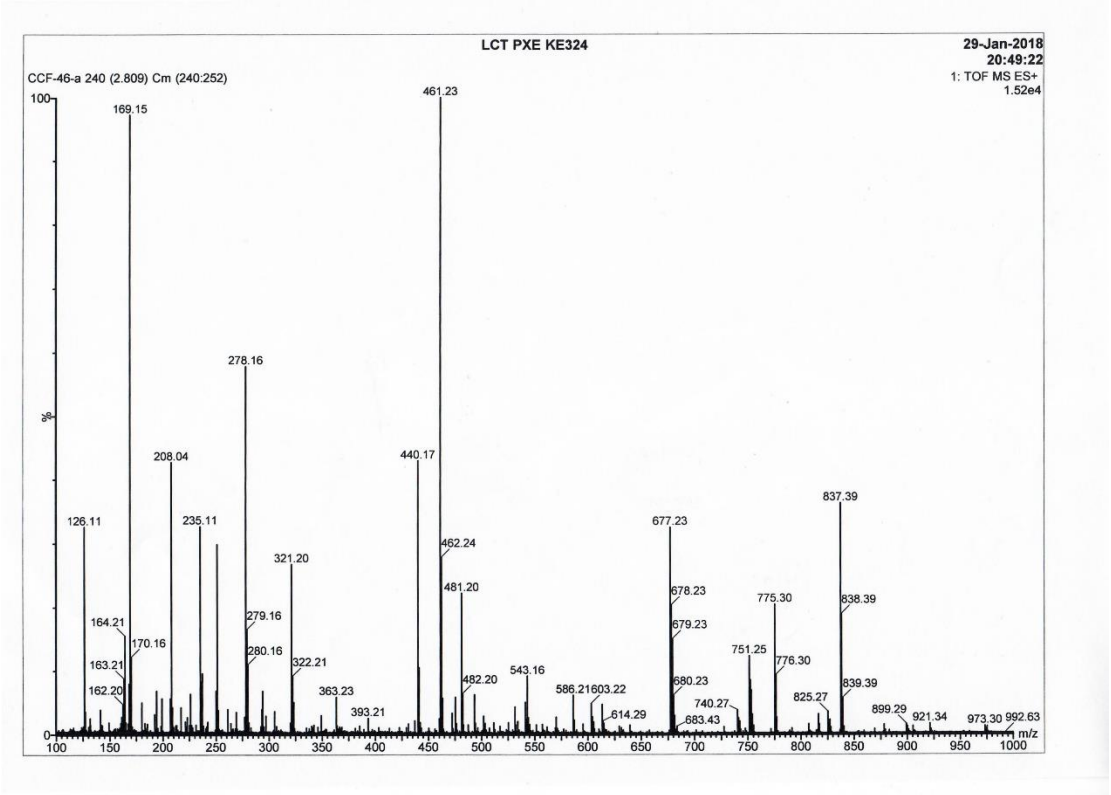


**Figure S90**. (−)-ESIMS spectrum of fortalide G (**7**).

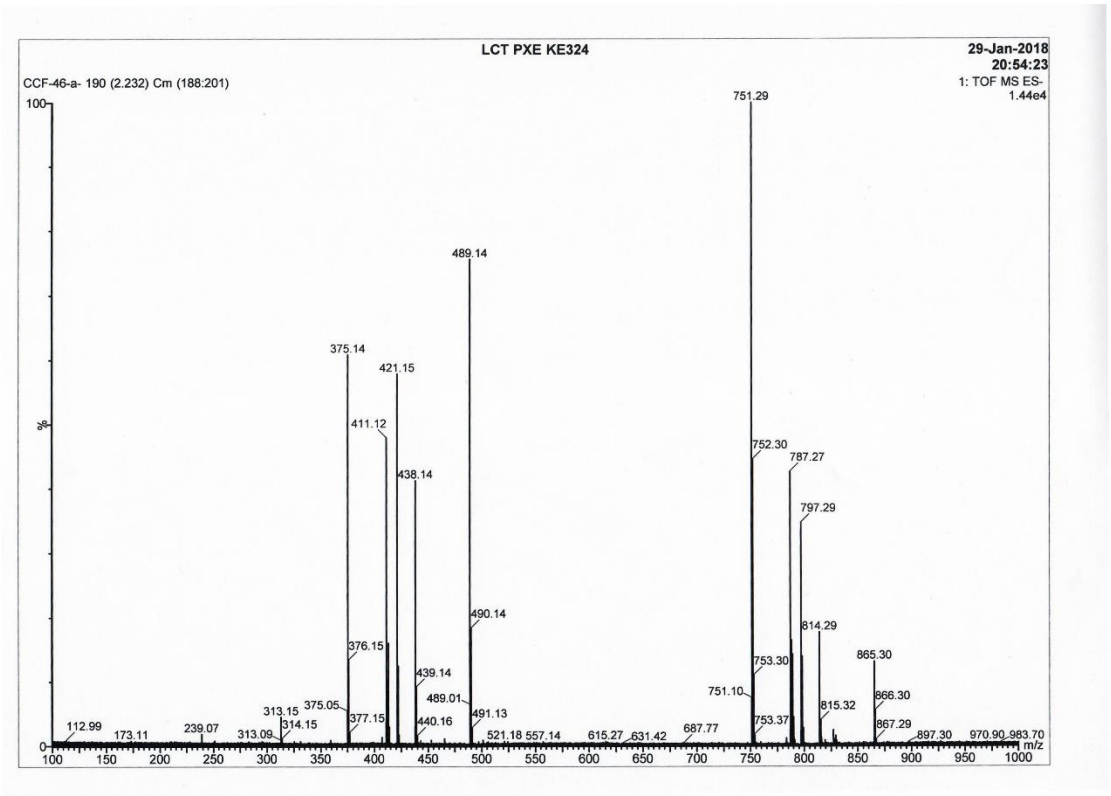

**Figure S91**. (−)-HRESIMS spectrum of fortalide G (**7**).

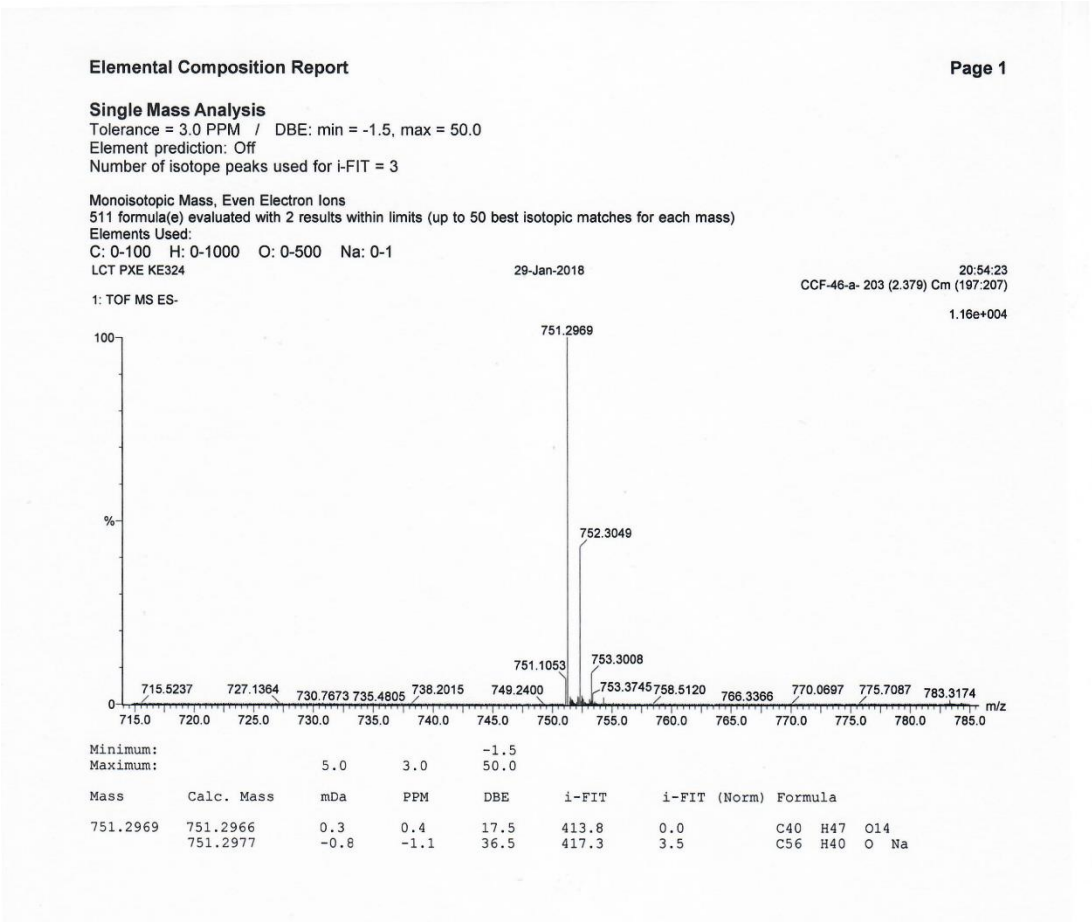

**Elemental Composition Report** **Page 1**

**Single Mass Analysis**
Tolerance = 3.0 PPM / DBE: min = -1.5, max = 50.0
Element prediction: Off
Number of isotope peaks used for i-FIT = 3

Monoisotopic Mass, Even Electron Ions
511 formula(e) evaluated with 2 results within limits (up to 50 best isotopic matches for each mass)
Elements Used:
C: 0-100 H: 0-1000 O: 0-500 Na: 0-1

LCT PXE KE324 29-Jan-2018 20:54:23
CCF-46-a- 203 (2.379) Cm (197:207)
1: TOF MS ES- 1.16e+004



| | | | | | | | |
|---|---|---|---|---|---|---|---|
| Minimum: | | 5.0 | 3.0 | -1.5 | | | |
| Maximum: | | | | 50.0 | | | |
| Mass | Calc. Mass | mDa | PPM | DBE | i-FIT | i-FIT (Norm) | Formula |
| 751.2969 | 751.2966 | 0.3 | 0.4 | 17.5 | 413.8 | 0.0 | C40 H47 O14 |
| | 751.2977 | -0.8 | -1.1 | 36.5 | 417.3 | 3.5 | C56 H40 O Na |

**Figure S92**. IR spectrum of fortalide G (**7**).

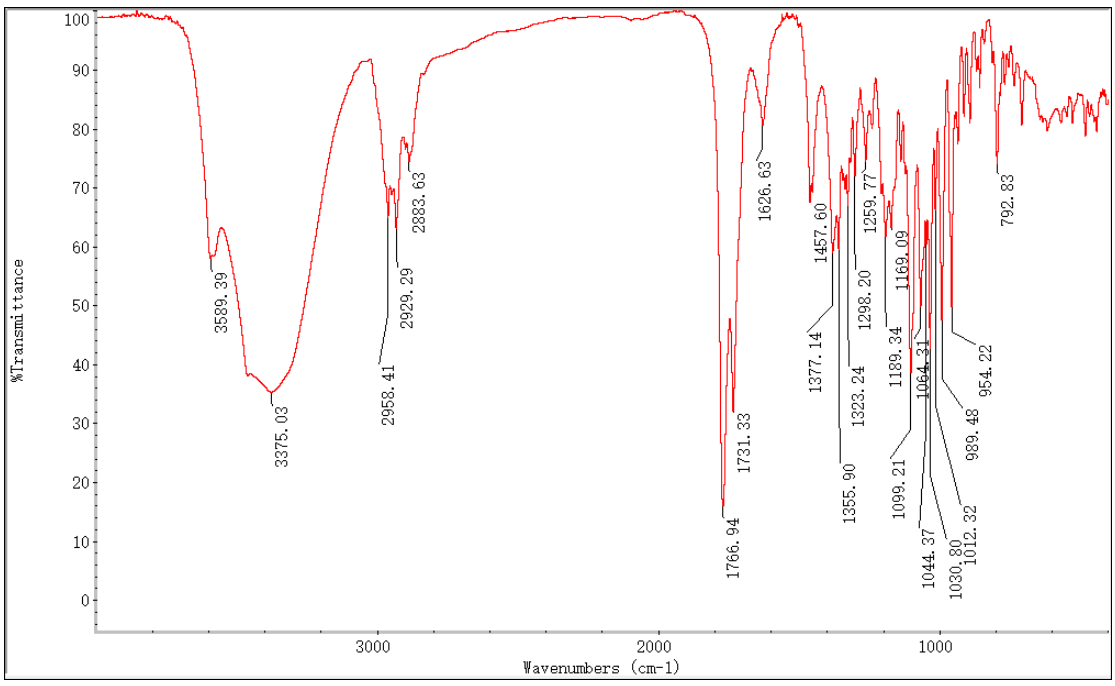

**Figure S93–S102.** 1D and 2D NMR, MS, and IR spectra of fortalide H (**8**)

**Figure S93**. $^{1}$H NMR spectrum of fortalide H (**8**) in methanol-$d_4$.

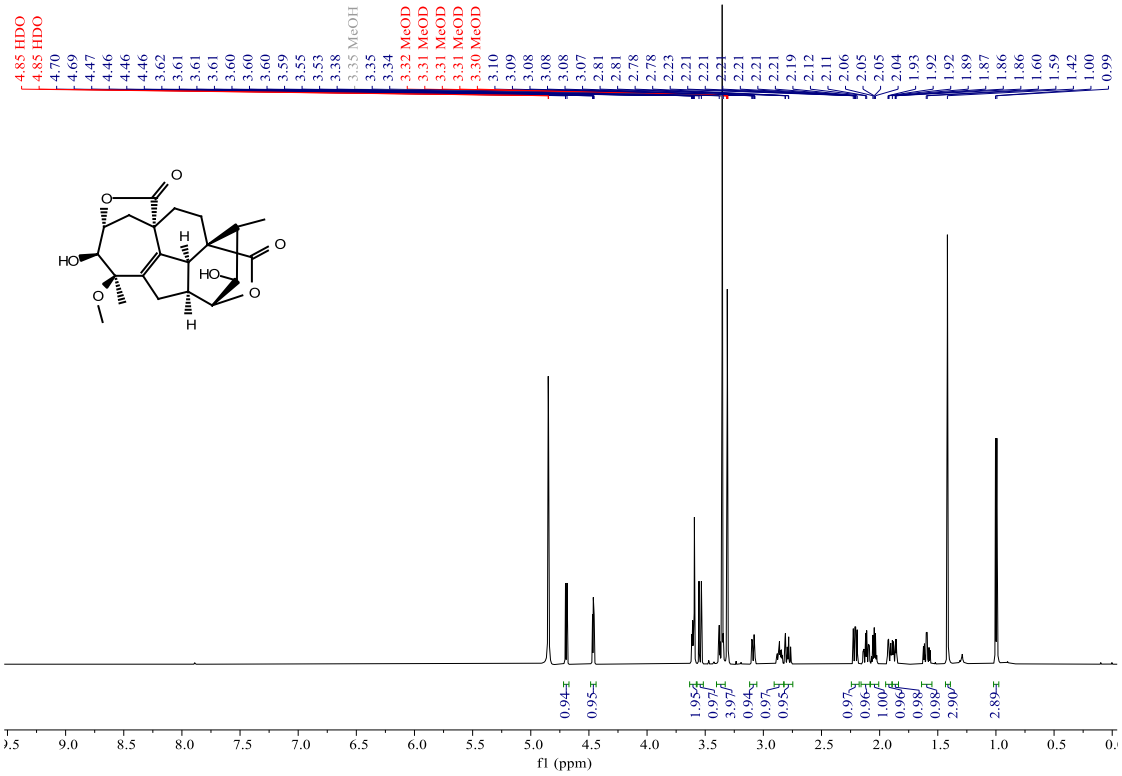


**Figure S94**. $^{13}$C NMR (BB and DEPT-135) spectra of fortalide H (**8**) in methanol-$d_4$.

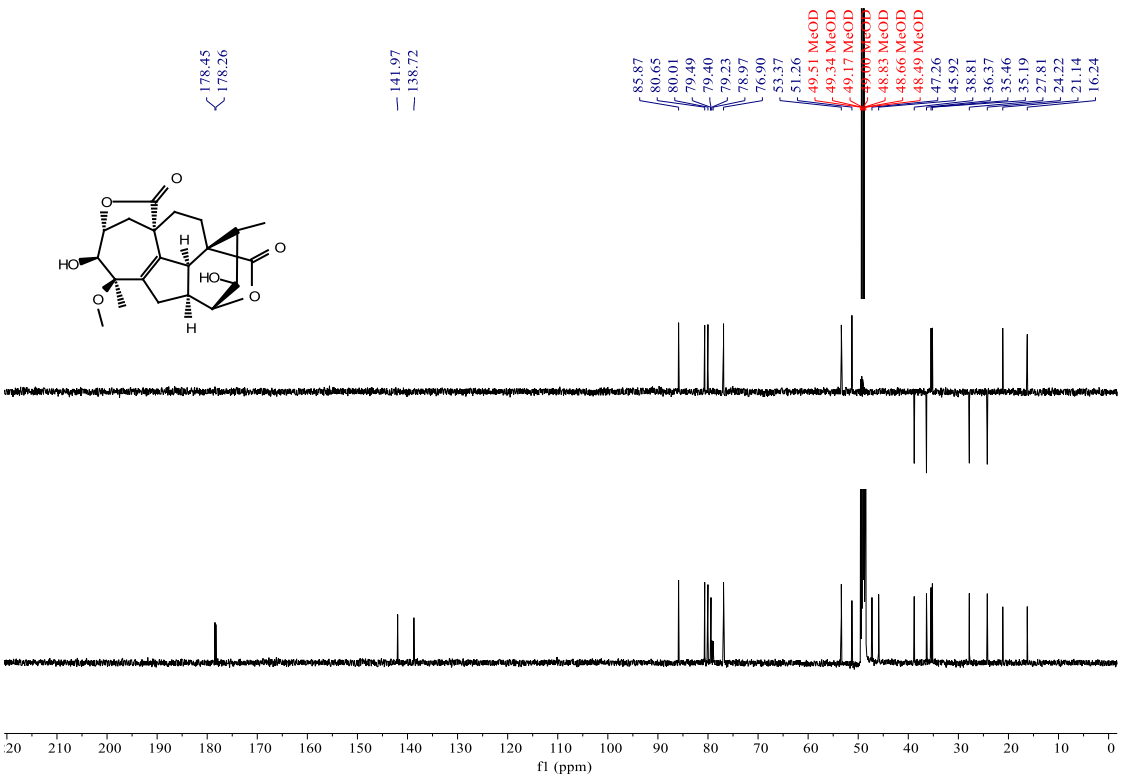

**Figure S95**. HSQC spectrum of fortalide H (**8**) in methanol-$d_4$.

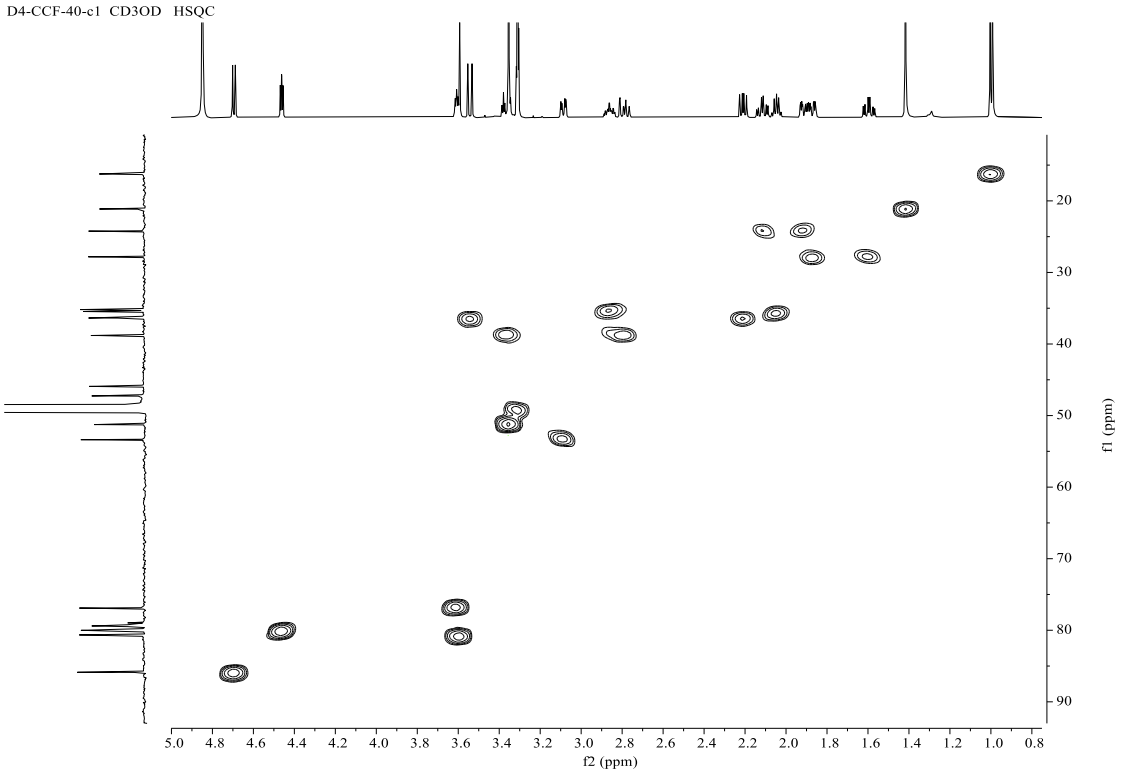


**Figure S96** HMBC spectrum of fortalide H (**8**) in methanol-$d_4$.

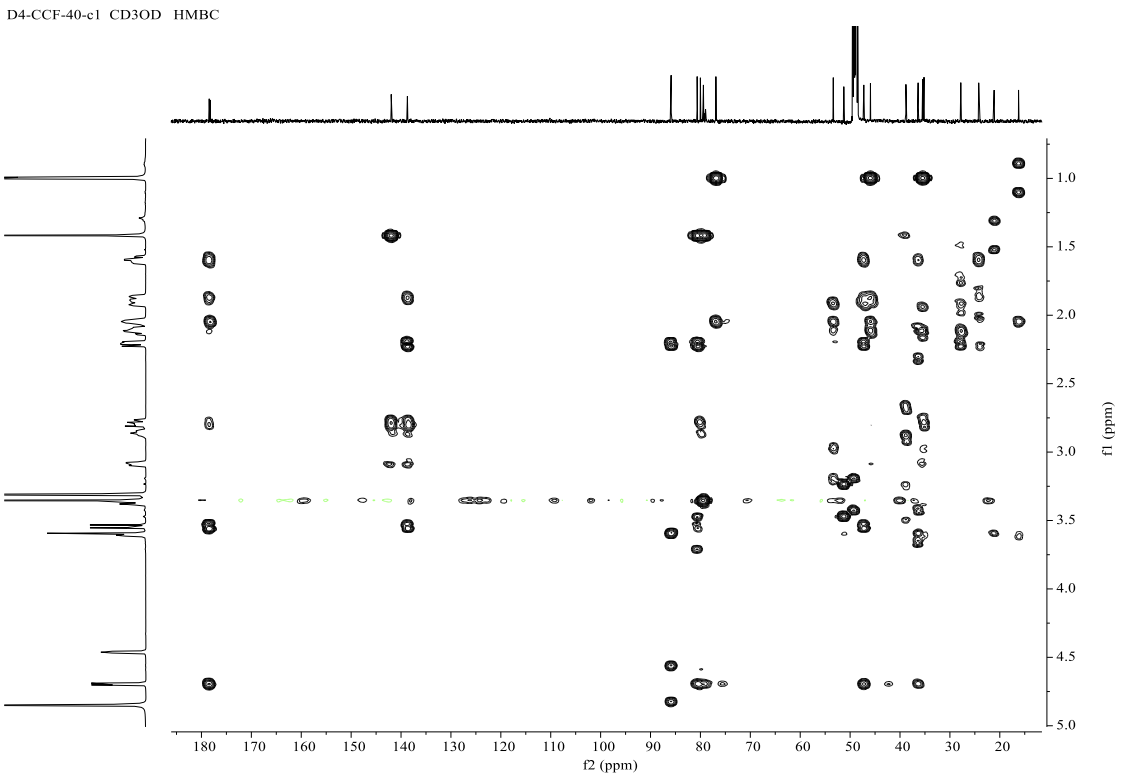

**Figure S97**. $^{1}$H-$^{1}$H COSY spectrum of fortalide H (**8**) in methanol-$d_4$.

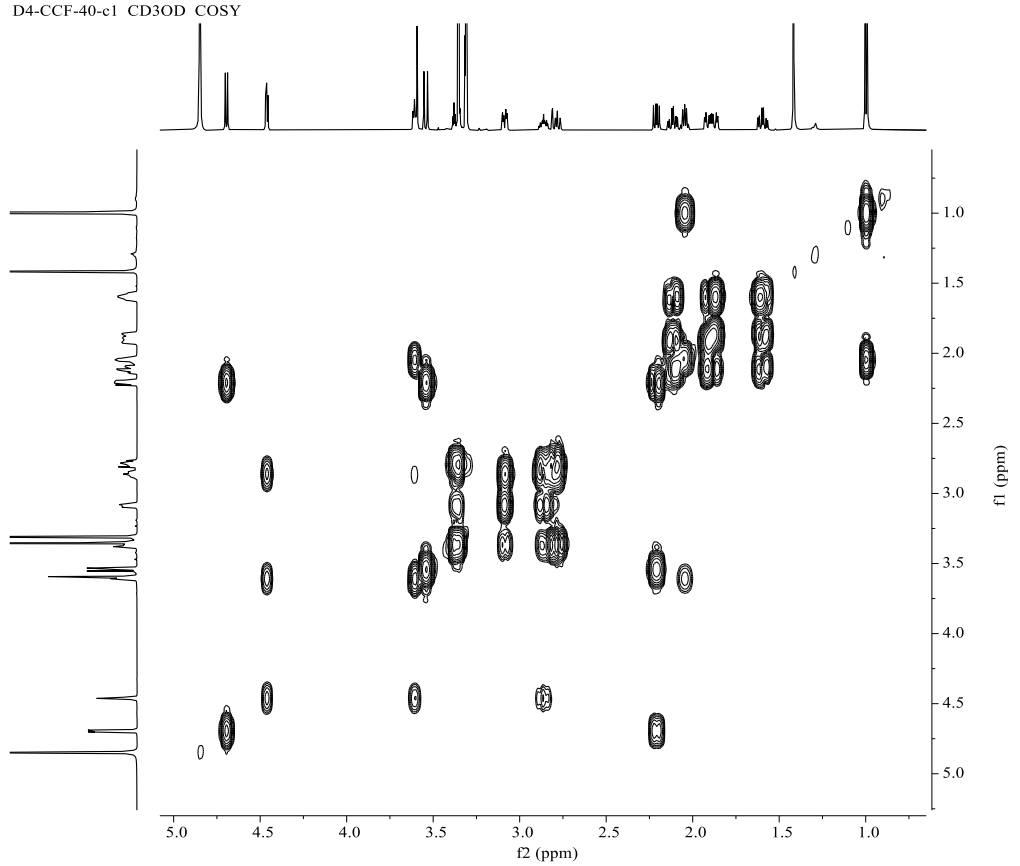


**Figure S98**. NOESY spectrum of fortalide H (**8**) in methanol-$d_4$.

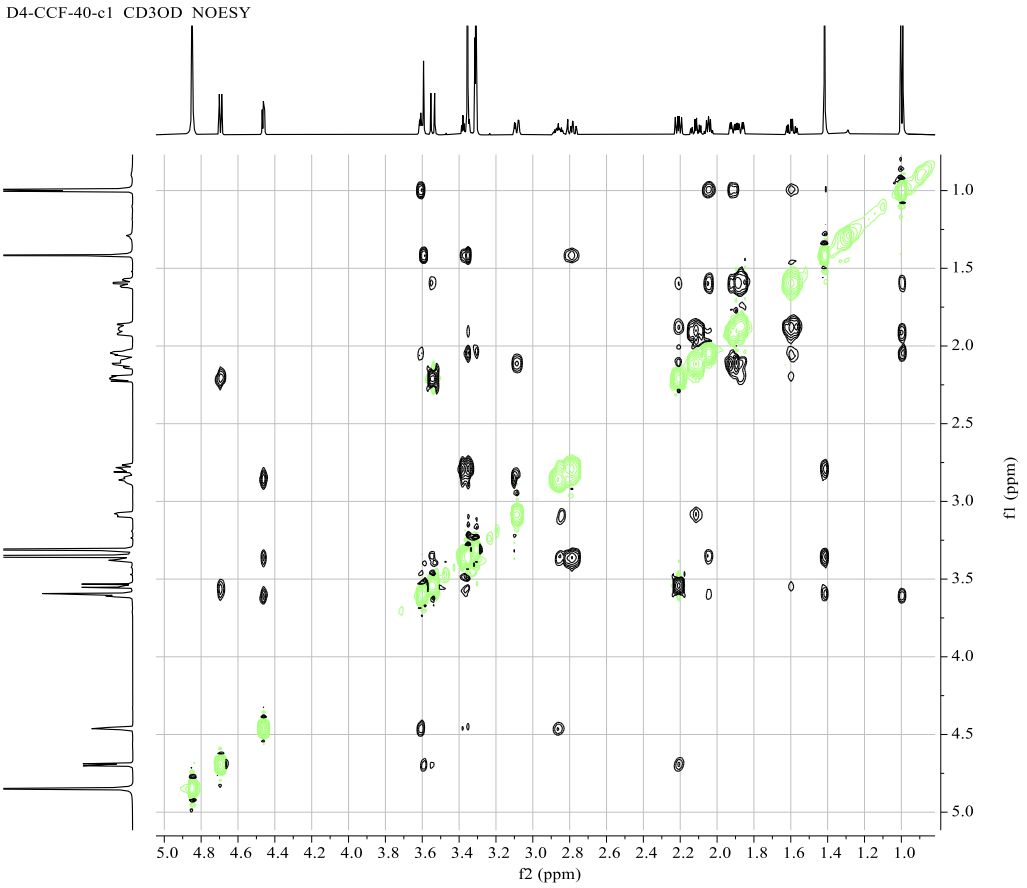

**Figure S99**. (+)-ESIMS spectrum of fortalide H (**8**).

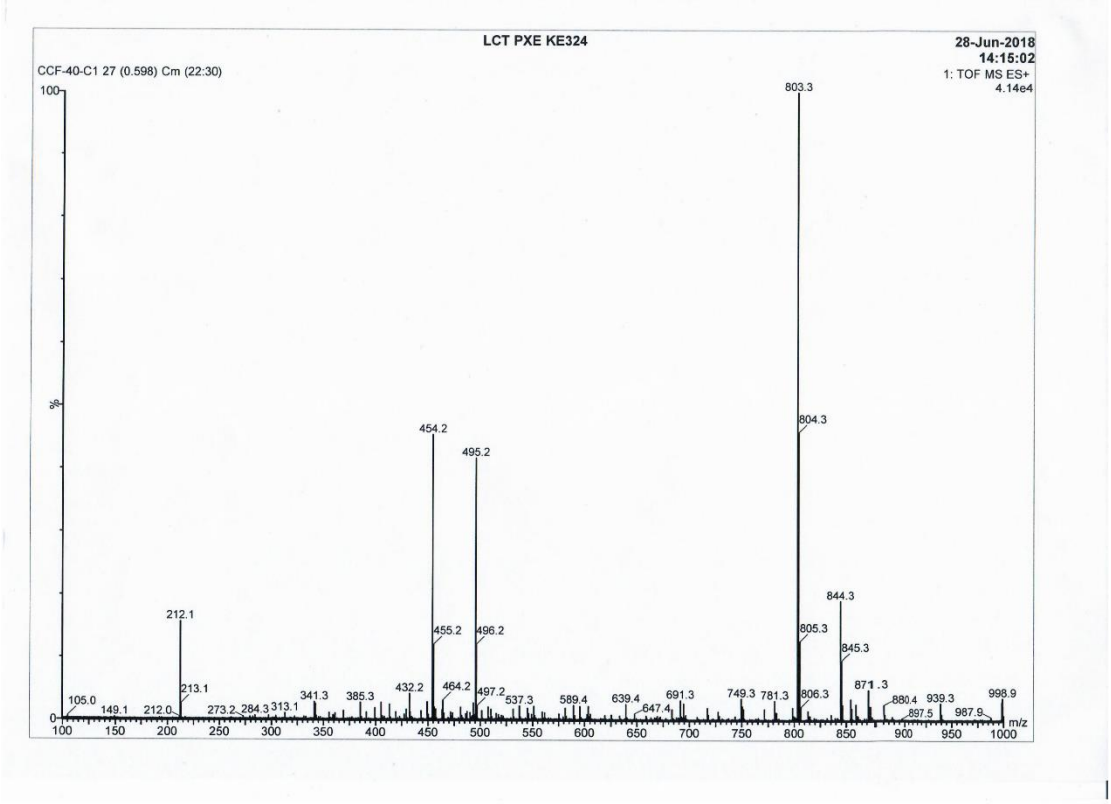


**Figure S100**. (−)-ESIMS spectrum of fortalide H (**8**).

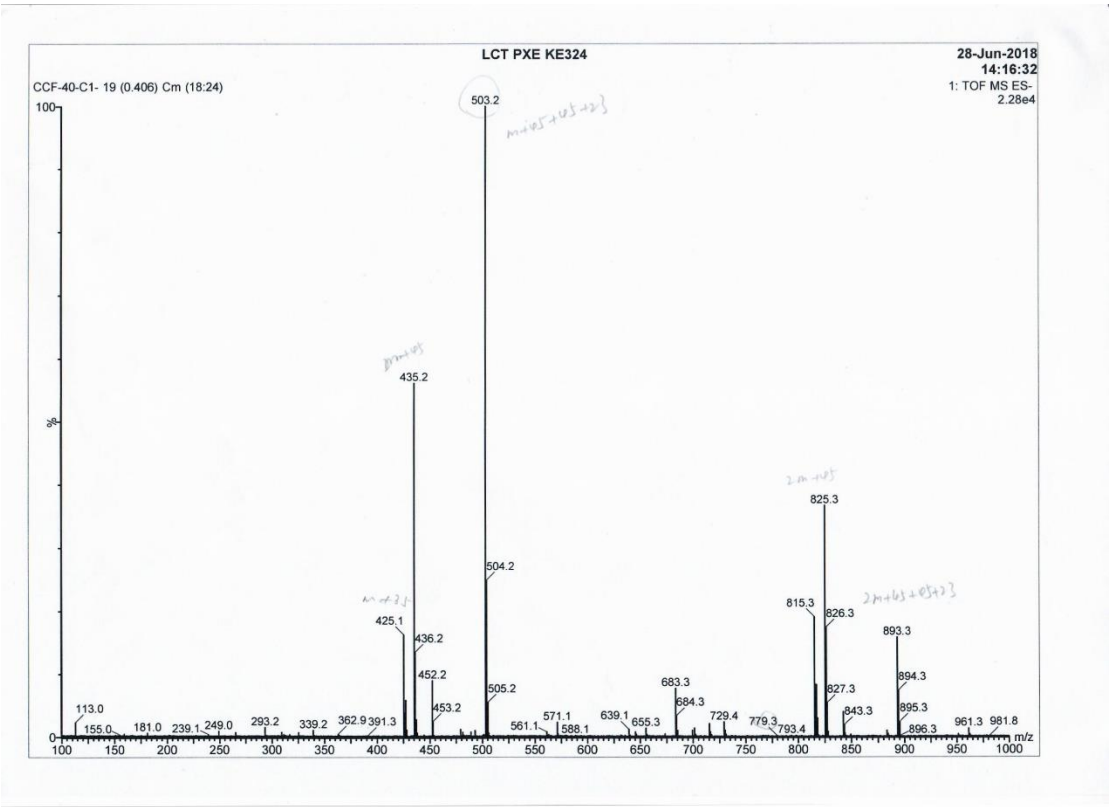

**Figure S101**. (−)-HRESIMS spectrum of fortalide H (**8**).

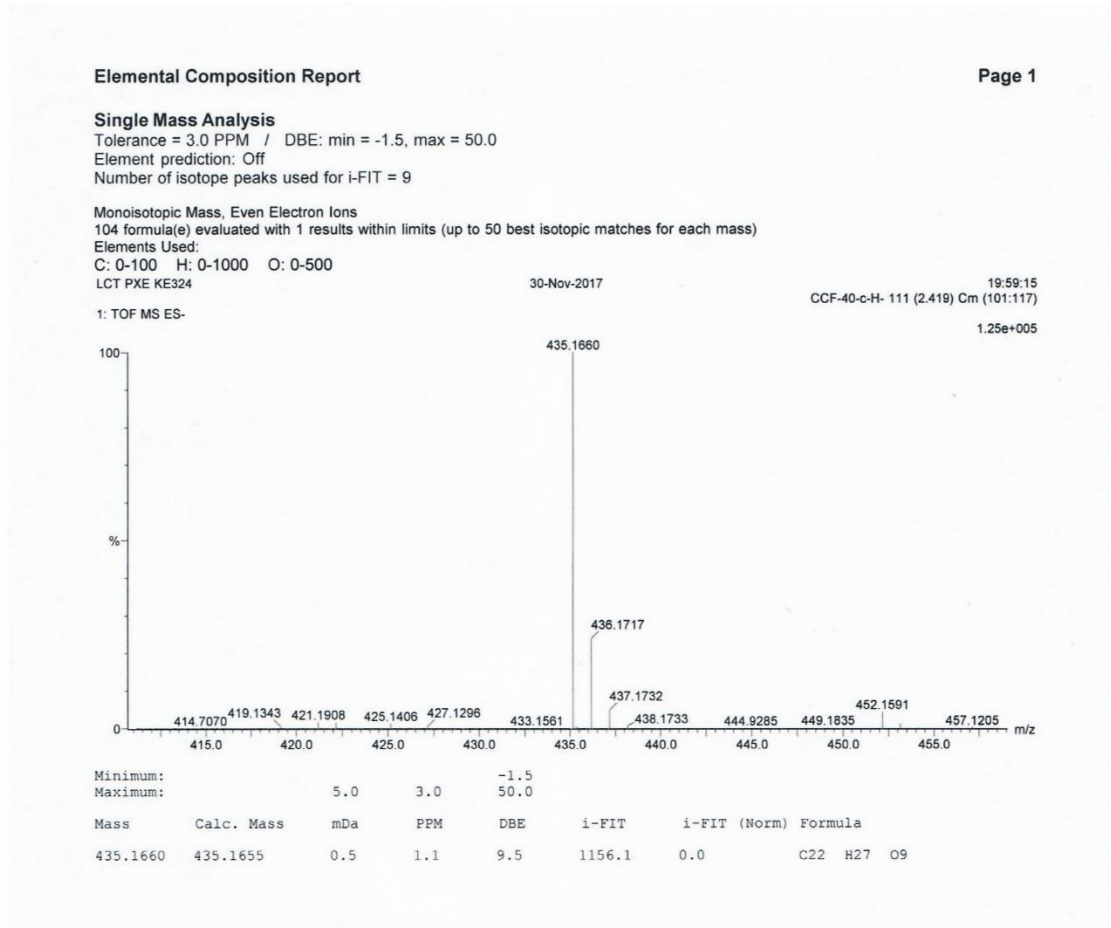


**Figure S102**. IR spectrum of fortalide H (**8**).

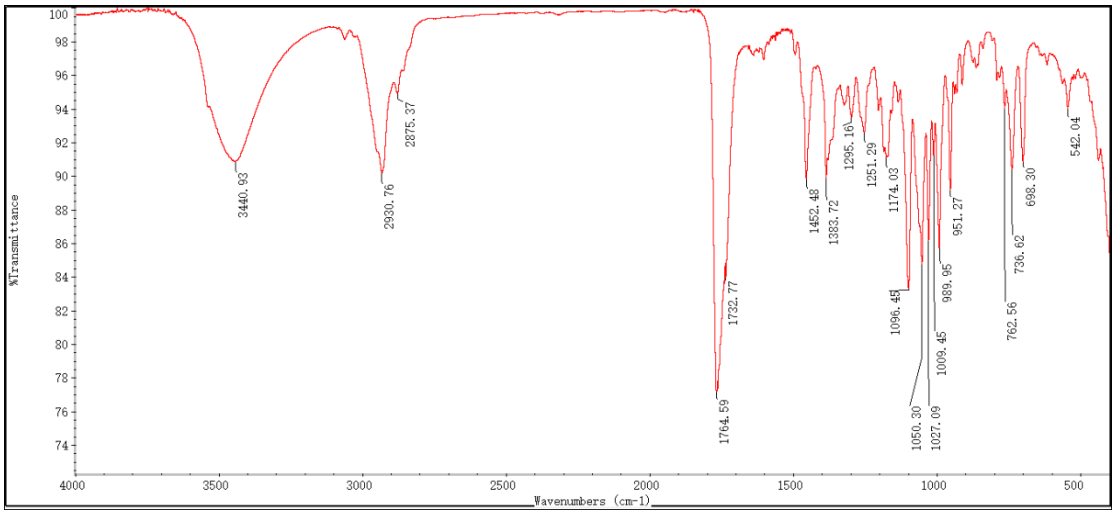

**Figure S103–S112.** 1D and 2D NMR, MS, and IR spectra of fortalide I (**9**)

**Figure S103**. $^{1}$H NMR spectrum of fortalide I (**9**) in methanol-$d_4$.

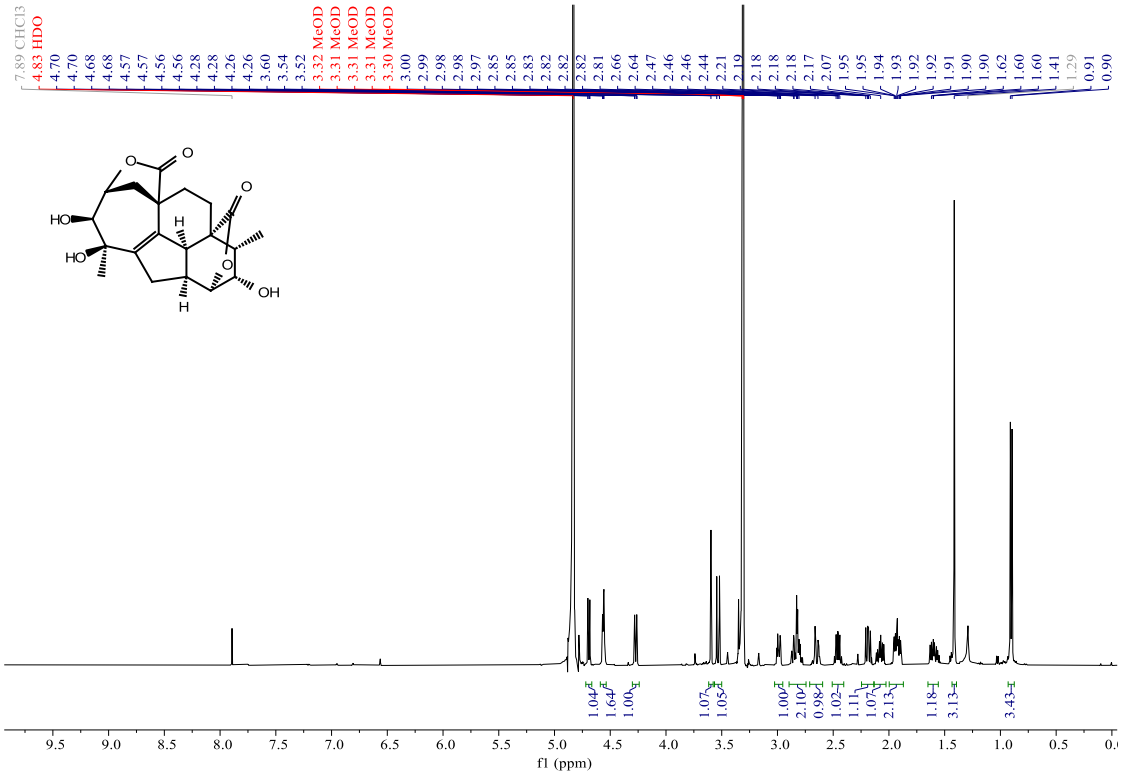


**Figure S104**. $^{13}$C NMR (BB and DEPT-135) spectra of fortalide I (**9**) in methanol-$d_4$.

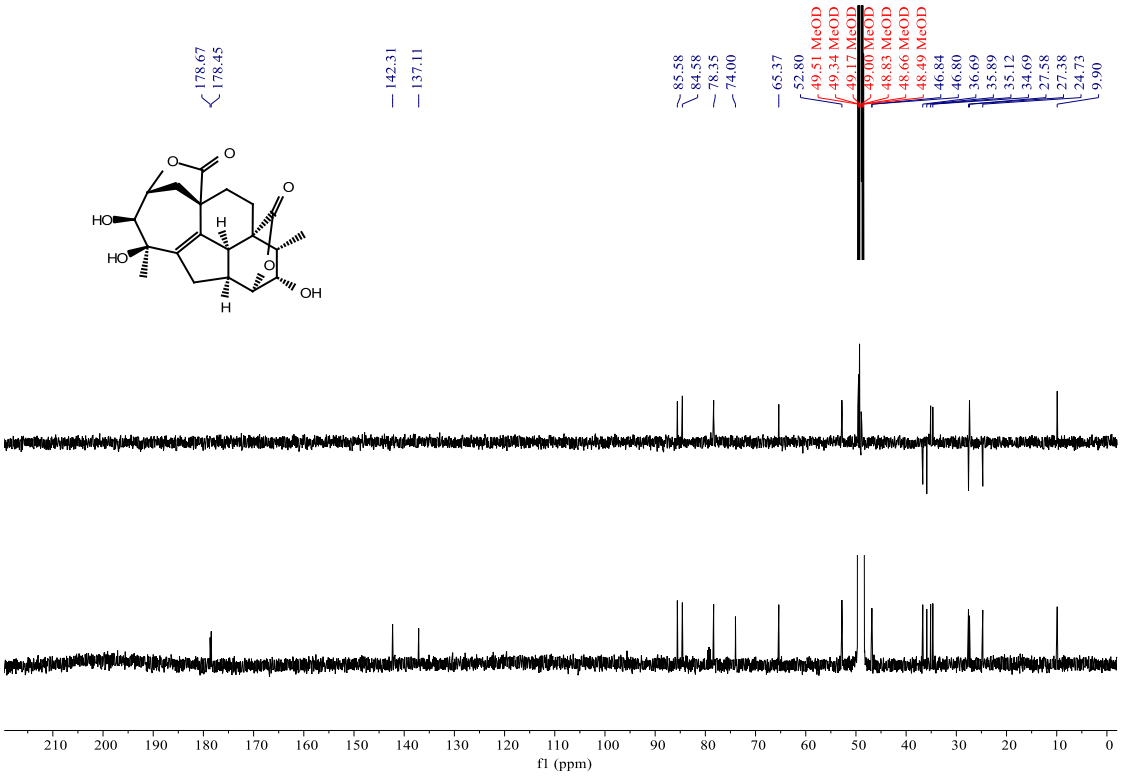

**Figure S105**. HSQC spectrum of fortalide I (**9**) in methanol-$d_4$.

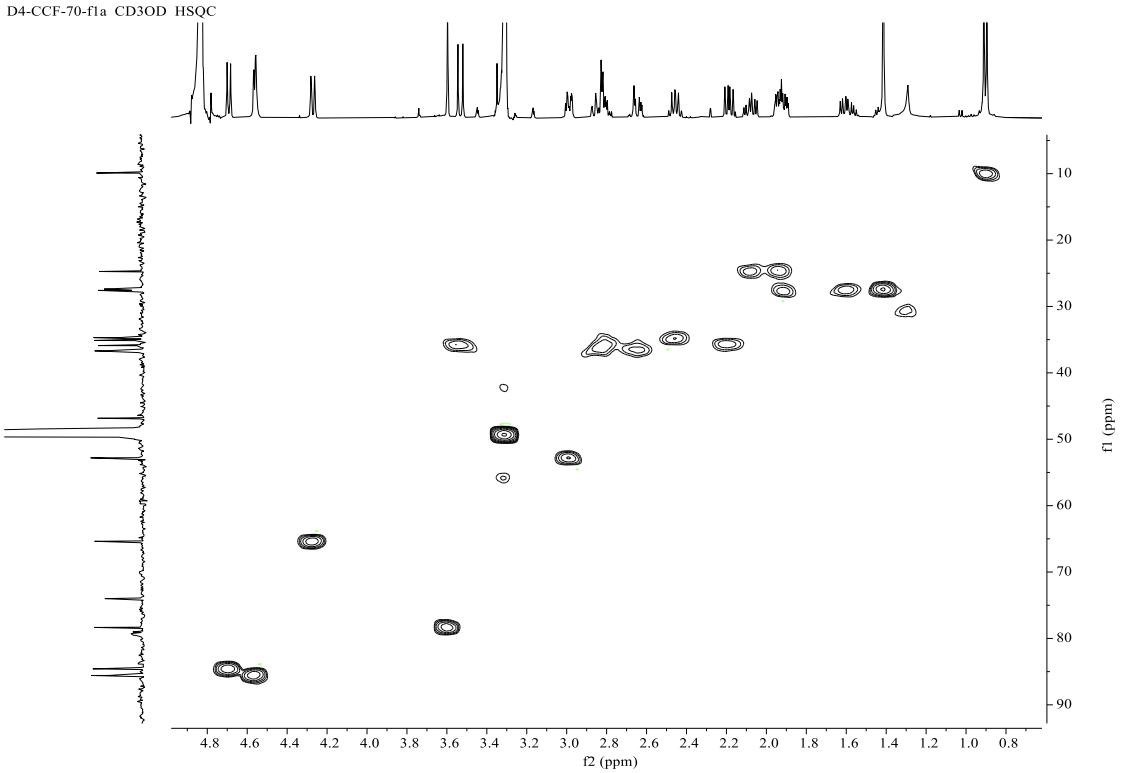


**Figure S106**. HMBC spectrum of fortalide I (**9**) in methanol-$d_4$.

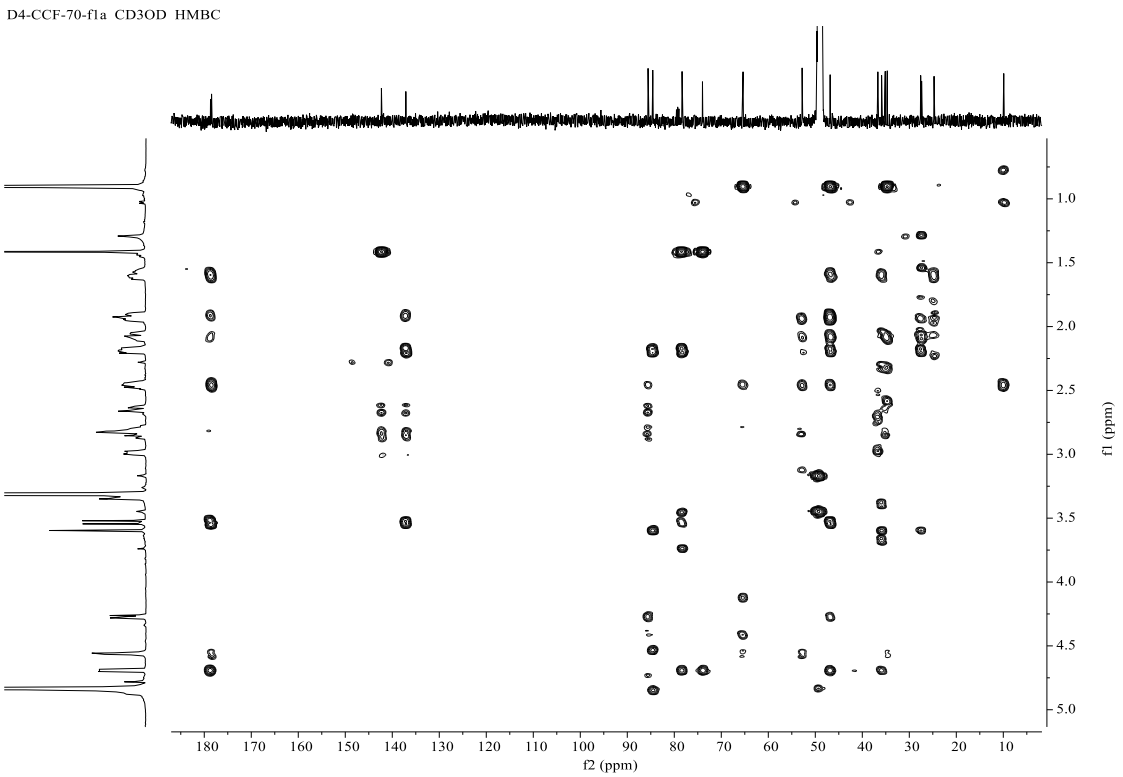

**Figure S107** $^{1}$H-$^{1}$H COSY spectrum of fortalide I (**9**) in methanol-$d_4$.

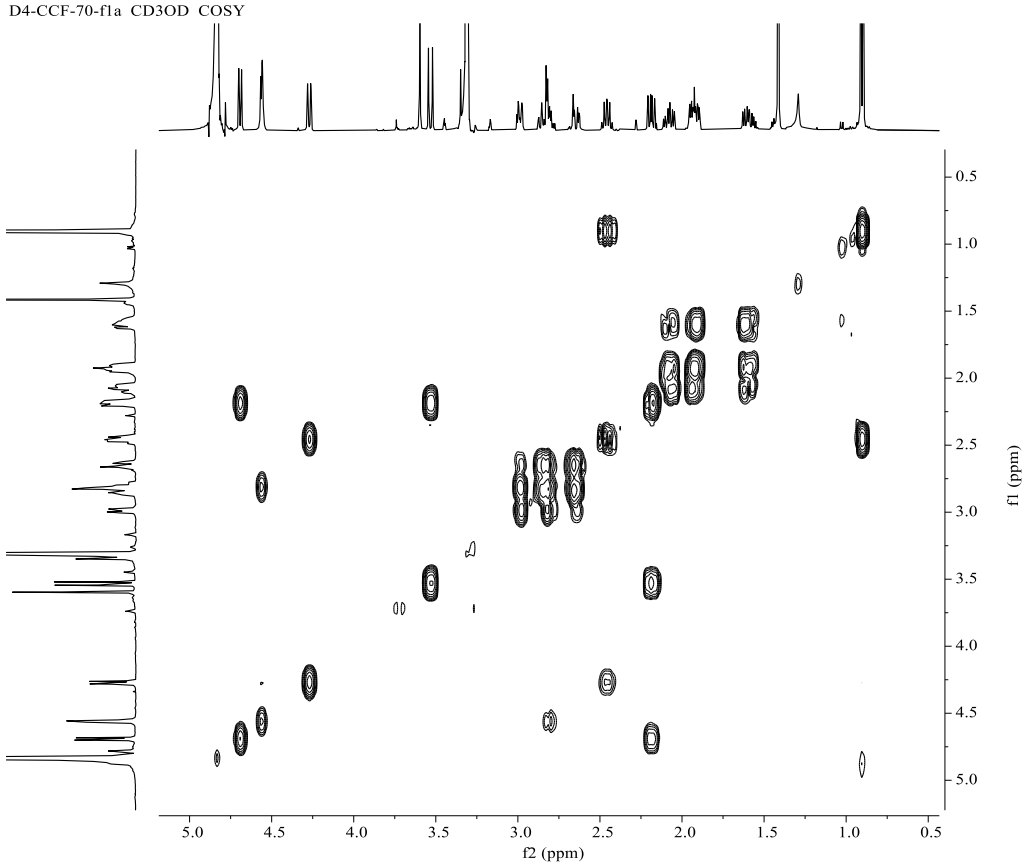


**Figure S108**. NOESY spectrum of fortalide I (**9**) in methanol-$d_4$.

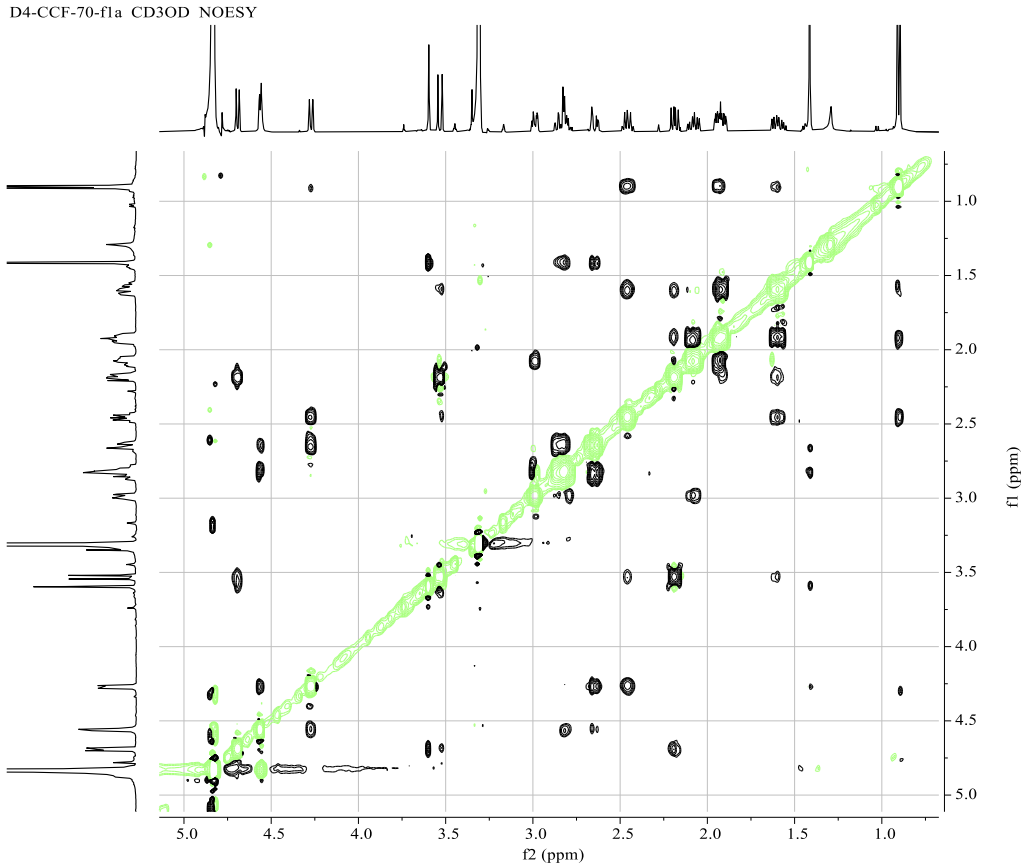

**Figure S109**. (+)-ESIMS spectrum of fortalide I (**9**).

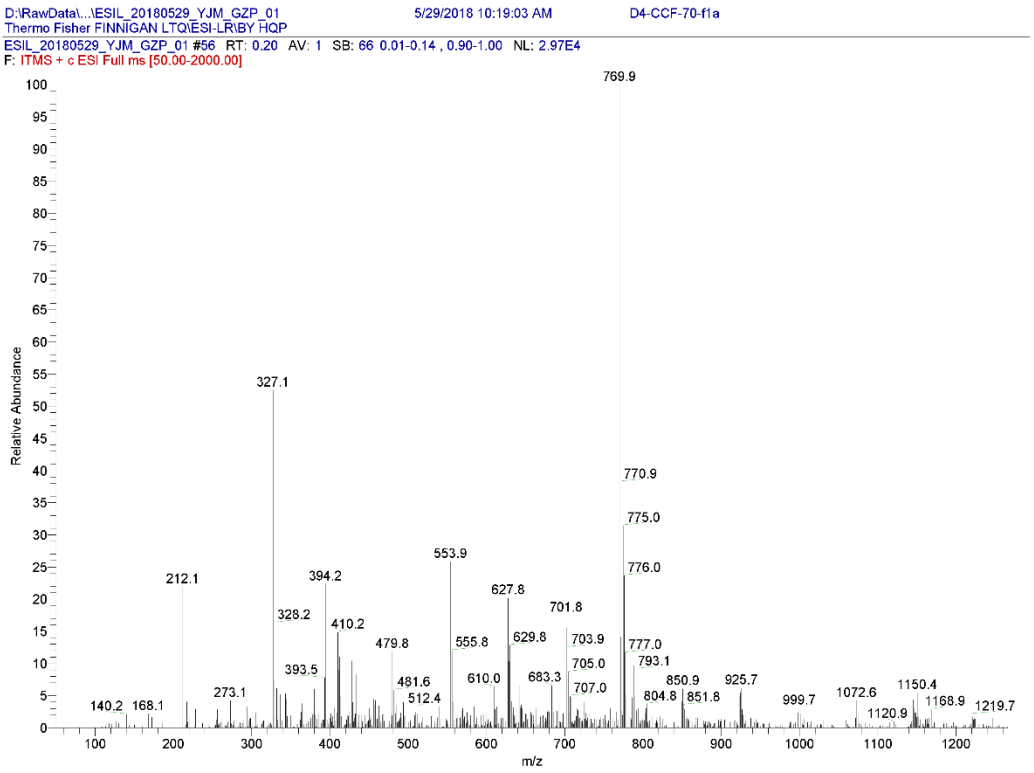


**Figure S110**. (−)-ESIMS spectrum of fortalide I (**9**).

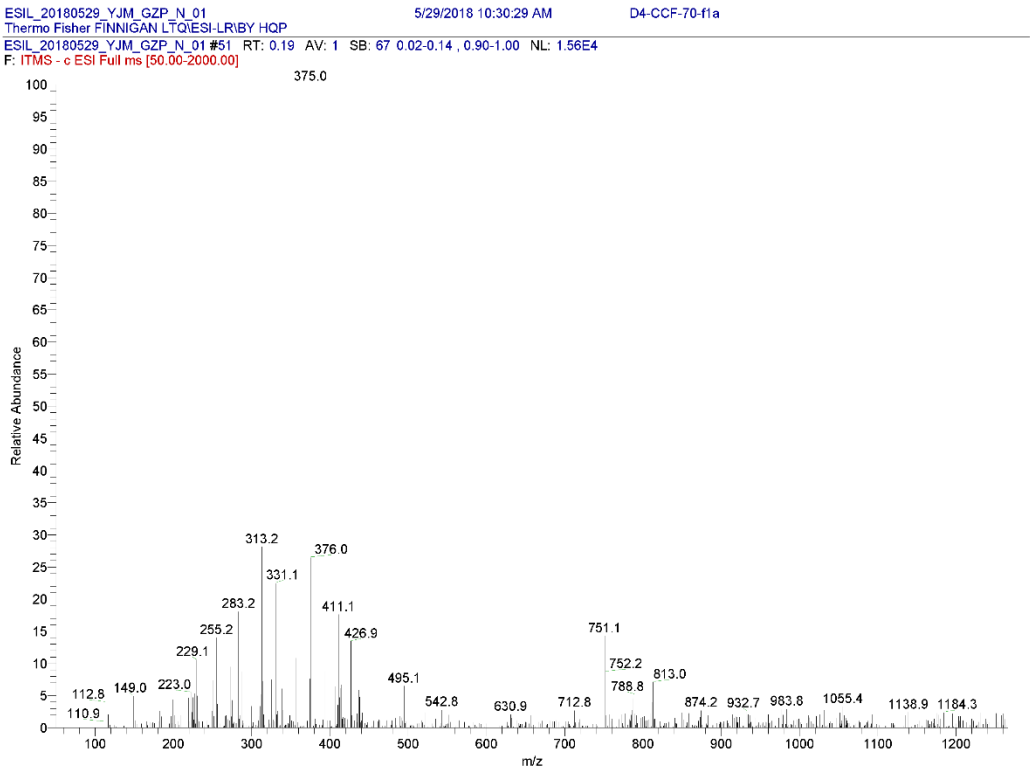

**Figure S111**. (+)-HRESIMS spectrum of fortalide I (**9**).

**Qualitative Analysis Report**

| | | | |
|---|---|---|---|
| **Data Filename** | ESIH_20180529_YJM_GZP_07.d | **Sample Name** | D4-CCF-70-f1a |
| **Sample Type** | Sample | **Position** | P1-A8 |
| **Instrument Name** | Agilent G6520 Q-TOF | **Acq Method** | 20160324_MS_ESIH_NEG_1min.m |
| **Acquired Time** | 5/29/2018 14:35:29 | **IRM Calibration Status** | Success |
| **DA Method** | small molecular data analysis method.m | **Comment** | ESIH by ZZY |

User Spectra

| Fragmentor Voltage | Collision Energy | Ionization Mode |
|---|---|---|
| 175 | 0 | ESI |

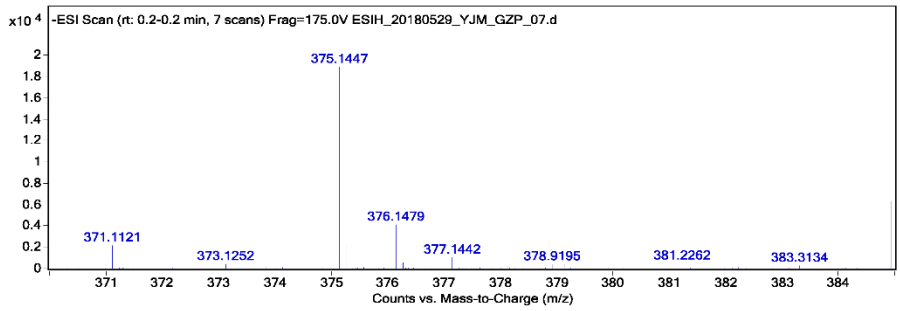


**Formula Calculator Results**

| m/z | Calc m/z | Diff (mDa) | Diff (ppm) | Ion Formula | Ion |
|---|---|---|---|---|---|
| 375.1447 | 375.1449 | 0.27 | 0.71 | C20 H23 O7 | (M-H)- |

--- End Of Report ---

Agilent Technologies Page 1 of 1 Printed at: 14:39 on: 5/29/2018

**Figure S112**. IR spectrum of fortalide I (**9**).

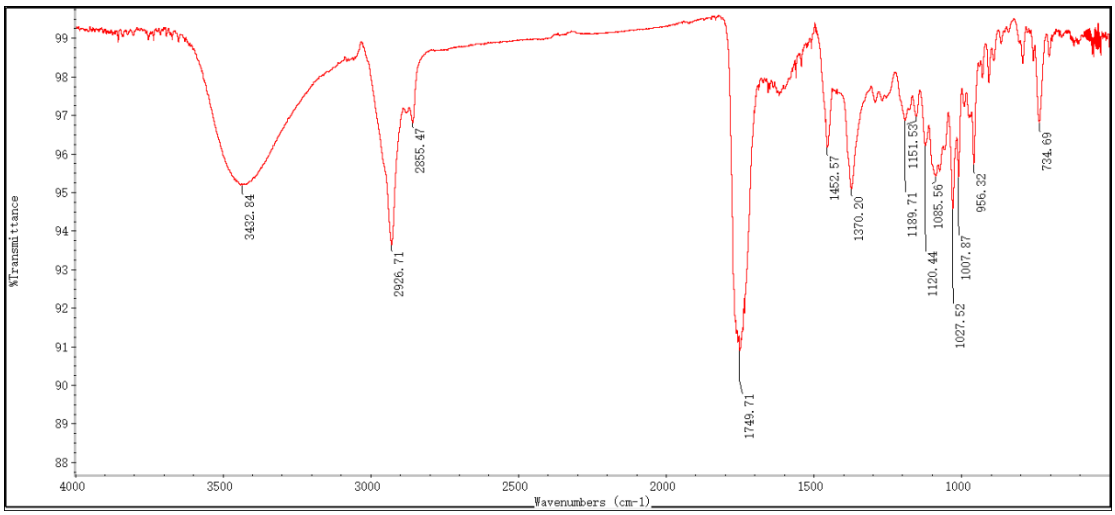

**Figure S113–S122.** 1D and 2D NMR, MS, and IR spectra of fortalide J (**10**)

**Figure S113**. $^{1}$H NMR spectrum of fortalide J (**10**) in methanol-$d_4$.

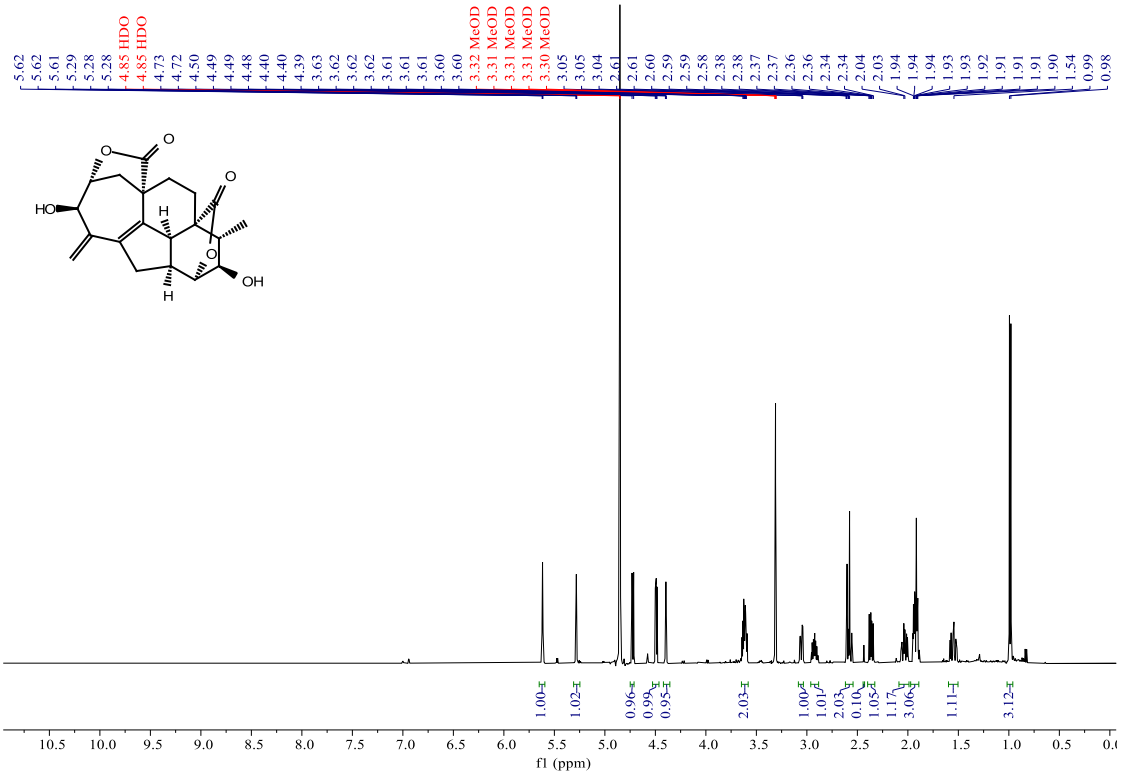


**Figure S114**. $^{13}$C NMR (BB and DEPT-135) spectra of fortalide J (**10**) in methanol-$d_4$.

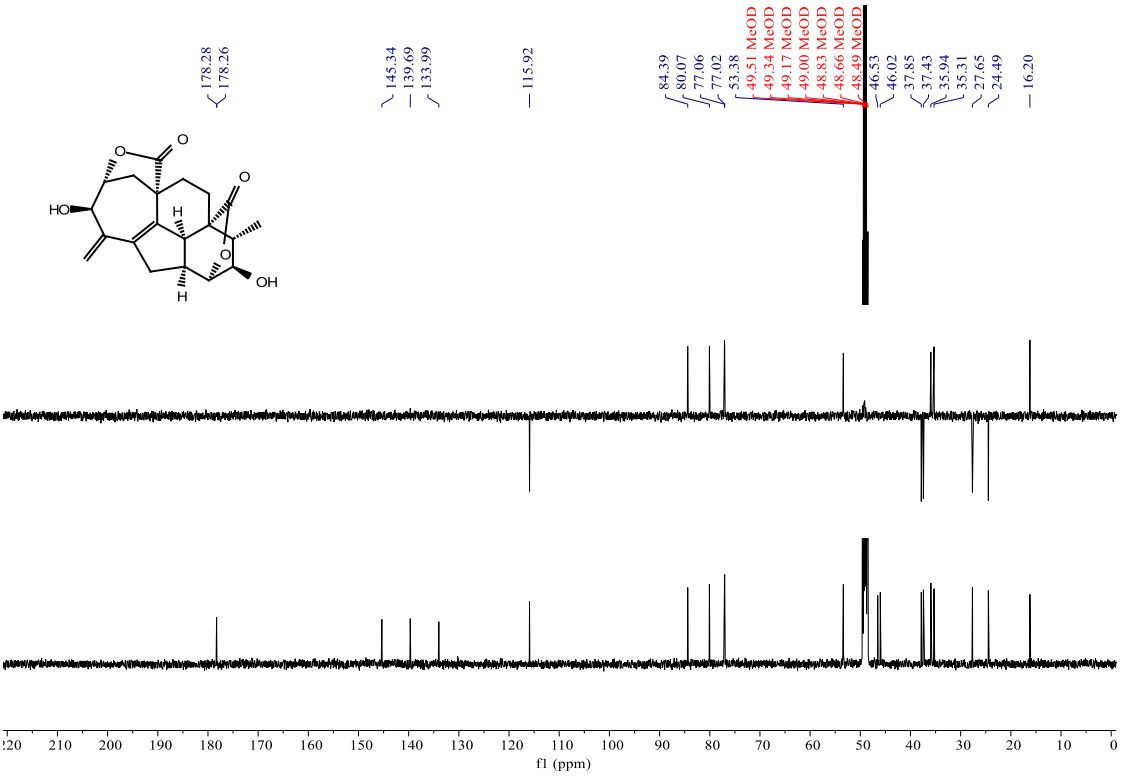

**Figure S115**. HSQC spectrum of fortalide J (**10**) in methanol-$d_4$.

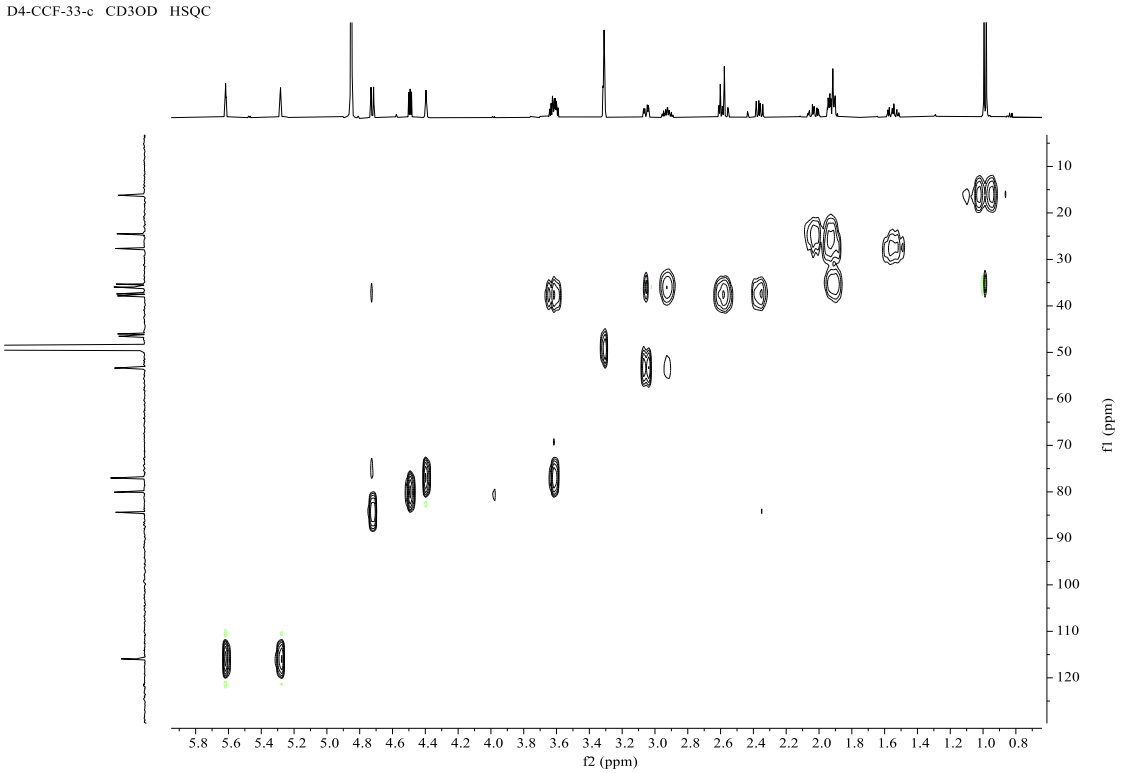


**Figure S116**. HMBC spectrum of fortalide J (**10**) in methanol-$d_4$.

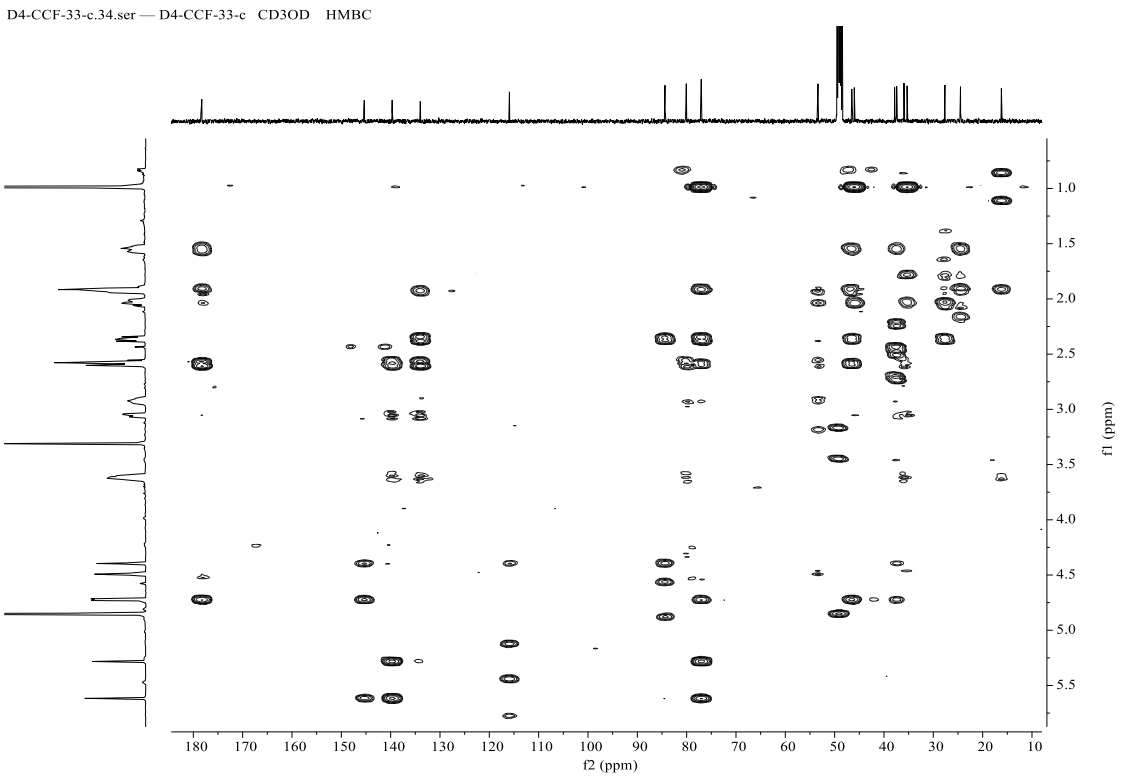

**Figure S117**. $^{1}$H-$^{1}$H COSY spectrum of fortalide J (**10**) in methanol-$d_4$.

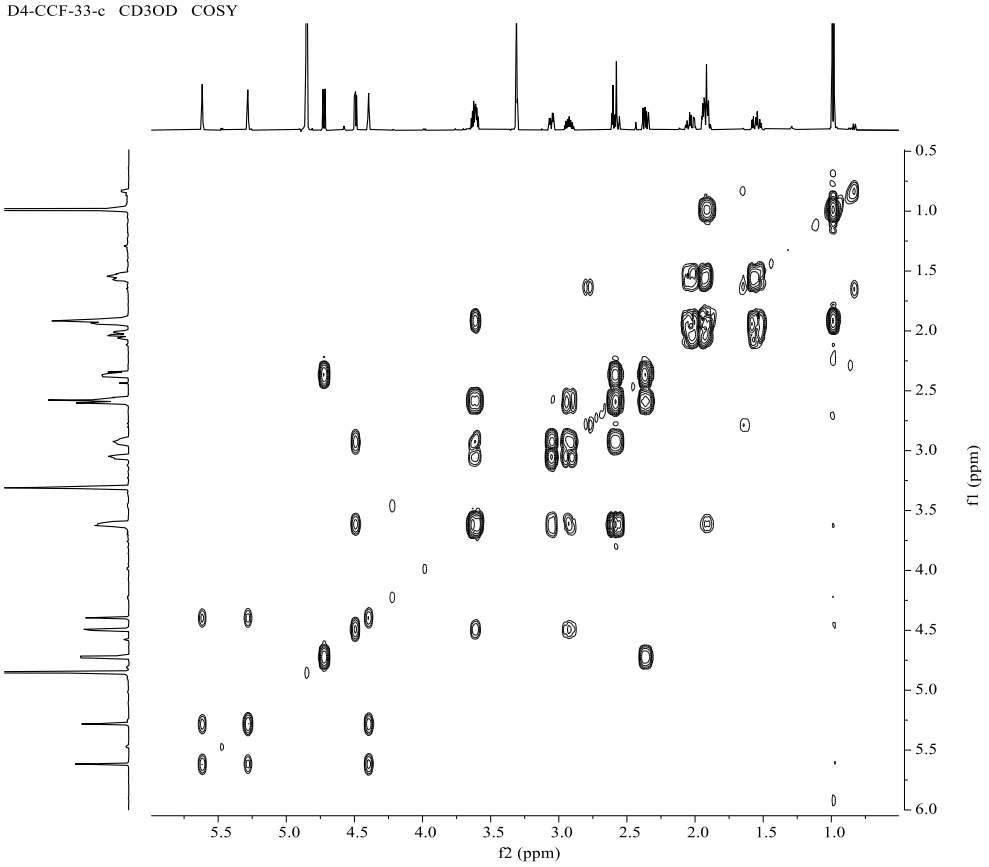


**Figure S118**. NOESY spectrum of fortalide J (**10**) in methanol-$d_4$.

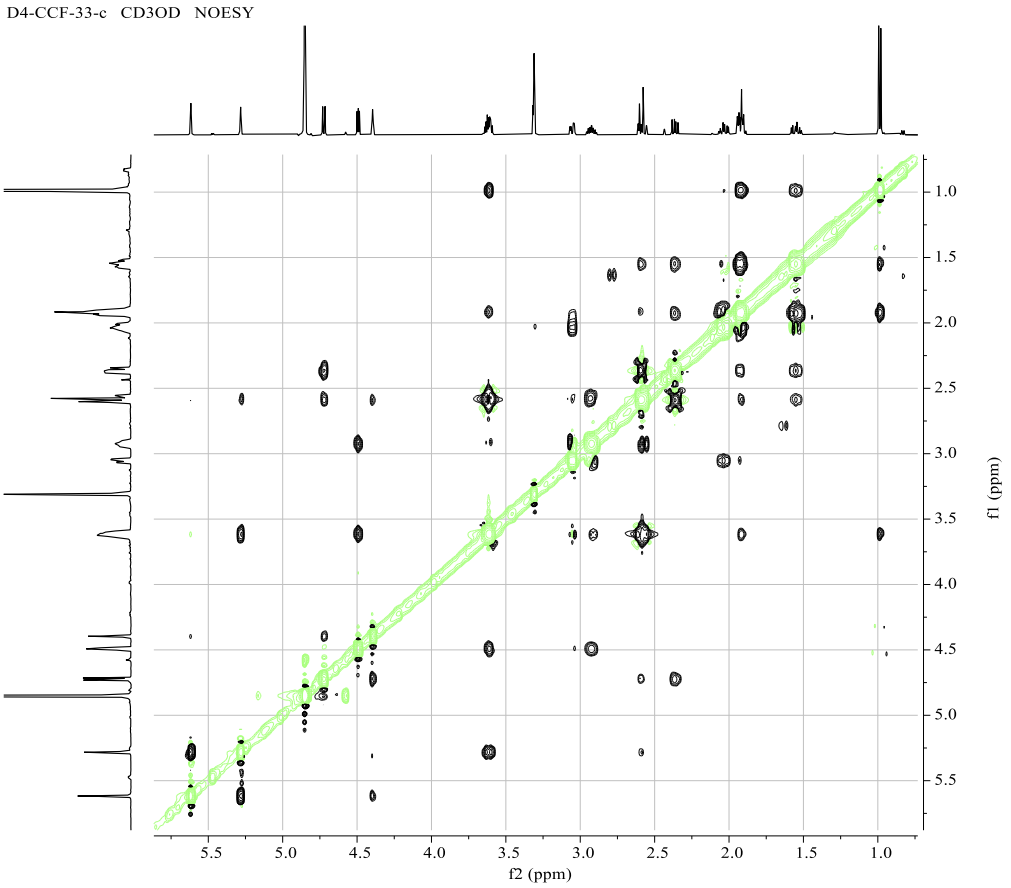

**Figure S119**. (+)-ESIMS spectrum of fortalide J (**10**).

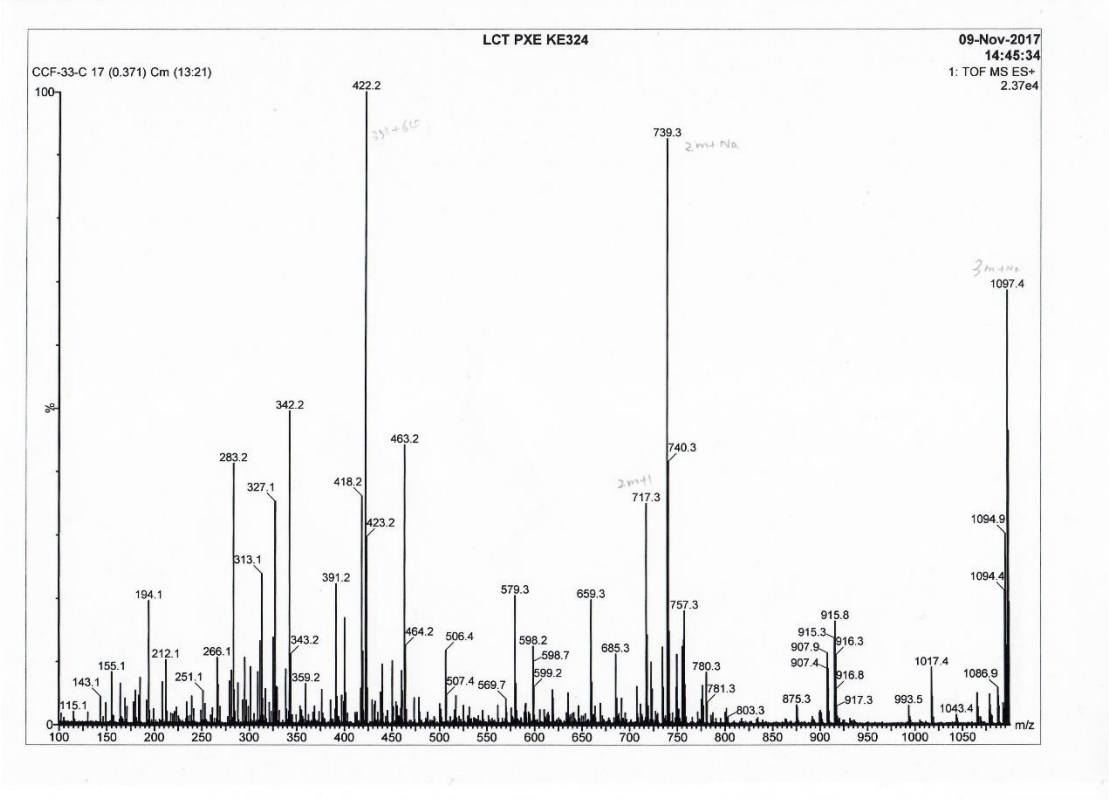


**Figure S120**. (−)-ESIMS spectrum of fortalide J (**10**).

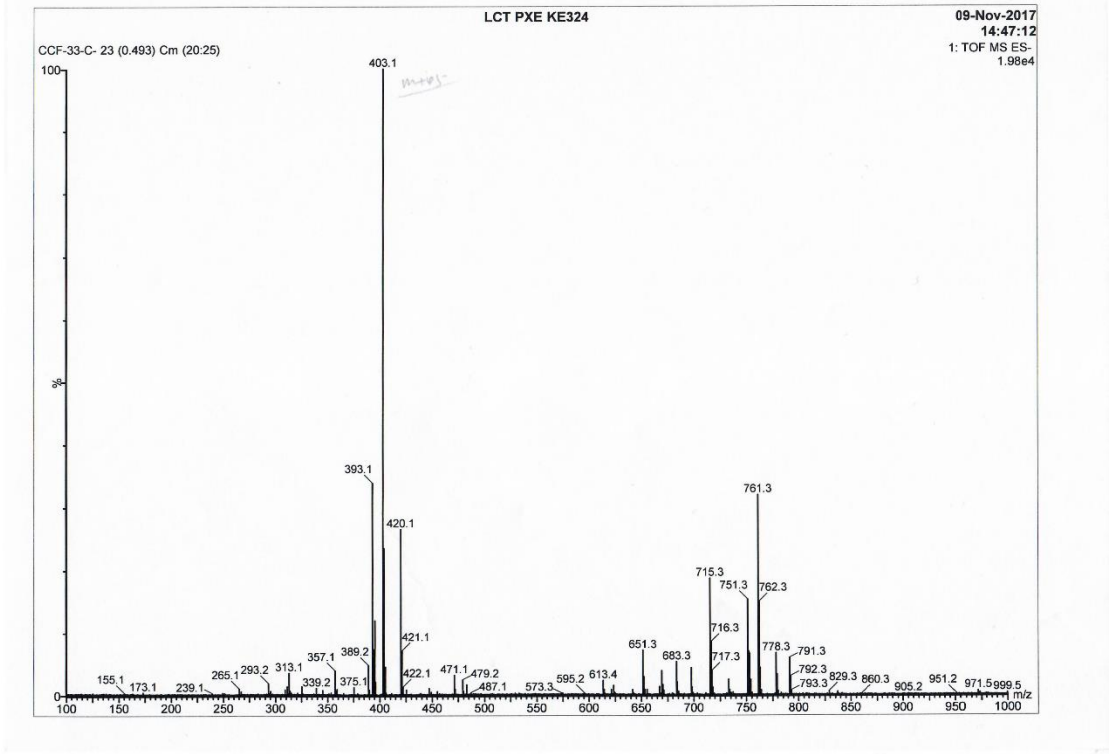

**Figure S121**. (−)-HRESIMS spectrum of fortalide J (**10**).

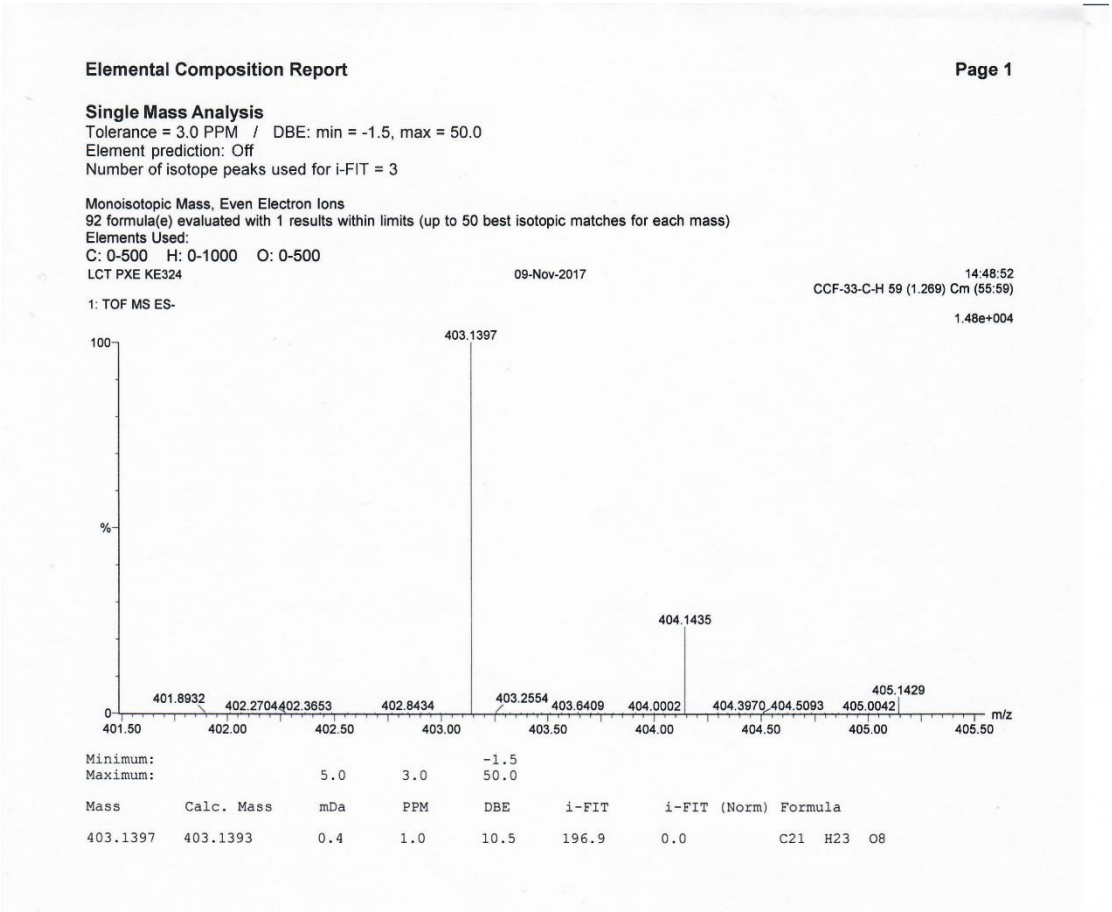

Elemental Composition Report — Page 1

Single Mass Analysis
Tolerance = 3.0 PPM / DBE: min = -1.5, max = 50.0
Element prediction: Off
Number of isotope peaks used for i-FIT = 3

Monoisotopic Mass, Even Electron Ions
92 formula(e) evaluated with 1 results within limits (up to 50 best isotopic matches for each mass)
Elements Used:
C: 0-500 H: 0-1000 O: 0-500

LCT PXE KE324 09-Nov-2017 14:48:52
CCF-33-C-H 59 (1.269) Cm (55:59)
1: TOF MS ES- 1.48e+004



| | | | | | | | |
|---|---|---|---|---|---|---|---|
| Minimum: | | | | -1.5 | | | |
| Maximum: | | 5.0 | 3.0 | 50.0 | | | |
| Mass | Calc. Mass | mDa | PPM | DBE | i-FIT | i-FIT (Norm) | Formula |
| 403.1397 | 403.1393 | 0.4 | 1.0 | 10.5 | 196.9 | 0.0 | C21 H23 O8 |

**Figure S122**. IR spectrum of fortalide J (**10**).

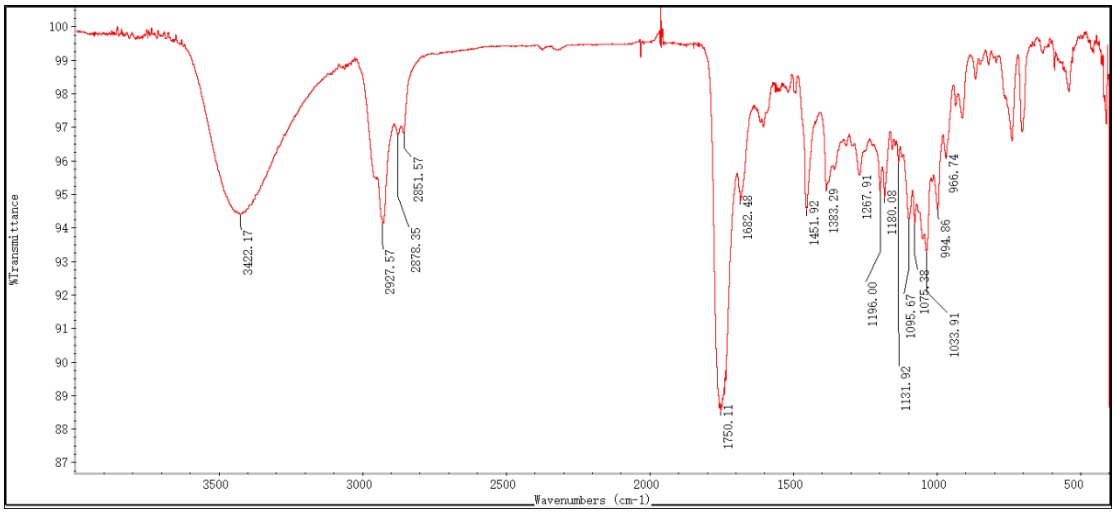

**Figure S123–S134.** 1D and 2D NMR, MS, and IR spectra of fortalide K (**11**)

**Figure S123**. $^{1}$H NMR spectrum of fortalide K (**11**) in $CDCl_3$.

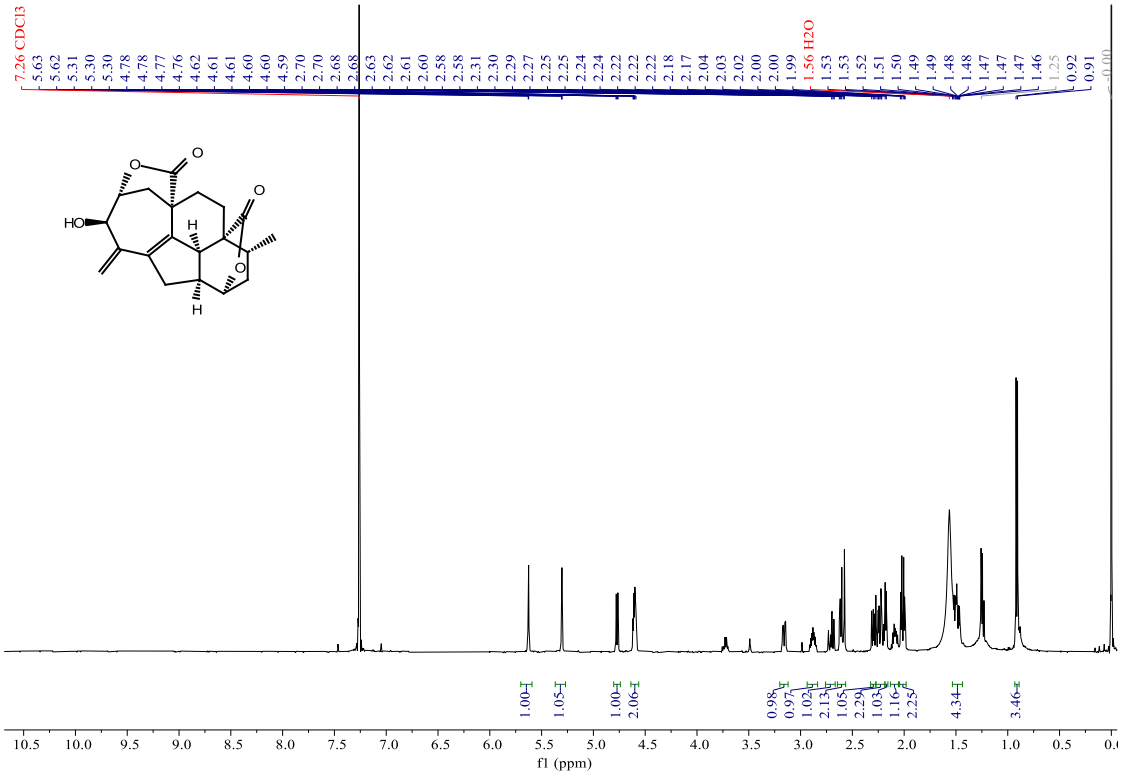


**Figure S124**. $^{13}$C NMR (BB and DEPT-135) spectra of fortalide K (**11**) in $CDCl_3$.

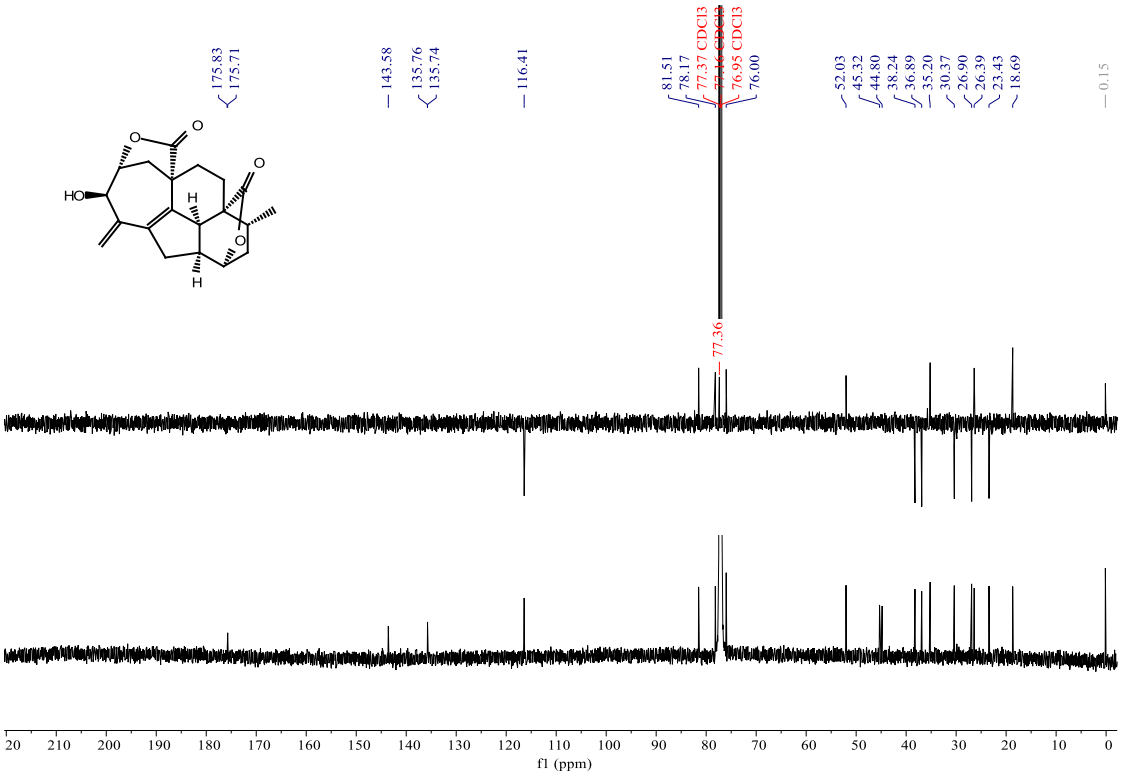

**Figure S125**. $^{1}$H NMR spectrum of fortalide K (**11**) in pyridine-$d_5$.

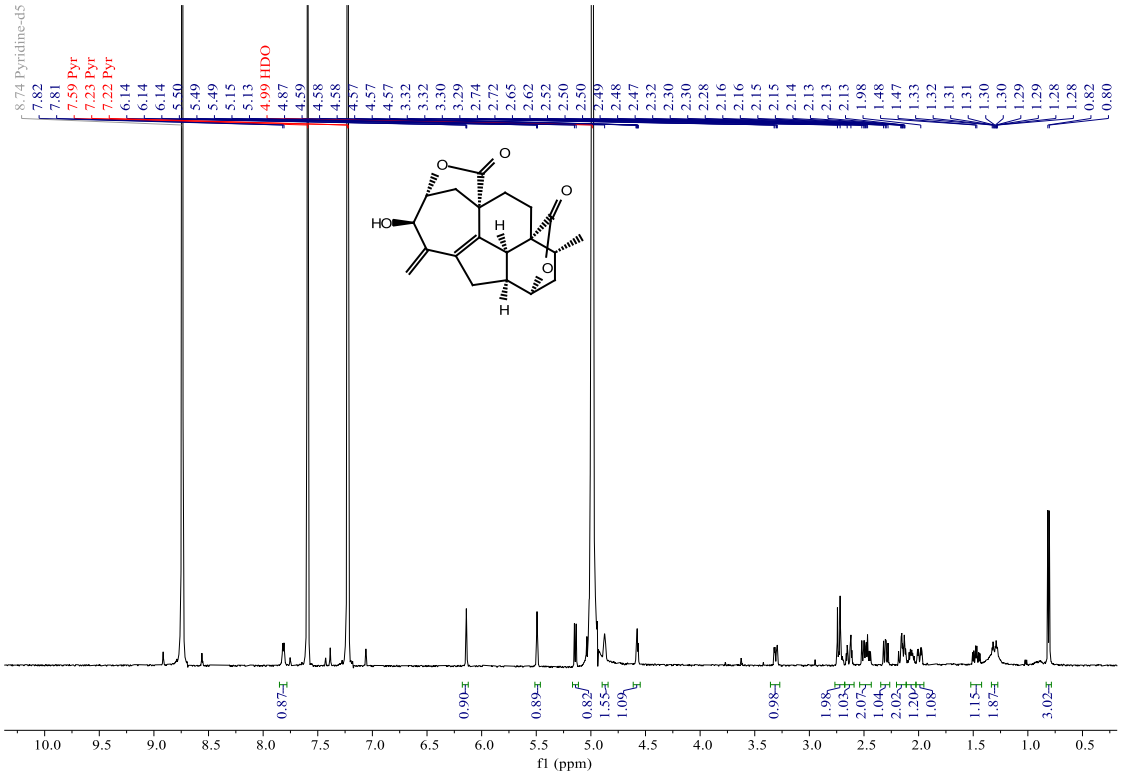


**Figure S126**. HSQC spectrum of fortalide K (**11**) in $CDCl_3$.

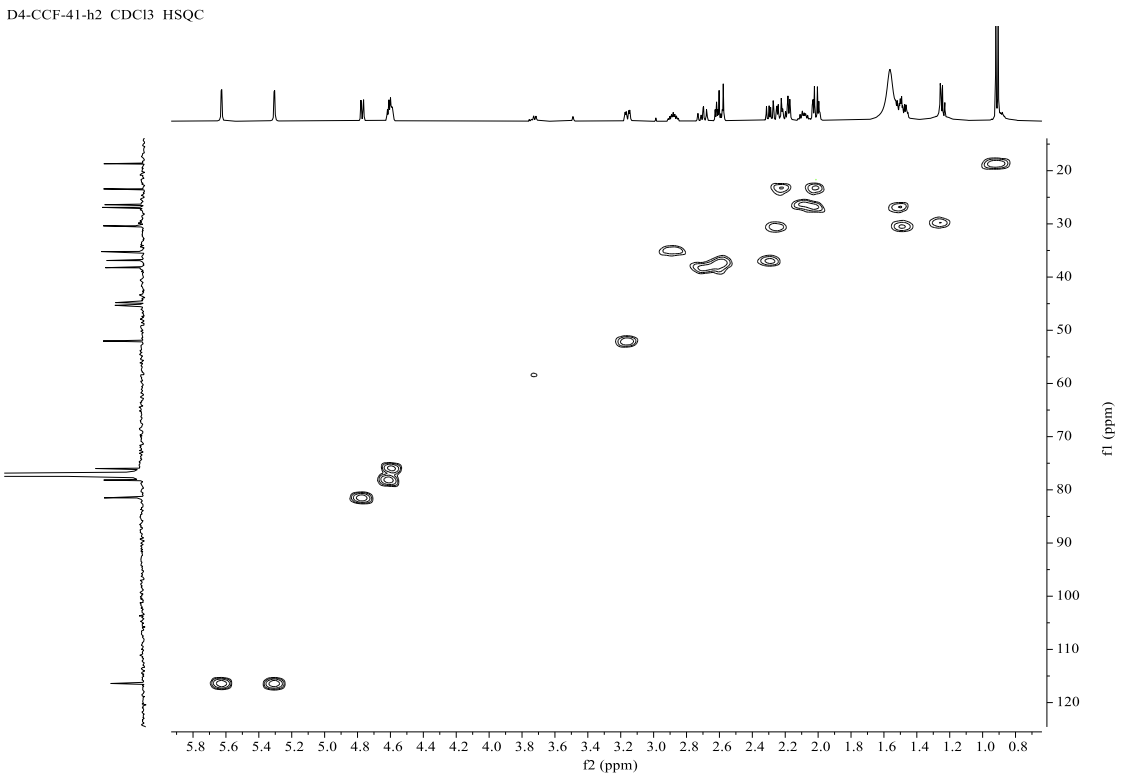

**Figure S127**. HMBC spectrum of fortalide K (**11**) in $CDCl_3$.

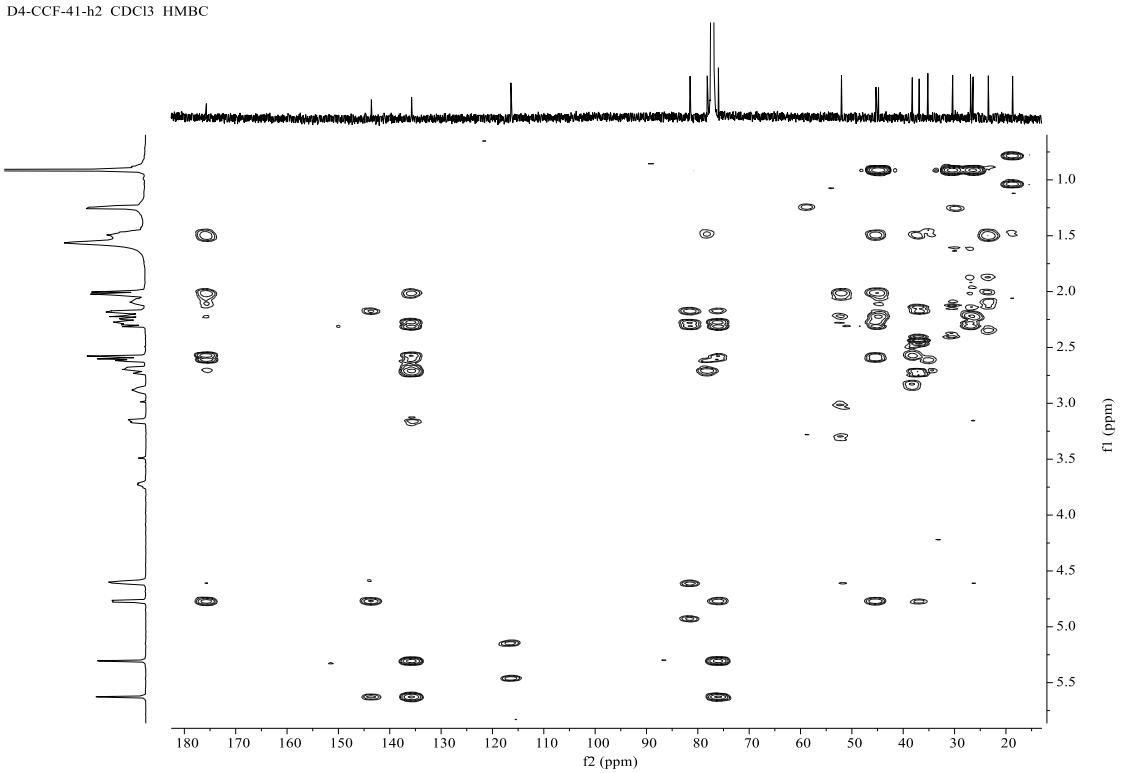


**Figure S128**. $^{1}H$-$^{1}H$ COSY spectrum of fortalide K (**11**) in $CDCl_3$.

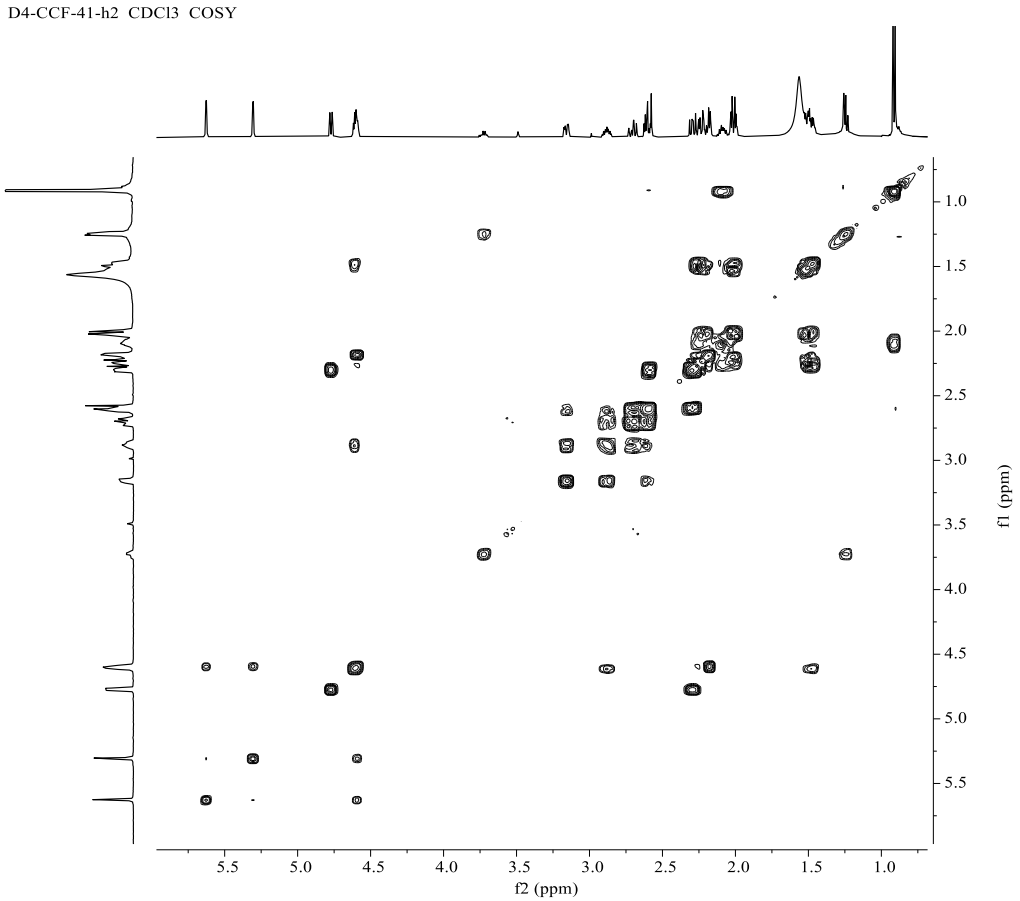

**Figure S129**. NOESY spectrum of fortalide K (**11**) in $CDCl_3$.

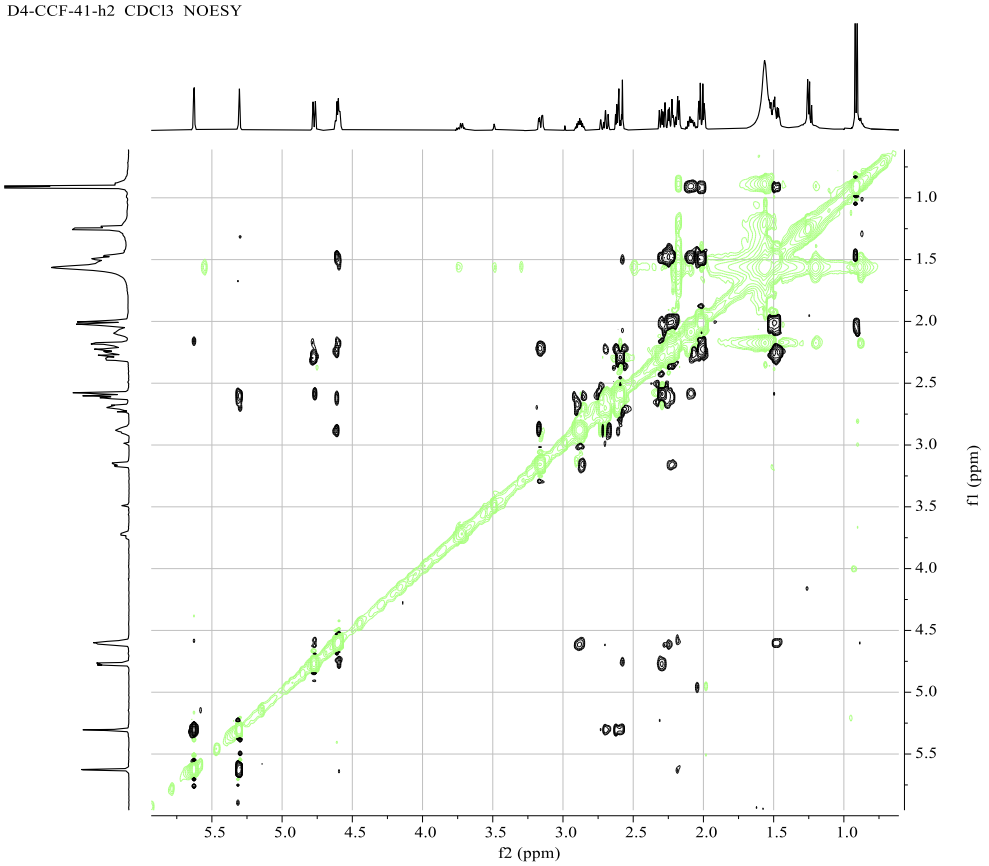


**Figure S130**. NOESY spectrum of fortalide K (**11**) in pyridine-$d_5$.

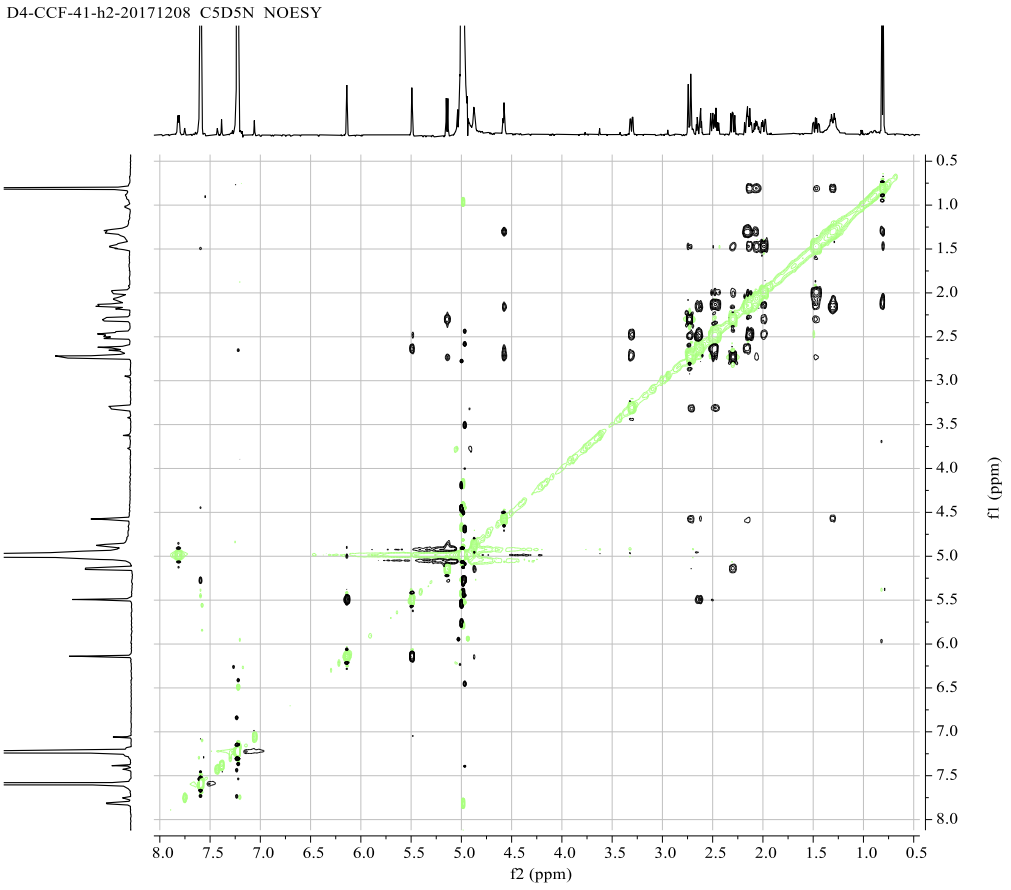

**Figure S131**. (+)-ESIMS spectrum of fortalide K (**11**).

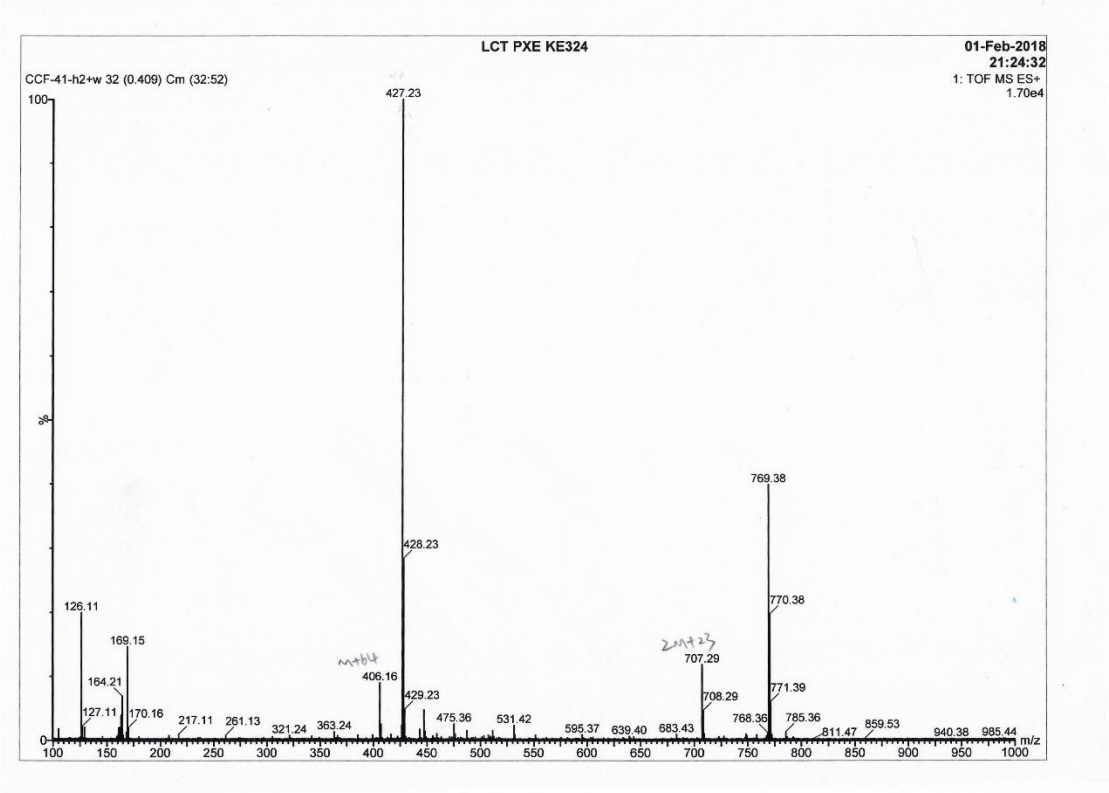


**Figure S132**. (−)-ESIMS spectrum of fortalide K (**11**).

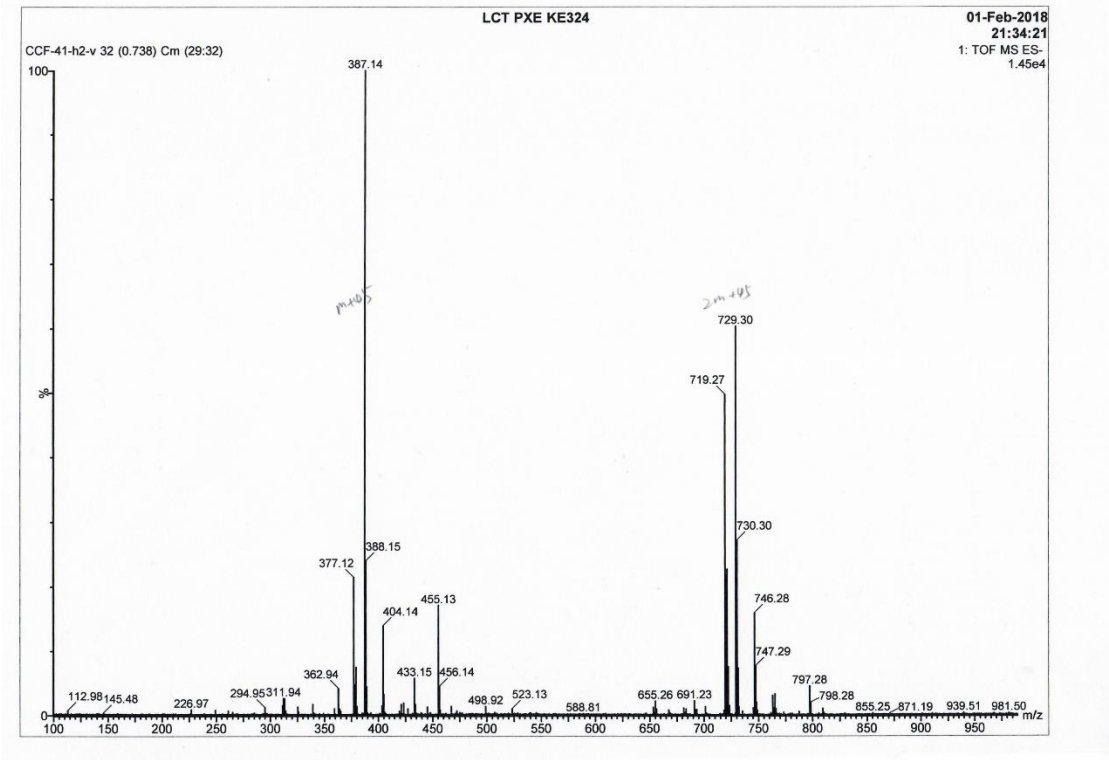

**Figure S133**. (+)-HRESIMS spectrum of fortalide K (**11**).

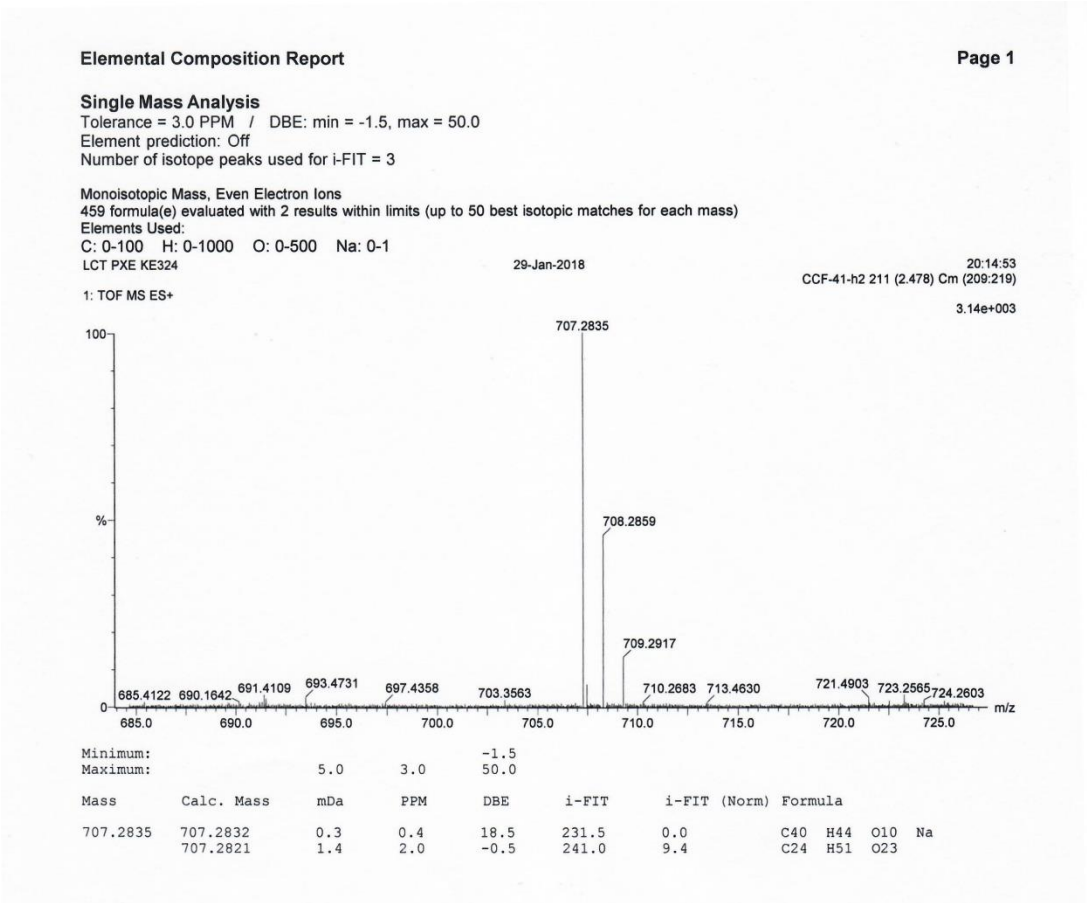


**Figure S134**. IR spectrum of fortalide K (**11**).

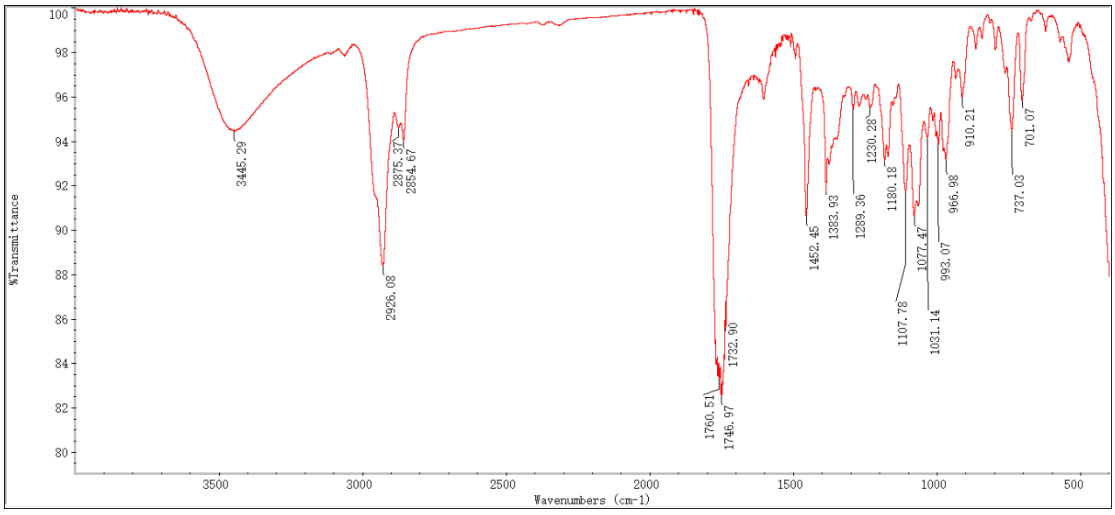

**Figure S135–S143.** 1D and 2D NMR, MS, and IR spectra of fortalide L (**12**)

**Figure S135**. $^{1}$H NMR spectrum of fortalide L (**12**) in $CDCl_3$.

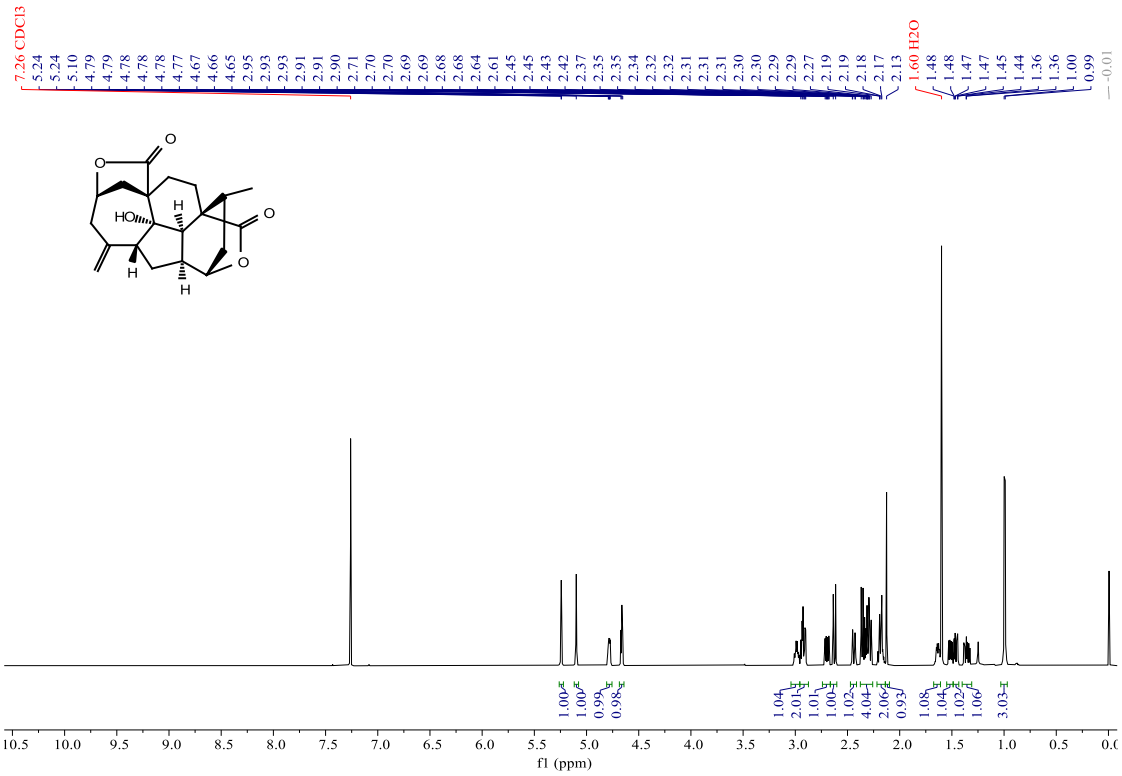


**Figure S136**. $^{13}$C NMR (BB and DEPT-135) spectra of fortalide L (**12**) in $CDCl_3$.

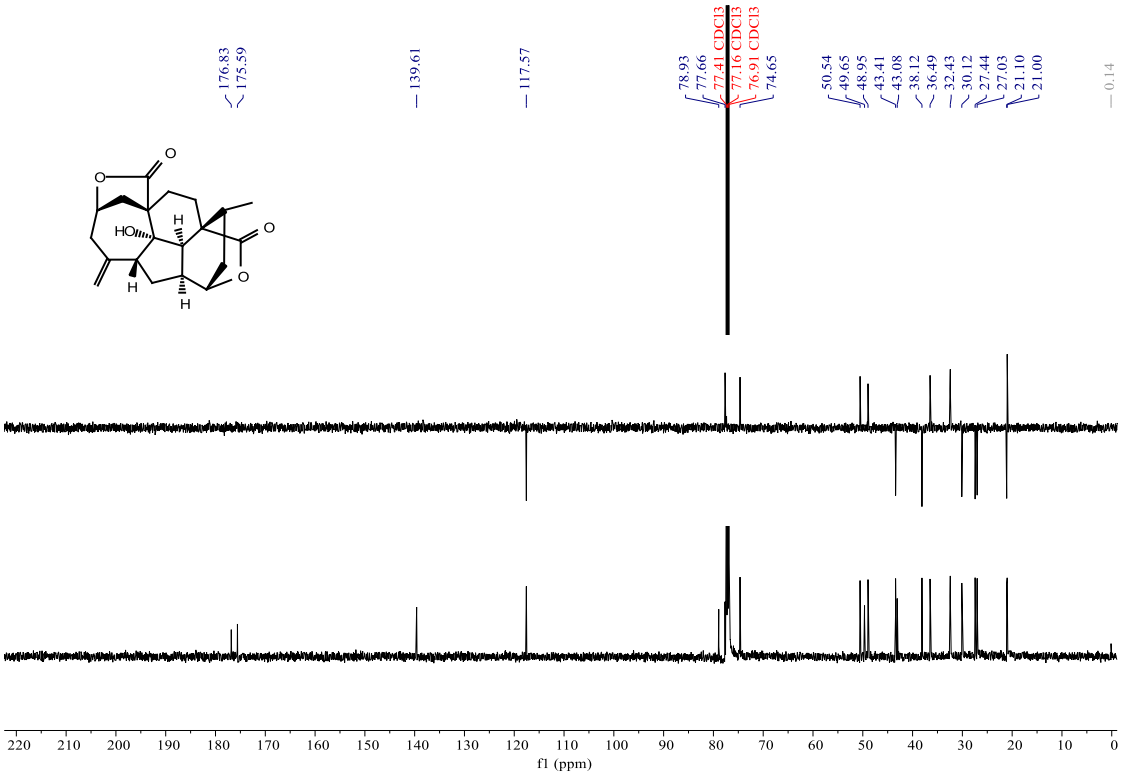

**Figure S137**. HSQC spectrum of fortalide L (**12**) in $CDCl_3$.

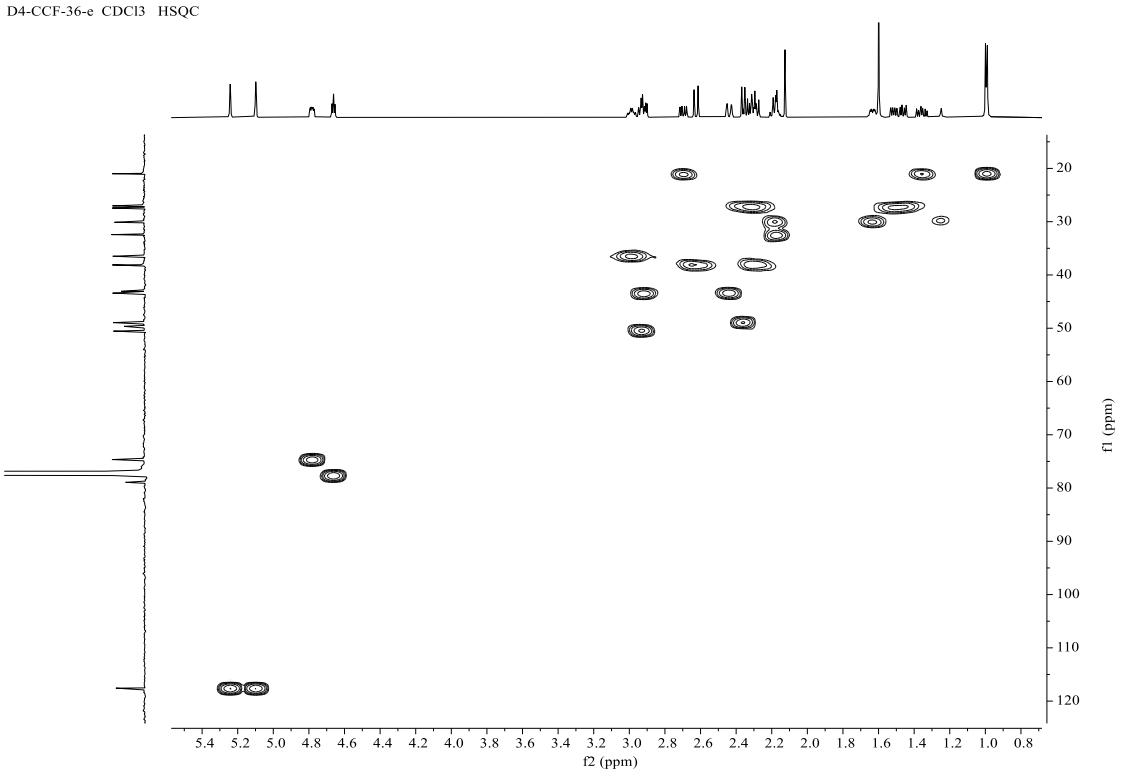


**Figure S138**. HMBC spectrum of fortalide L (**12**) in $CDCl_3$.

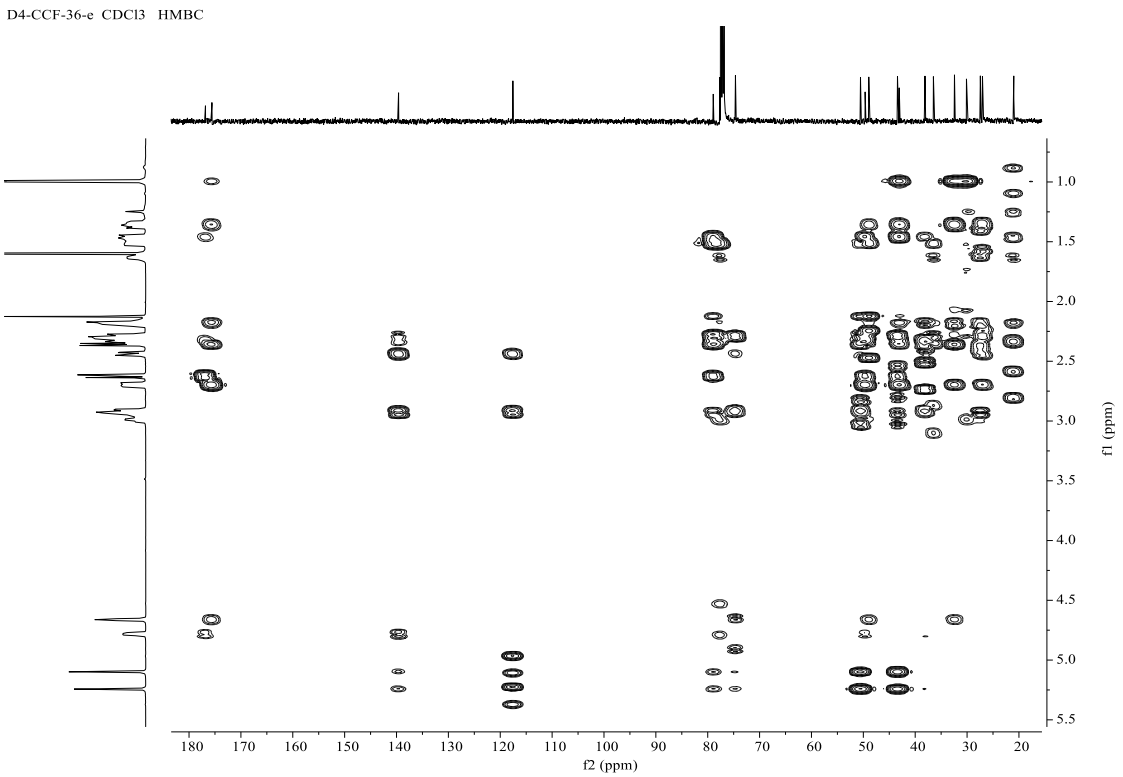

**Figure S139**. $^{1}H$-$^{1}H$ COSY spectrum of fortalide L (**12**) in $CDCl_3$.

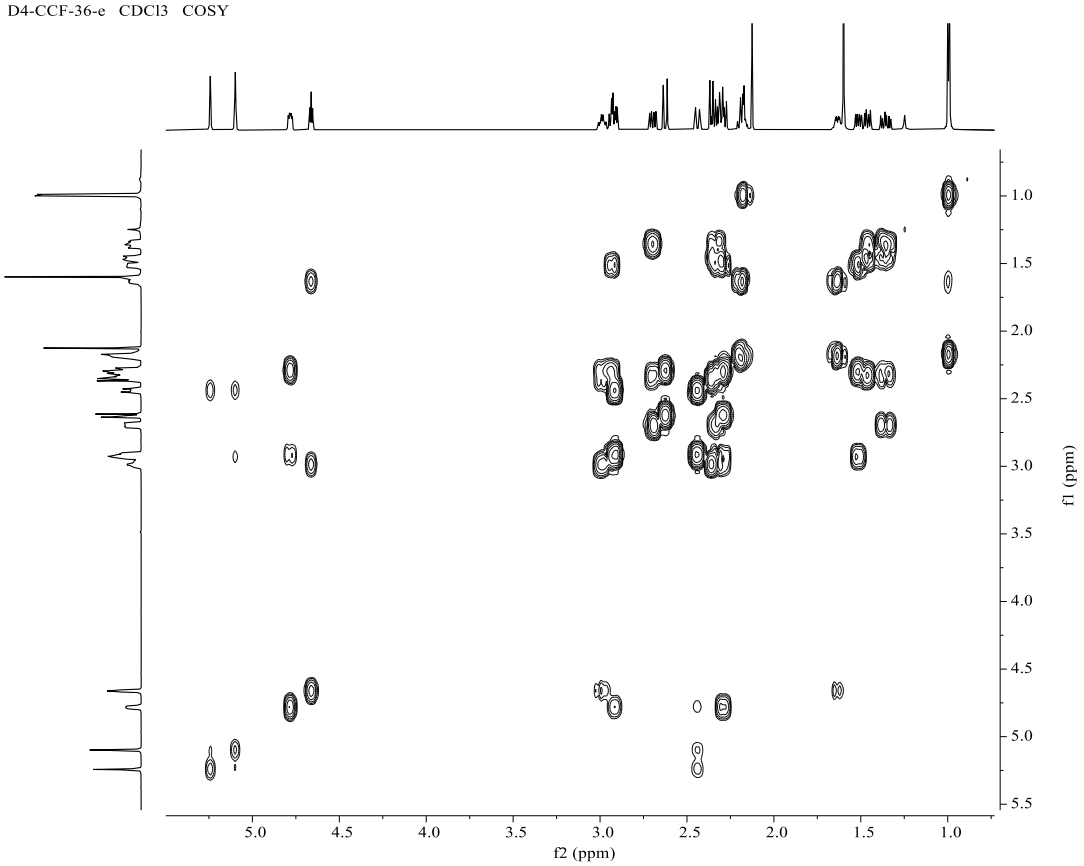


**Figure S140**. NOESY spectrum of fortalide L (**12**) in $CDCl_3$.

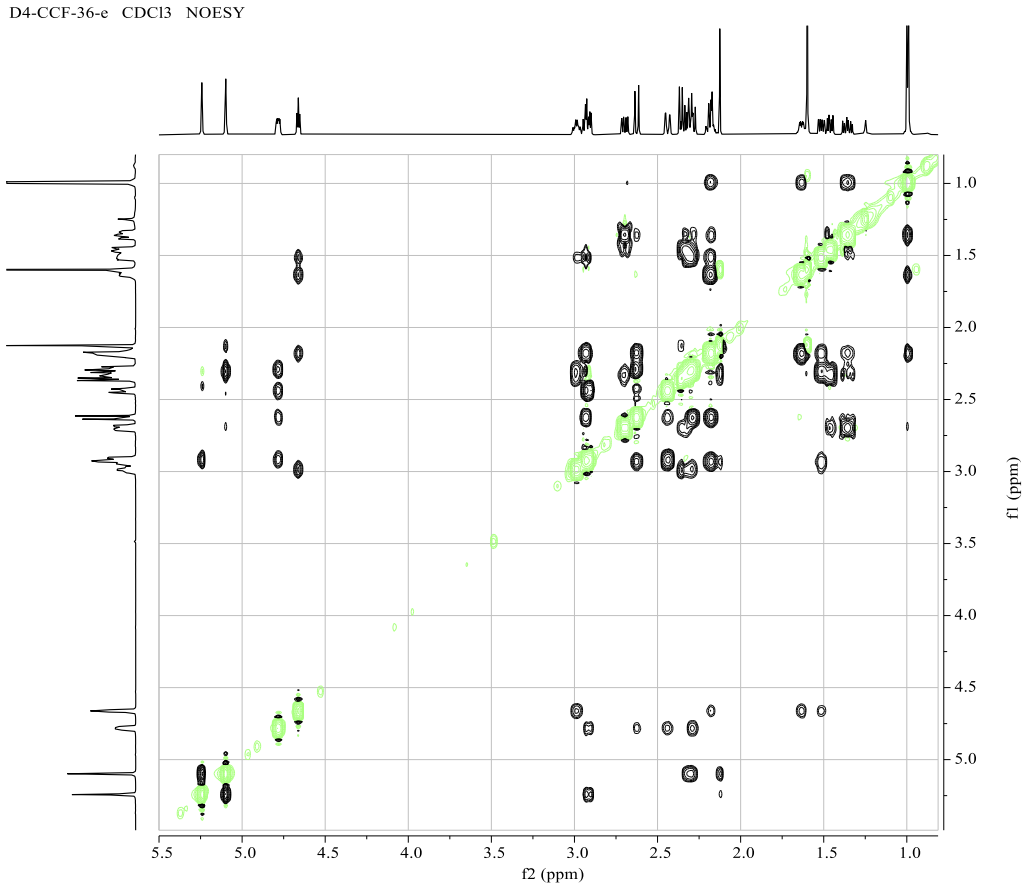

**Figure S141**. (+)-ESIMS spectrum of fortalide L (**12**).

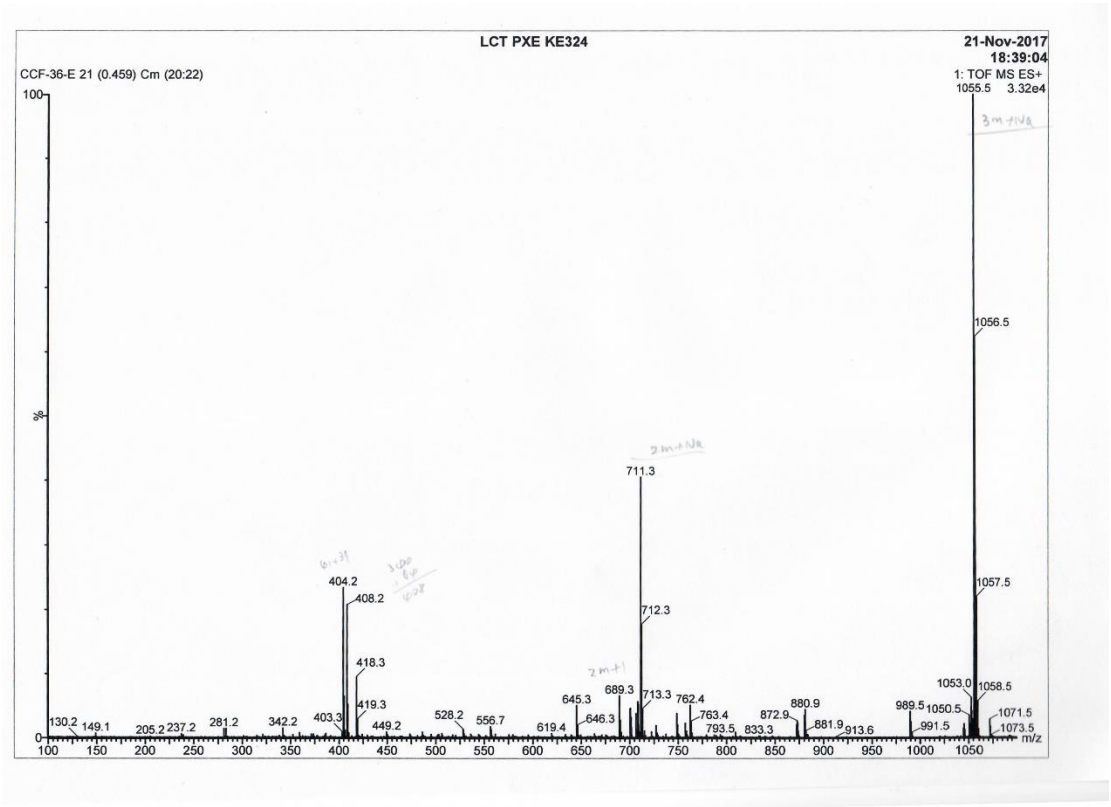


**Figure S142**. (+)-HRESIMS spectrum of fortalide L (**12**).

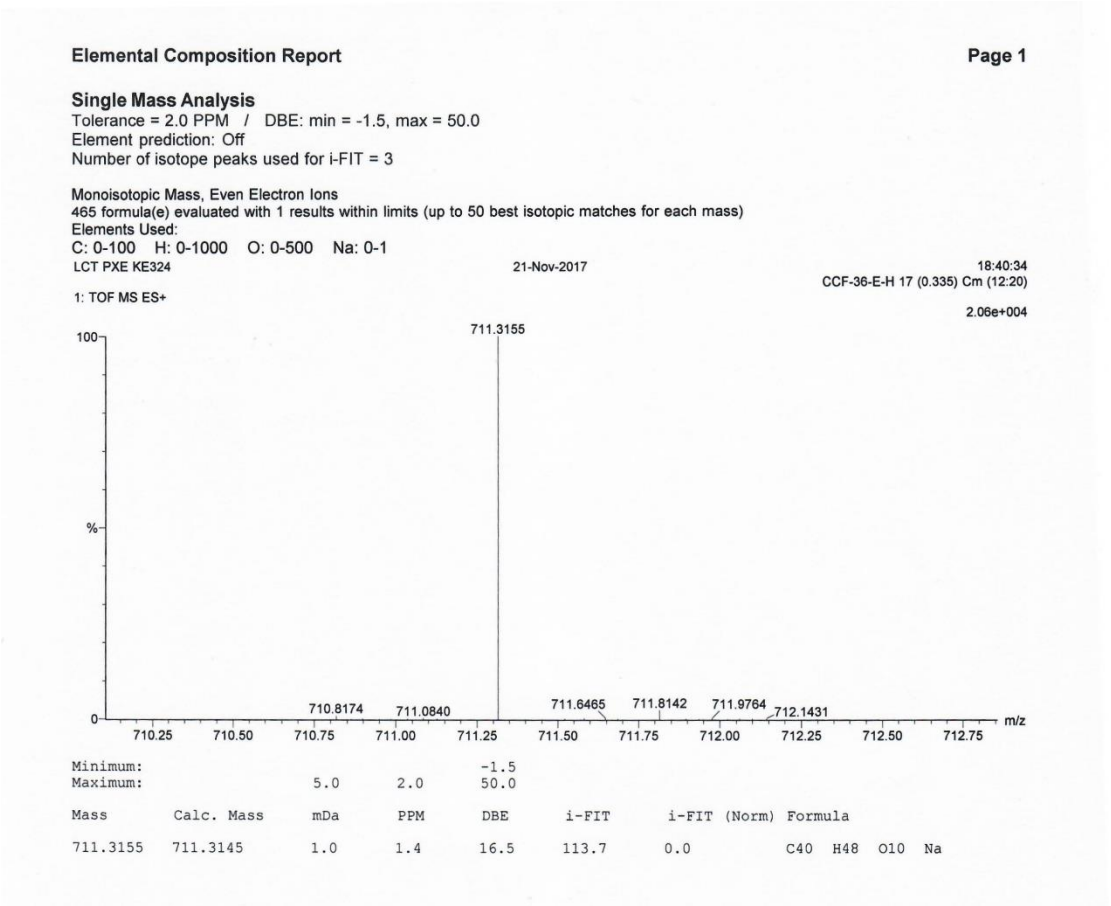

**Figure S143**. IR spectrum of fortalide L (**12**).

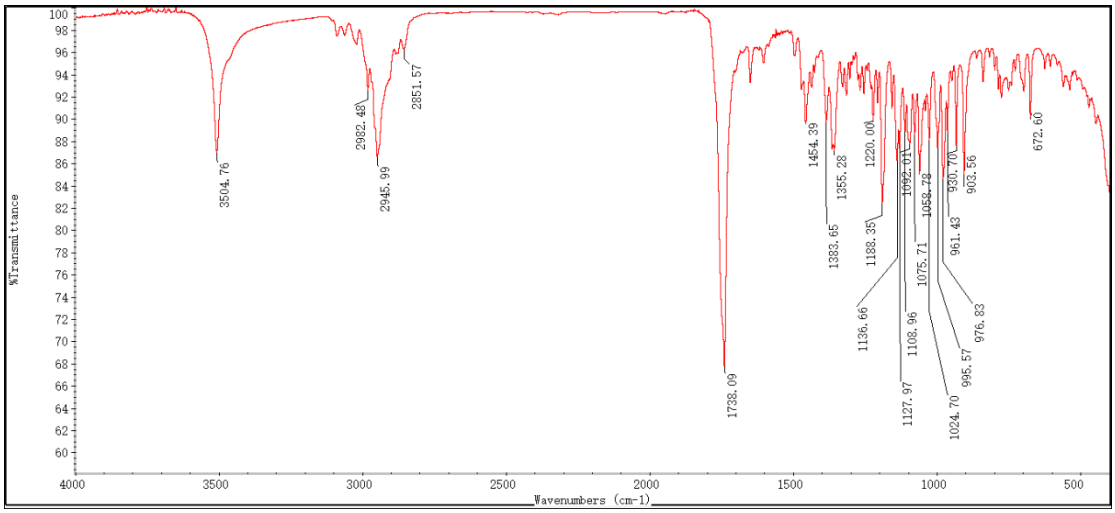


**Figure S144–S153.** 1D and 2D NMR, MS, and IR spectra of fortalide M (**13**)

**Figure S144**. $^{1}$H NMR spectrum of fortalide M (**13**) in pyridine-$d_5$.

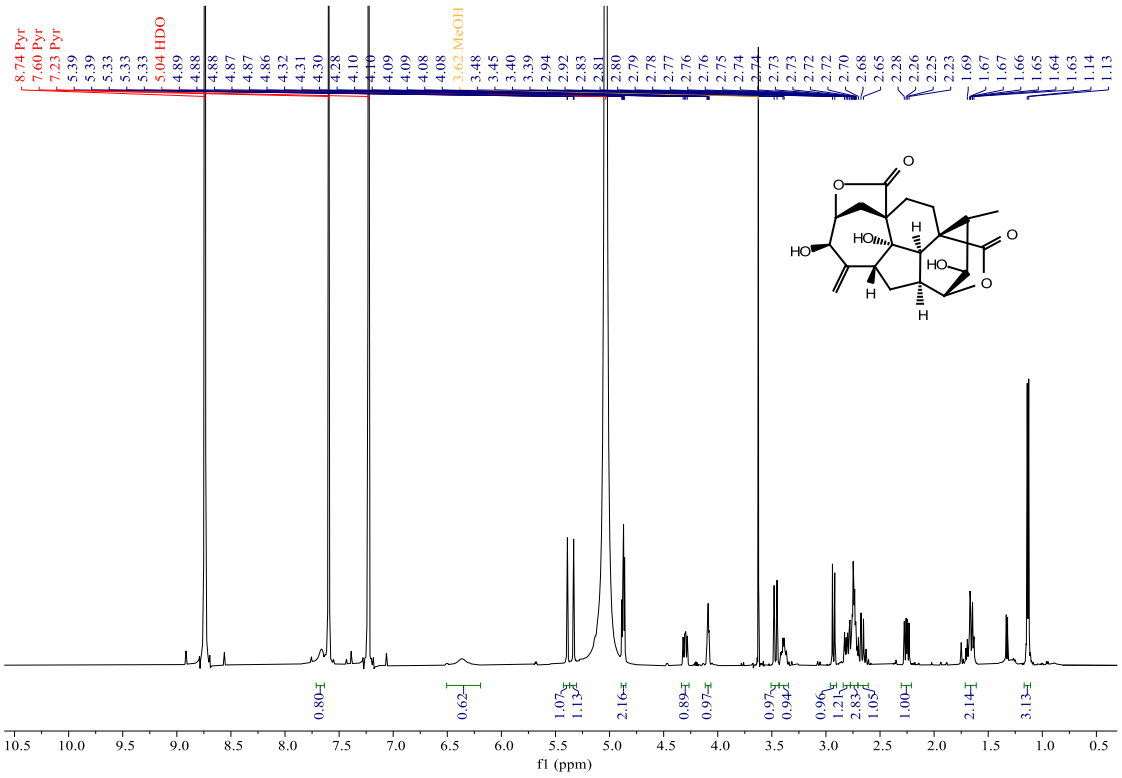

**Figure S145**. $^{13}$C NMR (BB and DEPT-135) spectra of fortalide M (**13**) in pyridine-$d_5$.

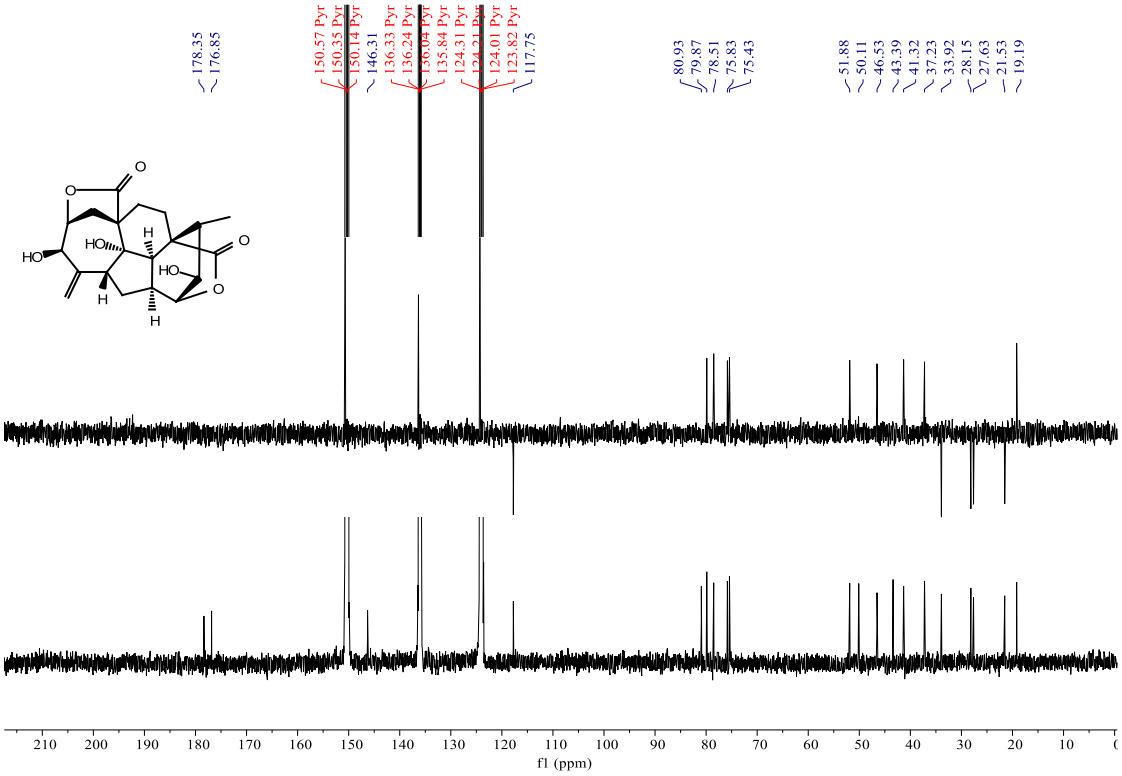


**Figure S146**. HSQC spectrum of fortalide M (**13**) in pyridine-$d_5$.

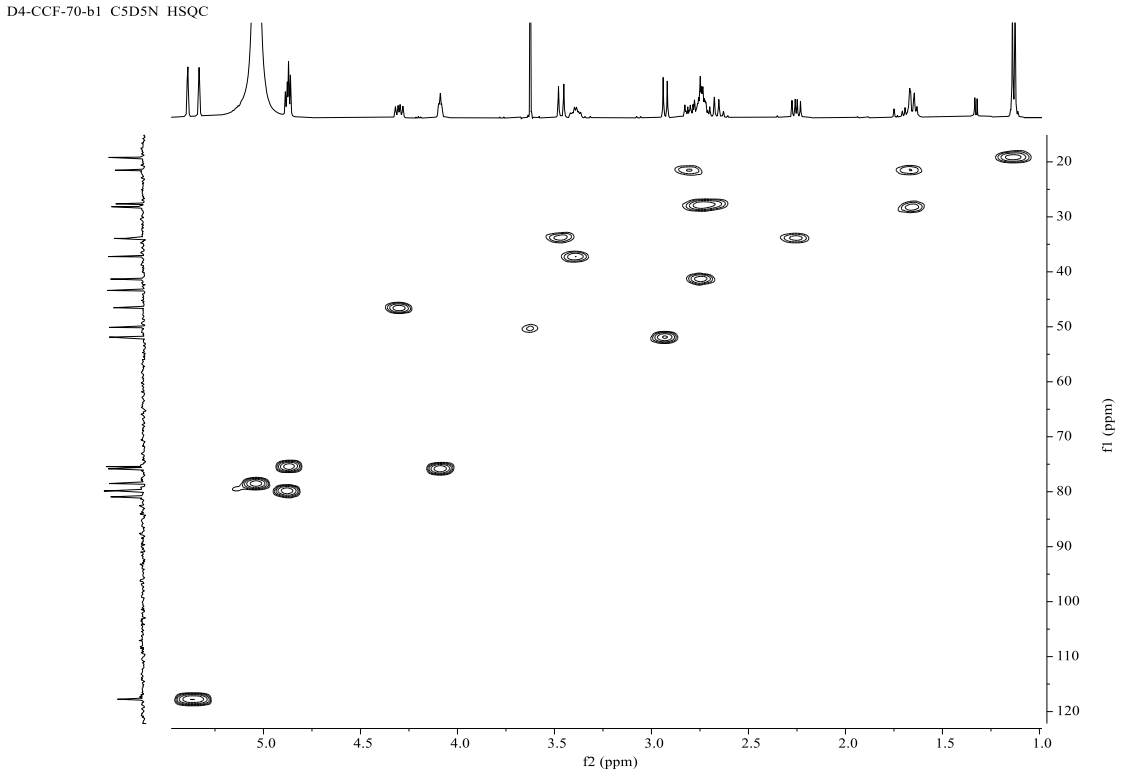

**Figure S147**. HMBC spectrum of fortalide M (**13**) in pyridine-$d_5$.

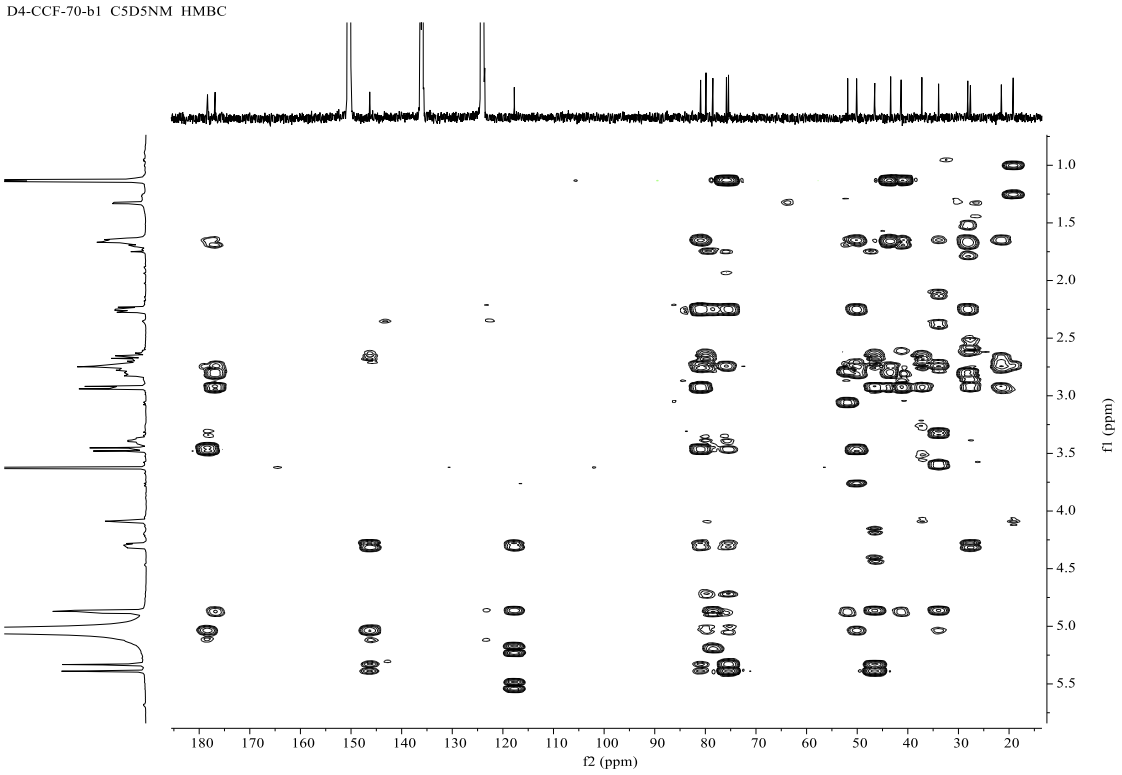


**Figure S148**. $^{1}$H-$^{1}$H COSY spectrum of fortalide M (**13**) in pyridine-$d_5$.

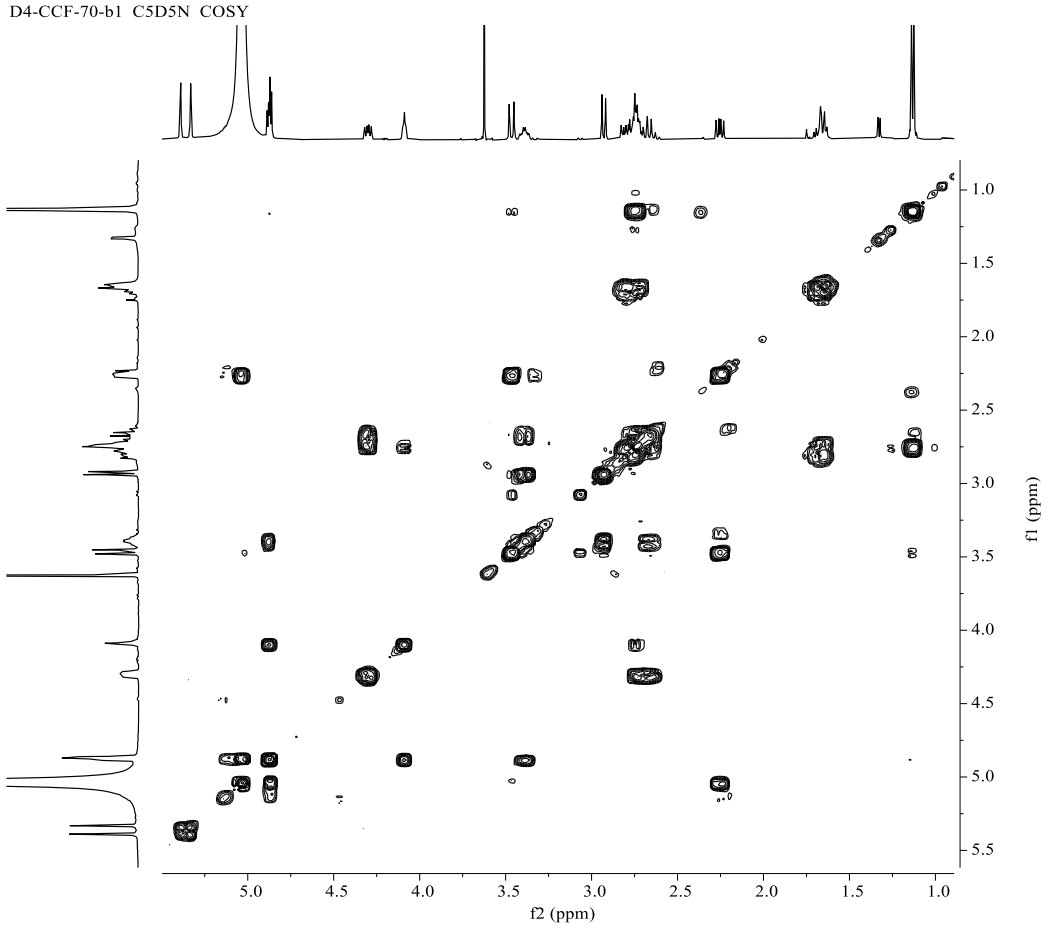

**Figure S149**. NOESY spectrum of fortalide M (**13**) in pyridine-$d_5$.

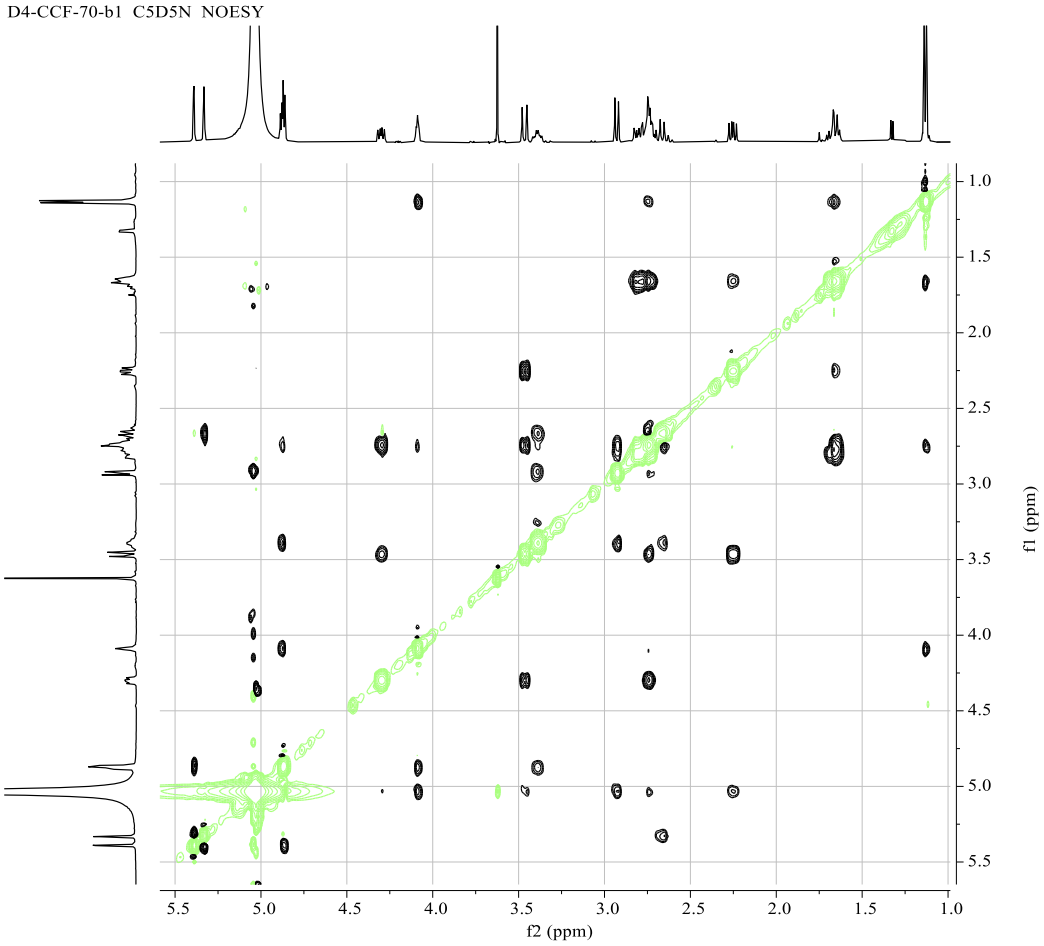


**Figure S150**. (+)-ESIMS spectrum of fortalide M (**13**).

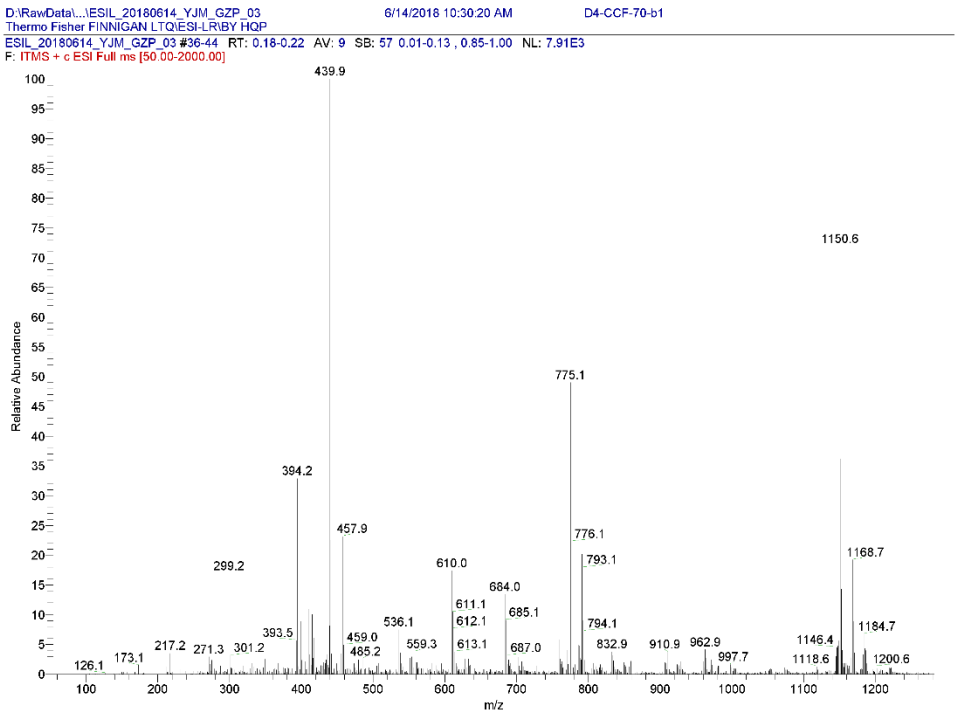

**Figure S151**. (−)-ESIMS spectrum of fortalide M (**13**).

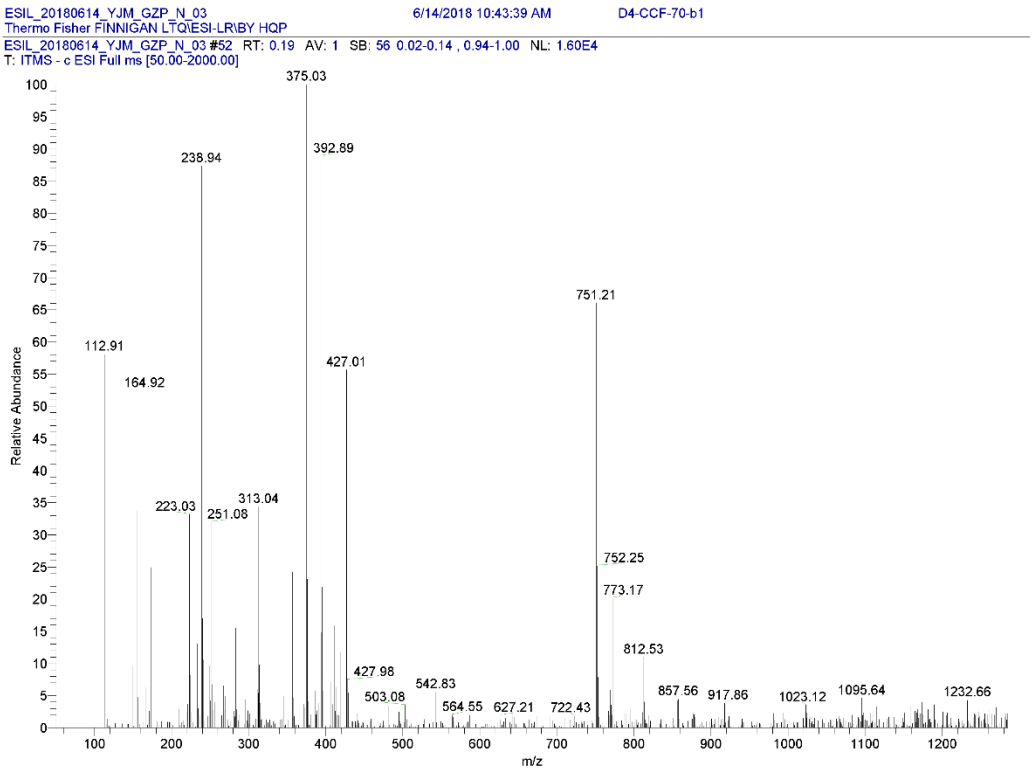


**Figure S152**. (−)-HRESIMS spectrum of fortalide M (**13**).

**Qualitative Analysis Report**

| | | | |
|---|---|---|---|
| **Data Filename** | ESIH_20180614_YJM_GZP_03.d | **Sample Name** | D4-CCF-70-b1 |
| **Sample Type** | Sample | **Position** | P1-B3 |
| **Instrument Name** | Agilent G6520 Q-TOF | **Acq Method** | 20160324_MS_ESIH_NEG_1min.m |
| **Acquired Time** | 6/14/2018 14:49:44 | **IRM Calibration Status** | Success |
| **DA Method** | small molecular data analysis method.m | **Comment** | ESIH by ZZY |

**User Spectra**

| Fragmentor Voltage | Collision Energy | Ionization Mode |
|---|---|---|
| 175 | 0 | ESI |

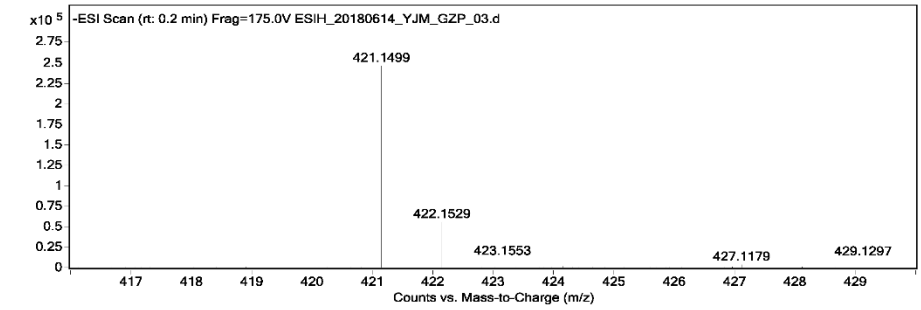


**Formula Calculator Results**

| m/z | Calc m/z | Diff (mDa) | Diff (ppm) | Ion Formula | Ion |
|---|---|---|---|---|---|
| 421.1499 | 421.1504 | 0.5 | 1.19 | C21 H25 O9 | (M+COOH)- |

--- End Of Report ---

Agilent Technologies Page 1 of 1 Printed at: 15:35 on: 6/14/2018

**Figure S153**. IR spectrum of fortalide M (**13**).

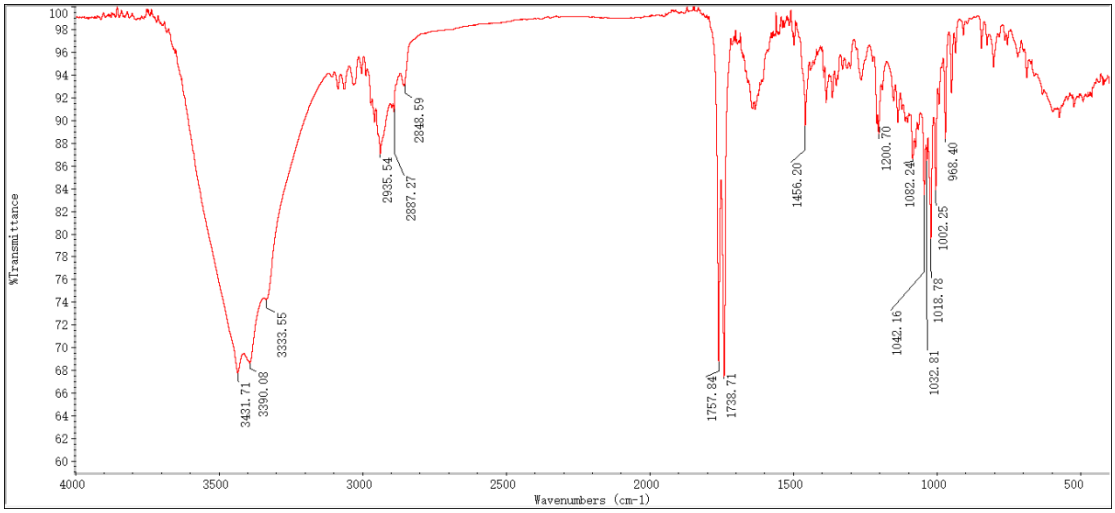


**Figure S154–S163.** 1D and 2D NMR, MS, and IR spectra of fortalide N (**14**)

**Figure S154**. $^{1}$H NMR spectrum of fortalide N (**14**) in pyridine-$d_5$.

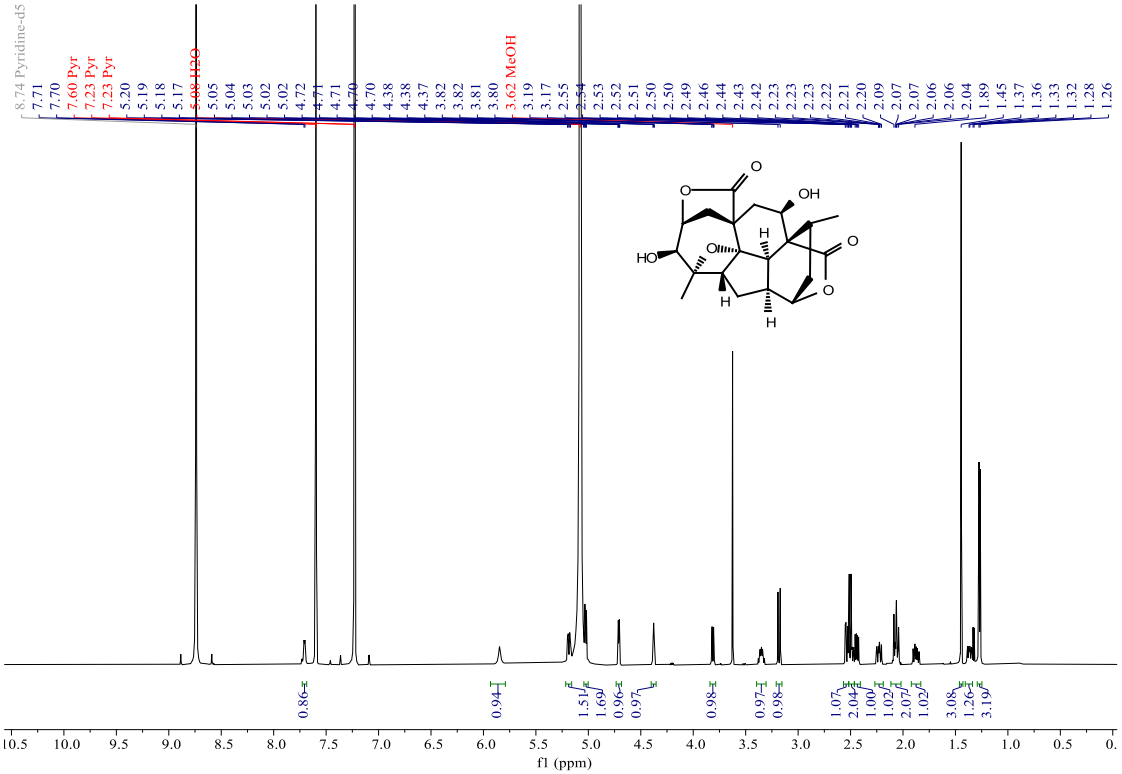

**Figure S155**. $^{13}$C NMR (BB and DEPT-135) spectra of fortalide N (**14**) in pyridine-$d_5$.

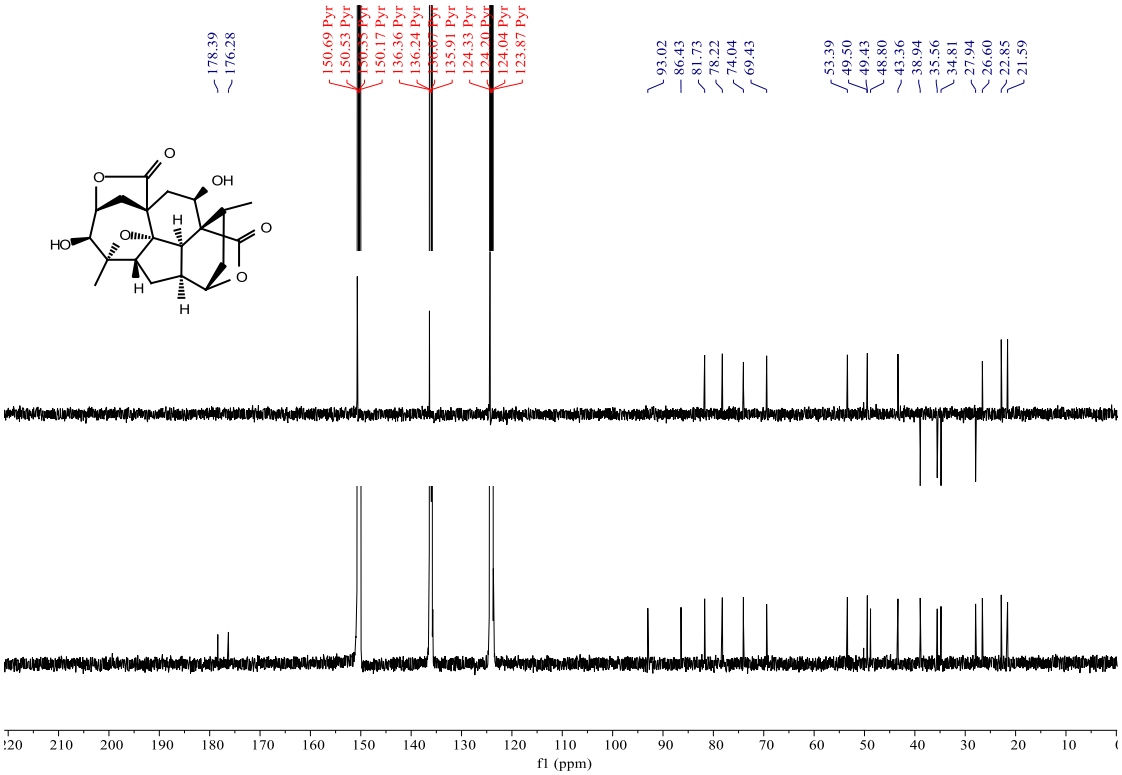


**Figure S156**. HSQC spectrum of fortalide N (**14**) in pyridine-$d_5$.

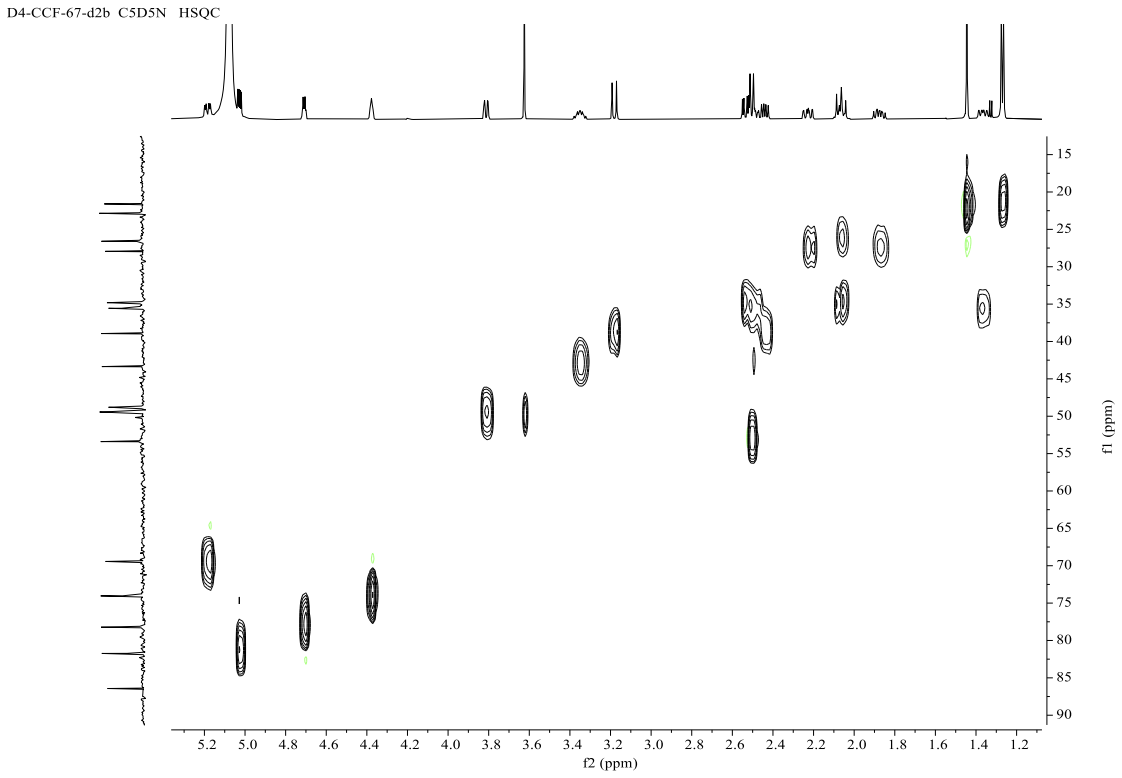

**Figure S157**. HMBC spectrum of fortalide N (**14**) in pyridine-$d_5$.

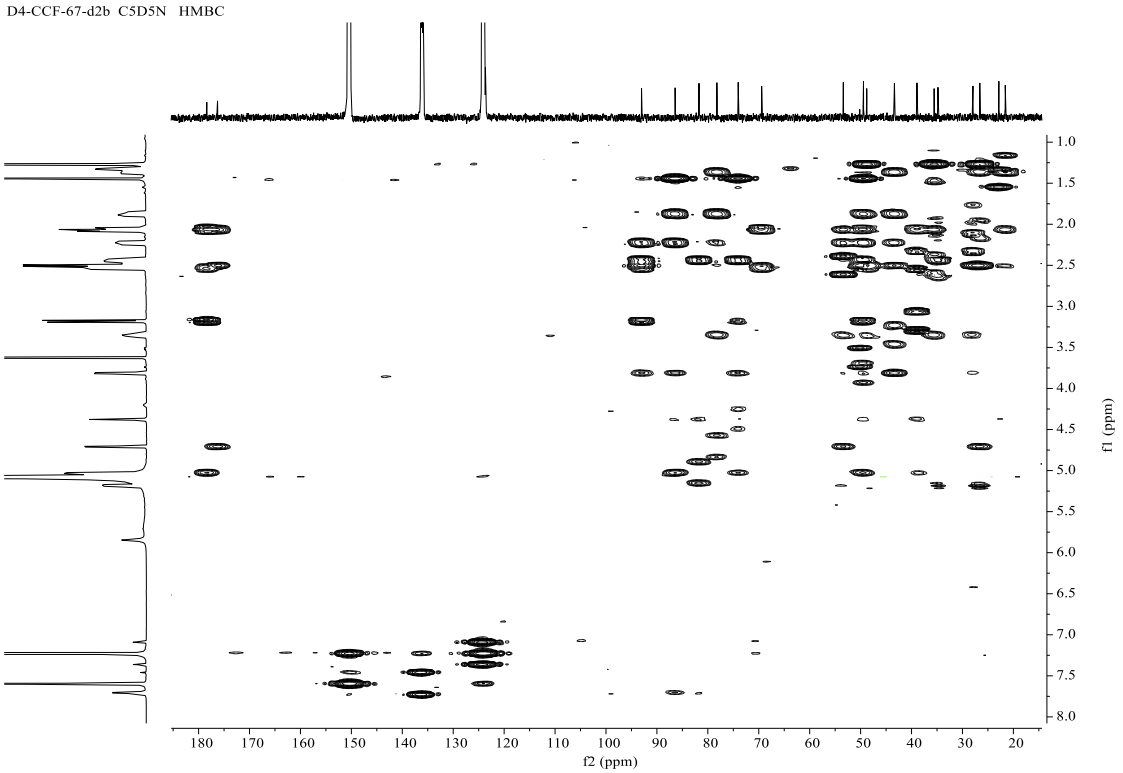


**Figure S158**. $^{1}$H-$^{1}$H COSY spectrum of fortalide N (**14**) in pyridine-$d_5$.

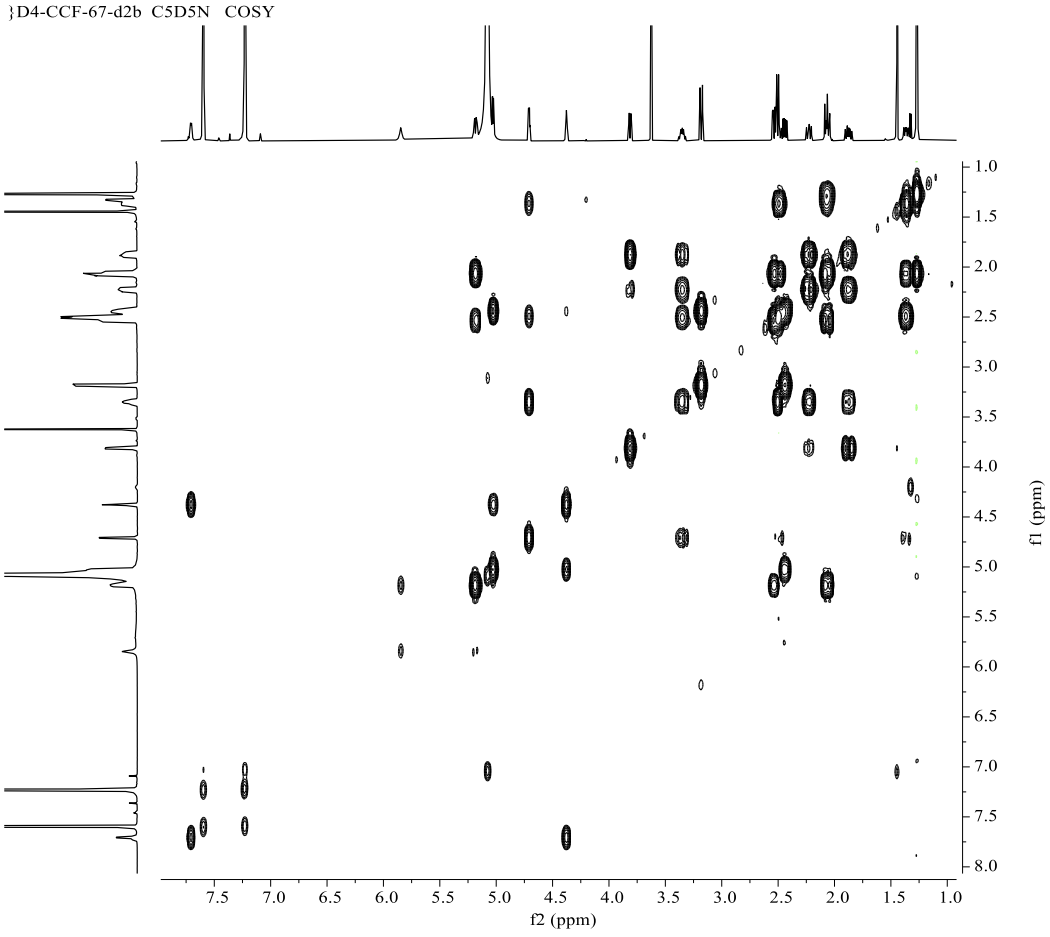

**Figure S159**. NOESY spectrum of fortalide N (**14**) in pyridine-$d_5$.

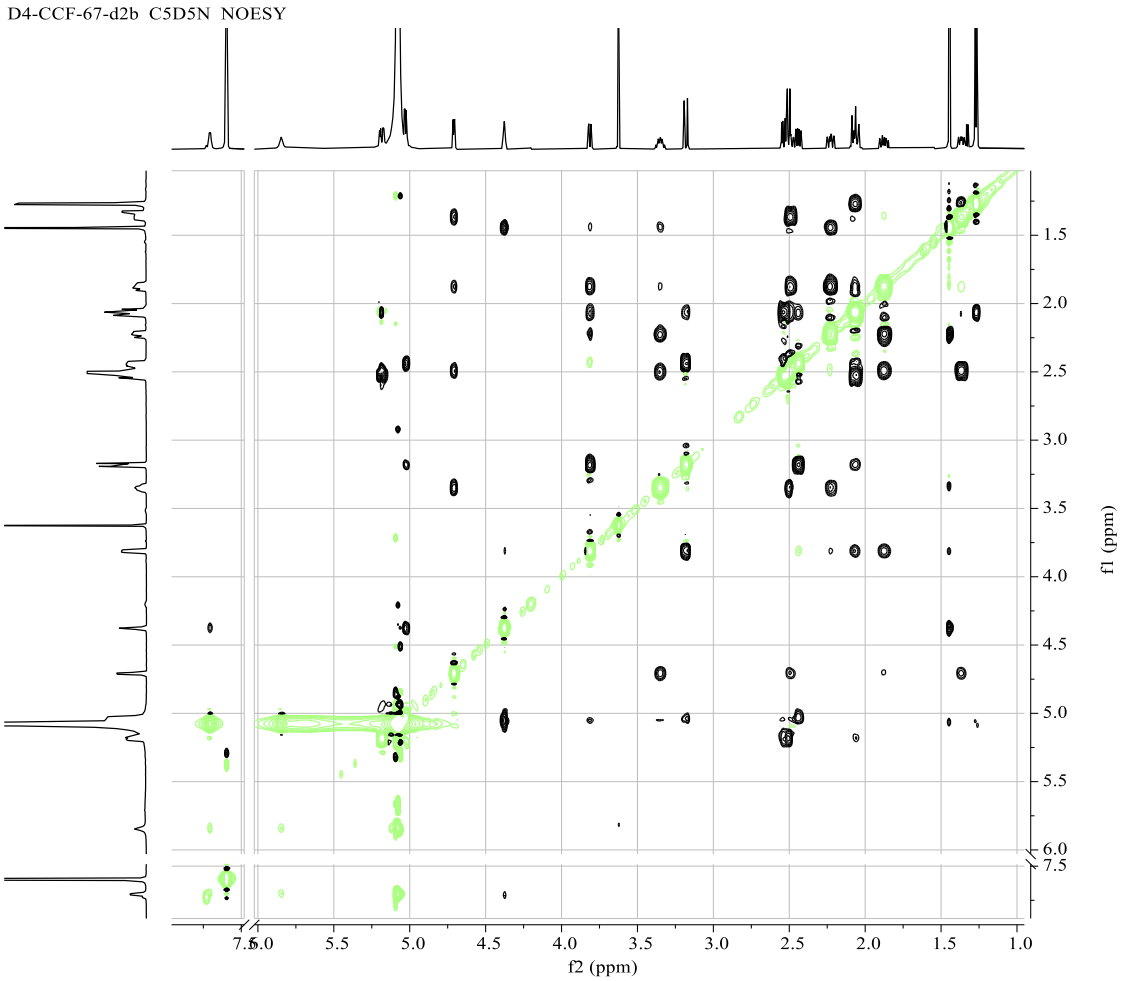


**Figure S160**. (+)-ESIMS spectrum of fortalide N (**14**).

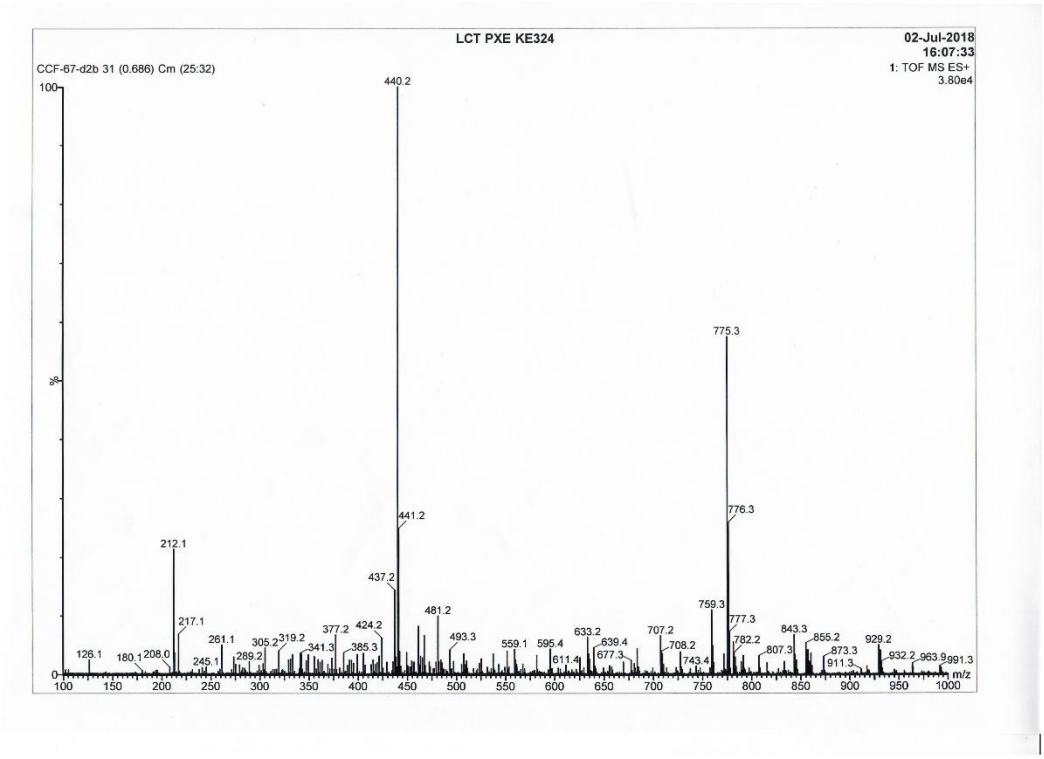

**Figure S161**. (−)-ESIMS spectrum of fortalide N (**14**).

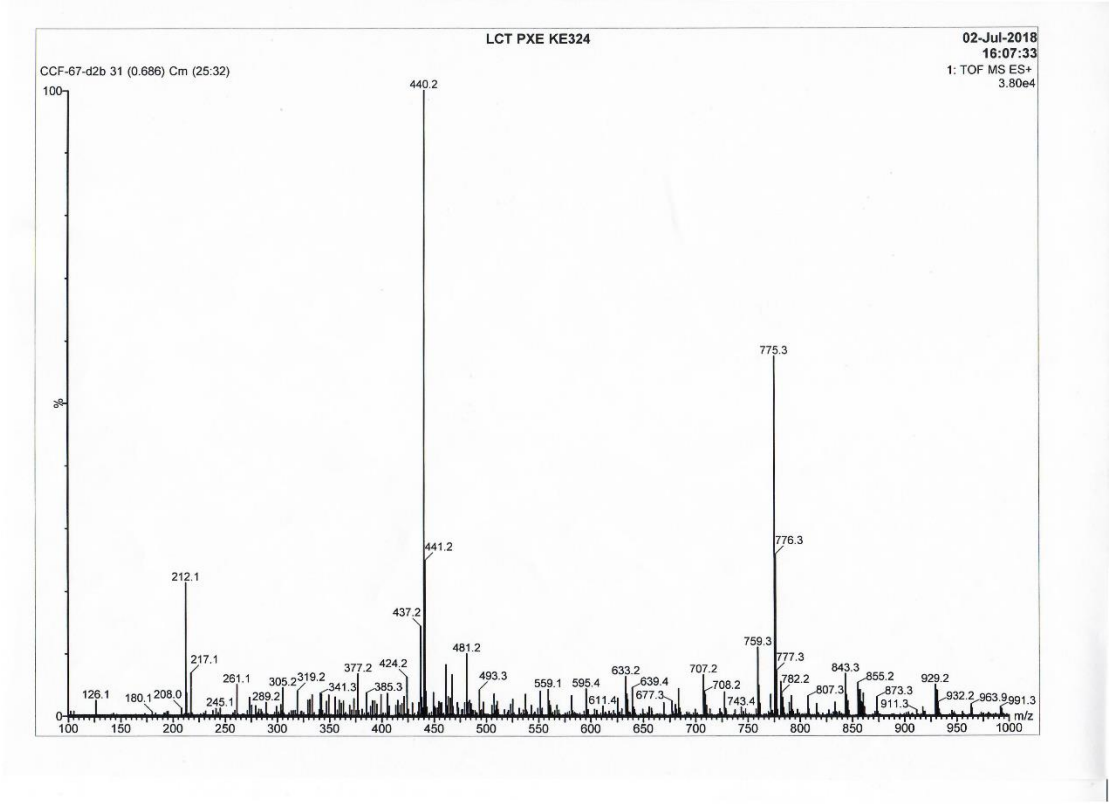


**Figure S162**. (−)-HRESIMS spectrum of fortalide N (**14**).

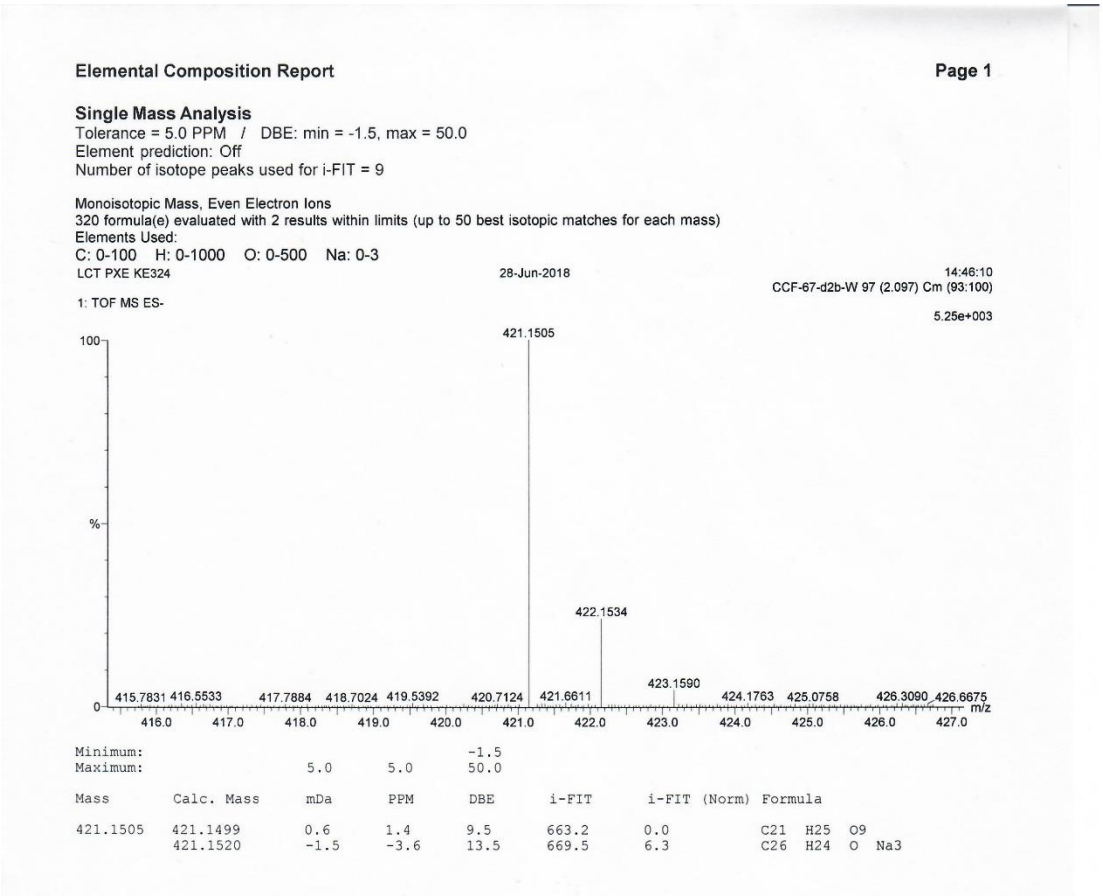

**Figure S163**. IR spectrum of fortalide N (**14**).

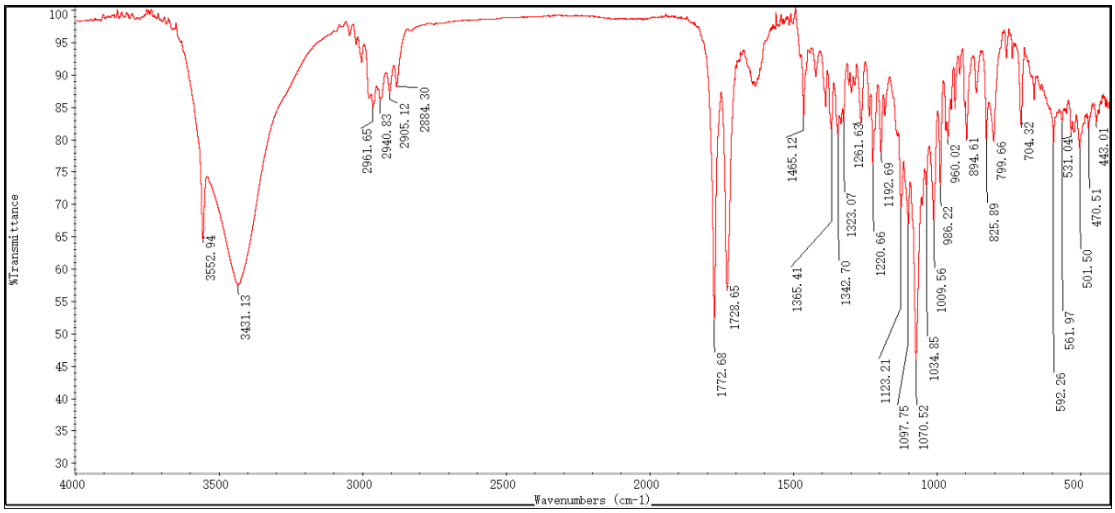


**Figure S164–S172.** 1D and 2D NMR, MS, and IR spectra of fortalide O (**15**)

**Figure S164**. $^{1}$H NMR spectrum of fortalide O (**15**) in pyridine-$d_5$.

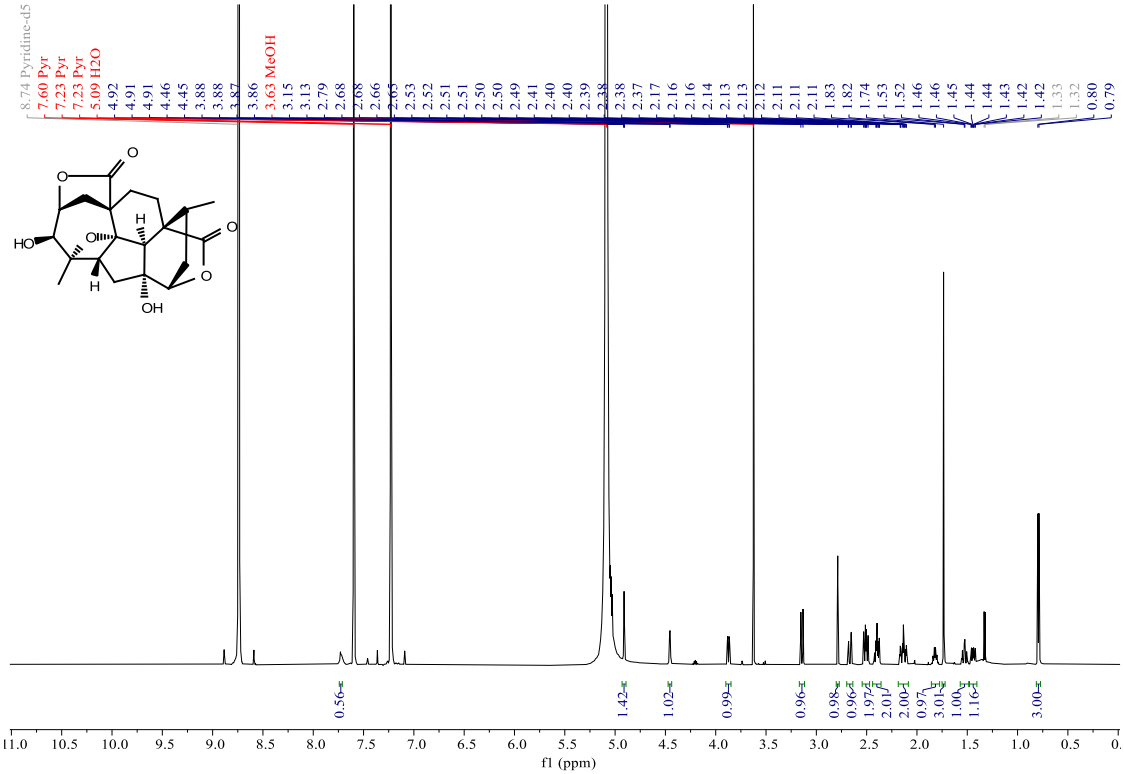

**Figure S165**. $^{13}$C NMR (BB and DEPT-135) spectra of fortalide O (**15**) in pyridine-$d_5$.

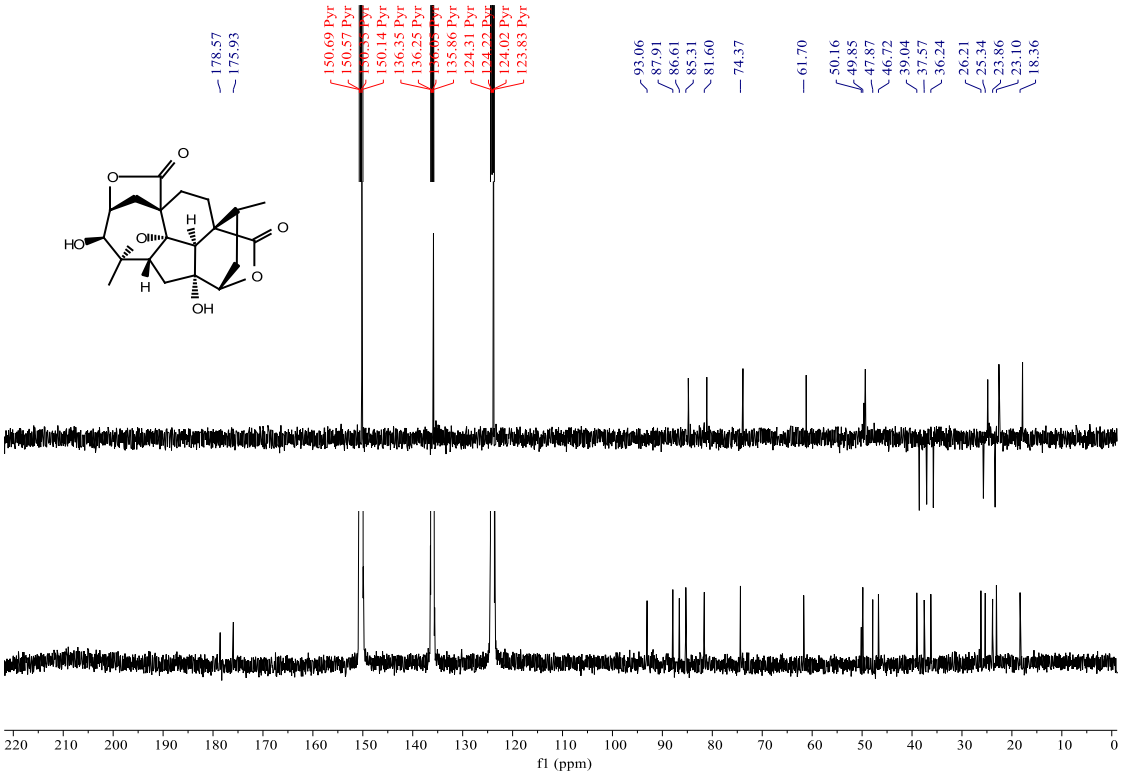


**Figure S166**. HSQC spectrum of fortalide O (**15**) in pyridine-$d_5$.

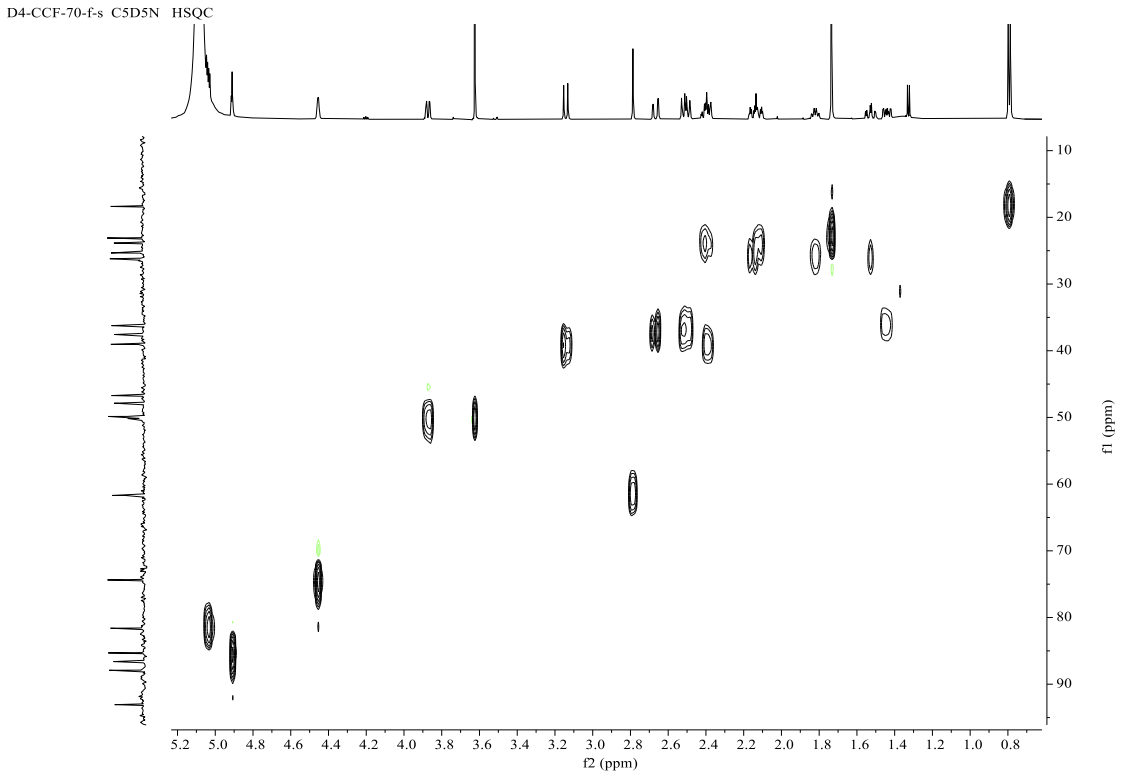

**Figure S167**. HMBC spectrum of fortalide O (**15**) in pyridine-$d_5$.

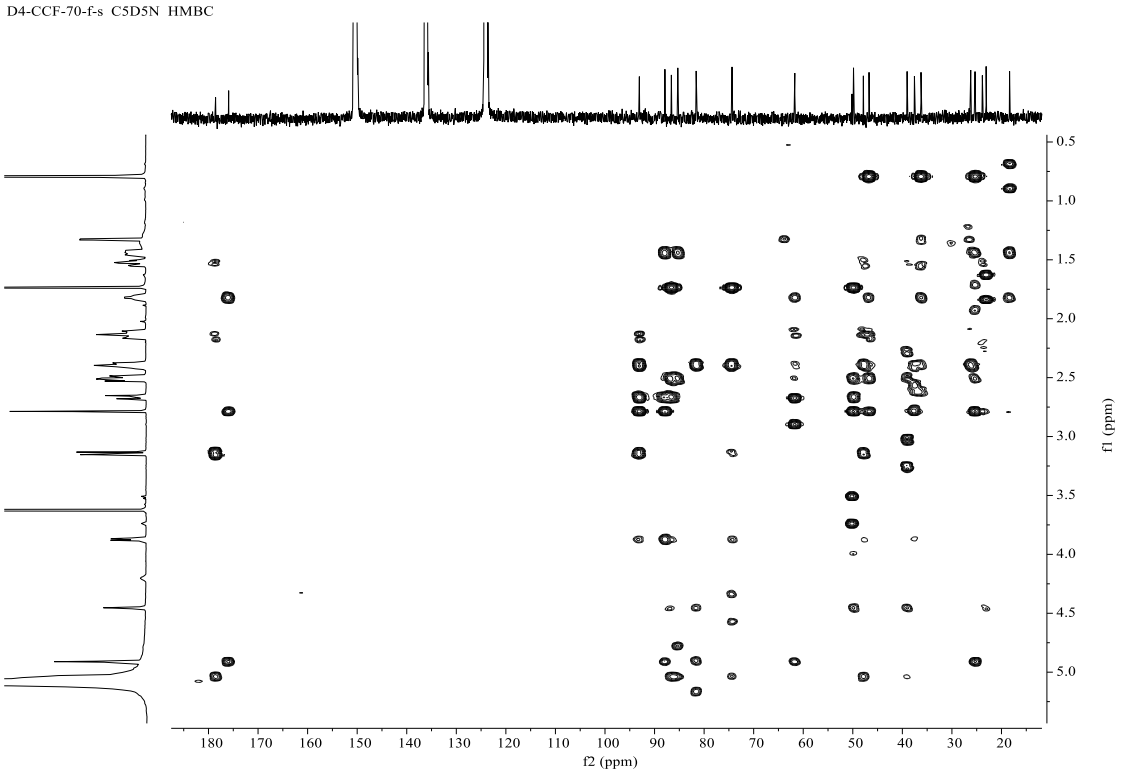


**Figure S168**. $^{1}$H-$^{1}$H COSY spectrum of fortalide O (**15**) in pyridine-$d_5$.

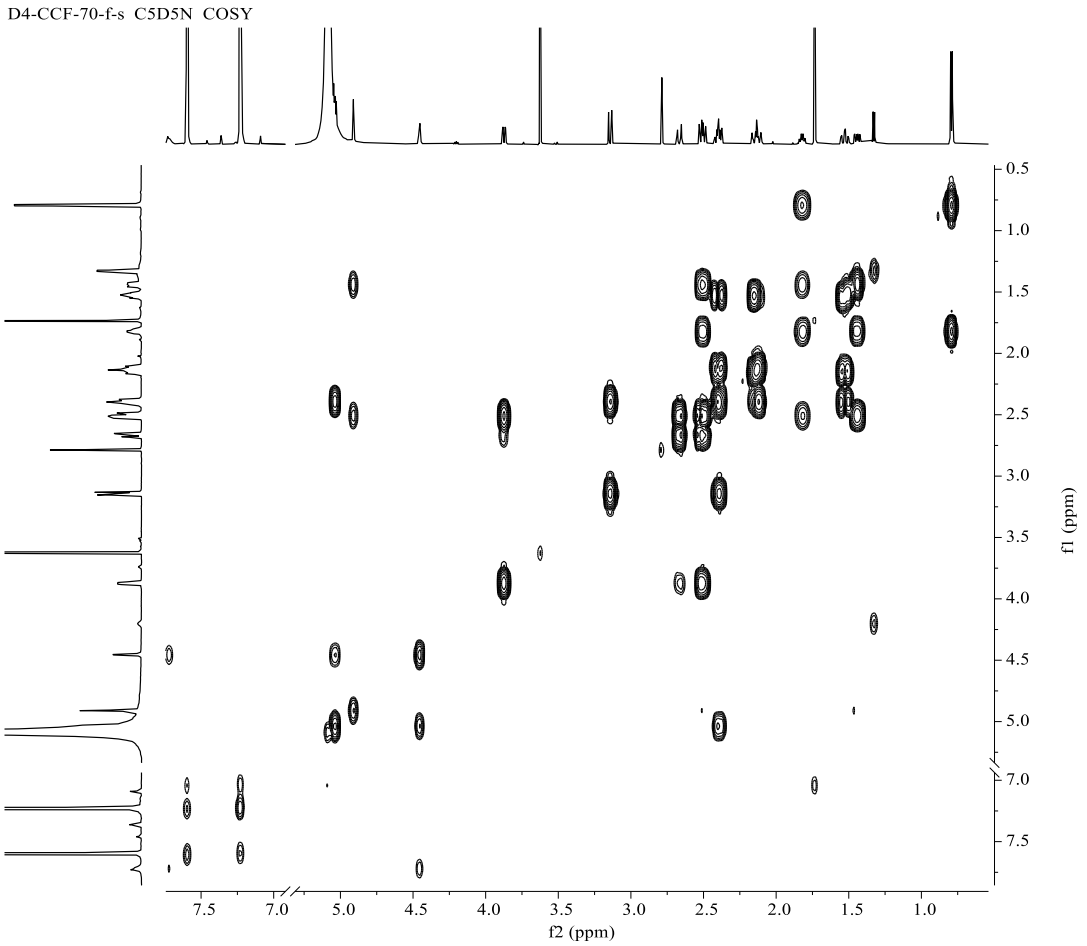

**Figure S169**. NOESY spectrum of fortalide O (**15**) in pyridine-$d_5$.

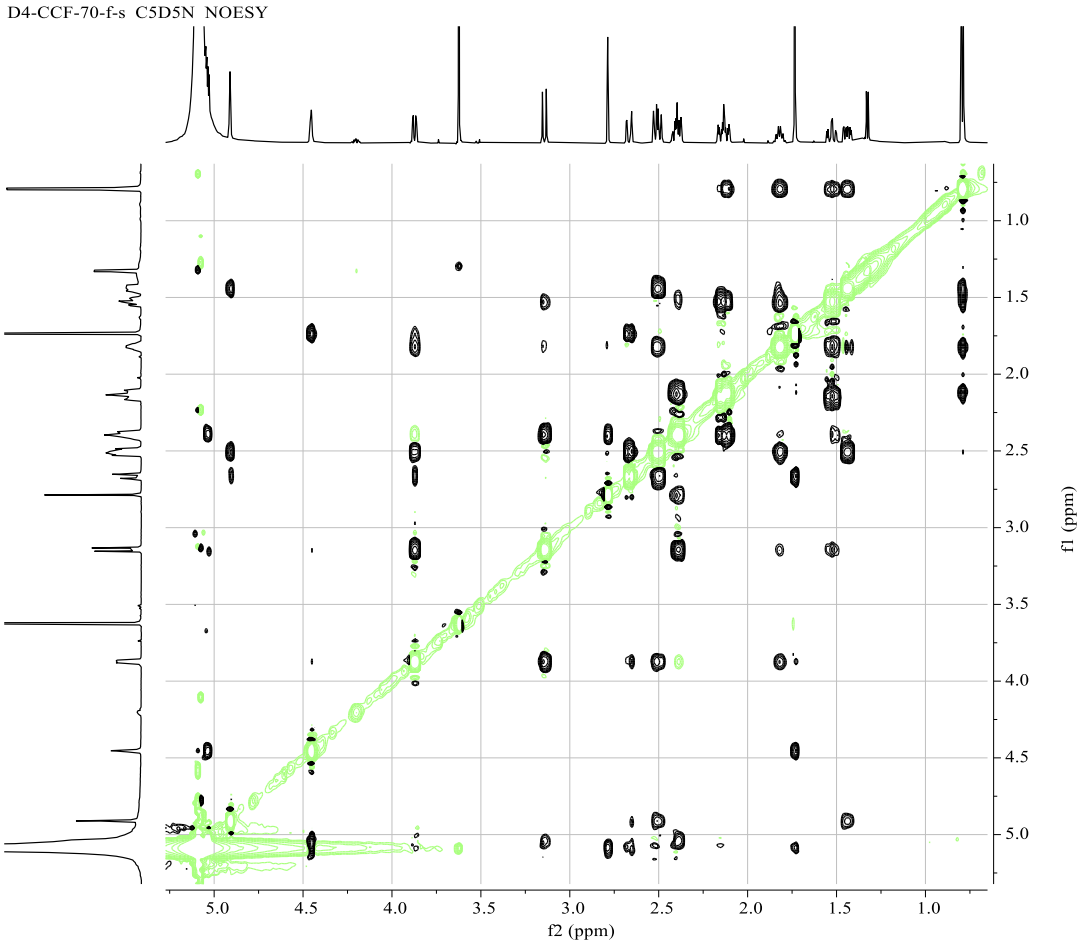


**Figure S170**. (−)-ESIMS spectrum of fortalide O (**15**).

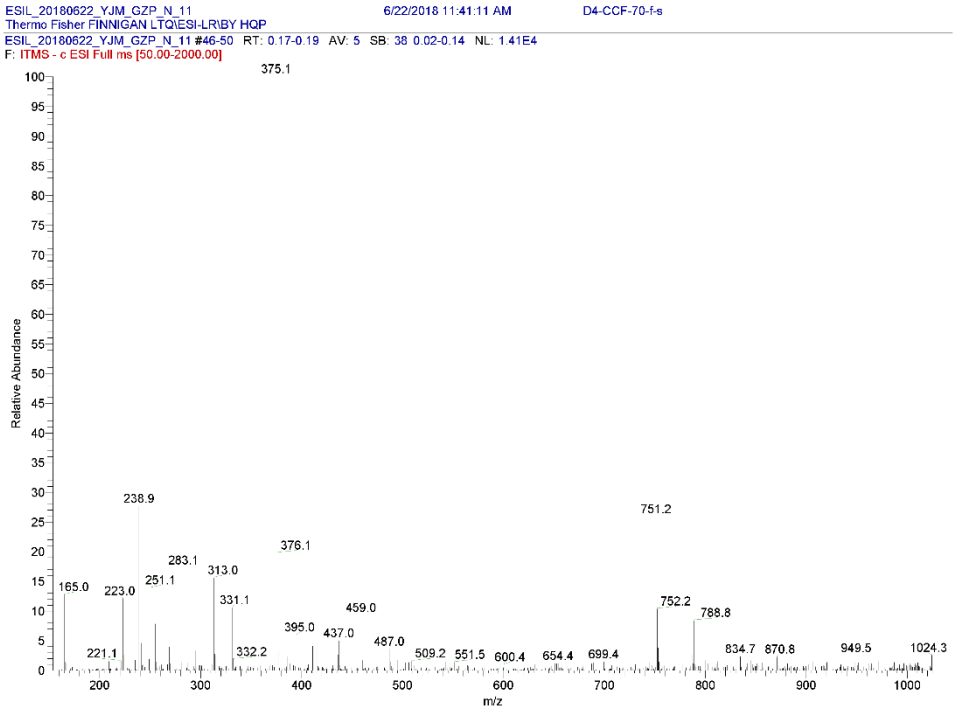

**Figure S171**. (−)-HRESIMS spectrum of fortalide O (**15**).

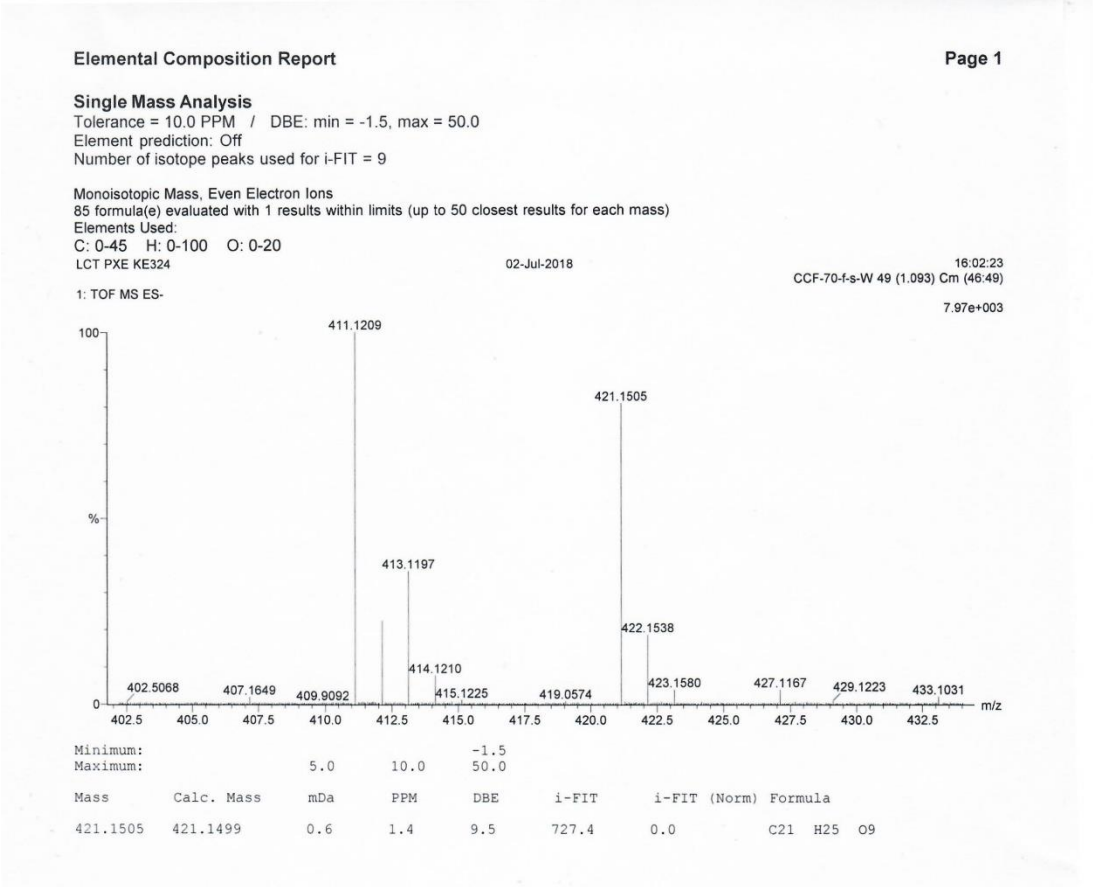


**Figure S172**. IR spectrum of fortalide O (**15**).

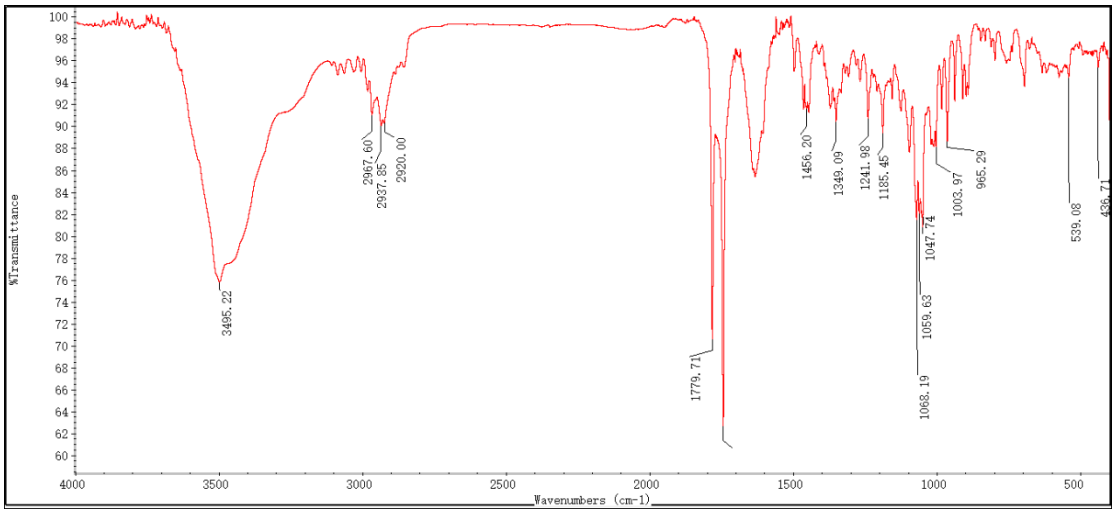

**Figure S173–S181.** 1D and 2D NMR, MS, and IR spectra of fortalide P (**16**)

**Figure S173**. $^{1}$H NMR spectrum of fortalide P (**16**) in $CDCl_3$.

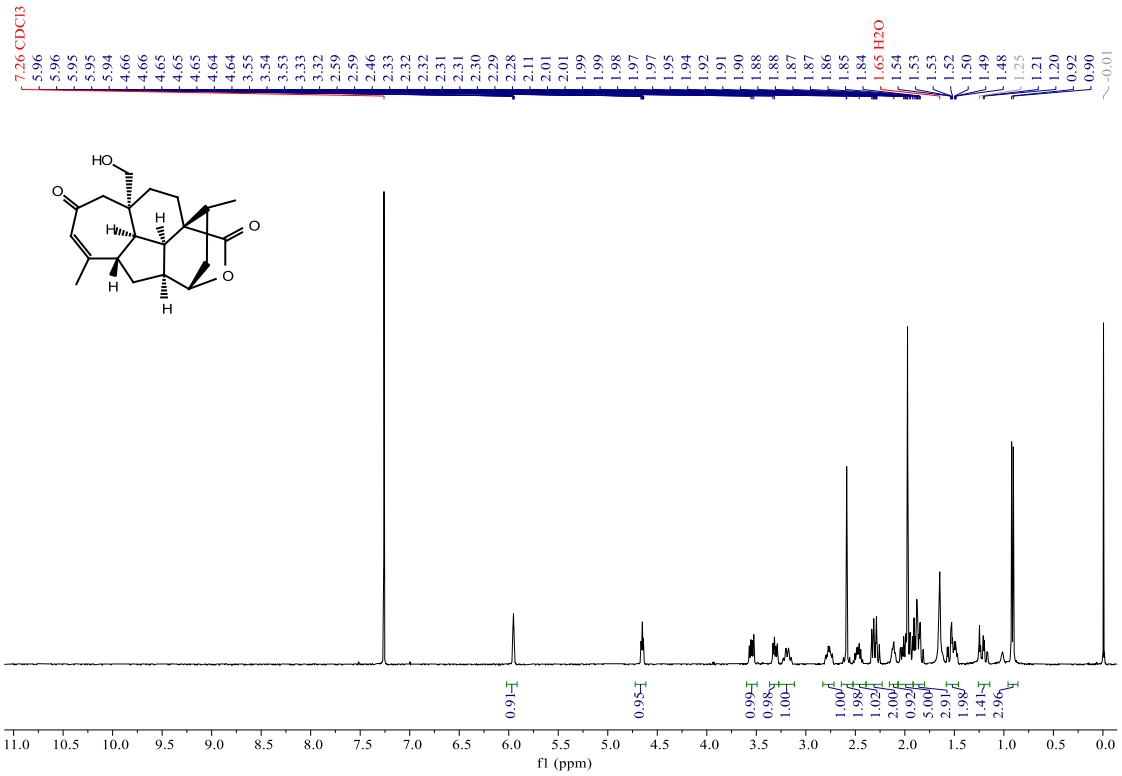


**Figure S174**. $^{13}$C NMR (BB and DEPT-135) spectra of fortalide P (**16**) in $CDCl_3$.

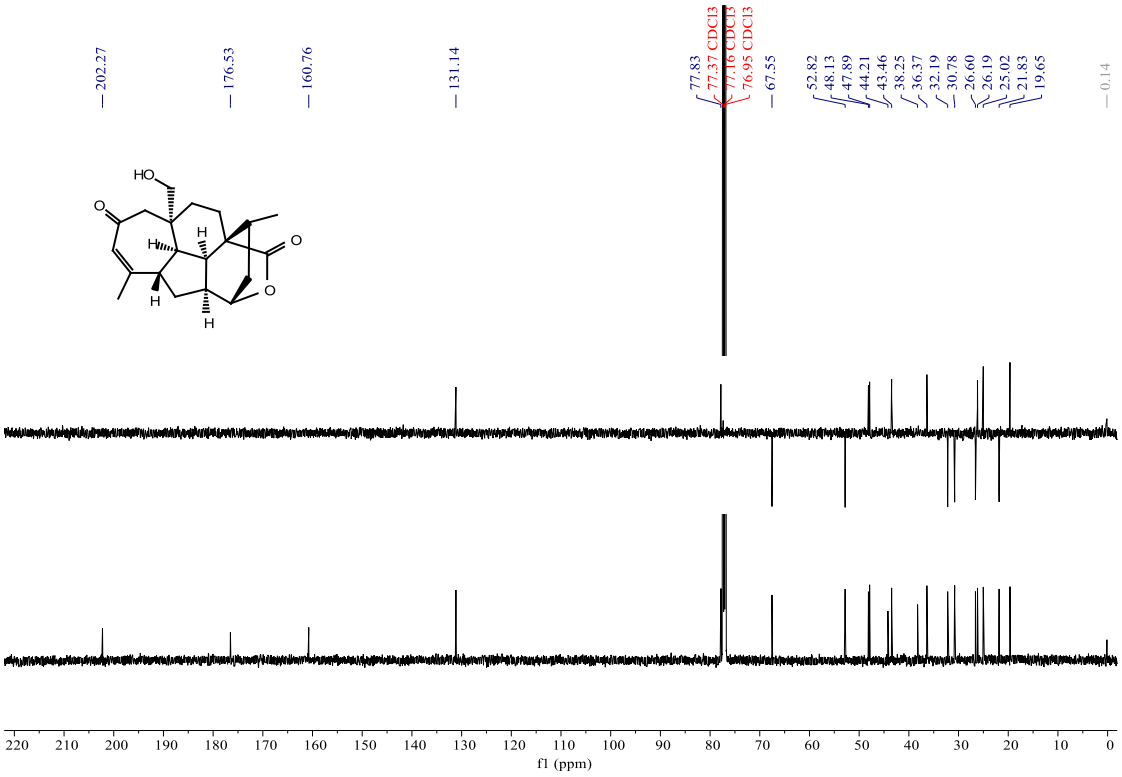

**Figure S175**. HSQC spectrum of fortalide P (**16**) in $CDCl_3$.

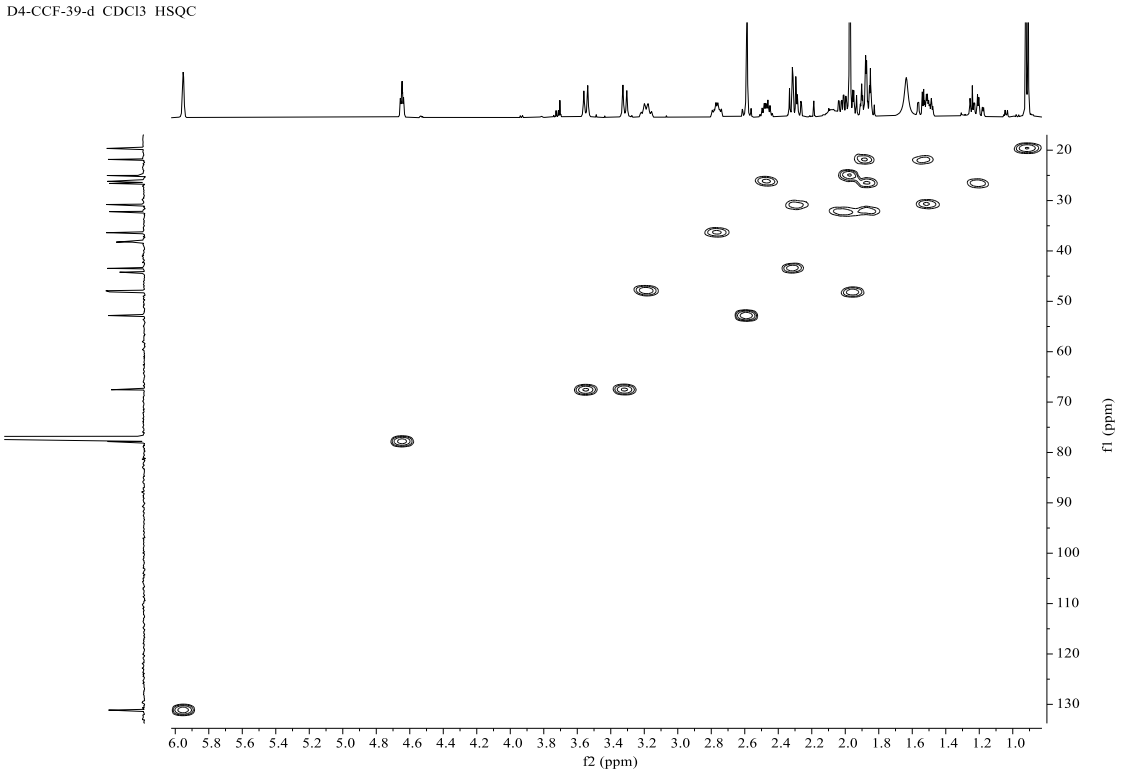


**Figure S176**. HMBC spectrum of fortalide P (**16**) in $CDCl_3$.

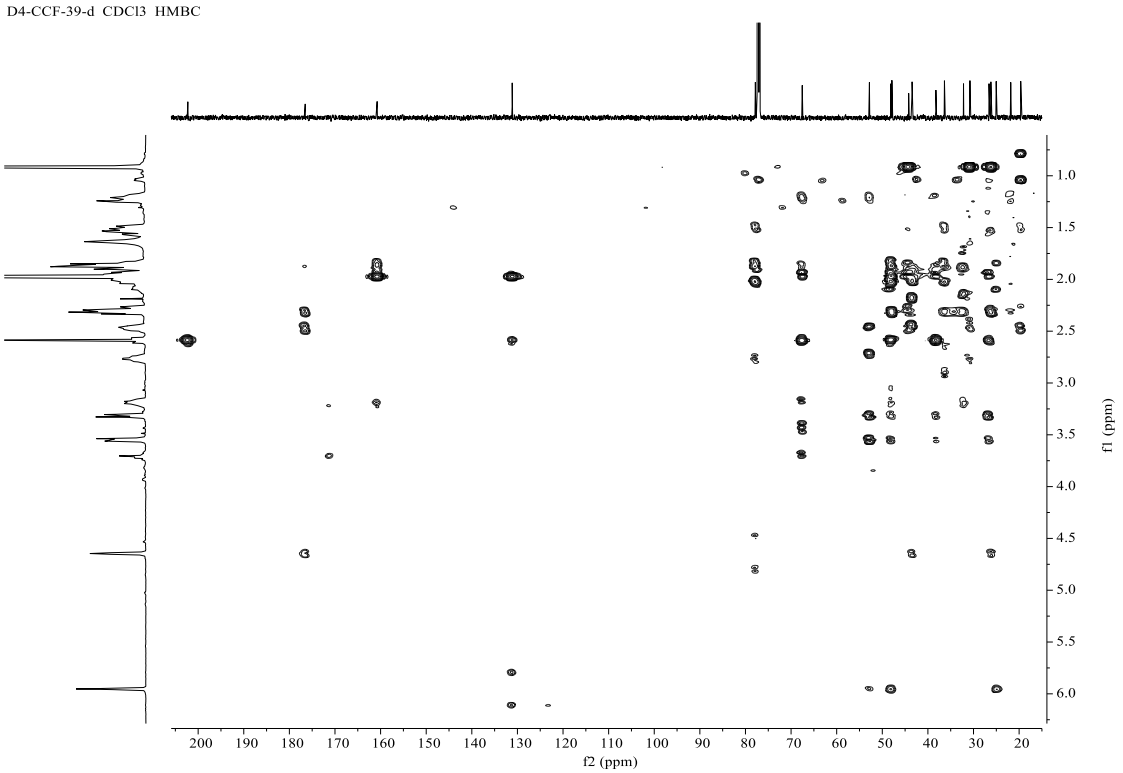

**Figure S177**. $^{1}H$-$^{1}H$ COSY spectrum of fortalide P (**16**) in $CDCl_3$.

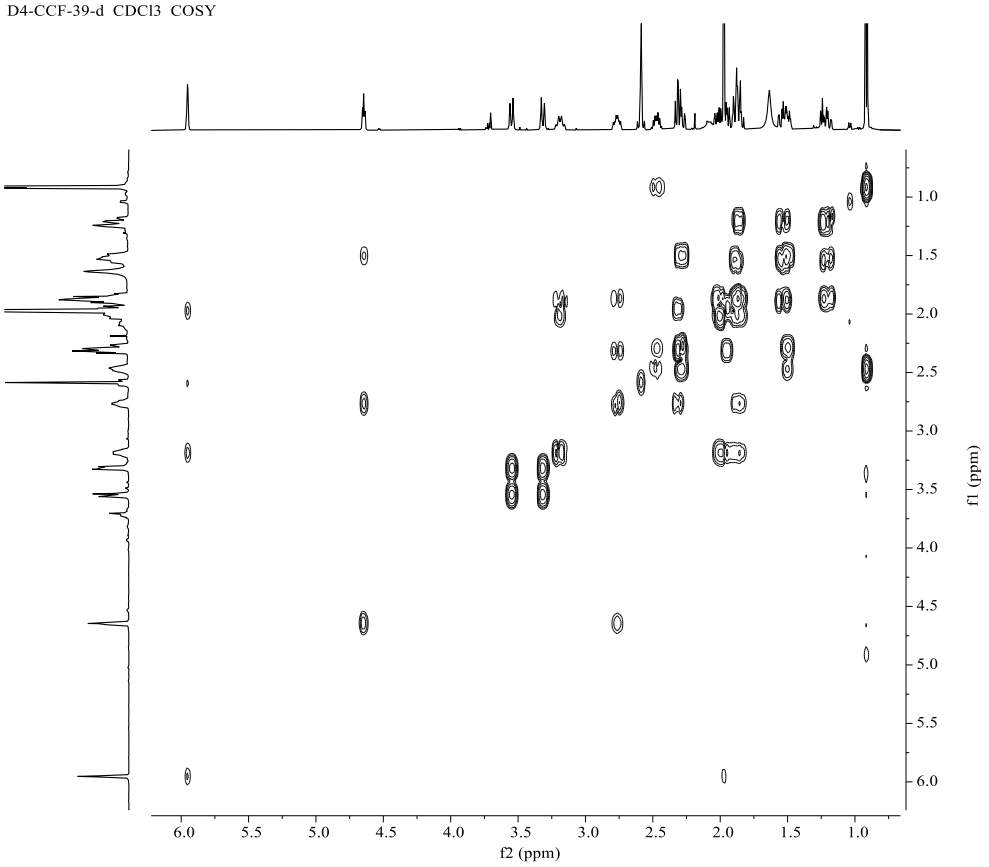


**Figure S178**. NOESY spectrum of fortalide P (**16**) in $CDCl_3$.

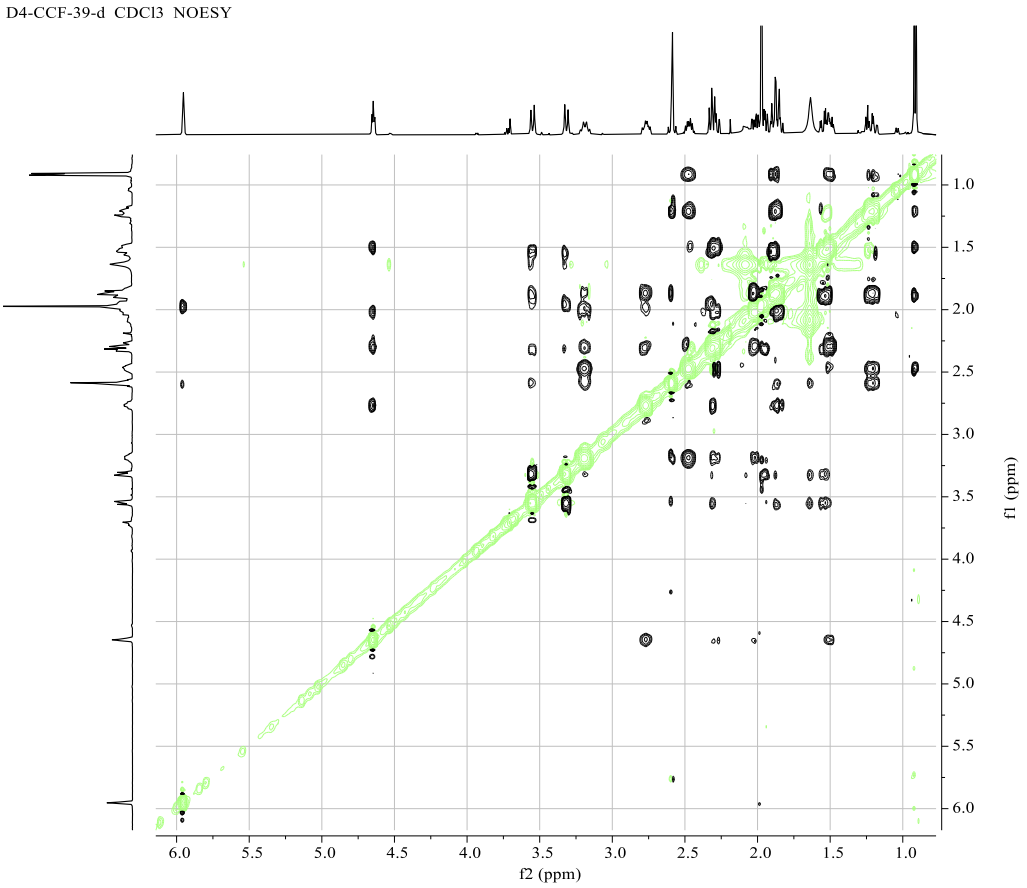

**Figure S179**. (+)-ESIMS spectrum of fortalide P (**16**).

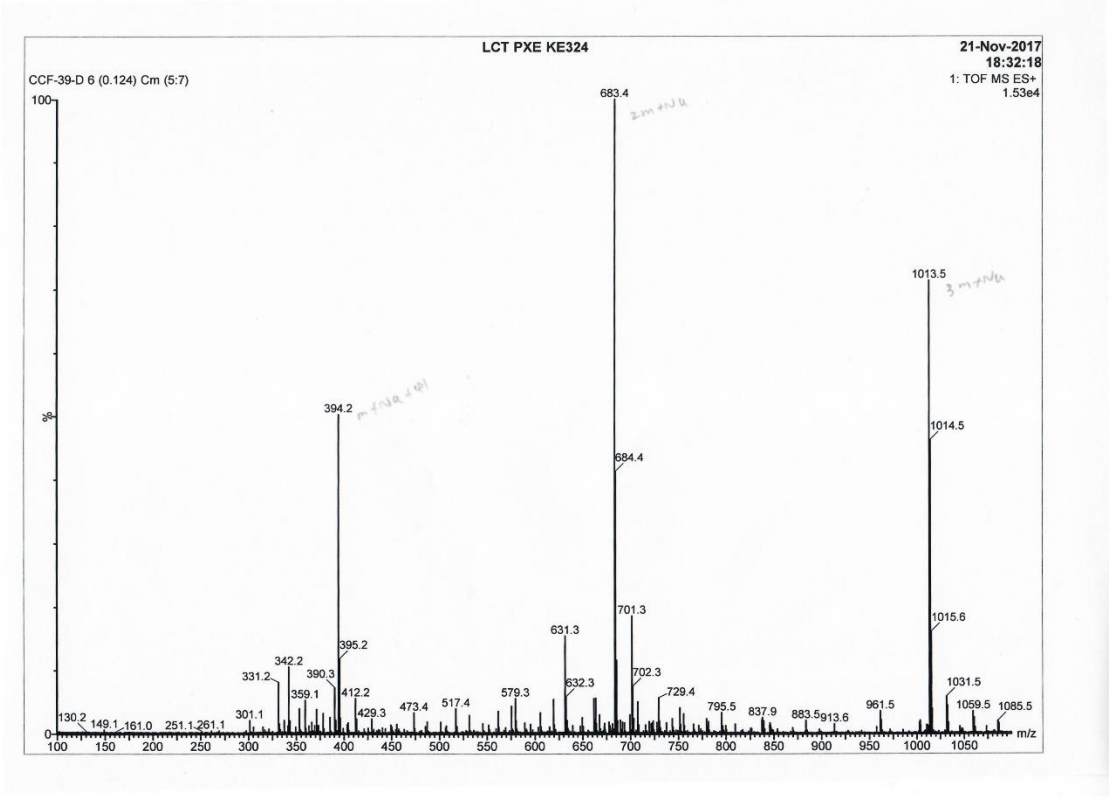


**Figure S180**. (+)-HRESIMS spectrum of fortalide P (**16**).

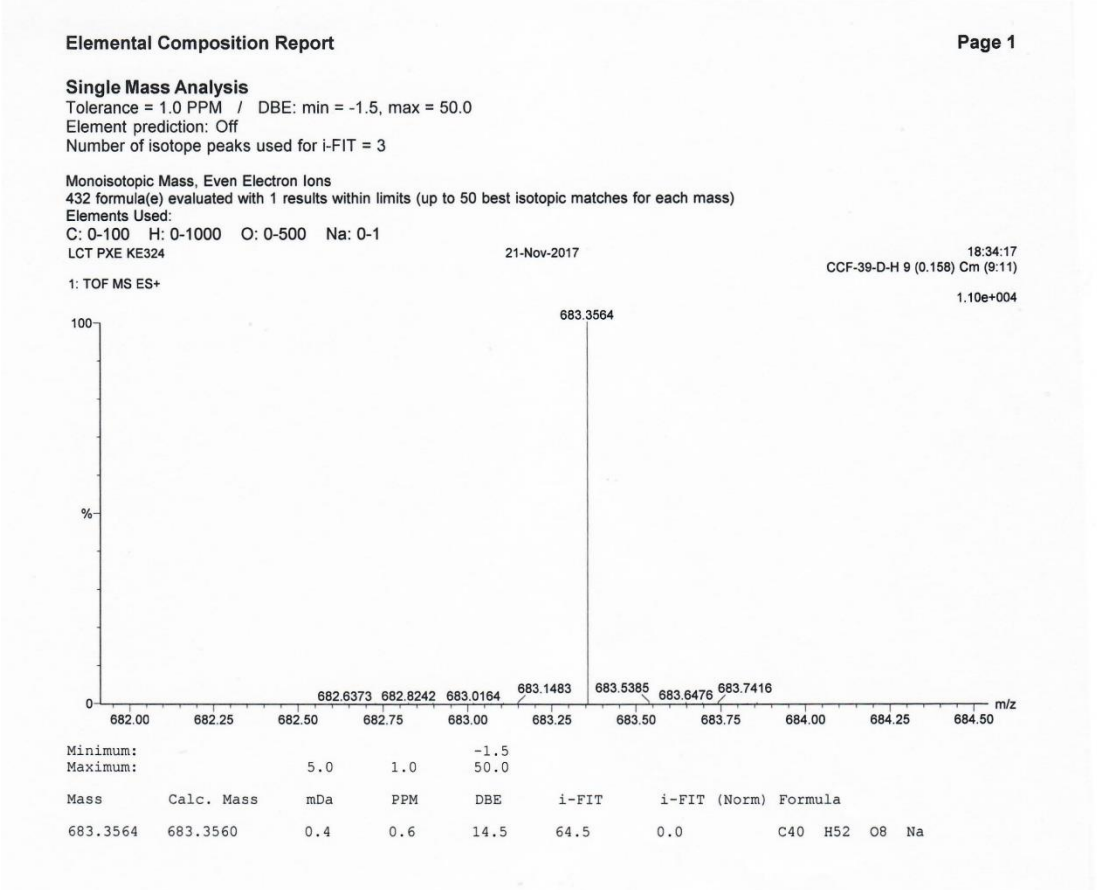

**Figure S181**. IR spectrum of fortalide P (**16**).

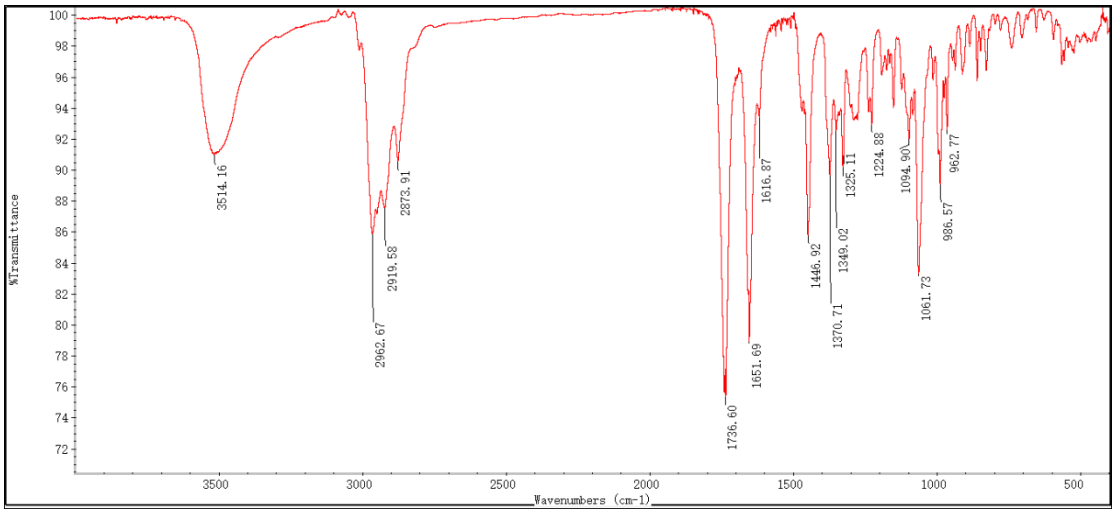


**Figure S182–S191.** 1D and 2D NMR, MS, and IR spectra of fortalide Q (**17**)

**Figure S182**. $^{1}$H NMR spectrum of fortalide Q (**17**) in methanol-$d_4$.

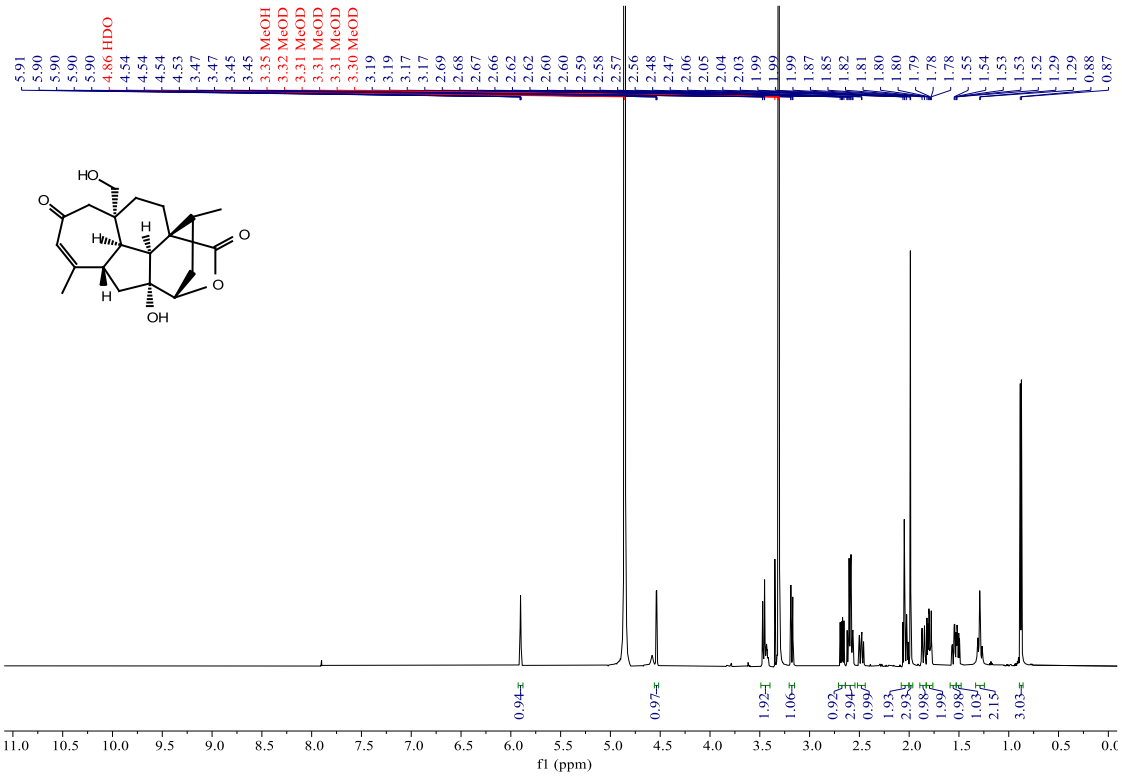

**Figure S183**. $^{13}$C NMR (BB and DEPT-135) spectra of fortalide Q (**17**) in methanol-$d_4$.

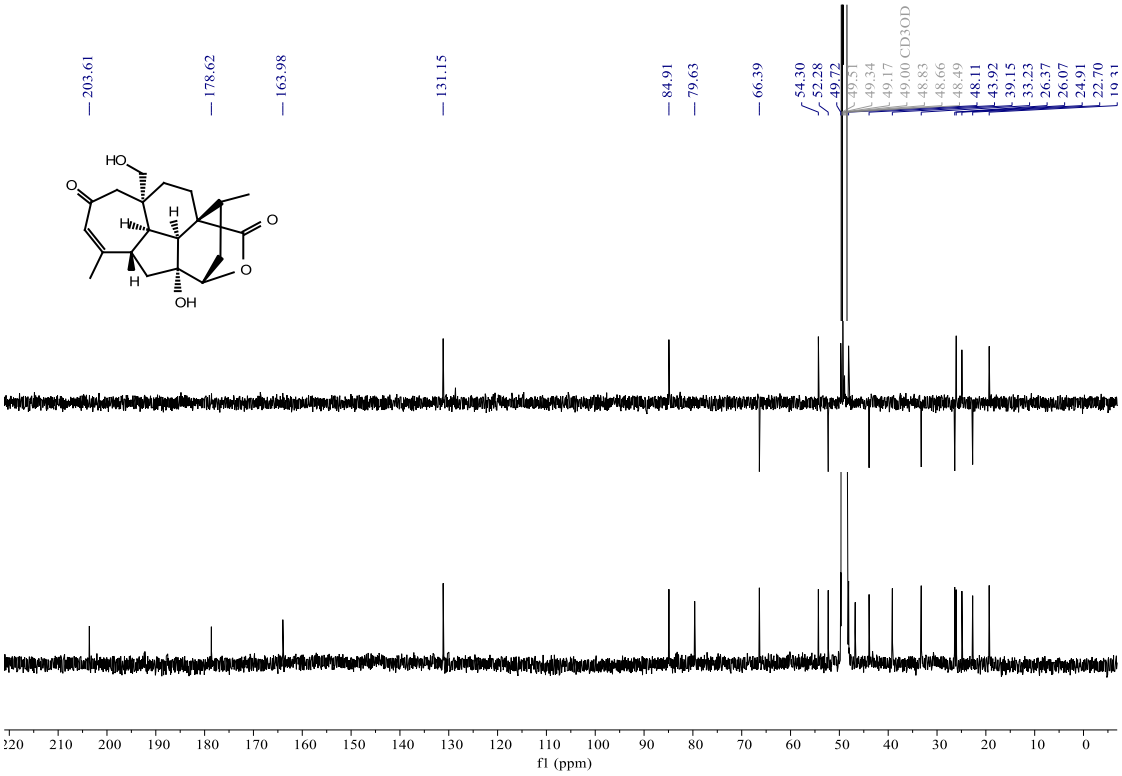


**Figure S184.** HSQC spectrum of fortalide Q (**17**) in methanol-$d_4$.

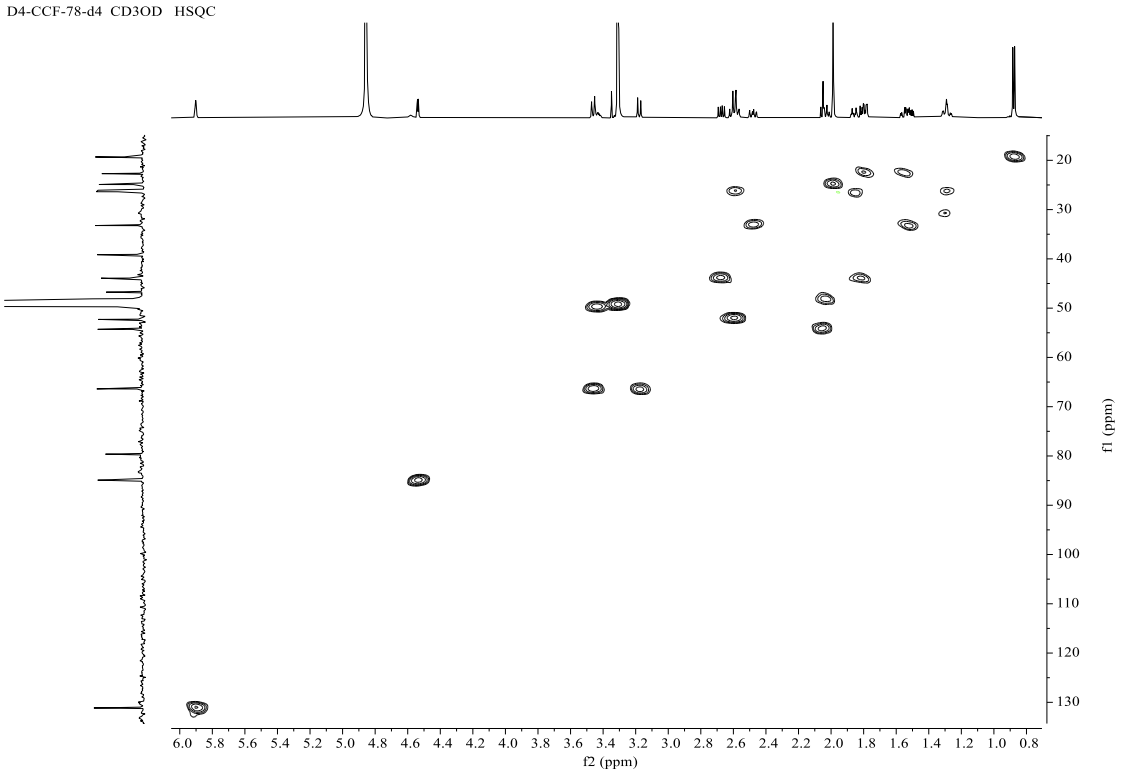

**Figure S185.** HMBC spectrum of fortalide Q (**17**) in methanol-$d_4$.

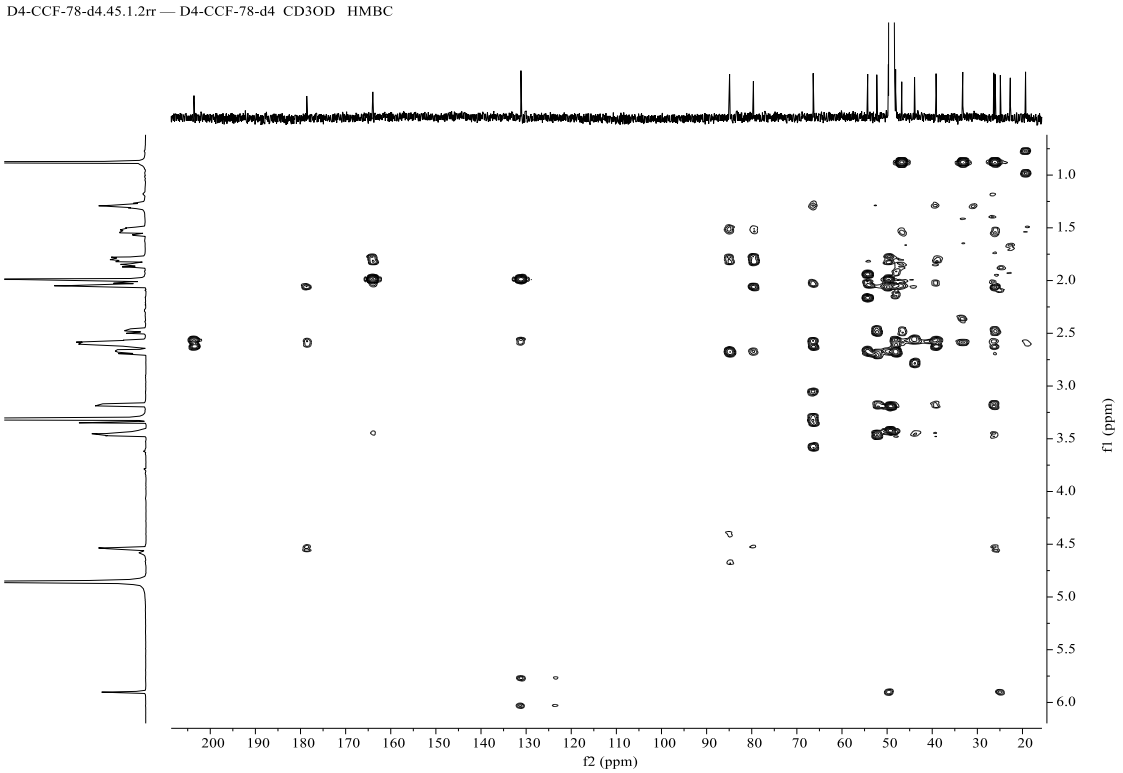


**Figure S186**. $^{1}$H-$^{1}$H COSY spectrum of fortalide Q (**17**) in methanol-$d_4$.

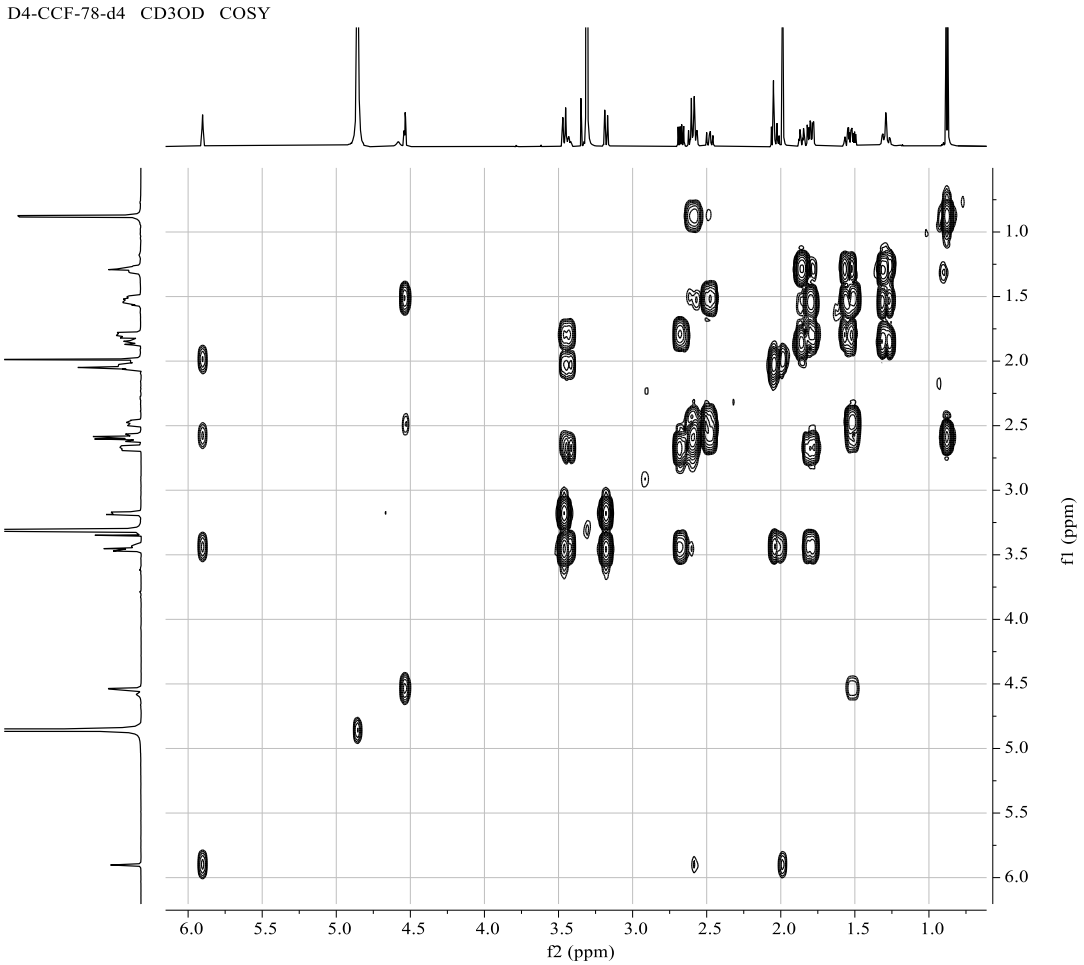

**Figure S187**. NOESY spectrum of fortalide Q (**17**) in methanol-$d_4$.

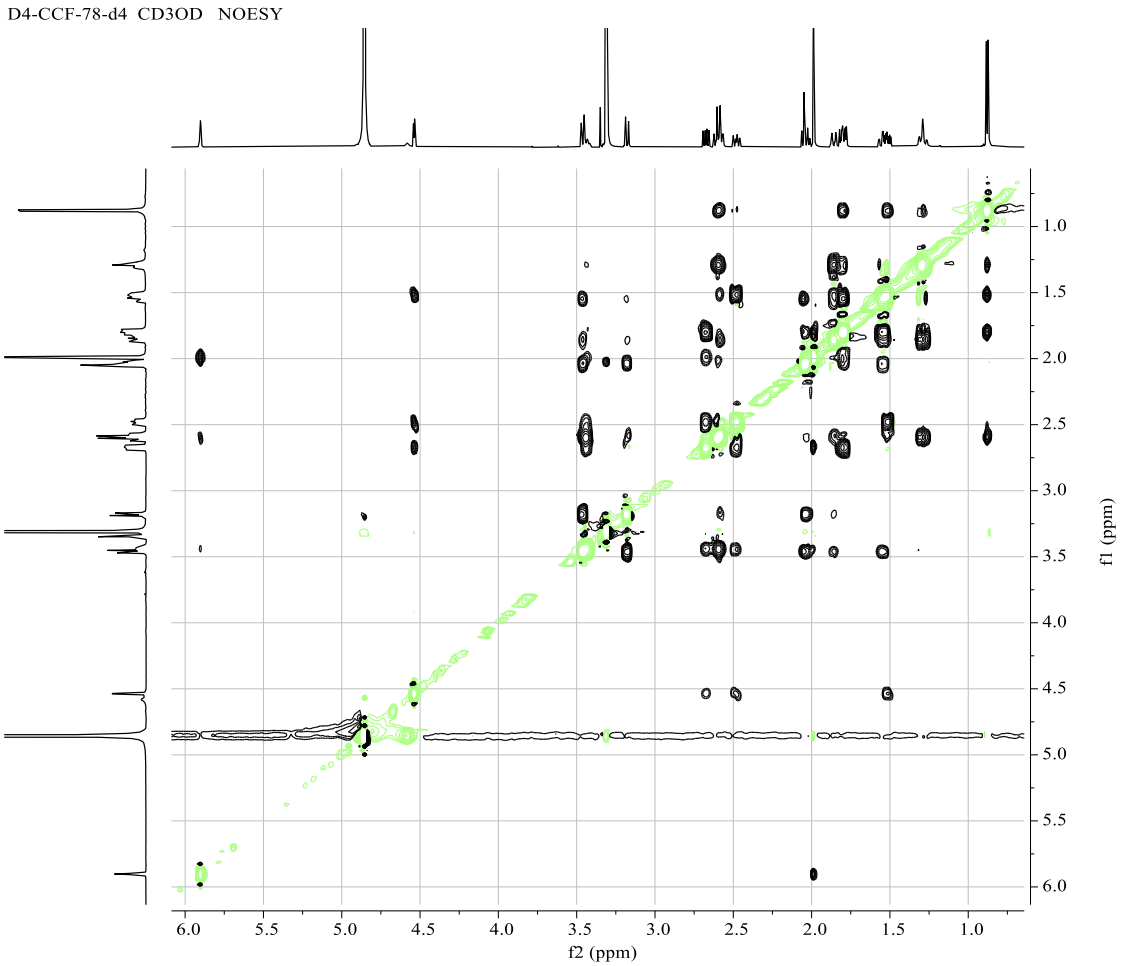


**Figure S188**. (+)-ESIMS spectrum of fortalide Q (**17**).

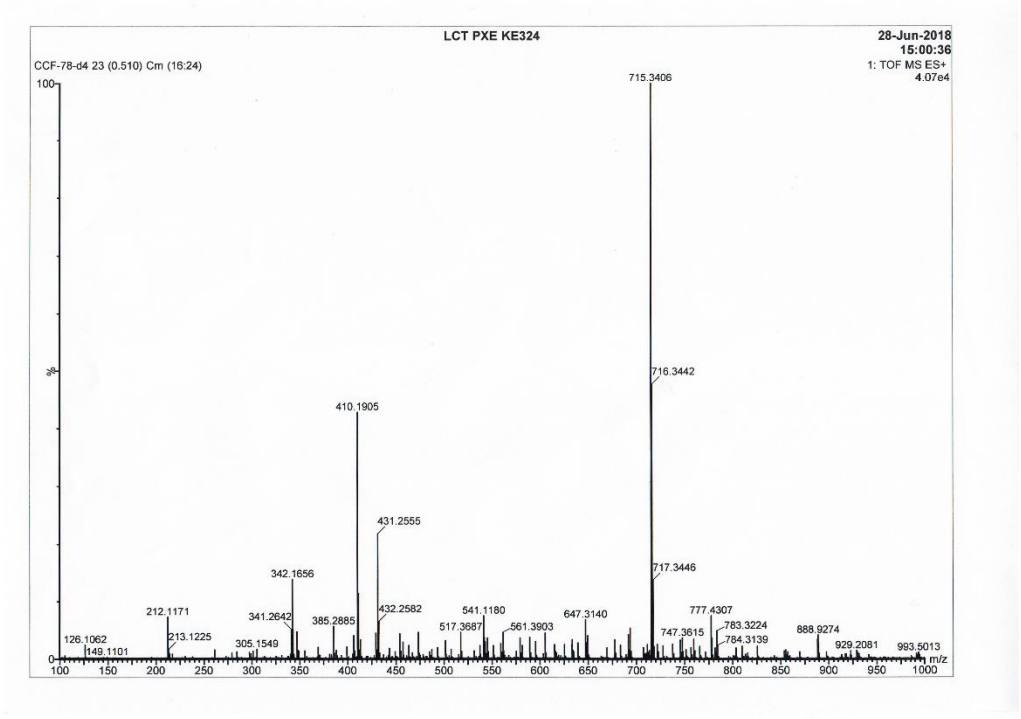

**Figure S189**. (−)-ESIMS spectrum of fortalide Q (**17**).

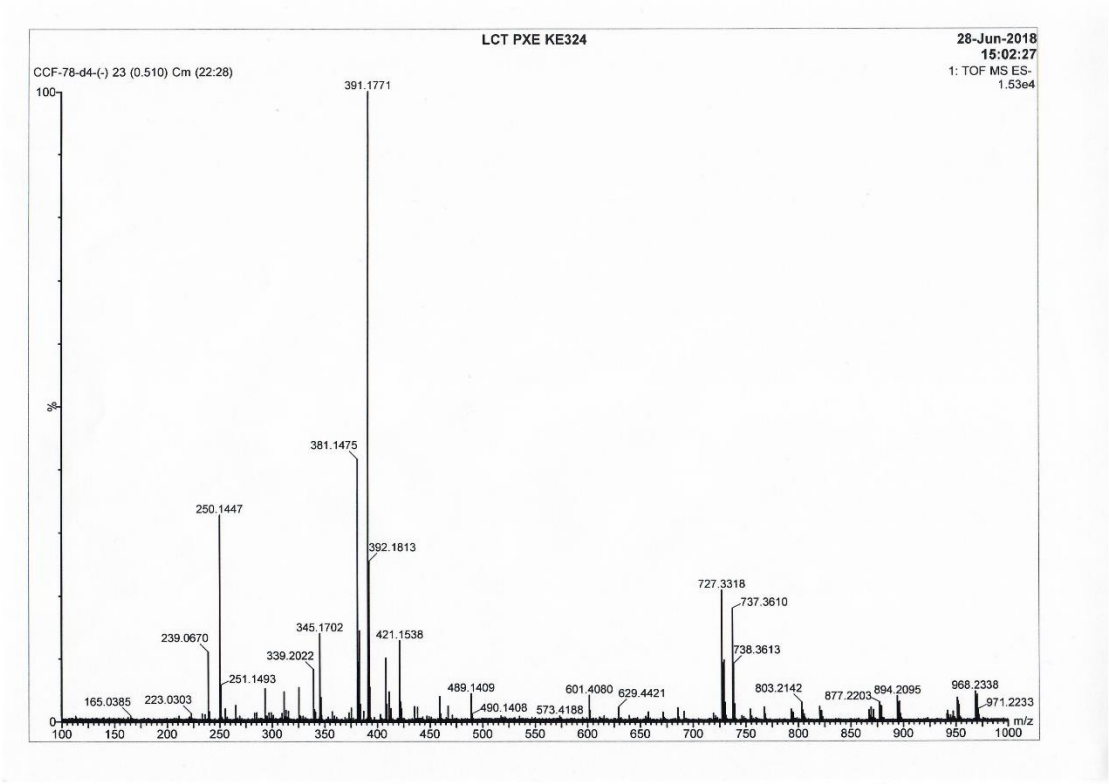


**Figure S190**. (−)-HRESIMS spectrum of fortalide Q (**17**).

**Elemental Composition Report** **Page 1**

**Single Mass Analysis**
Tolerance = 5.0 PPM / DBE: min = -1.5, max = 50.0
Element prediction: Off
Number of isotope peaks used for i-FIT = 9

Monoisotopic Mass, Even Electron Ions
87 formula(e) evaluated with 1 results within limits (up to 50 best isotopic matches for each mass)
Elements Used:
C: 0-100 H: 0-1000 O: 0-500

LCT PXE KE324 28-Jun-2018 15:04:10
CCF-78-d4-W 57 (1.216) Cm (52:58)
1: TOF MS ES- 1.16e+004

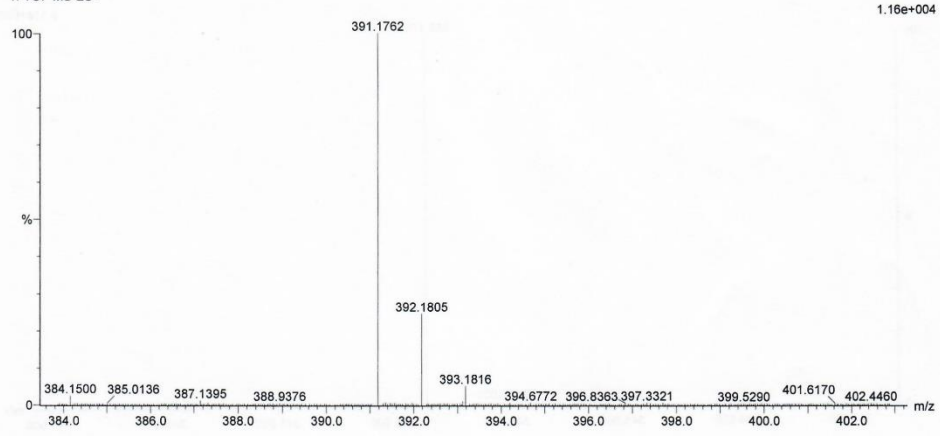


| | | | | | | | |
|---|---|---|---|---|---|---|---|
| Minimum: | | | | -1.5 | | | |
| Maximum: | | 5.0 | 5.0 | 50.0 | | | |
| Mass | Calc. Mass | mDa | PPM | DBE | i-FIT | i-FIT (Norm) | Formula |
| 391.1762 | 391.1757 | 0.5 | 1.3 | 8.5 | 1077.9 | 0.0 | C21 H27 O7 |

**Figure S191**. IR spectrum of fortalide Q (**17**).